A THREE COMPONENT METHOD OF ANALYZING ICEBREAKING RESISTANCE

D. BRUCE COLBOURNE, B.Eng. S.M. P.Eng.

ISBN 0-315-55033-3

Canada

A THREE COMPONENT METHOD OF ANALYZING ICEBREAKING RESISTANCE

© D.Bruce Colbourne, B.Eng. S.M. P.Eng.

A thesis submitted to the School of Graduate Studies in partial fulfilment of the requirements for the degree of Doctor of Philosophy

Faculty of Engineering
Memorial University of Newfoundland
October 1989

St. John's Newfoundland

ABSTRACT

This thesis presents a broad based review of current literature in the field of ship icebreaking and ice mechanics relevant to icebreaking.

A dimensional analysis of the ship icebreaking problem is presented, leading to a system of non-dimensional numbers based on division of the problem into three independent components; an ice breaking component, an ice clearing component and a viscous drag component. Results from a comprehensive set of model tests are presented, validating the three component analysis method. In addition the method is applied to a number of model scale and full scale data sets with considerable success. It is concluded that testing and analysis of icebreaking by dividing the problem into components is practically feasible and offers an improved method of analysis, presentation and scaling.

Acknowledgments

I would like to express my sincere appreciation to the following people for their help and encouragement with this work.

Dr. Jim Lever
Dr. Mike Hinchey
Prof. Bill Milne

Mr. Spence Butt
Mr. Brian Hill

Mr. Norman Jeffery
Dr. Ross Peters
Dr. Fred Aldrich

CONTENTS

PART TWO RESEARCH AND RESULTS

LIST OF SYMBOLS

Symbol	Description	Units
A	Area	m^2
a	Ice Flaw Size	m
B	Ship Beam	m
C	Non Dimensional Coefficient	-
D	Depth	m
E	Elastic Modulus	MPa
E_s	Energy (Milano)	J
e	Energy	J
F	Force	N
f	Friction Coefficient (also μ)	-
G	Fracture Toughness	kPa-m
g	Gravitational Acceleration	m/s^2
h	Thickness	m
K	Stress Intensity	$N/m^{3/2}$
k	Non Dimensional Coefficient	-
L	Length	m
M	Mass	kg
N	Normal Force	N
p	Pressure	kPa
R	Resistance	N
S	Shape Coefficient	-
S_c	Ice Floe Concentration	-
r	Ice Floe Radius	m
T	Ship Draft	m
t	Time	s
V	Velocity	m/s
v	Viscosity	m^2/s
x	Axis Label	m
y	Axis Label	m
z	Axis Label	m
Fn	Froude Number	-
Re	Reynolds Number	-
Cn	Cauchy Number	-
Sn	Strength Number	-
C_C	Clearing Coefficient	-
C_B	Breaking Coefficient	-
C_R	Resistance Coefficient	-
ϕ	Stem Angle	deg
α	Waterline Angle	deg
β	Flare Angle	deg
δ	Specific Weight	N/m^3
$\Gamma_{(i,w,d)}$	Mass Density (ice,water,difference)	kg/m^3
$\sigma_{(F,C,S)}$	Strength (Flexural,Compressive,Shear)	kPa
Ω	Scale Factor	-
μ	Friction Coefficient (also f)	-

LIST OF FIGURES

LIST OF TABLES

LIST OF PHOTOGRAPHS

1. INTRODUCTION

The understanding of forces acting on vessels operating in ice covered waters has increased remarkably in the past twenty years. Despite this, it is difficult to make a prediction of the in-ice performance of a new design, particularly if it is not within the shape and size parameters of those ships for which there is some experience. There have been many efforts to develop numerical and experimental methods for full scale ice performance prediction. Although each new development has advanced the field, a universally accepted comprehension of the problem has not yet emerged.

With discovery of oil and minerals in the Arctic and increased interest in exploration of the Antarctic, the need for information on vessel performance in ice became more urgent. This urgency, combined with the fact that the mechanism of breaking ice is complex and difficult to understand, led to a bypass of fundamental research in favour of model testing and analysis of very specific applications. The result has been a large body of information with a narrow range of application.

There have been many theories attempting to explain icebreaking. To date, none of these has been entirely successful and considerable reliance is placed on model testing. In this area, test results have been scattered and difficult to correlate between test facilities. This is related to lack of standardization, different test materials

and differing ideas on important aspects of testing. Considerable effort has been put into development of model ice formulations to satisfy strength, elastic modulus and other scaling requirements but much less has gone into development of test procedures or investigation of basic icebreaking mechanisms.

At the start of the work detailed in this thesis, the intent was to identify two basic components of icebreaking: breaking the ice and clearing it away. It was hypothesized that these two mechanisms were equally important but fundamentally different phenomena. Thus they should be experimentally separated for analysis and scaling. It was thought that many problems in interpreting results from icebreaking model tests could be related to inability to discriminate between these two mechanisms. The aim of this research was to provide a practical experimental method for dividing icebreaking resistance into these two components and to provide the analytical backup and similitude requirements for a method of individual scaling.

Along the way it became necessary to develop and modify some testing techniques and methods of analyzing and presenting data. The end result is a method of conducting and analyzing ship ice model tests. This method has been exercised on a number of data sets and found to be an improvement over previous methods. It makes better use of scarce and expensive data although it does require a more involved model test.

It is believed that this type of analysis will provide a framework within which model test procedures and data analysis can be standardized. This should result in a more expedient development of icebreaking theory and icebreakers.

The following three chapters (2,3,4) present a review of the icebreaking and ice mechanics literature covering major developments up to the present time. Following this, a dimensional analysis for ice breaking and ice clearing is presented (Chap 5). The subsequent three chapters (6,7,8) describe experiments carried out to verify the developed expressions. Chapter 9 covers application of the analysis to a number of other model and full scale data sets. Some discussion of the method, its strengths and shortcomings, is contained in Chapter 10, along with discussion of some characteristics of the two primary icebreaking components. Conclusions and recommendations for further work are identified in Chapter 11. The raw experimental data are contained in the appendices.

PART ONE LITERATURE REVIEW

2. DEVELOPMENTS IN NAVAL ARCHITECTURE

Attempts to analytically describe or experimentally model the icebreaking problem have been ongoing for almost a century. The object of most developments has been to estimate required power to propel a vessel through ice. Success has been limited in that formulations have lacked general applicability, and even where good results have been shown, they have been confined to a narrow range of vessel or ice parameters.

Such poor predictions reflect the limited understanding of the processes involved, but this has been difficult to rectify given the complexity of icebreaking and practical problems associated with experimentation. In many respects, the problem has not been critical because numerous icebreaking ships have been built and operated successfully. Nevertheless work on icebreaking continues with the expectation that gains in understanding will lead to more efficient ships and operations.

In recent history, refrigerated model towing tanks have been introduced for vessel and structure testing in ice. Scaling requirements are well documented, but it has been difficult to achieve desired ice properties at small scale. As with analytical models, lack of knowledge of primary

processes has made it difficult to judge which ice material properties are most relevant thus requiring closest scaling.

The following sections review developments in the area of ships and models in ice. Developments relevant to ice mechanics are mentioned but covered in more detail in Chapter 3.

2.1 Kashteljan Poznjak and Ryvlin

The work of Kashteljan et al., published in Russian in 1968 and translated in 1969 [2.1], is the first major treatise on ships in ice. Until recently, principles laid down in this publication formed the basis for much of the icebreaker design work conducted worldwide. The resistance equations still form a baseline for analytical developments in ship ice resistance. Although more recent studies have revealed weaknesses in the work, it offers valuable insights into performance and operation of ships breaking ice or transiting ice filled channels.

Kashteljan et al. cover a range of subjects related to ships in ice including review of mechanical and physical ice properties, resistance of ships in level continuous ice, and ice model testing. A second part deals with ships operating in broken ice. This is a subject not extensively covered by other authors.

The document provides a narrative description of icebreaking and states that although roll motion may develop, ships do not exhibit periodic pitch motions while icebreaking. This is contrary to later descriptions which report pitch motions caused by repeated riding up on the ice, followed by failure in the sheet under the bow.

It is stated that ice fails by developing radial and circumferential cracks around the bow leading to formation of

one or more rows of broken floes down the side of the vessel. The size of ice pieces and number of rows is dependent on ship speed and ice thickness. Generally, higher speeds and lower thicknesses result in higher numbers of rows of smaller ice floes.

The total resistance of a ship in ice is divided into components attributable to:

1. Breaking ice at the stem and bow sides.
2. Submerging broken ice.
3. Turning ice floes.
4. Motions of the vessel.
5. Impact with the ice.
6. Pushing broken ice aside.
7. Ice friction.
8. The water.

This list is consolidated into two primary components, a Direct Resistance and a Velocity Resistance. The direct resistance is made up of velocity independent terms ie. breaking at the bow, some part of the submerging and turning, and frictional resistance. The velocity resistance includes inertial effects and open water resistance. This division is maintained through the work and applied to model testing and analytical expressions for ship ice resistance.

Similarity conditions for scaling model test results are derived. By satisfying geometric, kinematic and dynamic similarity, Froude, Reynolds and Cauchy numbers are shown to be relevant to icebreaking vessels. It is stated that a part of the resistance to pushing ice aside is viscous drag which should satisfy Reynolds scaling. Because it is not possible

to satisfy Reynolds scaling in a ship model towing situation, some error may be realized in testing for these components. It is noted that the Froude condition can be satisfied and if so, leads to the requirement, based on the Cauchy number, that ice strength and elastic properties be scaled by the geometric scale ratio. Thus the scaling requirements become:

$$L_S/L_M = E_S/E_M = h_S/h_M = \sigma_S/\sigma_M = \Omega \qquad (2.1)$$
$$V_S/V_M = (\Omega)^{1/2}$$

where Ω is the geometric scale factor,
S indicates the full scale ship,
M indicates the model.

Friction coefficient is maintained at both scales and Poisson's Ratio of the model ice should be the same as the full scale. These relations are based on assumption that, under the loading conditions imposed by icebreaking, ice acts as a linear elastic material and fails in a brittle manner. Anisotropy in sea ice is treated by introducing a reduced Elastic Modulus.

The work deals at length with model testing but states that the method is laborious and subject to scaling errors. It is proposed that an analytical expression without dependence on model test results would offer better prediction. Development of this expression draws from the historical review presented in the paper but is based on the

breakdown of components presented earlier. These are condensed to;

$$R_T = R_1 + R_2 + R_3 + R_B \qquad (2.2)$$

R_T total resistance
R_1 resistance due to breaking ice
R_2 resistance associated with weight forces (ie. submersion, turning floes, dry friction)
R_3 resistance due to penetration through broken ice
R_B open water resistance

Components are assumed independent of each other and the ship is assumed to be moving at steady speed. Components are calculated by determining energy expended over a unit length of ship travel. The Direct Resistance is the sum of R_1 and R_2 while the Velocity Resistance is the sum of R_3 and R_B.

Breaking resistance is sub-divided into a term for the sides of the bow and a term for the stem. A term for the sides is given as;

$$R_1' = k_1 B \sigma h \mu_0 \qquad (2.3)$$

where μ_0 is, in this case, a hull shape factor and k_1 is determined from model experiments. This is somewhat at odds with the originally stated objective of the analytical expression. The term for the stem is;

$$R_1'' = k_1 \sigma h^2 \tan \Phi \qquad (2.4)$$

where ϕ is stem angle. Rather than use both, the first expression is taken as the best approximation and the component associated with the stem is distributed among remaining direct components. The second direct component is taken to be the sum of resistances due to:

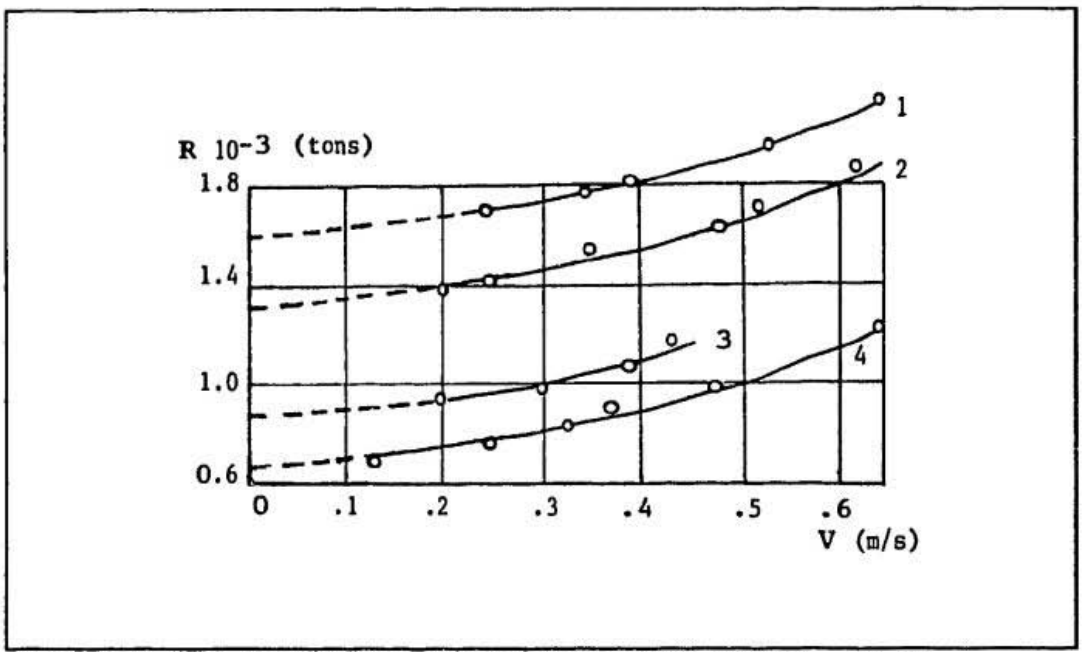

FIGURE 2.1 Model Ice Resistance USSR ERMAK [2.1]
1 σ = 28 T/m^2
2 σ = 19 T/m^2
3 σ = 11 T/m^2
4 σ = 6 T/m^2

(a) Changing the Vessel Position:

$$R_2' = k_2' C h^{1.75} \sigma^{1.25} \mu_0 \qquad (2.5)$$

(b) Turning Ice Floes:

$$R_2'' = k_2'' \delta B h^{1.75} E^{0.25} \mu_0 \qquad (2.6)$$

and (c) Submerging Broken Ice:

$$R_2''' = k_2'''\delta Bh^2 \mu_0 \qquad (2.7)$$

The basis for these is obscure but appears to be largely the authors' intuition. The component associated with changes in vessel position is neglected, as is the turning component. The R_2 is taken as follows:

$$R_2 = k_2\delta Bh^2\mu_0 \qquad (2.8)$$

and the direct resistance becomes:

$$R_D = k_1B\sigma h\mu_0 + k_2\delta Bh^2\mu_0 \qquad (2.9)$$

Velocity resistance is a combination of hydrodynamic and inertial effects. Open water resistance is separated and inertial resistance given as:

$$R_3 = k_3B^xhV^y/n_2 \qquad (2.10)$$

where n_2 is another hull shape factor.

This expression is strange because k_3 is has dimensions. The k factors for all three components and the exponents x and y are determined from model tests on a single vessel and the final expression given as;

$$R = 0.004B\sigma h\mu_0 + 3.6\delta Bh^2\mu_0 + 0.25B^{1.65}hV/n_2 + R_B \qquad (2.11)$$

This expression is said to be applicable to all vessels because μ_0 and n_2 are form dependent. However, no evidence is given and later data for other ships has not borne this out.

Following the work on continuous ice, considerable

explanation is devoted to ship resistance in broken ice. This is interesting because if icebreaking can be divided into independent components then resistance in broken ice should be a sub-case of the continuous ice situation, assuming that floe sizes are comparable. The case of complete coverage in finely broken ice is relevant for comparison with breaking consolidated ice. Some description of model testing in broken ice is given, but of greater interest is development of analytical expressions covering the situation. The earlier work is not followed, but resistance is reduced to components attributed to inertia, impact, ice deflection, submersion, turning, and elastic compression. Submersion and turning components are neglected and the broken ice resistance expression presented as;

$$\begin{aligned} R_{BI} = {} & \delta(rh)^{1/2}(B/2)^2[k_1(1+2f\alpha L/B)+k_4 f\alpha L/BS_c] \\ & + k_2\delta rhB(f+\alpha_c \tan(\alpha))Fn \\ & + k_3\delta rhL \tan^2(\alpha)Fn^2 \end{aligned} \qquad (2.12)$$

This is quite different from the non-breaking components presented earlier. This equation is semi-empirical in nature with constant values dependent both on the ship and ice concentration. Coefficients are given, but are derived from a single ship case. This case in turn is presented as proof of the expression. While hardly a valid approach, so little work has been done in the area that few further improvements have been made.

2.2 White

In a Doctoral Thesis and paper, White [2.2,2.3] presents a simplified treatment of icebreaking. The basis is that most effective icebreaking is done by generating downward force at the stem of the vessel. Energy components associated with ice crushing, floe inertia, submergence and side friction are neglected. However effects of friction pertaining to the ability of the bow to ride up onto the ice sheet are considered.

White does not deal extensively with continuous transit in ice but is concerned mainly with ramming. Conclusions deal more with design of an effective bow shape than a predictive method, although scaling laws for modelling in ice are derived. This paper prompted some discussion regarding neglect of other components of resistance. White, however, maintained that the primary icebreaking resistance was breaking the ice. He also expressed strong disagreement with the conclusions of Kashteljan, particularly regarding the submergence component.

Although treatment of the icebreaking mechanism is simple and considers only a single component of resistance, the parabolic stem line and forebody shape developed by White has been a successful bow form for a number of icebreaking ships (see Fig.2.2).

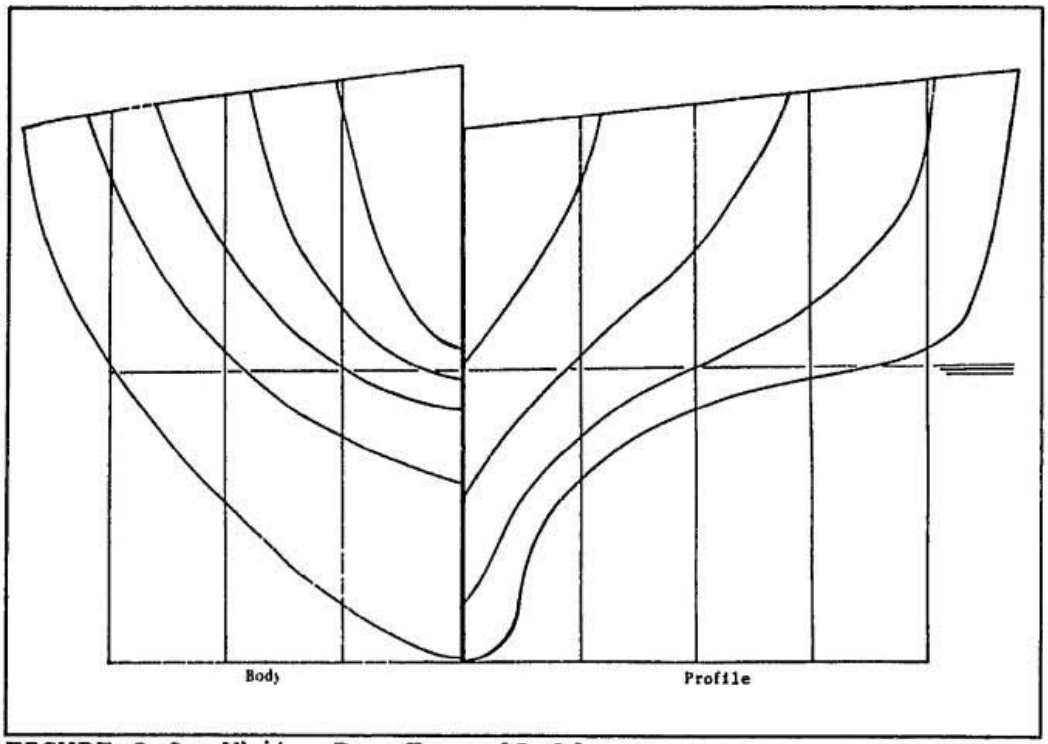

FIGURE 2.2 White Bow Form [2.3]

The design, or variations on it were used on MANHATTAN, the USCG Polar class and the CCG R-Class. All these vessels have shown good performance in polar and sub polar regions.

2.3 Lewis and Edwards

Lewis and Edwards [2.4] present a theoretically based expression for ship resistance in level ice. Ship, or ice dependent coefficients are determined by regression analysis of model data. Scaled results are compared with a regression equation from full scale trials data.

The expression takes the form:

$$R_i = C_0\sigma h^2 + C_1\Gamma_i g B h^2 + C_2\Gamma_i B h V^2 \qquad (2.13)$$

where the first term is the resistance associated with breaking the ice cover, the second is submergence resistance and the third is inertial or velocity resistance. Coefficients are derived from model test data of the USCG Wind Class.

The breaking component is derived from an analytical solution for bending failure in a semi-infinite wedge on an elastic foundation. Wedge type failure, resulting from formation of radial and circumferential cracks in the ice is assumed to be the mode of failure at the bow of a vessel. Thus, solution of the simplified problem should give an indication of forces at the bow. However, it is also apparent that the volume of ice broken depends on ship beam and consequently one would expect some beam dependence in a breaking term.

The submergence term indicates that ice will be pushed

down to a depth h (ice thickness). It is more likely that the degree of submergence is a ship related parameter, probably related best to vessel draft (T). This, and lack of a beam dependent breaking term, is noted in discussions of the paper.

Friction is not explicitly identified, although the authors state that the coefficients account for friction associated with each component. This is not an ideal approach, because different coefficients are required if the friction changes.

Full scale predictions for a Wind Class vessel are given (Figure 2.3). These are compared with ice trials data for USCGC STATEN ISLAND. Predictions show good agreement, regarding effects of ice thickness. Agreement on velocity is not as good. A major difference is that the full scale data show a linear dependence on velocity. The range of forces is, however, fairly narrow. The full scale data do not exhibit any dependence on ice flexural strength, which is attributed to a limited range of ice strengths tested at full scale.

While this method shows promise, there are some weaknesses. Ice resistance is presented in terms of σ (ice strength), h (ice thickness), B (beam), and V (velocity). Given that all terms in the regression equation contain h or h^2, two out of three contain B, the coefficient of the breaking term (involving σ) is small and, the velocity term does not show good agreement with full scale data, it appears that the regression is really in terms of B and some power of

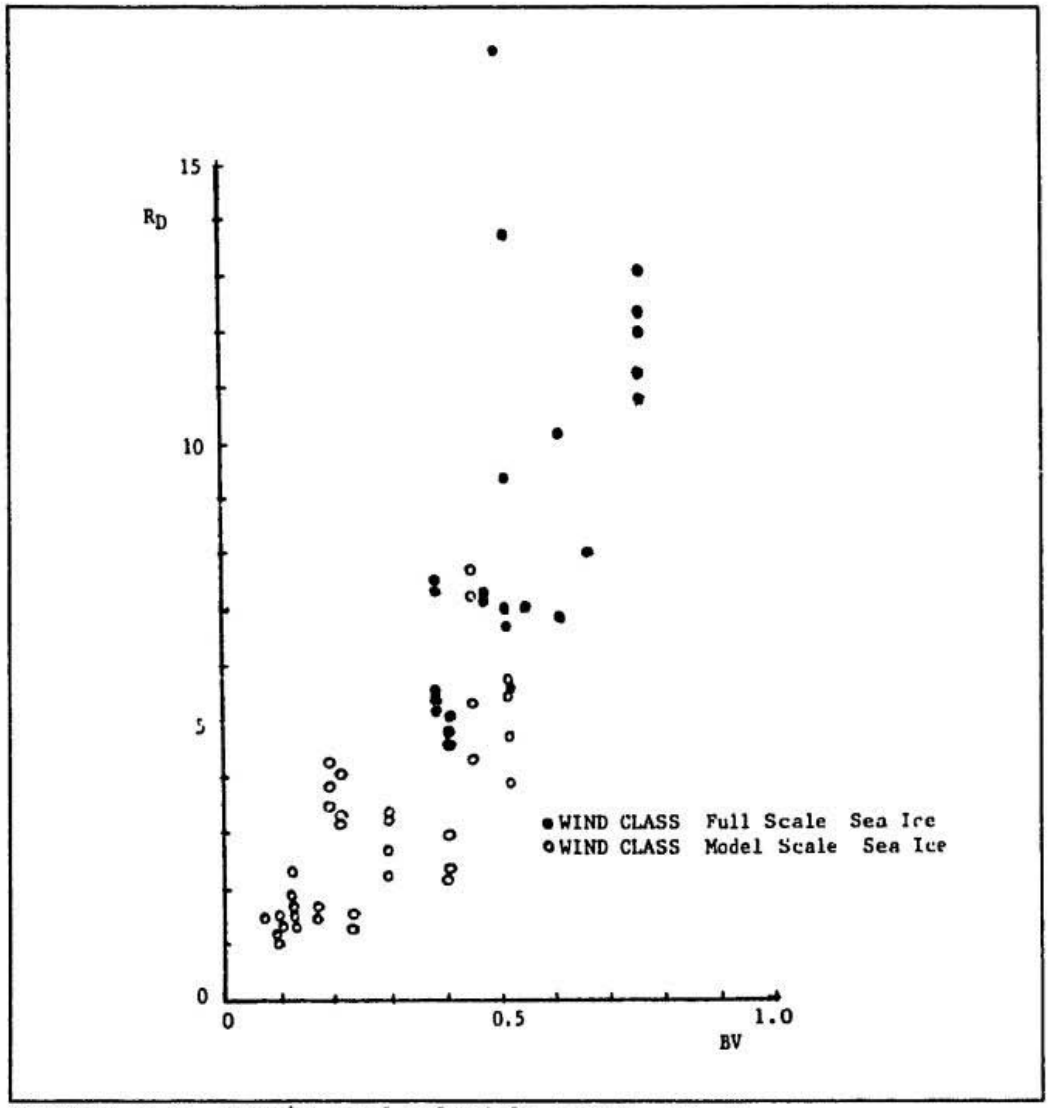

FIGURE 2.3 Lewis and Edwards 1970 [2.4]
$BV = (B/h)_2(\Gamma gh/\sigma)$
$R_D = R/(\sigma h^2)$

h. This narrowing of the range is furthered by the fact that the proof data are for a single ship, eliminating variation in B and leaving the only demonstrated effect as that of ice thickness. Thus, much more verification would be required before it could be widely applied.

2.3.1 Edwards and Lewis et al 1972

In 1972 Edwards, Lewis and others [2.5] presented results of model and full scale resistance tests on USCGC MACKINAW. A set of dimensionless icebreaking coefficients, which differ from those used earlier, are presented.

Full scale trials detailed in the paper were performed in fresh water ice, on the Great Lakes. There are a number of factors leading to error in the figures. The MACKINAW has a single bow propeller which complicates the icebreaking mechanism at the bow. In estimating thrust, propeller shaft torque was measured and thrust estimated from open water propeller charts. This takes no account of loss of thrust due to passage of ice through the propeller which could lead to significant errors. A better method would have been direct measurement of thrust.

The model test data show some scatter in ice properties particularly flexural strength. Elastic modulus is not considered and in scaling model data, open water resistance is not separately accounted for.

Dimensionless groups for the ice resistance are presented as follows:

$R/(\Gamma_w g B h^2)$	Dimensionless Resistance
$V/(gh)^{1/2}$	Froude Number
$\sigma/(\Gamma_w gh)$	Dimensionless Strength
h_s/h	Dimensionless Snow Cover

These groups are different from the expression presented in 1970. Translating back to a dimensional resistance expression, one obtains:

$$R_i = C_0\sigma Bh + C_1\Gamma_w gBh^2 + C_2\Gamma_w V^2 Bh \qquad (2.14)$$

Neglecting snow cover

It can be seen that the breaking term has been changed to σBh from σh^2. In addition the non-dimensionalizing factor is $\Gamma_w gBh^2$ (the submergence term) rather than σh^2 (the strength term). No explanation is given for these changes, although this equation is more in keeping with more current publications.

In performing regression analysis on the full scale data it was found that ice strength is not a significant contributor to the resistance. The major parameters are stated to be ice thickness, velocity and snow cover thickness. No conclusions are drawn about vessel parameters as only one ship was tested. In general, correlation between model data and full scale data is reasonable for low Froude numbers but divergence increases with velocity.

2.4 Milano

In 1973, Milano [2.6] provided a new approach to determination of ship resistance in ice. It considers icebreaking a cyclic process for which average resistance is the total energy lost over a cycle divided by distance travelled per cycle. The work covers a purely analytical expression for energy lost in an icebreaking cycle. Total energy consumption is broken down as:

$$E_T = E_1 + E_2 + E_3 + E_4 + E_5 \qquad (2.15)$$

where;
- E_T= Total expended energy.
- E_1= Energy associated with movement through a broken ice filled channel.
- E_2= Energy associated with impact and crushing of the ice sheet.
- E_3= Energy associated with the ships bow moving up onto the ice sheet.
- E_4= Energy associated with the ships bow falling after failure in the ice sheet.
- E_5= Energy associated with forward motion and submergence of ice subsequent to failure.

Complicated expressions are developed for each component and developed into a numerical computer program.

This approach is significant for a number of reasons. It does not involve regression analysis of model or full scale data, eliminating the limited applicability associated with that method. The algorithm recognizes that many mechanisms resist transit of a ship through ice and that they may not all

act at the same time or to the same degree.

Milano's formulation does raise some questions however. Breaking ice is not a separate term but is included with the E_2 and E_3 terms. Thus energy lost to breaking ice is not explicitly identified. The E_4 term due to the ship falling after failure appears to be double counting because this energy is regained from the E_3 term (Energy associated with climbing on to the ice sheet). Thus potential energy of E_3 is converted to kinetic energy in E_4. It is not logical to consider this a further loss in energy. Finally, the method only deals with energy lost at the bow (back to the section of maximum beam). For older icebreaking forms this is fine, as there is really no flat midsection. However for newer vessels and non-icebreakers this is a more serious omission.

In comparison with full scale results, (Figure 2.4) Milano's method shows good agreement at low velocity. At higher speeds the method predicts overly high resistances. In discussion, J. W. Lewis reveals that the analytical line is for an ice strength higher than that recorded in the full scale trials. Had recorded strength been used, correlation with the full scale data would have been worse than that shown.

In a second paper, presented in 1975, Milano [2.7] exercised the method further. This comprises results from variations in ship and ice parameters, including relative magnitudes of the energy components for a single ship-ice

case. It shows that E_3 and E_4 terms are similar in magnitude and identical in form when plotted against velocity. This is evidence that these two terms represent the same energy in different forms. Remaining illustrations provide insight into effects of various ship parameters on predicted resistance but do not provide verification of the underlying assumptions.

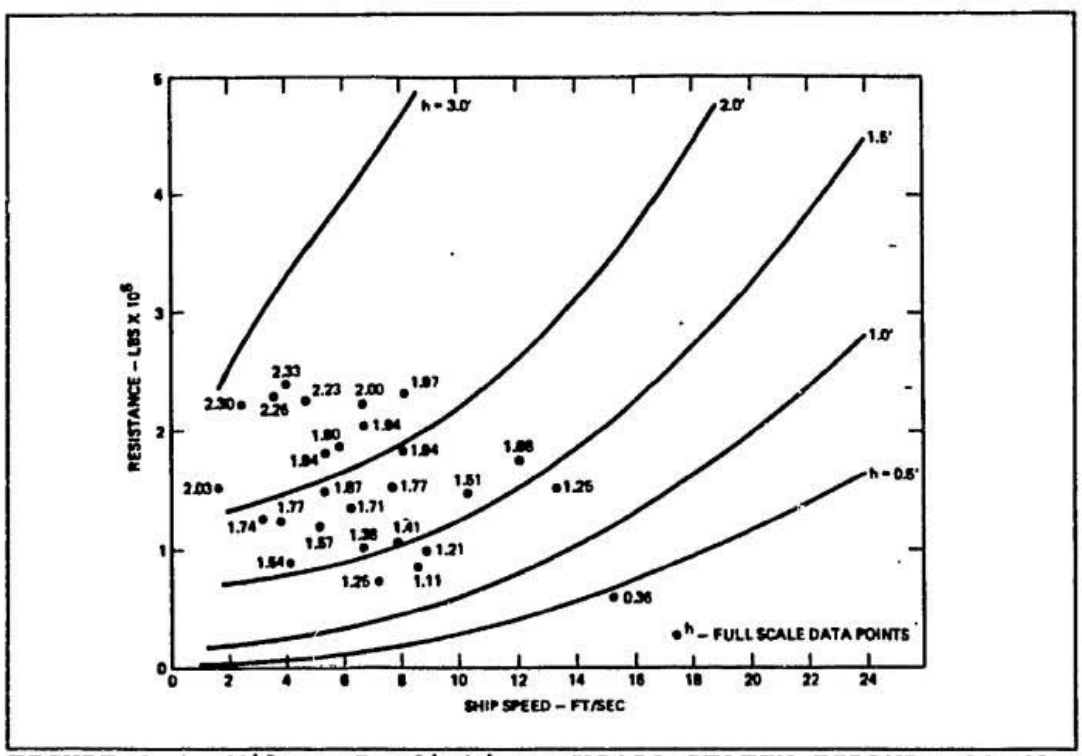

FIGURE 2.4 Milano Prediction USCGC STATEN ISLAND [2.6]

2.5 Enkvist

Enkvist [2.8] presents a broad based work covering ice properties, full scale trials, model tests and analytic developments. The stated objective is to provide a means of predicting full scale ice performance based on model testing but with a degree of analytical back up. Enkvist maintains that icebreaking is too complex for analytical methods to replace model testing.

In discussion of ice properties at model and full scale, Enkvist notes two important problems in model testing. First, the ratio of Elastic Modulus to Flexural Strength (E/σ) is lower in model ice than real sea ice. For failure in flexure, this lack of similarity leads to error in model test prediction. The second phenomena is residual plasticity in model ice. Natural ice fails as a brittle material with a clean break. Model ice, on the other hand, suffers brittle failure in the top layer and plastic failure in the underlying material (Figure 2.5). The result of this is that model ice consumes proportionally more energy in failure than the full scale.

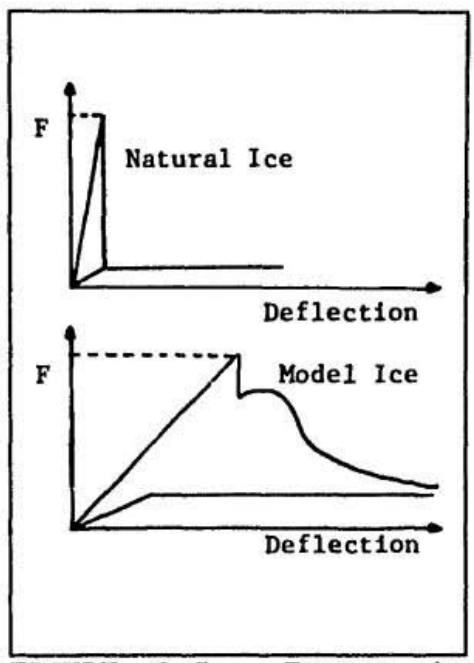

FIGURE 2.5 Energy to Break Model and Full Scale Ice [2.8]

Enkvist notes the importance of these problems to the breaking component of total ship resistance but states that breaking resistance is a small component of the total and thus the error is small.

The relation between cantilever beam tests and strength experienced when breaking cusped ice pieces, normally observed at the ship bow, is also discussed. For a limited number of cases, no relation was found between strength recorded during beam tests and strength measured in cusp breaking tests. Under ice properties, a discussion of the role of friction in icebreaking is presented. This is reinforced with results from experiments at model and full scale (Figure 2.6). A

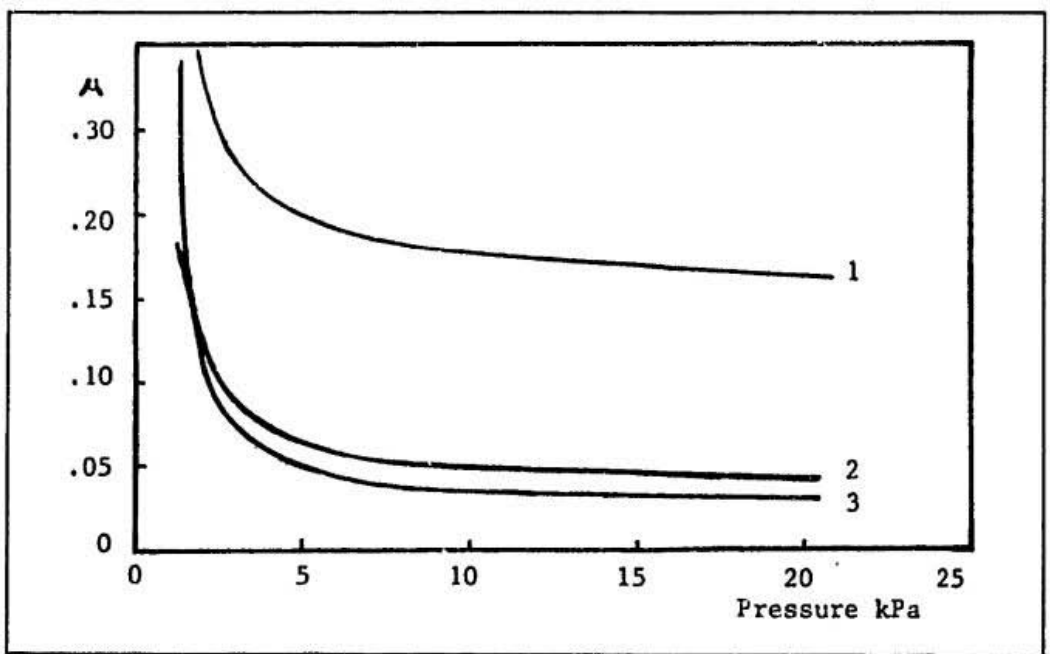

FIGURE 2.6 Hull Friction Measurements [2.8]
1 Dry Snow
2 Dry Ice
3 Wet Snow

major concern is hull roughness and how it should be scaled. Although definite conclusions are not drawn, it is recommended that standards be established for dealing with ice friction at model scale.

In development of a predictive method, Enkvist verifies his formulation with three vessels for which model and full scale data were available. These are the Russian MOSKVA Class icebreakers, the icebreaking RO-RO vessel FINNCARRIER and the icebreaking tug JELPPARI, representing a cross section of icebreaking vessel types.

During full scale trials, vessel speed, pitch motions and the size of broken ice pieces were recorded. Engine power and shaft rpm were logged as a means of estimating thrust. Difficulties are reported in estimating actual thrust and this is recognized as a source of error.

A methodology employed in model testing is described and problems maintaining ice thickness and properties are noted. Analysis of data is based on division of resistance into three components:

$$R_i = R_\sigma + R_S + R_V \qquad (2.16)$$

where;

R_i = Total ice resistance.
R_σ = Resistance due to breaking the ice cover.
R_S = Resistance due to submerging broken ice.
R_V = Resistance due to velocity effects.

By dimensional analysis, the following formulations are developed:

$$\begin{aligned} R_\sigma &= C_\sigma Bh\sigma \\ R_S &= C_S BhT\Gamma_d g \\ R_V &= C_V Bh\Gamma_i V^2 \end{aligned} \qquad (2.17)$$

which are combined to give the equation:

$$R_i/(BhT\Gamma_d g) = C_\sigma \sigma/(T\Gamma_d g) + C_S + C_V \Gamma_i V^2/(T\Gamma_d g) \qquad (2.18)$$

A term for friction is added and a draft vs. thickness factor T/h introduced. The final result is:

$$R_i/(BhT\Gamma_d g) = [1 + C_\mu(\mu)][C_\sigma(S_\sigma, G_T) + C_S + C_V(F_T, G_T)] \qquad (2.19)$$

where:

$$S_\sigma = \sigma/(T\Gamma_d g) \qquad F_T = V/(gT)^{1/2} \qquad G_T = T/h$$

This is similar in form to earlier equations with addition of the friction factor $C_\mu(\mu)$.

Enkvist calculates constants in the equation by regression analysis of model test results. Constants are dimensionless and assumed applicable to full scale predictions. On comparison with vessel trials, correlation is reasonable when assumed friction coefficients are in the range 0.3 - 0.4. These coefficients are quite high although Enkvist asserts that they are reasonable. Because of the way friction is included in the expression, adjustments to it act as multiplicative correction factors. It is not clear if the friction coefficient is at fault or if other factors influence the resistance prediction.

On the analytical side, Enkvist presents the same components, with methods for calculating constants based on ship parameters. For C_o and C_s, agreement between calculated values and measured values is poor, but for C_v agreement is good. The majority of velocity resistance is attributed to turning ice floes. As part of this mechanism, a phenomena called ventilation is introduced. This occurs when the edge of a floe is pushed down by the ship side and water is unable to flood the top of the ice piece. Thus there is a hydrostatic pressure on the floe in addition to buoyancy and dynamic forces. This increases force on the ship and consequently resistance. It is stated that ventilation is only observed at higher ship speeds.

In summary, Enkvist's formulation does not depart sharply from previous developments except in the explicit addition of a friction term. Discussion of the issues in icebreaking is however very detailed and complete.

2.5.1 Enkvist 1983

In 1983 Enkvist [2.9] showed that the breaking component of total in-ice resistance is higher than originally estimated. Breaking is said to represent between 40% and 80% of the total "near zero speed" full scale ice resistance. It is not indicated how this information affects earlier predictors but an expression for resistance due to submergence

at low speeds is given. A new formulation for breaking resistance is not offered. It is concluded that the high breaking resistance cannot be attributed to bending in the ice sheet alone, and that other failure mechanisms, such as shear or crushing must come into play.

2.6 Vance

In 1974 and 1975 Vance [2.10,2.11] published work on scaling, model testing and regression analysis applied to ships in ice. This led to another formulation for predicting full scale ship resistance from model tests.

Prior to discussion of scaling, Vance lists ice material properties relevant to icebreaking. Non-dimensional numbers are developed based on similitude for weight, inertial, elastic and viscous forces. Weight similarity is satisfied through geometric scaling and Froude, Cauchy and Reynolds Numbers are derived as factors to satisfy the remaining conditions. Ice characteristic length and frictional forces are included. Similarity for characteristic length is said to insure that the size of broken ice pieces is proportional at model scale. Vance indicates that requirements for characteristic length are satisfied if Poisson's Ratio for model ice is the same as full scale. It is shown that the friction coefficient for model and full scale should be the same.

As with open water tests, Froude and Reynolds numbers cannot be satisfied at the same time. Because inertial effects are more important, Reynolds scaling is not satisfied and correction is made by calculation. Other factors can be more or less satisfied, except the ratio of elastic modulus to flexural strength is not properly scaled in model ice. Vance

lists parameters relevant to the icebreaking process and develops expressions for components of icebreaking resistance. These are based on Kashteljan and Enkvist and the resulting expression is similar to their equations. Total resistance is divided into three components (breaking, submergence and velocity) and the friction factor included as an overall multiplier.

An expression for the breaking component is based on the equation for a cantilever beam. The more realistic case of a semi-infinite plate is not analyzed. Vance states that there is no evidence to indicate that there is a velocity effect in the breaking component of resistance.

Derivation of a submergence resistance term is similar to Enkvist's and results in an expression of the same form. For velocity resistance, Vance assumes momentum transfer as the dominant phenomena and the expression takes the form $\frac{1}{2}MV^2$. This is contrary to Enkvist who assumed the dominant speed effect as turning ice floes.

Open water resistance is calculated by Reynolds friction only. No account is taken of any wave generation or form drag. This is probably a valid approach, given the low speeds normally used in icebreaking.

The result is:

$$R = C_f[R_S + R_B + R_V] + R_{OW} \qquad (2.20)$$

where; C_f is a frictional multiplier ie. 1+f

$R_S = C_S\Gamma_d g B^x h^y T^z$

$R_B = C_B\sigma_f Bh$

$R_V = C_V\Gamma_i V^2 L^m h^n B^p$

and; $x+y+z = 3$

$m+n+p = 3$ for dimensional homogeneity

Values for constants and exponents in this expression are derived by an involved process. Model test data sets for five ships are used in a stepwise regression analysis to derive a set of 64 expressions in the form presented above, for each vessel (a total set of 320 expressions). Each of the sixty four expressions uses a different set of exponents, subject to certain constraints and the same exponents are used for each vessel. The multiple r (statistical measure of goodness of fit) is used to rate expressions.

Each set of five resistance expressions is used to make full scale predictions by retaining C values calculated in the regression and substituting vessel and ice parameters as per the full scale situation. These predictions are compared to regression lines for each vessel based on available full scale data. The expression with the best average fit over five

vessels, between full scale prediction and full scale regression is selected as the "best" form.

$$R_i = C_s\Gamma_d gBh^2 + C_B\sigma_f Bh + C_V\Gamma_i V^2 Lh^{.65}B^{.35} \qquad (2.21)$$

Friction is left out, apparently due to lack of data at model or full scale.

Although this expression offers the best average prediction, it does not give best prediction for all vessels in the analysis. Vance attributes this to shape factors or poor data.

Following the predictor equation, there is discussion on design of an adequate ice resistance test, considering confidence intervals on predictions. This is interesting because Vance suggests 64 data points per friction factor and tests at three friction factors for a total of 192 points. This results in a mid band confidence interval of about 10%. Given the expense of full scale or model tests it is unlikely that 192 or even 64 good data points are often obtained for a vessel. This indicates that confidence intervals on most model tests in ice are very wide.

In discussion of the predictor equation, plots are presented showing model scale regressions, full scale regression, full scale data points and predictions by other methods (ie. Milano, Lewis and Edwards, Kashteljan etc.). Although it is not clear where the full scale regression lines come from, model scale predictions show good agreement with

full scale data points. This is not surprising, given that the predictor is based on a regression of the same data points.

A prediction for a vessel not used in the regression analysis is presented, but does not show such good agreement. This is, however, stretching the regression because this vessel (The JELPPARI) is substantially different from the others in hullform and size.

As a final note, relative magnitudes of resistance components against ship velocity are mentioned. It is shown that the submergence component is disproportionately high for model tests but that the sum of breaking and submergence is equal for both model and full scale. This is contrary to conventional wisdom that model ice absorbs more energy in breaking due to residual plastic tearing. This phenomena is presented by Enkvist and reviewed by Vance, but not included in the discussion.

2.7 Naegle

Naegle [2.12] develops a motion simulation algorithm for icebreaking vessels with three degrees of freedom (surge, pitch and heave). This is based on a theory that forces at the bow in level continuous ice, are cyclic and related to the length of the broken ice cusps. As each pair of cusps approaches the breaking point, force becomes maximum in both horizontal and vertical directions.

Considerable work is devoted to defining hydrodynamic coefficients for an icebreaking hull. A second portion involves analysis of the cusped breaking pattern created in the ice as the vessel progresses. This relates the icebreaking force cycle to characteristic cusp length, as a function of ice properties and vessel properties. Inertial and submergence components are calculated using methods presented by Enkvist including effects of ventilation. Force at the vessel stem is assumed to be generated by shear failure in the ice.

Expressions for icebreaking forces and hydrodynamic coefficients are used in three coupled equations of motion, which form the basis for a motion prediction computer program. Horizontal forces generated at each time step in the motion simulation are averaged over each icebreaking cycle (cusp to cusp) to give a mean resistance for the vessel.

On comparison with full scale and model data (Figure 2.7), Naegle's motion simulation tends to under predict

resistance and agreement gets worse with increasing ice thickness. In motion simulation, the program predicts a degree of sinusoidal pitch motion which has not been observed in the limited number of cases for which such data has been recorded.

Lack of correlation is attributed to poor estimation of forces related to turning broken ice floes. This may be the

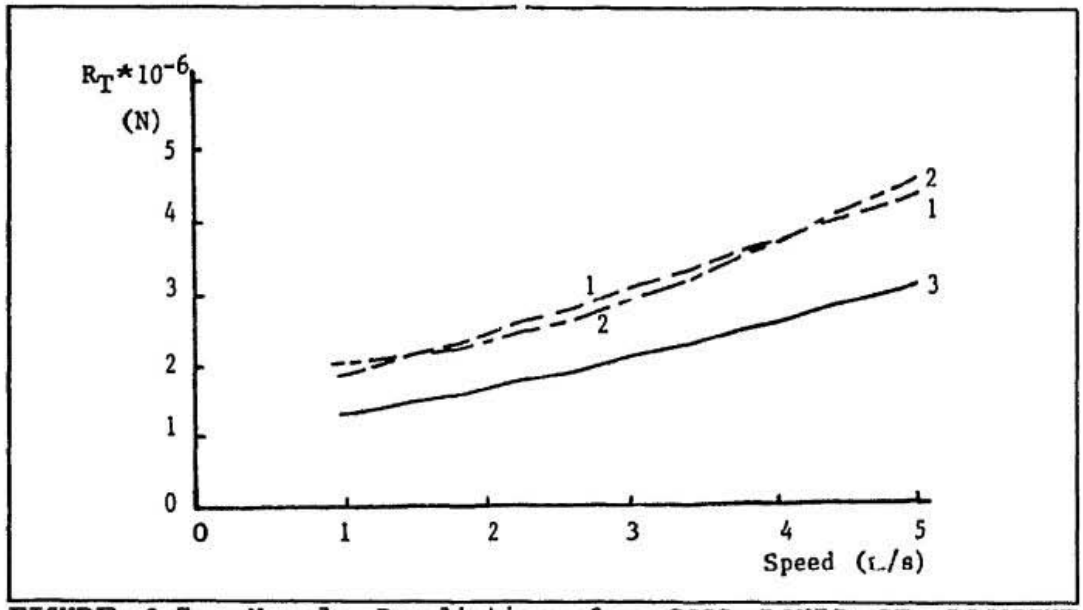

FIGURE 2.7 Naegle Prediction for CCGS LOUIS ST. LAURENT [2.12]
Ice thickness = .914 m.
1 Full Scale
2 Model Scale
3 Naegle Predictor

case, as Enkvist indicated in 1983 that the resistance caused by turning and submersion were poorly estimated in his 1972 paper. Given that this was the method used by Naegle, an overall under estimation would appear likely.

There is another issue which may contribute to poor resistance calculation and could explain the discrepancy in

predicted vs. observed pitch motions. As a basis for the analytical model it is assumed that vessel roll will not be an important factor and the ice will break symmetrically on both sides of the vessel bow. On consideration, this is not likely. It is probable that ice cusps will fail in a staggered pattern, first one side and then the other. This would give rise to a roll excitation which would augment the asymmetric breaking pattern. An asymmetric pattern would introduce a number of modifications to the model. Pitch motions would be reduced, because the excitation force is reduced. The same rationale would apply to reduction in peak breaking resistance although average resistance may be unaffected.

Although Naegle's model is not perfect, it represents an important step in the understanding of icebreaking by recognizing that ice forces induce motions in the vessel which affect the icebreaking performance. Secondly it presents an analysis of the breaking pattern at the bow, including size and aspect ratio of floes and resulting cusp pattern in the broken channel. Relationships between these parameters, ice properties and vessel characteristics have implications for the exciting forces and frequencies experienced by vessels breaking ice.

2.7.1 Kotras, Baird and Naegle

This paper [2.13], published in 1983, further develops Naegle's model. Resistance is divided into breaking, floe turning and floe submerging components with a frictional component associated with each. Further analysis of a simplified cusped breaking pattern around the bow is presented and considerable attention is devoted to turning ice floes and associated forces on the vessel. An algorithm for submergence forces is not well explained.

A departure from the original work is the neglect of pitch and heave motions in the expressions. Although predicted to be significant in the original model their effect on estimated resistance is said to be small.

Although the final model is not clearly presented, some results are. As with previous models, coefficients come from regression analysis of full scale data. The resulting expressions show good agreement with this data but really only illustrate the degree of scatter in the full scale data.

2.8 Carter

In a 1983 report, Carter [2.14] presents an analytical method for estimating resistance of a ship transiting level continuous ice. Resistance is divided into ice resistance and open water resistance. The ice portion is split into two components attributable to the maximum force generated in the ice sheet prior to failure. The first component is due to force generated at the vessel stem and the second to forces generated along the sides of the bow. The model assumes that ice fails in flexure through radial, followed by circumferential cracking. Maximum force occurs prior to failure along the circumferential crack. This force is calculated and summed over the bow area to give the two icebreaking components.

In Carter's expression, resistance associated with breaking ice at the stem is independent of vessel beam. Both components are functions of ice thickness squared and the side component includes effects of friction. Expressions for the two are developed for a static case and a velocity correction applied, based on dynamic response of a floating wedge. This acts to increase the breaking resistance with increasing velocity. This is contrary to previous developments, in which the breaking mechanism is assumed to be velocity independent.

A correction for lateral pressure in the ice and an empirical addition for resistance due to snow are added to give the following:

$$R_T = R_{IS}(1+0.4V^2l^2/\sigma h^2)^{1/2}((\sigma+\sigma_o)/\sigma) + \sigma_o h(2L-L^*)f + 900h_s + R_{OW} \tag{2.22}$$

$$R_{IS} = R_1 + R_2$$

$$R_1 = .5483(\pi/2-\alpha)\left(\frac{\sin\alpha\sin\phi + f\cos\phi}{\sin\alpha\cos\phi - f\sin\phi}\right)\sigma h^2 \tag{2.22a}$$

$$R_2 = .75\sigma h^2 B/l\frac{1+2\cos\phi}{(\sin\alpha+\cos\alpha)(1+2\sin\delta)}(\tan\phi + f(2L^*/B(1+2\cos\alpha)+1.732\tan\alpha)) \tag{2.22b}$$

where R_1 is the force associated with the stem,

R_2 is the force associated with the sides,

$(1+0.4V^2l^2/\sigma h^2)^{1/2}$ is a velocity correction,

$((\sigma+\sigma_o)/\sigma) + \sigma_o h(2L-L^*)f$ is a pressure correction,

$900h_s$ is resistance due to snow cover, (h_s=snow depth),

R_{OW} is vessel open water resistance,

L^* is the length of the vessel forebody,

ϕ,α are bow angles.

There are some points to be noted about this expression. It is an equation for maximum force at the bow and assumes the entire bow area is in contact with ice at, or close to, the

failure point. No account is taken of forces required to submerge, turn or accelerate ice pieces after breaking. All effects of velocity are attributed to dynamic increase in forces required to break ice. This is at odds with most other investigators in the field.

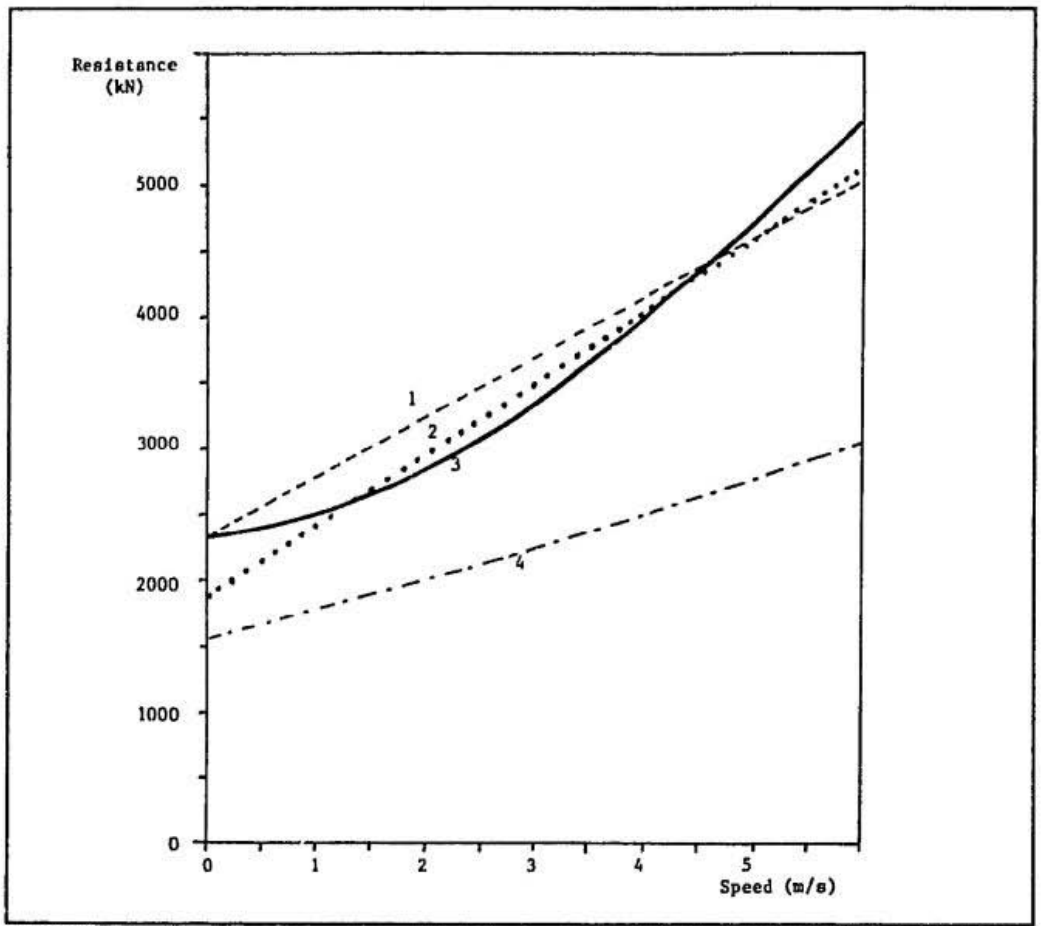

FIGURE 2.8 Carter Prediction for CCGS LOUIS ST. LAURENT [2.14]
Ice thickness = 1.0 m.
1 Full Scale
2 Model Scale
3 Carter Predictor
4 Kashteljan Predictor

Carter compares his equation with available full scale and model data and includes predictions using the Kashteljan method (Figure 2.8). In all cases, correlation between the analytical expression and published data is good. This agreement is a strong case for the presented expression as an accurate representation of icebreaking resistance.

On the other hand the expression calculates maximum force during an icebreaking cycle. Traditional theory indicates that force on a vessel during ice transit fluctuates. If this is the case then average force should be something less than that calculated by Carter. His expression however neglects components, notably the turning and clearing of floes. It is conceivable that the neglect of some elements is compensated by the conservative assumptions of the expression, in calculating peak forces.

2.9 Poznyak and Ionov

In 1981 Poznyak and Ionov [2.15] presented a paper describing a method of analyzing ship-ice resistance. In addition to breaking, submergence and velocity components, a separate component for frictional effects is included. In the final analysis the frictional component is separated into terms associated with each of the components. The resulting expression takes the form:

$$R_T = R_\sigma + R_{f\sigma} + R_s + R_{fs} + R_V + R_{fV} \qquad (2.23)$$

where R_σ, R_s, and R_V are as defined previously (eqn. (2.16)) and $R_{f\sigma}$, R_{fs}, and R_{fV} are frictional components associated with R_σ, R_s and R_V. This recognizes that different frictional coefficients or mechanisms may be at work during the icebreaking process.

A methodology for estimating the magnitude of components from model tests is presented. For an unidentified model moving at a speed of 0.13 m/sec. (said to be near the design point for the vessel) in 29 mm of ice, the relative magnitudes of the components come out as follows:

$$\begin{aligned} R_\sigma &= 41.3\ \% \\ R_s &= 15.8\ \% \\ R_V &= 12.4\ \% \\ R_f &= 30.0\ \% \\ \hline R_T &= 100\ \% = 17\ N. \end{aligned}$$

In this case the frictional components were lumped into a single value.

An expression based on the component breakdown is presented as follows:

$$R_i = 0.14\sigma h^2[a_1(\beta)B + f_d a_2(\beta)L] + 0.1\,\delta_o hBL(\tan\alpha_o/(\tan\alpha_o + B/L))[a_1(\beta)\sin\alpha_o + f_d a_2(\beta)(1+\cos\alpha_o)] + 1.5\,\delta_f hB^2 Fn(1+1/\cos\alpha_o)[(\tan\alpha_o)^2/(2\tan\alpha_o - B/L) + f_d] \quad (2.24)$$

Without going into detail on the derivation it is interesting to note that the first term (breaking) contains h^2 contrary to recent formulations. As previously mentioned, each term has a frictional coefficient, f_d. A further improvement would be to carry on with the original idea of different frictional coefficients for each term, supposing these could be determined.

2.10 Model Trials

Most model tests have been in support of specific designs and are not available in the open literature. Ice testing facilities have their own methods of testing and extrapolating which are not public knowledge and this reduces the value of much model test data. Ice formulations, test methods and data analysis are still developing, making older results less reliable and less comparable to current tests. These factors dictate caution in use and interpretation of much data.

2.10.1 ITTC Standard Model Ice Trials

In an attempt to assess the degree of standardization in the worldwide ice testing community, the International Towing Tank Conference (ITTC) initiated a series of Standard Model Tests in 1982. The purpose of these tests was to provide a standard model for testing at all major tanks. The model selected was the Canadian Coast Guard R-Class hull at scales of 1:40 and 1:20. First results of this program have been collected and presented at the 17th. ITTC [2.16].

Initial presentation of results (Figure 2.9) serves to illustrate the wide variety of values obtained at different facilities. For example, the reported frictional coefficients ranged from 0.038 to 1.3 for the same surface. Of the tanks

reporting, three use Saline ice, two use Carbamide (Urea) and one uses artificial (wax) ice.

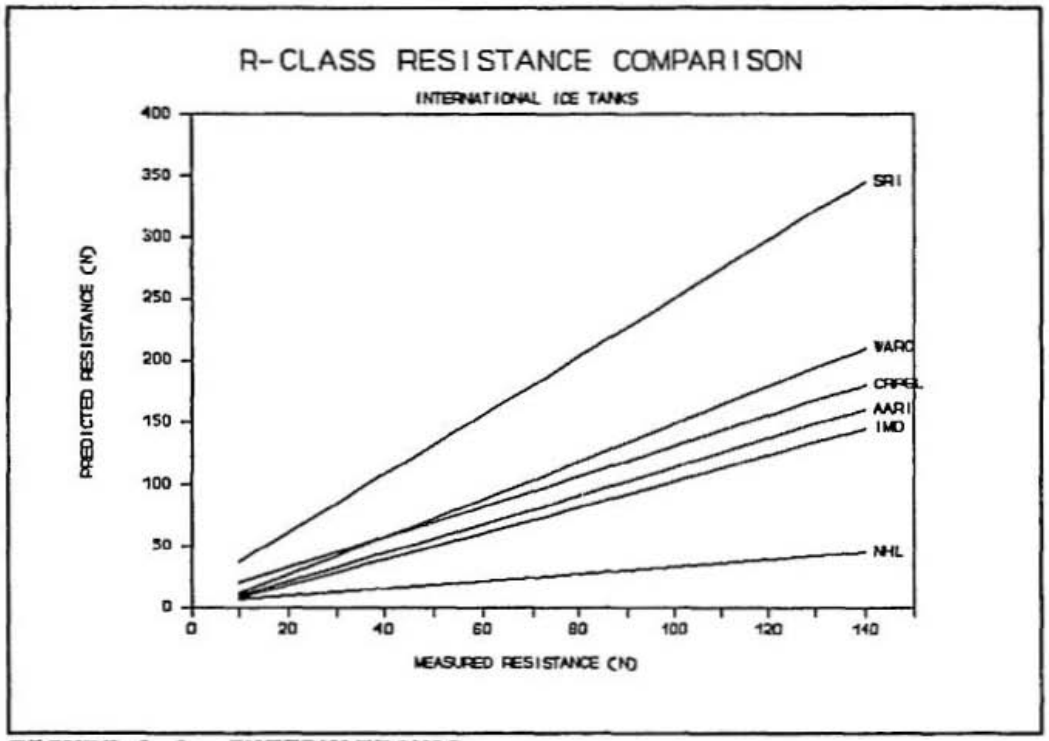

FIGURE 2.9 INTERNATIONAL R-CLASS MODEL TEST DATA

Although the committee suggested full scale target values for ice flexural strength, ice thickness and velocity, results show that difficulty is experienced in achieving and maintaining target values.

Overall results indicate a difference of about 50% between lowest values and highest. Because of high scatter and lack of data on effects of friction, results have not been scaled up for comparison with ship data.

The standard model tests served mainly to illustrate a degree of scatter and non-conformity in ice model testing. It is clear that extreme care would be required in comparing results from different tanks. Further to this, it would seem that predictions based on these results should show an even higher degree of variability. This can be overcome by more basic work, standardization and data.

2.10.2 Atkins and Caddell

In papers published in 1974 and 1975 Atkins and Caddell [2.17,2.18] develop a non dimensional scaling parameter for use in ice model tests. This number is related to fracture toughness and velocity of crack propagation for ice at model and full scale. The assumption is that forces required to propagate cracks in an ice sheet are more important than elastic forces in determining icebreaking resistance.

This is reasonable given that ice broken by ships fails through generation and propagation of cracks. It is also obvious that natural ice contains many existing flaws due to brine pockets, air inclusion and pressure cracks. Thus fracture mechanisms and crack propagation should play a role.

Following consideration of similitude for cracking forces a dimensionless "number" is developed. This takes the form:

$$I_n = V^2 \Gamma (L)^{1/2} / K \qquad (2.25)$$

where V is the ship velocity
Γ ice density
L ship length
$K = (EG)^{1/2}$ stress intensity factor
E ice Elastic Modulus
G ice Fracture toughness

This is called the Ice Number by the authors and is shown to be a combination of the Cauchy number and a factor $(EL/G)^{1/2}$. It is explained as the Cauchy number corrected for effects of a cracked material.

Although this is relevant to testing models in ice, it has not attracted much attention. It appears that fracture mechanics deserve more attention as the approach seems more valid than the traditional Elastic Material approach.

2.10.3 Timco

Timco [2.19] presents an overview of issues involved in model testing ships and other structures in ice. For vessels and structures where flexural failure is thought to be the prime mode of icebreaking, Timco derives scaling laws using a rationale identical to that of Vance. He gives a history of model ice development and a list of ice types employed worldwide. This is followed by discussion of the mechanical properties of ice and the degree to which they are properly modelled in Urea (Carbamide) doped model ice. Explanation of the crystal structure of model ice and its effect on mechanical properties is included. It is noted that the commonly used cantilever beam test is not a good indication of the actual flexural strength of the ice but serves as a relative index. The problem of plastic failure in model ice, opposed to brittle failure in un-doped ice, is also mentioned. Elastic modulus problems in model ice are identified along with difficulties in scaling fracture toughness (Figure 2.10). Timco gives the best obtainable E/σ (Elastic modulus/Flexural strength) ratio as 2500 for model ice compared to a mean of about 5000 for full scale ice.

The paper discusses ice-structure interactions briefly, and presents recommendations for future work, followed by a comprehensive list of references.

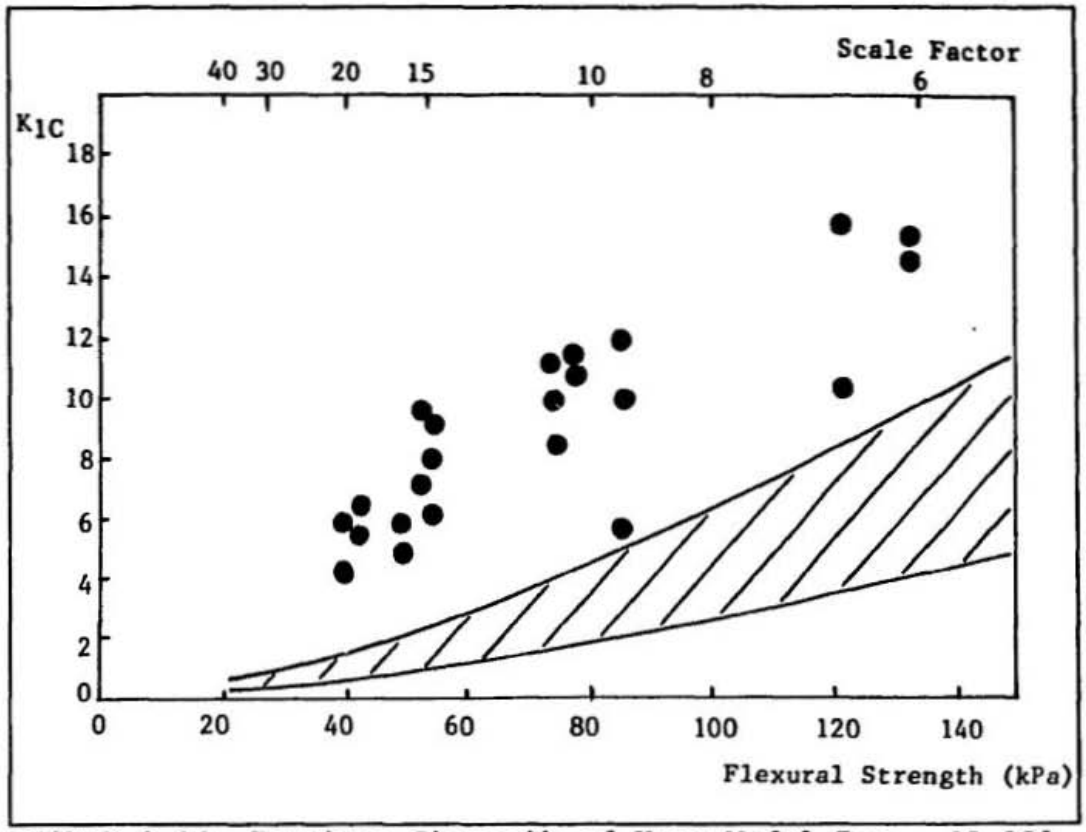

FIGURE 2.10 Fracture Strength of Urea Model Ice [2.19]
Ice thickness = 40 mm
Shaded area = Scaled sea ice
Points = Test results

2.11 Full Scale Trials

There have been a number of full scale ice trials conducted worldwide. A list of vessels and related publications is given in Table 2.1. As a rule, full scale tests are expensive to conduct and present considerable measurement difficulties. The major problem is translating vessel thrust into resistance, compounded by difficulties in measuring true thrust on propulsion shafts. It is shown by Lewis et al [2.20] that the propulsive characteristics of propellers are affected by the presence of ice but it is not clear to what degree. This introduces error in estimating thrust deductions and hull resistance. Where shaft torque is measured, errors are compounded because correlation between torque and thrust is dependent on unknown hydrodynamic conditions.

Further problems arise in measurement of ice properties. It is difficult to measure thickness and flexural strength at a sufficient number of points along the ships track to give an indication of ice properties along the entire route.

Despite these, and other problems such as velocity measurement, full scale trials continue and are improving. In fact they supply the only data which can be used to calibrate model tests or analytic methods. Chapter 9 presents full scale results for three vessels in comparison with resistance predicted on the basis of the present work. However

caution in the use of these data is required in view of experimental scatter and necessarily crude techniques.

Table 2.1 Full Scale Icebreaking Trials

SHIP	YEAR	LOCATION	REF.
USSR Ermak	-	Baltic	2.1
M.V. Finncarrier	1970	Baltic	2.8
M.V. Jelppari	1971	Baltic	2.8
USCGC Staten Island			2.5
USCGC Mackinaw	1970	Great Lakes	2.5
USCGC Katmai Bay	1979	Great Lakes	2.21
M.V. Manhattan		Arctic	
M.V. Arctic	1979-81	Arctic/ Lake Melville	2.22
USSR Moskva	1969	Baltic	2.8
CCGS Louis St. Laurent	1970	Arctic	2.23
CCGS Pierre Radisson	1978-79	Arctic/ St. Lawrence	2.24
CCGS Franklin	1980	Lake Melville	2.25

3. REVIEW OF ICE PROPERTIES

To date, ice has been a difficult material to quantify. Within broad limits, the strength of ice in any mode of failure is dependent on many factors including loading rate, geometry and temperature. Temperature is particularly important because natural ice is usually close to the melting point. At high homologous temperatures, most materials exhibit unsteady material properties and ice is no exception. This has led to conservative design practice for structures and vessels in ice encountering applications and has fostered a great deal of effort towards better defining the material properties of ice.

This chapter presents the state of ice mechanics applied to offshore structures and ice transiting vessels. Interest is generally in vessels which penetrate ice in one way or another and consequently in ice failure. At present, work in this area is advancing rapidly, particularly in the study of fracture mechanics and ice friction. The relevance of some new theories to traditional failure modes is also discussed.

3.1 Ice in Nature

The freezing point of fresh water is 0°C. and salt water about -2°C.. Given that large portions of the globe experience temperatures below 0°C. for at least a portion of the year, ice occurs naturally in many areas and covers some ocean areas permanently. On the other hand, temperatures over most of the globe do not drop below -40°C. for extended periods. This limits the temperature of natural ice to a range close to the melting point.

Natural ice is usually not pure because foreign materials are present in the water from which it is formed. The most common impurity is salt from seawater, which has a significant influence on the properties of sea ice.

3.1.1 Material Structure

Pure ice is crystalline with a hexagonal molecular structure at normal temperatures and pressures (Figure 3.1). Oxygen atoms are linked by hydrogen bonds in a lattice of planes of closely grouped oxygen atoms known as Basal Planes [3.1]. The axis normal to these planes is called the C axis. The hexagonal molecular structure often carries over to the shape of individual ice crystals which are known as grains when agglomerated in a solid. Crystal growth is more pronounced in the basal plane directions and shear strength

is least between basal planes.

Ice has little ability to absorb interstitial or substitutional impurities so foreign elements in water are rejected during crystal formation. These impurities are rejected along the growth interface and often trapped between grains.

The crystal lattice of ice does contain dislocations in the structure. These are areas where gaps or overlaps occur in the lattice. Under load, dislocations are able to move within the crystal leading to permanent deformation in the material. As discontinuities move within a grain they tend to pile up at grain boundaries creating areas of high stress.

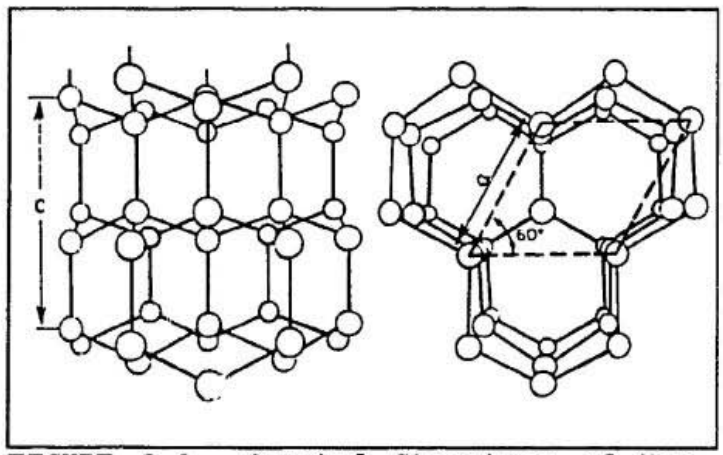

FIGURE 3.1 Crystal Structure of Ice [3.1]

3.1.2 Freshwater Ice

The structure of ice and consequently its material properties are dependent on the way in which the ice formed. Ice on lakes and rivers represent two different formation and growth conditions.

Lake ice will form (nucleate) naturally provided the water temperature is slightly below zero. Grain size depends on the concentration of nucleating agents at the surface and the rate of cooling. Finer grained ice will result from high concentrations and high cooling rates. A common nucleating agent is snow or falling ice crystals but in many cases ice will nucleate on small impurities in the water. Nuclei grow preferentially in basal plane directions until lateral growth is restricted by other crystals. If the water surface is calm and the growth rate not great, a surface skim of crystals with C axes oriented vertically will be formed. If the water surface is turbulent or the cooling rate high, orientation of crystals will be more random. Subsequent growth is vertically downward with crystal structure dependent on orientation of grains in the initially formed ice. For initial cover with vertically oriented C axes growth will be along the C axis and the ice will maintain this structure across its depth. For randomly oriented grains, those with horizontal C axes will dominate because of higher growth rates in the basal plane directions. Thus the primary crystal orientation will become

C axis horizontal with random orientation in the horizontal plane. A layer of completely randomly oriented grains up to a few cm. thick will exist at the top surface of the sheet.

River ice in a rapid flow situation is initiated by frazil nucleation. This is a process whereby river water is slightly supercooled and well mixed to the point where ice crystals start to form across the depth of the water. While these crystals are small they remain entrained in the water flow where they tend to agglomerate and form slush. As the size of individual ice pieces grows, they float to the top where further consolidation occurs leading to an ice cover or ice floes. In slow moving rivers the formation of ice is similar to that for lakes.

3.1.3 Sea Ice

Initial ice cover formation on salt water is similar to that for fresh water. However the sea surface is rarely calm so the surface layer contains randomly oriented grains leading to subsequent domination of crystals with horizontal C axes. The presence of salts leads to the formation of pockets of brine within the ice structure (Figure 3.2).

As sea ice grows, salts are rejected from the crystal structure resulting in a layer of highly saline water along the growth interface. This causes nonuniform growth at the

boundary with thin platelets of ice growing at higher rates than the bulk of the ice sheet. The platelets penetrate though the brine layer and grow laterally, trapping brine in spaces between platelets [3.1]. This forms elongated brine pockets in the ice which do not freeze because of high salinity (Figure 3.3).

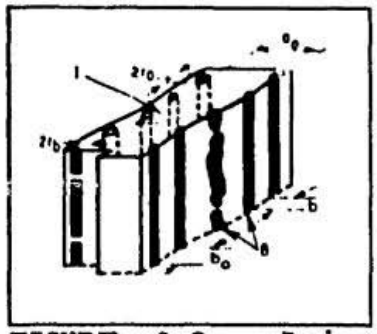

FIGURE 3.2 Brine Pockets [3.1]

As sea ice ages, brine travels downward in the ice sheet forming brine drainage channels and causing a reduction in salinity of the ice. First year ice, which is quite saline and contains a high fraction of drainage channels is weaker than freshwater ice. As the ice ages, salinity is reduced by drainage and seawater flushing, leading to reduction in the volume of drainage channels and an increase in strength. Ice that survives one or more years becomes stronger and is known as second or multi-year ice depending on age.

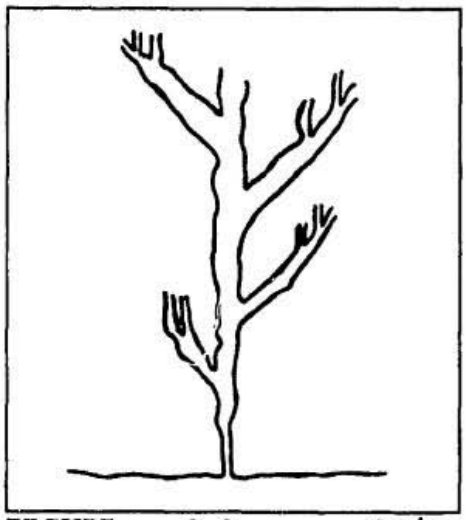

FIGURE 3.3 Brine Drainage Channels

3.2 Material Properties

In dealing with ice it is useful to discuss material properties and note where common concepts present difficulties in application. In cases where ice and man made structures come together, interest is usually in failure of the ice. Thus it must fracture or deform. This is an area of material science that is not well understood, even for extensively studied materials.

3.2.1 Deformation Properties

Deformation can be broken down into three categories: elastic, plastic and creep deformation [3.2].

Elastic deformation is defined as reversible deformation where strain is linearly proportional to applied stress. For isotropic polycrystalline materials this is true of the three modes of deformation; tension, compression and shear. A frequently used test for elastic properties is the uniaxial tensile test. However for brittle materials the compressive test is more commonly used because of higher strength in the compressive direction and the unpredictable nature of brittle failure in tension.

On the molecular level, elastic behaviour manifests itself as stretching or compression in inter-molecular bonds without permanent deformation in either the crystal lattice

or the boundaries between adjacent crystals. Elastic properties are highly dependent on the strength of molecular bonds in the crystal lattice.

Plastic deformation is permanent, non-recoverable strain in a material which occurs at some stress level higher than a threshold level defined as the elastic limit or yield stress. It is the stage following elastic deformation for a ductile material. (Distinction between brittle and ductile is discussed in the next section)

At the molecular level, plastic deformation is associated with sliding between crystal lattice planes. Slip between these planes is made easier by movement of dislocations in the crystal lattice. In polycrystalline solids, plastic deformation can also result from sliding between crystal (grain) boundaries and rearrangement of the grain structure.

Creep deformation is time delayed strain which may be recoverable or non-recoverable. Unlike elastic or plastic strains which occur simultaneously with the applied stress, creep strains are time dependent and may continue indefinitely if stress levels are maintained. Creep deformation is temperature dependent and at low homologous temperatures for most materials creep rates are almost zero.

Non-recoverable creep is plastic strain which is delayed because of finite dislocation velocity. Recoverable creep is associated with grain boundary sliding and is sometimes referred to as delayed elastic strain.

3.2.2 Failure Mechanisms

Essentially, failure and fracture are the same. However in some circumstances, particularly compressive failure, a material may be severely fractured but still able to support load and thus not failed. It is traditional to divide fracture or failure into two classes, brittle failure and ductile failure. The basic difference between these is the presence or absence of plastic deformation prior to generation and propagation of cracks of sufficient magnitude to cause failure.

With brittle failure there is little or no plastic deformation prior to fracture. Failure starts at a pre-existing crack in the material when the applied load induces a sufficiently high stress concentration around the crack tip giving rise to unstable propagation of the crack.

Ductile failure is more complicated because there is considerable plastic deformation leading to formation of small cavities in the material. This process is not dependent on pre-existing flaws because these are blunted by prior plastic deformation. When sufficient cavities in the material have come together to form a crack, it propagates outward to the surface causing failure in the material.

3.2.3 Applications to Ice

Ice is unlike most materials in ways which confound application of conventional materials terminology and test methods. The primary reason for this is it's high homologous temperature [3.3]. Ice is also a very brittle material. Thus it exhibits recoverable and non-recoverable creep deformation but not true plastic deformation. Creep in ice occurs so quickly that it appears to be plastic deformation. This leads to confusion in identifying the deformation mechanism. Although ice exhibits linear elastic deformation behaviour, it is often difficult to measure because of creep.

Natural ice is not isotropic and consequently material properties are not the same in all directions. Like other brittle materials, ice is not strong in tension and does not lend itself to tensile testing.

Classical fracture theory is thought to apply to ice with slight modification for plastic deformation at the crack tip. This modification is commonly applied to polycrystalline materials but the mechanism for ice is likely to be creep rather than true plastic deformation. In this case, crack velocity and creep mechanisms compete in time, complicating the required theory. Unpredictable material properties result from a combination of active creep mechanisms and brittle material properties. This has made it difficult to define or determine commonly used measures of strength.

3.3 Ice Forces

There are many ways ice can exert forces on a structure, or a vessel can exert forces on ice. In either event, it is desirable to quantify the force between the ice and the object of interest. Usually the problem is divided into local pressures and global forces. Local pressures are of interest for structural design because the structure must be able to withstand ice pressure without rupture or permanent deformation. Global forces are of interest in design of large elements and foundations. In the case of vessels, global force dictates the size of propulsion package to drive a ship through ice of given characteristics, whereas local pressures dictate the thickness of hull plating and size and spacing of stiffeners.

3.3.1 Causes of Ice Forces

Ice forces on fixed structures are caused by natural movements in surrounding ice. These movements are induced by winds, currents or changes in temperature. Winds and currents have similar effects in that the stress is due to fluid drag across the ice surface.

These may be described in terms of a semi-empirical law of fluid drag for example,

$$F = C_d \Gamma A V^2 \qquad (3.1)$$

where
- F drag force
- C_d drag coefficient
- Γ fluid density
- A ice surface area
- V fluid velocity

Drag coefficients for air or water over ice depend on the roughness of the ice surface exposed to the fluid. Ranges of coefficients are published and available to calculate wind and current forces on ice sheets.

Movements due to thermal expansion and contraction can also be calculated but high thermal inertia in ice coupled with temperature moderating effects of water result in slow application of thermal forces. Creep deformation under slow loadings usually relieves stress due to thermal effects. Thus extreme ice loads due to temperature variations only occur under relatively unusual conditions.

Ice forces on vessels are induced by attempts to progress through the ice. There is some control of the ice forces in this case because power output of the vessel can be regulated up to the maximum available. Nevertheless, maximum ice forces govern the rate of progress for a given hull form and propulsion package.

3.3.2 Limiting Values

Ice forces are limited by one of two factors [3.4]. Either the driving force reaches an upper limit or the ice fails in some manner against the structure (Figure 3.4). In cases where the driving force reaches a limit, there may be small scale local failure in the ice. An example of this would be a floe pushed against a structure with insufficient energy

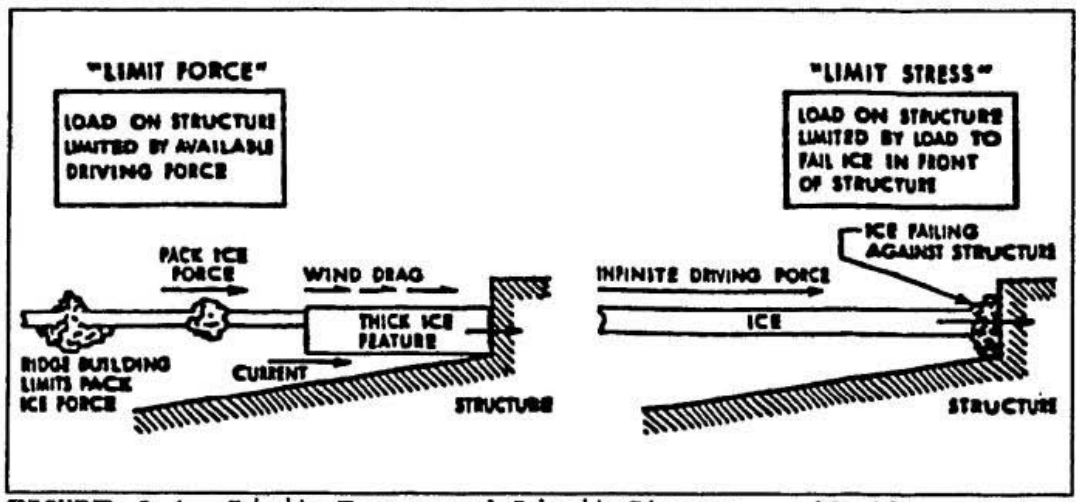

FIGURE 3.4 Limit Force and Limit Stress [3.4]

to cause widespread failure in the ice or the structure. Thus, the global force on the structure would be limited by forces driving the floe but local pressures sufficient to cause small scale ice crushing or structural denting would be evident.

Where the driving force can be arbitrarily large, ice failure at the interface dictates the maximum load. In this case force is dependent on a number of factors including mode of failure and rate of strain (Figure 3.5).

3.4 Failure Modes

Failure modes for ice are primarily dependent on geometry at the interface. Ice has little ability to withstand tensile loads and it is common practice to take advantage of this by

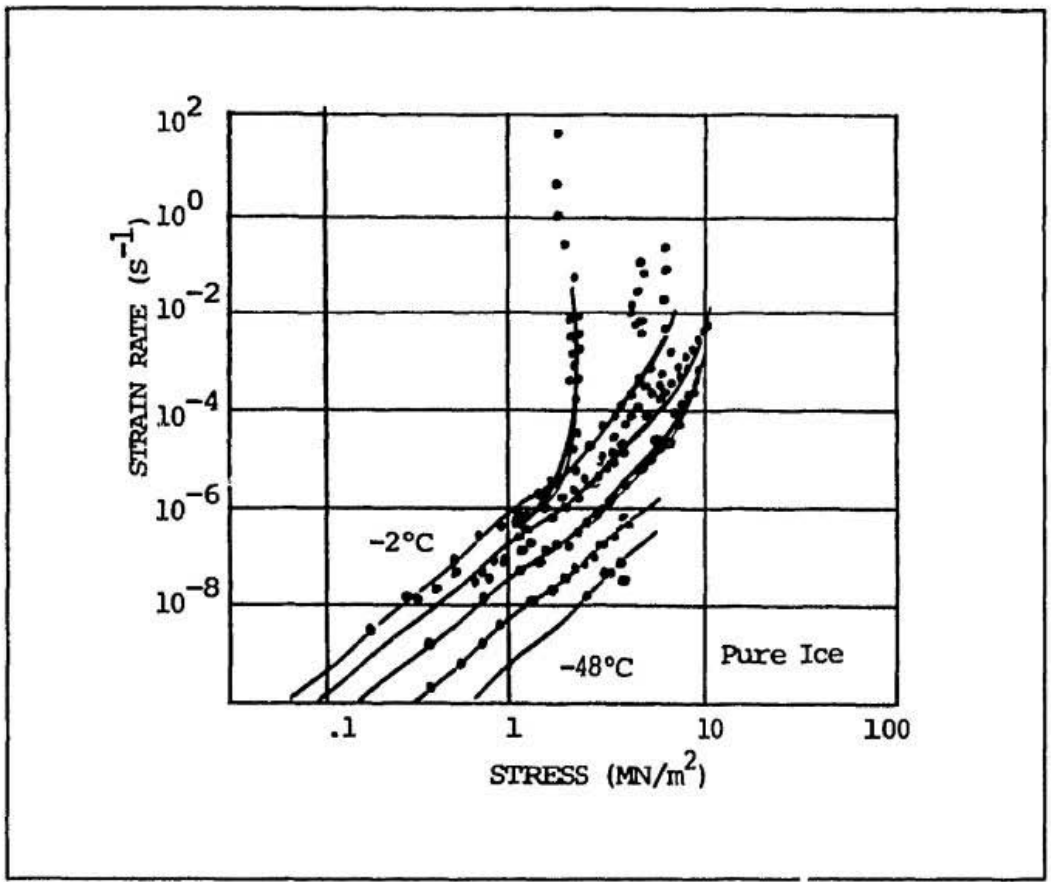

FIGURE 3.5 Load vs. Strain Rate [3.5]

designing the structure or vessel to induce failure in bending. Other modes which are commonly encountered are compression, shear and buckling. Pure tensile loads are rarely encountered in a natural situation.

3.4.1 Compression

Compressive strength of ice has been studied by a number of authors with a great deal of emphasis on time dependent deformation [3.6]. There is a wide range of reported values even at similar strain rates. The compressive strength of ice shows apparent scale effects in that increasing sample sizes exhibit lower strength. There have been a number of theories presented to explain the reduction in strength with increasing size.

One explanation is a theory that as sample size increases the size of existing flaws in the ice increases and thus by fracture mechanics a larger ice piece will fail at a lower load. However evidence to date suggests that this is not so because significant populations of larger flaws have not been observed in larger samples.

Another approach has been to consider non-simultaneous failure over the area of a large sample. Ice is assumed to fail randomly in smaller areas leading to high local stresses but lower average stress. There are difficulties with this concept as well, but it appears the more promising theory.

Despite the fact that reasons for scale effects are not clear, a number of publications have given pressure-area curves for ice. An example is shown in Figure 3.6.

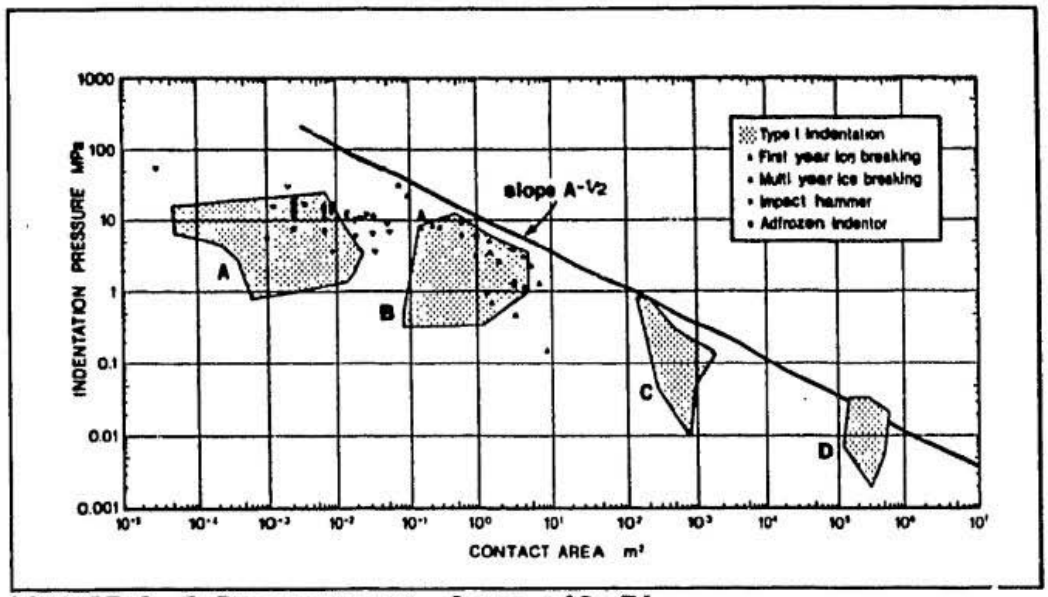

FIGURE 3.6 Pressure vs. Area [3.7]
A. Laboratory Tests
B. Mid Scale In Situ Tests
C. Full Scale Structures
D. Meso-scale Models

3.4.2 Tension / Flexure

Tensile strength tests of ice and other brittle materials are difficult due to the nature of brittle failure. At all strain rates, tensile failure is dominated by formation of cracks [3.5]. Critical crack size for tensile loading is small and as soon as a crack is formed it propagates. Tensile tests are also complicated by difficulties in attaching apparatus for load application to the ice sample. Attachment points often create stress concentrations leading to premature crack formation and failure in the wrong part of the sample. For these reasons the tensile test is not often employed and

reports of uniaxial tensile strengths for ice are rare.

A common means of measuring tensile strength of ice has been to test for flexural strength by beam bending tests. This can be done with cantilever beams or simply supported beams. A drawback is that assumptions have to be made about stress distributions in the beam sample, and thus flexural strength is not a material property but an indirect measure of one. However, the test is easy to perform and of particular relevance to icebreakers because the usual mode of ice failure is in flexure.

Cantilever beam tests are employed both in full scale trials and model basins as a measure of ice strength. A test involves sawing a beam out in the ice leaving one end attached to the sheet as a cantilever (Figure 3.7). The free end is loaded until failure occurs and the load to cause failure recorded. Flexural strength is calculated based on the geometry of the beam and a correction for buoyancy.

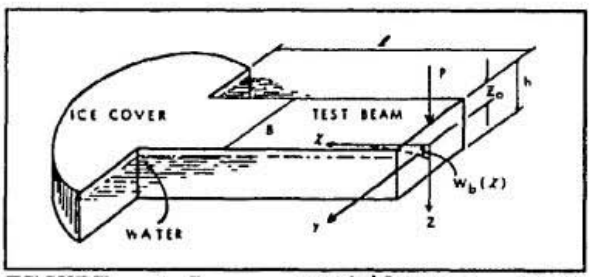

FIGURE 3.7 Cantilever Beam [3.8]

Frederking and Hausler [3.8] deal with the assumptions implicit in the test, including effects of buoyancy and non-homogeneity in the beam. They develop an equivalent stiffness for an ice beam with varying brine volume in the vertical direction. They state that a beam length to thickness

ratio of 10 or less results in a negligible buoyancy effect on the bending moment distribution. Results from experiments are plotted in Figure 3.8. The authors indicate that the theory worked well but that some plastic deformation was

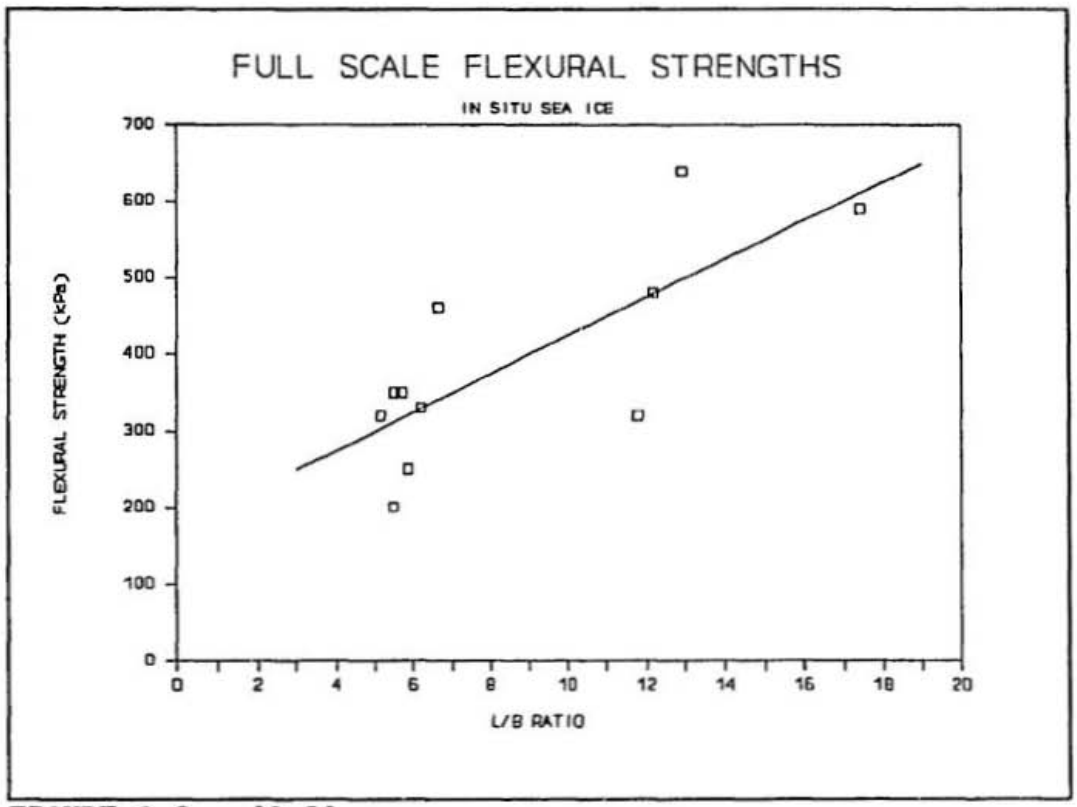

FIGURE 3.8 [3.8]

evident at the root of the beams. This was probably creep deformation but in either event would be a violation of the initial assumption of linear elastic behaviour.

3.4.3 Buckling

Ice does not often fail in buckling. This mode results from in-plane forces which cause the ice sheet to lose stability prior to failure in bending. However, there are cases where buckling is the lowest energy mode of failure. Buckling strength is calculated by the theory of a thin plate on an elastic foundation. A number of experimental studies have been carried out at small scales [3.9]. These studies have shown that buckling loads increase with relative velocity and that buckling is more likely to occur as the ratio of structure width to ice thickness (B/h) increases.

Most experimental results match theoretical calculations, falling between two extremes of boundary conditions. Assumption of a frictionless interface predicts lower loads than calculations for a hinge type boundary condition. Experimental results usually lie between the two. Use of a theoretical solution based on the hinged boundary condition results in a conservative estimation of buckling loads.

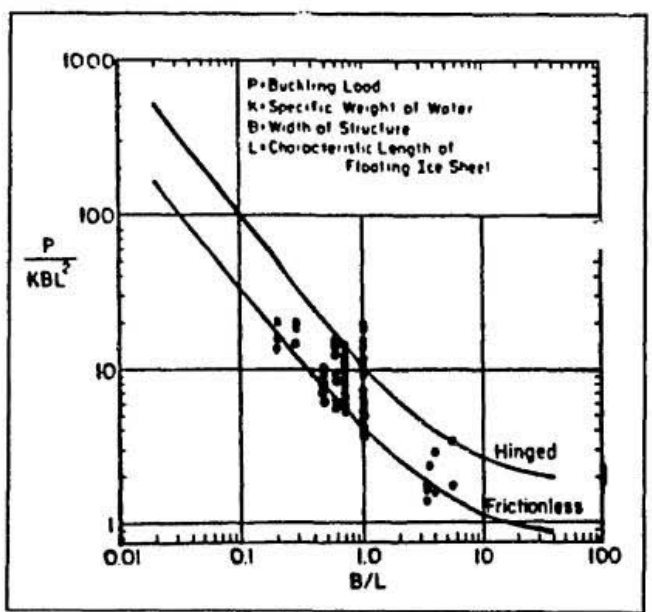

FIGURE 3.9 Buckling Loads [3.9]

At low strain rates, an ice sheet may undergo creep-buckling which has not been extensively studied [3.10]. Under this condition the ice sheet deforms into the buckled shape and may achieve a wave-like pattern of considerable amplitude without breaking. It has been proposed that creep-buckling loads would be lower than those resulting from elastic buckling.

3.4.4 Shear

Until recently there was little interest in shear strength from the ship/structure point of view because it was uncommon for ice failure to occur in shear when impinging on

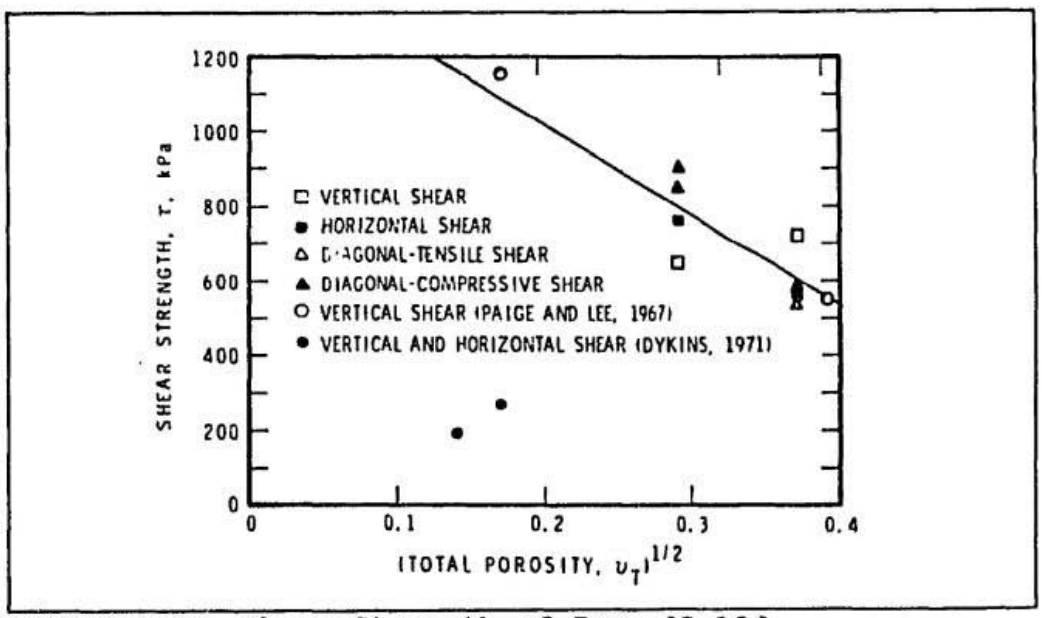

FIGURE 3.10 Shear Strength of Ice [3.11]

a structure. Recently however, ship designs have been developed to take advantage of low shear strength in ice (Figure 3.10) and thus more interest in the property has developed [3.11].

3.5. Friction

Material properties of natural ice make it difficult to determine friction coefficients in the normal sense. Ice is a relatively low friction material, but for icebreaking ships or structures in moving ice fields, friction generates substantial forces.

There have been a number of theories generated to explain the frictional properties of ice. Two have emerged as most likely, and it appears that both mechanisms act to a greater or lesser degree depending on the situation. It is generally agreed that the low friction is due to the presence of a thin water layer between the ice and the slider. It is the mechanism generating this layer which is the subject of study.

The most promising theory appears to be that of a liquid-like layer at the surface of the ice. This layer is thought to arise because natural ice at high homologous temperatures has a surface molecular structure which is disordered and amorphous compared to the regular crystal structure of the solid material [3.12]. This layer exhibits properties similar to a liquid layer and reduces the friction between ice and other materials.

The second idea explaining the presence of liquid at the surface is frictional heating between ice and the slider leading to melting at the interface. Although evidence has been generated to support this hypothesis [3.13] there has

also been some to disprove it [3.14]. It appears that in some cases the liquid-like layer is the major source of lubrication while in other cases frictional heating is the dominant mechanism of lubrication. An example of a case where frictional heating would be dominant is a high slider velocity on ice at a low ambient temperature. On the other hand the disordered surface layer would dominate at temperatures close to melting and low slider velocities. In intermediate cases the mechanisms would interact.

There have been a number of experimental studies of ice friction coefficient and results of these are summarized in the following table.

TABLE 3.1 ICE FRICTIONAL COEFFICIENTS

MATERIAL	STATIC		DYNAMIC				
Steel	.26		.04		.05	.045	.098
Aluminum	.30			.035		.033	.094
Brass	.25		.13				.079
Glass			.13				.009
Granite			.75				
Teflon	.04						
Inerta 160				.025			.066
Stainless Steel				.040		.025	.064
REFERENCE	3.16	3.12	3.12	3.15	3.14	2.8	3.16

Although these are presented as frictional coefficients implying that the classical frictional law:

$$F = \mu N \qquad (3.2)$$

holds, most investigators have observed that frictional coefficients change with slider velocity and normal pressure (Figures 3.11 and 3.12). Both aspects are consistent with the presence of a water lubricating layer. Variation in frictional coefficient with pressure and velocity has implications for testing ship and structure models in ice. In these cases, pressures are reduced by the linear scale factor so, if a frictional coefficient based on similar measurements is maintained, the tangential frictional force will not scale by the cube of the linear scale factor even if the normal force does. Similar arguments apply to full scale and model scale velocities.

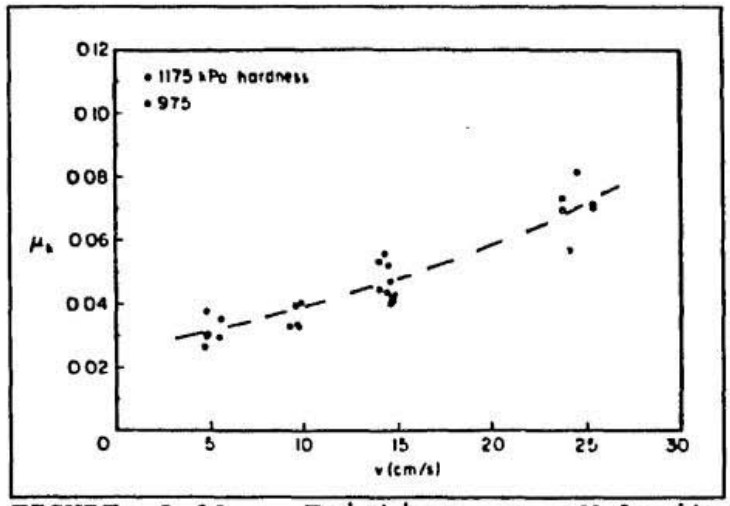

FIGURE 3.11 Friction vs. Velocity [3.15]

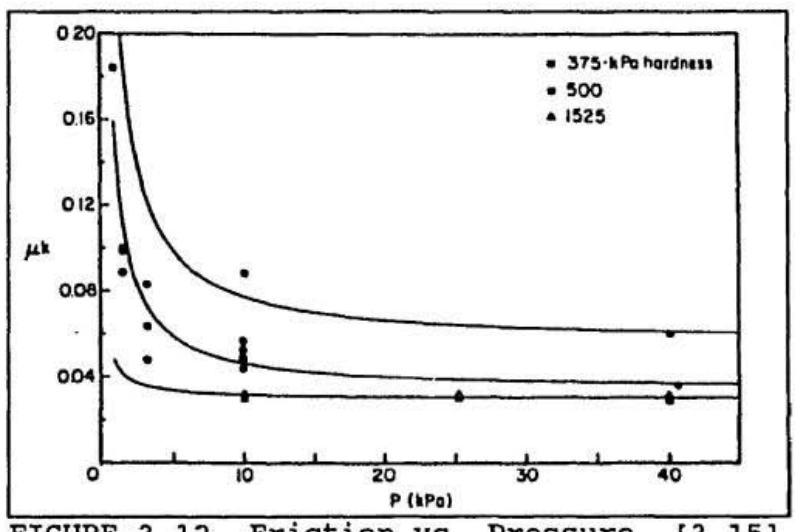

FIGURE 3.12 Friction vs. Pressure [3.15]

3.6 Fracture

Fracture mechanics applied to ice has gained increasing prominence in recent years. It is now believed that the generation and propagation of cracks in ice are relevant to most modes of failure at all but very low strain rates.

Miller [3.17] reviews application of fracture mechanics to ice. This paper considers plastic deformation mechanisms at the crack tip and required modifications to the classical theory of elastic fracture mechanics. The Griffith Equation:

$$\sigma_c = (2Ee/\pi a)^{1/2} \qquad (3.3)$$

where E is the Elastic Modulus
a is the crack length
σ_c is the critical stress
e is the surface energy

identifies creation of surface in the material as the consumer of elastic strain energy in crack propagation. This equation leads to a failure criterion of the form:

$$K = Y\sigma(\pi a)^{1/2} \qquad (3.4)$$

K is the critical stress intensity factor (a measure of stress at the crack tip)
Y is a calibration factor dependent on geometry

and

$$K^2 = GE \qquad (3.5)$$

G is the fracture toughness

The paper outlines criteria under which linear elastic fracture mechanics is valid for ice. The primary criterion is that the radius of the area of plastic deformation is small in comparison to crack length.

Goodman and Tabor [3.18] propose fracture toughness as the best measure of ice strength. It is indicated that the Griffith theory remains valid if the plastic zone at the crack tip is significantly smaller than the crack length, although it is observed that considerable energy is absorbed in plastic deformation in this area. The radius of the plastic zone is given as:

$$r_p = 1/6 \ (K^2/\sigma_y) \qquad (3.6)$$

where r_p is the plastic zone radius
K is the critical stress intensity
σ_y is the ideal plastic yield stress

Both papers identify the stress relieving mechanism at the crack tip as plastic deformation although it is more likely to be creep. Even though the effect would appear similar, the time element in creep deformation would make a difference in some crack growth scenarios. Creep mechanisms would also serve to blunt existing cracks, reducing their effectiveness in initiating failure.

Goodman [3.19] gives results from four point bending tests on pure polycrystalline ice samples. The four point test is used so that the test section of the sample is subjected to a constant bending moment and thus the initial crack is

under pure tensile loading. These tests were performed at three temperatures (-4C, -11C, -24C) and at a loading rate of 500 N/sec. Results show little or no temperature dependence.

Urabe et al. [3.20] performed in situ fracture toughness measurements on sea ice. These tests were three point bending tests with a notch located in one of three positions (top, bottom or side) on the beam sample. The results (Figure 3.13) show that the K_{IC} value is roughly constant up to a strain rate of about 10^{-3} sec^{-1}. Above this rate, Urabe gives the expression;

$$K_{IC} = -1.56 \ln(\delta) - 2.36 \qquad (3.7)$$

where δ is the strain rate

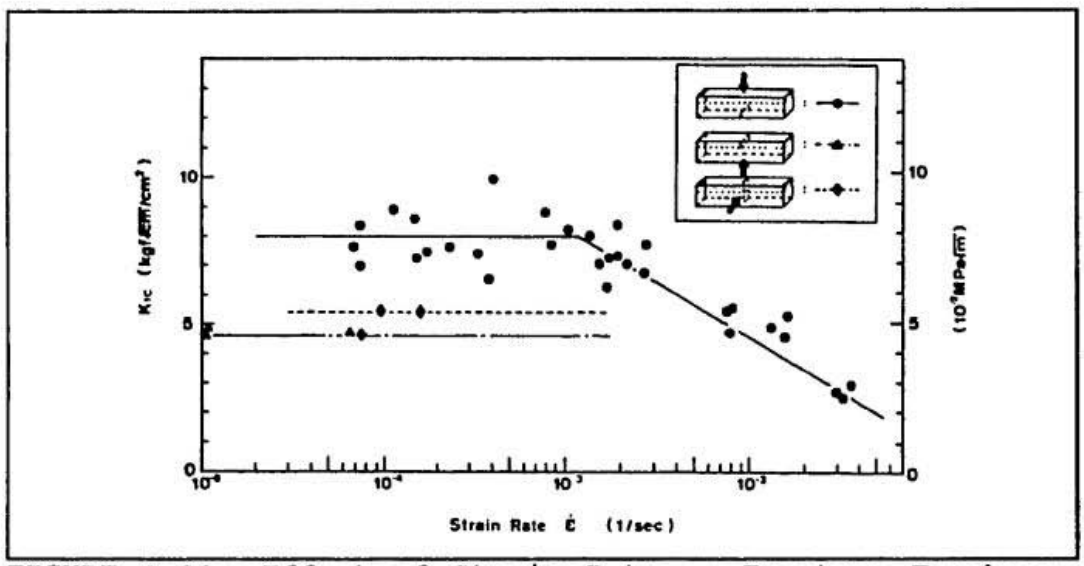

FIGURE 3.13 Effect of Strain Rate on Fracture Toughness [3.22]

The K_{IC} values for sea ice are lower than those recorded for pure ice. The explanation for this difference is the presence of brine pockets. In another paper, Urabe and Yoshitake [3.21] present an expression relating the change in fracture toughness to the ice brine volume or size of brine pockets.

In the same paper and a later publication [3.22] Urabe relates the difference in K_{IC} to grain size (Figure 3.14). This indicates that effective notch length is influenced by grain size. Areas where grains are large are not as significantly weakened by a notch as those areas where grain size is smaller.

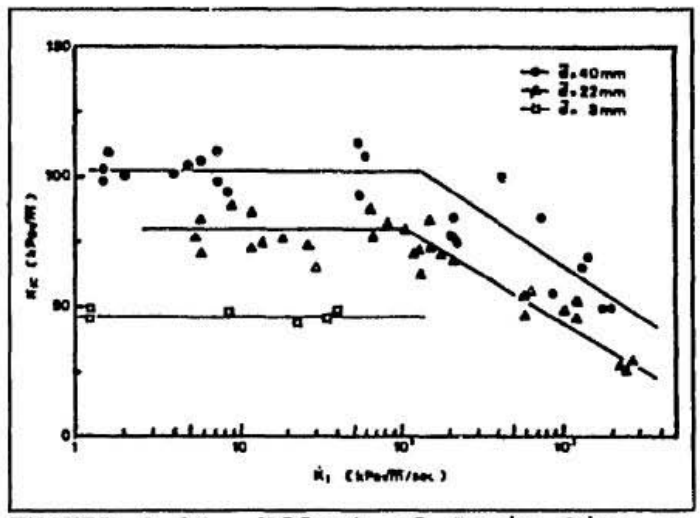

FIGURE 3.14 Effect of Grain Size on Fracture Toughness [3.22]

3.6.1 Flaw Populations in Ice

Although there are methods for measuring fracture toughness, failure load is dependent on another parameter, that being the flaw population. Fracture strength alone is not sufficient to predict a load at which failure will occur and it is in fact the load bearing capacity of the ice which is of interest in failure scenarios.

It is thought that the lowest order of crack nucleating locations in polycrystalline ice are grain boundaries. These represent the smallest discontinuities in the ice material structure, although crystal imperfections may represent an even smaller type of flaw. Mean length of grain boundary can be calculated given that grain size can be determined from ice samples.

With sea ice, particularly first year ice, the presence of brine pockets and brine drainage networks constitute another source of pre existing flaws in ice. Measurement of these discontinuities is more difficult than measurement of grain size. However the extent of brine drainage networks can be related to temperature and salinity. These parameters have been correlated with strength over certain ranges [3.23]. In general, the size of brine channels is an order of magnitude larger than grain size [3.1], so in cases where such channels are present and suitably sharp, they would dominate in terms of crack nucleation.

The largest flaws in natural ice are pressure cracks generated by thermal contraction or other movements in the ice. Flaws of this type are large and dominate any failure scenario provided the load is sufficiently large and widespread to take advantage of the crack extent. Effects of large flaws on ice strength has not been demonstrated although it is logical that they would significantly reduce strength in the area around the crack.

Given that fracture toughness of ice has been widely studied in recent years, the utility of the material property for icebreaking applications suffers from the lack of more definite research on flaw populations in natural ice. A further complication is that it is not clear if pre-existing flaws in ice serve as crack initiators or if they are effectively blunted by creep mechanisms. Until more information is generated in these areas, it remains difficult to predict failure loads for ice using fracture mechanics.

3.7 Ice Modelling

A common method of estimating ice forces has been to conduct model tests. However model testing is more complicated than it first appears. It has been standard procedure to try to scale all ice mechanical properties. This is done to satisfy force similitude considerations while maintaining Froude velocity scaling in ship model tests. Timco [2.19] gives a review of ice modelling and its associated problems. Strength reduction in model ice has been achieved by introducing dopants and controlling grain size. Dopants have included salt, carbamide (urea) and most recently combinations of glycol, detergent and sugar [3.24]. All these formulations exhibit controllable flexural strength in the range of 15 kPa to 100 kPa, with the lower strengths achieved by tempering (warming) the ice sheet. However, elastic modulus is in all cases disproportionately low, and for saline and urea formulations, fracture toughness is too high. It is generally believed that these factors lead to relatively high energy consumption in scale model icebreaking tests.

Synthetic model ice formulations based on paraffin or other wax like materials have been developed but have been found to improperly model frictional characteristics. These are not widely used.

To date, a model ice formulation which fully satisfies proper scaling of all mechanical properties of natural ice has

not been developed. Scale effects in crushing strength and frictional coefficient may require that these properties be adjusted by some factor other than the theoretical scale factor to give an adequate testing medium.

4. LITERATURE SUMMARY AND PROBLEM STATEMENT

Although there has been a large amount of work on ice and its effect on ships and structures, the problem of accurately quantifying global forces remains. The major difficulty appears to be the complexity of ice failure and interaction mechanisms.

Estimation of ice forces by calculation or model test is a science from which results are not yet fully reliable. The approach taken toward each individual problem is dependent on the geometry and environment of the situation. The saving grace of existing icebreakers and arctic structures has been conservative design and cautious operation.

In the area of ship resistance in ice, icebreaking has been shown to be a random phenomena involving a number of different processes. The basic deterministic mechanisms are not well understood nor are the statistical distributions of relevant parameters known. It is also not clear if mechanisms are linear such that their effects may be superimposed.

Analytical efforts have not emphasized primary icebreaking mechanisms. Although icebreaking has been conceptually divided into components since Kashteljan's work, it is only recently that experiments have been conducted to identify individual components.

Regression analysis, applied to expressions for overall resistance, presents a number of dangers. Most data sets from

model or full scale tests do not show sufficient variation in key parameters to allow confident application of regression. The only parameters which have consistently shown good variation are ice thickness, ship speed and depth of snow cover. Ship length, beam and ice strength are constant or nearly so for most exercises. Ice strength measurement is particularly suspect for full scale trials.

Friction is also an issue in ice resistance analysis. In many analytical expressions, the friction coefficient is used as an adjustment factor to bring end results in line with experimental data. This serves to confuse the issue and probably hides flaws in the developed expressions. Better understanding of frictional processes and consistent measuring methods are required at both model and full scale.

Scaling laws for model tests are well developed on the assumption that flexural failure is the dominant icebreaking mechanism. It appears, however, that fracture mechanics and crack propagation play a greater role. The fact that ship model tests are conducted under Froude scaling, resulting in errors in viscous forces, does not appear to be a significant problem.

Considerable emphasis has been placed on development of ice formulations to satisfy simultaneously all scaling requirements. Although steady progress has been made in improving properties of model ice, this is similar to attempting to formulate a test fluid to satisfy both Reynolds

and Froude scaling at the same time. An equally valid and potentially more fruitful approach would be to divide the problem into separate mechanisms which can then be scaled separately.

Full scale data, presented to date, must be treated with some scepticism. Measurement difficulties result in significant scatter in most full scale data. Nevertheless full scale data remains the primary standard against which model and analytical predictions are judged.

In summary, it appears that, through model testing and experience with existing vessels, reasonable predictions can be made for icebreaking vessels that do not stray from the size and shape limits of conventional vessels. However the icebreaking process is not yet well enough understood to allow confident prediction for unusual forms or optimization of existing forms.

New research could address the problem of icebreaking resistance in many ways, including tackling issues in basic ice mechanics and material properties. Nevertheless, a fundamental question is whether or not the total resistance can legitimately be divided into components for purposes of analysis. This encompasses a number of issues including what components exist, the relative magnitude of each, and whether the components can be isolated experimentally.

Icebreaking resistance components have been widely postulated in the literature and relative magnitudes addressed

by a few authors. Proof of existence, and questions of independence, separability and linearity in components have not been covered. Clearly the first step in verifying these components is to develop and validate a consistent experimental method of separating the primary mechanisms.

There is little point in dividing the problem into components analytically if they cannot be experimentally isolated. Once isolated, information on individual components may be used to better understand the total process. In addition, each model scale component may be separately scaled according to the appropriate requirements and the results summed at full scale to yield a total resistance.

The main objective of the present work was to develop a set of experiments to reveal the existence of primary components of icebreaking resistance. Some exploration of effects of certain parameter changes on these components was also undertaken.

Experiments were conducted at model scale, to permit better control over most parameters and in recognition of the impracticality of performing a large study at full scale. In principle, however, the methods developed are applicable at full scale.

Although other important aspects of icebreaking resistance were not extensively investigated (for example the influence of friction) it is felt that the issues addressed in this study offer considerable insight into the basic

icebreaking mechanisms and provide an improved method of conducting icebreaking model tests and scaling the results of such tests. Some limitations in the concept of independent components were identified during the work, but these appear to be second order in nature.

PART TWO RESEARCH AND RESULTS

5. DIMENSIONAL ANALYSIS

The major problem with modelling ships in ice is that many different mechanisms resist the vessel motion at the same time. These include hydrodynamic effects, friction, ice failure, buoyancy and inertia. It would be difficult to model and scale correctly all these phenomena at the same time. The issue is complicated by the fact that no agreement has emerged as to which mechanisms are dominant.

Previous analytical expressions and model scaling laws have been based on a single functional expression for the entire "ship in ice" resistance. This has not given credit to the idea of independent components, although many researchers have based their developments on the existence of such components. In contrast, vessel open water resistance has, since Froude's time, been divided into viscous and wavemaking components, each of which is scaled separately. As a first step to achieve this situation for icebreaking resistance, a dimensional analysis of the problem is performed based on separate components.

5.2 Analysis

The approach taken here is to treat the total ship-ice resistance as the sum of the following independent terms;

1. Open Water Resistance = R_O (5.1a)
2. Ice Breaking Resistance = R_B (5.1b)
3. Submergence Resistance = R_S (5.1c)
4. Inertial Resistance = R_I (5.1d)
5. Frictional Resistance = R_F (5.1e)
6. Snow Resistance = R_C (5.1f)

A method of modelling snow cover does not presently exist but is included for the sake of completeness and because full scale data usually reports some resistance due to snow on the ice.

Those variables associated with the identified components are taken as;

Open Water: $R_O = f_1(\mu, L, B, T, V, g, \Gamma_w, S)$ (5.2a)

Fracturing: $R_B = f_2(B, h, \sigma_F, \sigma_C, \sigma_S, G, a, E, S, V, \Gamma_i)$ (5.2b)

Submergence: $R_S = f_3(\Gamma_d, T, B, S, h, g)$ (5.2c)

Inertial: $R_I = f_4(V, \Gamma_i, h, B, S, g, \Gamma_w)$ (5.2d)

Frictional: $R_F = f_5(L, f_i, P, h)$ (5.2e)

Snow: $R_C = f_6(B, f_s, \sigma_{CS}, h_s)$ (5.2f)

The open water term is treated in the classical sense, covered in many previous works. Strength and elastic effects are included in the fracturing or breaking term. All mass, inertial, and added mass effects are included in the inertial term. Submergence is incorporated largely because it has been identified in previous developments, and is taken as the speed independent buoyancy effect. A frictional component is shown separately in order to explore the parameters relevant to friction independently.

Application of dimensional analysis to the equations 5.2a-5.2f leads to: (see Ref. 5.1 for details of dimensional analysis)

$$\frac{R_o}{\Gamma_w L T V^2} = \Phi_1\left(\frac{VL}{\nu}, \frac{V^2}{gL}, \frac{L}{B}, \frac{B}{T}, S\right) \text{ where } \nu=\mu/\Gamma_w \qquad (5.3a)$$

$$\frac{R_B}{\Gamma_i B h V^2} = \Phi_2\left(\frac{G}{\sigma_f h}, \frac{\sigma_c}{\sigma_f}, \frac{\sigma_c}{\sigma_f}, \frac{E}{\sigma_f}, \frac{B}{h}, \frac{G}{Ea}, \frac{\Gamma_i V^2}{E}, S\right) \qquad (5.3b)$$

$$\frac{R_S}{\Gamma_d g B h T} = \Phi_3\left(\frac{T}{h}, \frac{B}{h}, S\right) \qquad (5.3c)$$

$$\frac{R_I}{\Gamma_i B h V^2} = \Phi_4\left(\frac{V^2}{gh}, \frac{\Gamma_i}{\Gamma_w}, \frac{B}{h}, S\right) \qquad (5.3d)$$

$$\frac{R_f}{PLh} = \Phi_5\left(f_i, \frac{h}{L}\right) \qquad (5.3e)$$

$$\frac{R_C}{\sigma_{cs} B h_s} = \Phi_6\left(\frac{h_s}{B}, f_s\right) \qquad (5.3f)$$

Although many different arrangements of the variables are possible, those chosen here have been selected to follow traditionally developed formulations. Using this system, individual resistances have to be combined dimensionally to give a total resistance because a single group with units of force common to all components is not evident.

5.2 Discussion

Geometric similarity requires that all ship dimensions be scaled by a linear scale factor Ω ($L_p = \Omega L_m$, p = prototype m = model). Correct scaling of open water resistance (item a in eqns. 5.1-5.3) requires that geometric similarity be satisfied, along with Froude and Reynolds scaling of velocity. This is not possible with water, because for Froude scaling, $V_m=V_p/(\Omega)^{1/2}$ and for Reynolds scaling, $V_m=\Omega V_p$. This problem is well known and handled by further dividing into viscous and wavemaking components. Calculated corrections are made for the viscous term. It is interesting to note that at normal full scale icebreaking speeds (2-5 Knots), viscous drag dominates wavemaking resistance. Thus, the Froude similarity condition is not a primary scaling law for the open water component of icebreaking resistance.

It is common practice to subtract open water resistance from total resistance in ice to yield a net ice resistance:

$$R_I = R_T - R_W \qquad (5.4)$$

For this purpose, open water resistance is measured in a towing tank. This may not be a correct approach because of the presence of an ice sheet in both the ice model test and in the full scale. Viscous resistance should be largely unaffected, as there is no significant change in the vessel's boundary

layer flow conditions induced by the sheet. It is also unlikely that these conditions are altered by ice pieces passing over the bottom of the hull. On the other hand, boundary conditions for wavemaking resistance are significantly altered by the presence of the ice sheet. Although waves observed in an ice sheet are smaller in amplitude than those observed in open water, there is much greater capacity to absorb energy in the water-ice combination. The zero pressure boundary condition for a free surface is replaced by a more complicated condition such that the pressure at the ice/water interface is not constant but dependent on local motion of the ice sheet. This introduction of an elastic boundary yields a much more difficult solution to the fluid problem which is beyond the scope of this work. However some experiments were carried out to determine the effects of the floating ice sheet on wavemaking resistance. Results are detailed in later sections.

Considering dimensionless groups associated with the breaking component, (eqn. 5.3b), ice thickness is scaled to the same geometric ratio as the ship (Ω), and ratios of strength and elastic modulus for the model ice must be the same as full scale. If Froude velocity scaling is to be used, then it follows from the Cauchy number ($\Gamma_i V^2/E$) that the Elastic Modulus and all ice strengths must be scaled by the factor Ω (assuming ice density at both scales is the same). Fracture toughness (G not K_{IC}) on the other hand must be scaled

by the factor Ω^2 and the flaw size (a) by the factor Ω.

A dimensionless ratio similar to the Cauchy number can be derived by compounding it with the E/σ ratio to give $\Gamma V^2/\sigma$ or in another form $V/(\sigma/\Gamma)^{1/2}$. This number represents the ratio of ice Inertial forces to ice strength forces and will be referred to as the Strength Number.

Although velocity scaling is traditionally by Froude, if the breaking component can be measured in isolation, this need not be the case, and model velocity could be adjusted to maintain the relevant dimensionless ratio for varying flexural strength or fracture toughness in the model ice. It is, however, important that ratios of strength properties be maintained and this has been a difficulty with model ice formulations to date.

Many publications use water density in place of ice density in their developments on ice resistance. This is based on assumption that ice density and its ratio to water density is constant. This is not the case for model ice and thus ice density is used in this work.

Resistance associated with submerging broken ice (eqn. 5.3c) is a function of the volume of ice broken, the density difference between the ice and water and the depth of submergence. This is not a velocity dependent component but a function of ship shape and relative draft.

Inertial resistance (eqn. 5.3d) shows similar dimensionless ratios to the submergence term with the addition

of velocity effects. It appears reasonable to neglect submergence as a separate component and combine inertial and submergence resistances under a common ice clearing term. The only advantage of separating these two components is that the inertial resistance can be assumed to be zero at very low speeds while the submergence component remains. However as speed increases, the physical distinction between the two components is somewhat arbitrary. It is preferable to consider submergence resistance as the zero speed limiting value of the inertial resistance. Dimensionless ratios associated with inertial resistance dictate maintenance of the ice-water density ratio and geometric scaling of ice thickness. The ice thickness Froude Number in equation 5.3d indicates a requirement for Froude Velocity scaling in modelling this mechanism.

Frictional resistance (eqn. 5.3e) is primarily a function of the coefficient of friction between the ice and the ship. In principle the coefficient should be the same at full and model scale. However, reliable full scale measurements of the friction coefficient are practically nonexistent. Also a parameter which is often excluded from ice resistance formulations is lateral pressure in the ice sheet. It is logical that this would have an effect on frictional resistance, but only if the ship is in contact with the unbroken ice sheet. Usually the ice breaks some distance away from the vessel sides and there is no direct contact, but

force may be transmitted through ice pieces turned and jammed between the hull and the intact sheet. Furthermore there is still some question as to how friction should be treated because of evidence that frictional coefficients for ice are a function of pressure and sliding velocity (Figures 3.11 and 3.12). If this is the case, then the frictional coefficient for model tests will require adjustment due to lower absolute velocity and pressures at model scale. Friction is also intertwined with the other components of ice resistance and is probably not truly independent or separable from these mechanisms. Thus, consideration of a separate frictional component is a limited concept, at best applicable only to forces along the sides of a flat sided vessel. Even then, it may not scale solely according to the friction coefficient.

Resistance due to snow on the ice surface (eqn. 5.3f) is thought to be primarily a frictional problem. However if the snow is thick (i.e. of the order of the ice thickness) the compressive strength of the snow would play a role in resistance. If snow cover is to be modelled, then the frictional coefficient must be maintained and the thickness and compressive strength values scaled by the factor Ω.

Development of the preceding non-dimensional ratios illustrates that icebreaking mechanisms involve different parameters and different scaling laws. The fact that a single non-dimensional ratio, relevant to all resistive components, is not apparent presents a case for isolating components and

scaling them individually. Ideally, ice model tests would be performed to separate each component, with elements combined after scaling to generate a prototype prediction. As previously stated, this is similar to the technique used for open water resistance to deal with viscous and wavemaking resistance components. It is unrealistic to expect the more complicated case of ice resistance to yield to a single simple model test.

The most promising means of separating breaking and clearing resistance components is the pre-sawn ice test introduced by Enkvist [2.9]. This involves reduction of model ice strength to zero by sawing slots in the ice. Resistance due to breaking can be determined by subtracting resistance values recorded during a pre-sawn test from those recorded during a regular ice test. Enkvist, however, assumes that the breaking component is velocity independent and only conducts the pre-sawn test at low speeds. In addition, the effects of friction are not clearly separated by the procedure, but as previously discussed, this may not be practical in any event.

Despite some limitations, the pre-sawing technique was selected as the method of choice for the experimental portion of this research. Uncertainties associated with the technique required that some initial experimentation be carried out to provide verification, but this was deemed worthwhile as it would provide further information on both the technique and the icebreaking components.

5.3 A Simplified System

Having discussed icebreaking to a degree of completeness and developed a set of non-dimensional expressions, the problem arises that many of the variables either cannot be or are not routinely measured. Thus, a considerably reduced number of variables is available for analysis from a tank or full scale situation. In recognition of this, a reduced formulation, based on the previous development is required for practical application.

The open water component remains unchanged, but a number of variables are eliminated from the ice resistance component. The breaking term is essentially unaffected. Terms due to submergence and inertia are combined into a single component hereafter termed Ice Clearing Resistance. In the combination of the two terms, effects due to ice-water density differences (buoyancy) have been neglected because this is thought to be largely a low speed phenomena. As speed increases, buoyancy forces are quickly overwhelmed by inertial and added mass effects. These effects are more dependent on the absolute densities than the buoyant difference.

Frictional resistance is eliminated as a separate component because it is interrelated with each of the other components and thus cannot be treated as independent. Resistance due to snow cover is eliminated for the purposes of tank work because it is generally not modelled. This

reduces the problem to three resistive components.

$$\text{Open Water} \quad R_O = g_1(\mu, L, B, T, V, g, \Gamma_w, S) \tag{5.5a}$$

$$\text{Breaking} \quad R_B = g_2(B, h, \sigma_f, E, V, \Gamma_i, f_i, S) \tag{5.5b}$$

$$\text{Clearing} \quad R_C = g_3(B, h, g, V, T, \Gamma_i, \Gamma_w, f_i, S) \tag{5.5c}$$

Following on with the analysis:

$$\frac{R_O}{\Gamma_w L T V^2} = \Phi_1\left(\frac{VL}{\nu}, \frac{V^2}{gL}, \frac{L}{B}, \frac{B}{T}, S\right) \text{ where } \nu=\mu/\Gamma \tag{5.6a}$$

$$\frac{R_B}{\Gamma_i B h V^2} = \Phi_2\left(\frac{E}{\sigma_f}, \frac{B}{h}, \frac{\Gamma_i V^2}{\sigma_f}, S, f_i\right) \tag{5.6b}$$

$$\frac{R_C}{\Gamma_i B h V^2} = \Phi_3\left(\frac{V^2}{gh}, \frac{B}{h}, \frac{B}{T}, \frac{\Gamma_i}{\Gamma_w}, S, f_i\right) \tag{5.6d}$$

The open water term is treated in the same manner discussed previously. However, the ice related terms are considerably simplified from the previous case. This leads to a workable system of the form:

$$\frac{R_B}{\Gamma_i B h V^2} = f\left(\frac{V^2 \Gamma_i}{\sigma_f}\right) \tag{5.7a}$$

$$\frac{R_C}{\Gamma_i B h V^2} = f\left(\frac{V^2}{gh}\right) \tag{5.7b}$$

if it is assumed that E/σ_f, B/h, the shape factors, density ratio and friction coefficients preserve their full scale values. These two equations (neglecting the open water component briefly) cover the two components that should come out of a pre-sawing test: breaking the ice and clearing the broken pieces.

This same result can be reached by considering force ratios. Assuming four types of forces in the problem as a whole, all of which are influenced by friction in the interaction:

Resistive Forces	$F_R = R_B$ or R_C	(5.8a)
Gravitational Forces	$F_g = \Gamma_i g L^3$	(5.8b)
Strength Forces	$F_S = \sigma L^2$	(5.8c)
Inertial Forces	$F_I = \Gamma_i L^2 V^2$	(5.8d)

where L is a general length dimension.

Considering the breaking resistance:

$$F_R = f(F_S , F_I) = R_B \tag{5.9}$$

and the clearing resistance:

$$F_R = g(F_g , F_I) = R_C \tag{5.10}$$

the inertial force appears with both components and provides a common denominator:

$$\frac{R_B}{F_I} = f(\frac{F_S}{F_I}) \tag{5.11a}$$

$$\frac{R_C}{F_I} = g(\frac{F_g}{F_I}) \tag{5.11b}$$

Expanding these two expressions:

$$\frac{R_B}{\Gamma L^2 V^2} = f\left(\frac{\sigma L^3}{\Gamma L^2 V^2}\right)$$
$$= f\left(\frac{\sigma}{\Gamma V^2}\right) \qquad (5.12a)$$

$$\frac{R}{\Gamma L^2 V^2} = g\left(\frac{\Gamma q L^3}{\Gamma L^2 V^2}\right)$$
$$= g\left(\frac{qL}{V^2}\right) \qquad (5.12b)$$

Ship beam (B) and ice thickness (h) are the relevant linear dimensions and the equations rearranged to the previous form.

$$\frac{R_B}{\Gamma_i B h V^2} = f\left(\frac{V^2 \Gamma_i}{\sigma_f}\right) \qquad (5.7a)$$

$$\frac{R_C}{\Gamma_i B h V^2} = f\left(\frac{V^2}{gh}\right) \qquad (5.7b)$$

The result is the same as that from the dimensional analysis. These two expressions give what is believed to be the dominant relationship between parameters for the ice breaking and ice clearing components of the total resistance. It can be argued that other non-dimensional formulations are equally valid or offer advantages such as a more direct demonstration of the velocity effect. The forms shown in equations 5.7a and 5.7b have been selected for the following reasons.

The development and resulting expressions are similar in form to those used in other branches of fluid mechanics, for example, presentations of Drag Coefficient against Reynolds Number or Ship Resistance Coefficient against Froude Number. In addition, it is normal practice, when dealing with

accelerative fluid systems, to use the inertial term as a common non-dimensionalizing factor as has been done here.

It is also believed that there is a physical significance to the ratio $R/(\Gamma_i BhV^2)$ in that it represents a ratio of the resistive force to the inertial resistance of a block of ice B*h*1m. at the velocity of interest. Finally in Chapter 8 these expressions have been applied to experimental data with good results. When compared with a number of other possible formulations using weight or strength forces as the non-dimensionalizing factor the above forms demonstrated best collapse of the data.

This leads to the development of two ice resistance coefficients; an Ice Breaking Coefficient C_B and an Ice Clearing Coefficient C_C:

$$C_B = \frac{R_B}{\Gamma_i BhV^2} \quad (5.13a) \qquad C_C = \frac{R_C}{\Gamma_i BhV^2} \quad (5.13b)$$

Scaling for the clearing component is Froudian although the Froude number is based on ice thickness rather than ship length. Consequently, there needs to be some distinction between the two. The term $V/(gh)^{1/2}$ will be called the Thickness Froude Number. Scaling for the icebreaking component is dependent on the number $V/(\sigma/\Gamma)^{1/2}$ which has been previously named the Strength Number. Thus, the two fundamental mechanisms in icebreaking are subject to different scaling laws; with icebreaking a function of Strength Number, and ice clearing a function of Thickness Froude Number.

6. REMARKS ON MODEL TESTING IN ICE

Before detailing the experimental portion of this research, it is worthwhile to discuss some issues in model testing which are not generally covered in the literature. There are many ways in which conditions in a model tank differ from the full scale. Indeed, tests carried out in a tank are not so much models of the real situation as reference cases for comparison between forms. An icebreaking vessel rarely finds itself in a uniform sheet of level, continuous, flawless ice. This, however, is a repeatable and definable condition which provides a good baseline for testing. Although it can be criticized as unrealistic in terms of actual full scale conditions, it is preferable at this stage in the development of icebreaking theory to stick with a well defined and controlled condition for research purposes. This simplification is similar to that made by testing for open water resistance in perfectly calm tank conditions.

6.1 Towing System

While propelling a model through ice of limited dimensions, restraint must be placed on some model motions. Common practice is to tow from a point near the centre of gravity. This leads to a model which is not directionally stable and thus requires yaw restraint. Yaw control on a full scale vessel is provided by rudder which is a force exerting device but model yaw restraint is a rigid connection applying a fixed displacement. Under fixed restraint, the model is less able to deflect due to asymmetric loads at the bow. This results in higher forces at the bow, probably leading to increased resistance. Consequently, it is expected that the use of rigid yaw restraint results in higher tow forces than would be experienced with a soft restraint.

Restraint in heave, pitch and roll are not normally provided so these motions do not present problems.

A similar condition to the yaw restraint arises in towing. Usually a model is towed at constant speed through the ice. This is contrary to full scale, where propulsion is supplied by a force generating device. Alternately the model can be propelled with a scaled propulsion system. This is frequently used but suffers from some drawbacks, particularly the difficulty in reaching steady state, given the nature of a propeller drive system and variation in ice failure for even a uniform sheet. The problem is compounded when ice is

ingested by the propeller causing fluctuations in measured torque and thrust. Constant speed towing offers greater economy in use of tank time and ice, and improved control of test conditions. The cost is in the realism of the test.

Towing system dynamics are relevant to the nature of measured loads. With fixed speed towing, the towing post and model form a mass-spring combination which will vibrate when excited. Forces exerted on the model by ice are cyclic and of considerably higher magnitude than those in an open water test. It is desirable to avoid resonance, and thus the natural frequency of the tow post-model combination should be well removed from the range of fundamental frequencies arising from the ship model-ice interaction. The post can be stiff with a high natural frequency or soft with a low natural frequency. However, a soft system may not be able to generate sufficient force for adequate towing without increasing stiffness. It is more common to employ a rigid system but this also has an effect on recorded results. Given the nature of icebreaking, even at model scale, vibrational noise is generated and filtered by the towing system. This filtered noise is recorded as fluctuation in resistance at or near the natural frequency of the towing system. Indeed, most high peaks observed in resistance traces are due to vibration in the towing system and not model-ice interaction events. Account must be made for this in data analysis.

6.2 Ice Properties

In providing a sheet of ice for tank testing, the most desirable feature is consistent mechanical properties. Given the nature of ice and scaling requirements for very low strengths, it is difficult to maintain consistent mechanical properties. There is also spatial variation in sheet thickness and mechanical strength over the area of the ice surface. Both properties continually change in time and cannot be arrested in order to conduct a test. Thus, even in the best of tests there is a variation in results stemming from variation in ice properties. Strength measurement is destructive to the ice and very time consuming. Consequently, it is impractical to measure strength at a large number of locations, although thickness can be determined at any number of locations immediately after a test.

Also related to ice strength for testing and scaling purposes is the degree of variability in cantilever beam tests. Measured strength has been shown to be dependent on sample size, geometry and loading rate [3.8]. Thus the strength measured at model scale may not correspond directly to that measured in the field.

Another potential concern in a towing tank is the effect of in- plane confinement of ice by the tank walls. The effect of confinement on resistance is not yet clear, but it does not appear to have a great effect on measured resistance. Limited

trials with an ice sheet cut away from the tank walls did not record any significant change in resistance. Nevertheless, tests are normally conducted a minimum of 2-3 beam widths from the tank walls to minimize confinement effects.

It is widely reported in the literature on full scale icebreaking that radial cracks in the ice emanate from the bow area during icebreaking. This radial cracking is not observed in model testing, and generally the ice fails along circumferential lines with limited secondary radial cracking. The net result is still a cusped pattern of broken pieces in the channel similar to that reported for full scale icebreaking. It is believed that the absence of primary radial cracks is due to a degree of cohesiveness in the model ice which does not exist at full scale. Whether or not the lack of initial radial cracks in the model case causes an increase in the scaled ice resistance is as yet unproven.

Friction between ice and model surfaces is a problem for which adequate standards have not been established. Frictional coefficients are measured by moving ice samples over a model surface or similarly prepared friction plate. Normal load is varied and tangential force measured. Trends in results have been observed due to sample orientation and this has been attributed to water drainage leading to increased lubrication for some orientations. Trends have also been observed with sliding velocity, normal pressure, and ice temperature. This leaves a great deal of information to reconcile before

frictional coefficients can be established. Although frictional coefficients are routinely measured as part of ice testing procedure, they are of limited value except for comparison between models. At present it is not possible to scale frictional results with any accuracy.

6.3 Statistical Validity

Model testing in ice presents issues of data reliability which do not arise to as great a degree in other branches of testing. In fluid and aerodynamic fields, the small scale behaviour of the test medium is better understood on an empirical if not a purely theoretical basis. This is not the case for icebreaking. There is a degree of large scale randomness in ice failure, coupled with variation in mechanical properties over the duration and area of a test. Thus, the results of ice tests are really random variables.

If distributions of these variables are normal, then a resistance value recorded during a test would not be truly repeatable but given sufficient samples at the same conditions, a distribution would be obtained of which the mean could properly be called the mean resistance for the given conditions. This concept of random errors has not been widely adopted in ice testing, in spite of published results which show wide confidence intervals on recorded data.

A practical problem in gathering sufficient data for statistical validity is the high cost and time associated with ice testing. For a given sheet of ice it is rare to get more than four or five data points in a day. For thicker sheets the yield is lower , sometimes less than six points per week. Thus, it is a luxurious test program where runs are repeated purely to establish an average resistance for a given set of

conditions. In most cases, inherent error in measurement is not recognized and no published work could be found attempting to quantify the deviation. It has been stated that if ice properties could be adequately controlled, then tests would be repeatable with much smaller errors. Undoubtedly better uniformity in material properties would reduce error, but this would not eliminate the randomness in material failure. Although not covered in this research, it would be worthwhile to address distributions of mechanical properties and measured variables in ice testing in general.

7. EXPERIMENTAL METHOD

The objective of the experimental program conducted for this research was to demonstrate that icebreaking resistance can be physically separated into two components, and that these components are better presented and scaled individually.

A number of approaches were taken to the problem in an attempt to provide verification of the concept. Early on, it was recognized that it would be difficult to prove the existence and separability of the components in an absolute sense, based solely on the pre-sawing technique. The obvious first requirement was to prove the legitimacy of the technique. A first approach to this was to vary the basic parameters inherent in the technique to determine the effect on recorded results. The second approach was to develop another experiment which would allow at least one component to be measured by a different method for comparison with that measured by pre-sawing.

The final approach to the wider question of the behaviour of individual components was addressed by performing a range of experiments in which one parameter was varied at a time. Although neither one of these investigations offers a method of absolute proof, when taken together they offer a body of evidence which provides insight into both the concept and the techniques.

Experiments involving variations in pre-sawn pattern were the first approach to validating the technique itself. In this case a number of test parameters were varied to determine the effect on measured resistance. This was to provide data on the robustness of the technique and to give an indication of reliability and repeatability. In addition the relatively wide ranges of parameter variation allowed the limits of the technique to be determined.

Trials conducted with the so called shallow draft wedge formed the second experimental approach to validating both the concept of independent components and the technique of pre-sawing. By towing a partial hull which was really only a bow section without significant below water volume or after body it was intended to provide a test in which only the breaking component was measured. There would be no hull to displace the ice or give hydrodynamic drag. Thus the breaking component measured directly by this method should be comparable to that induced from the pre-sawing technique.

The third phase of the program was to perform a set of more or less standard ice tank tests in which the two components were measured while a number of parameters were varied. These included ice thickness, ice strength, vessel speed and vessel beam. Vessel beam was the only ship related dimensional parameter to be varied because it was judged to be the dominant linear dimension and thus the best used in a non-dimensional formulation. Unfortunately the full range of

all variables could not be cross correlated but sufficient information was gathered to identify relationships.

Testing was carried out in the ice tank of the Institute for Marine Dynamics, a large government/commercial research facility. As part of the experimental program, it was intended that testing procedures be developed appropriate for regular ship model trials. Under these conditions, procedures have to be carried out quickly, and to be useful, results should not be sensitive to small variations in ice conditions.

Initially it was hoped to cover a wide range of ice thickness and flexural strength, but this was limited by practical considerations and an extremely busy tank schedule. The range of ice thickness was limited to that which would allow one test per day. However, this limitation has been mitigated by incorporating a larger group of data gathered during other model test series covering a wider range of ice properties.

The test series conducted for this research was carried out as a normal set of tests at the IMD tank. The following two sections describe the ice tank and operations associated with ice production. Sections 7.3 and 7.4 describe features of the experiments specific to this research.

7.1 The Ice Tank

The Institute for Marine Dynamics Ice Tank has a usable ice sheet area of 76 m. by 12 m. and is presently the largest such facility in the world [7.1]. A 15 m. setting up area is located at one end of the tank separated from the main area by a thermal door. At the opposite end of the tank is a melt pit which enables one ice sheet to be grown while the previous one is melting (Figure 7.1).

A service carriage is provided for ice preparation and measurement work. This carriage is fitted with a work platform

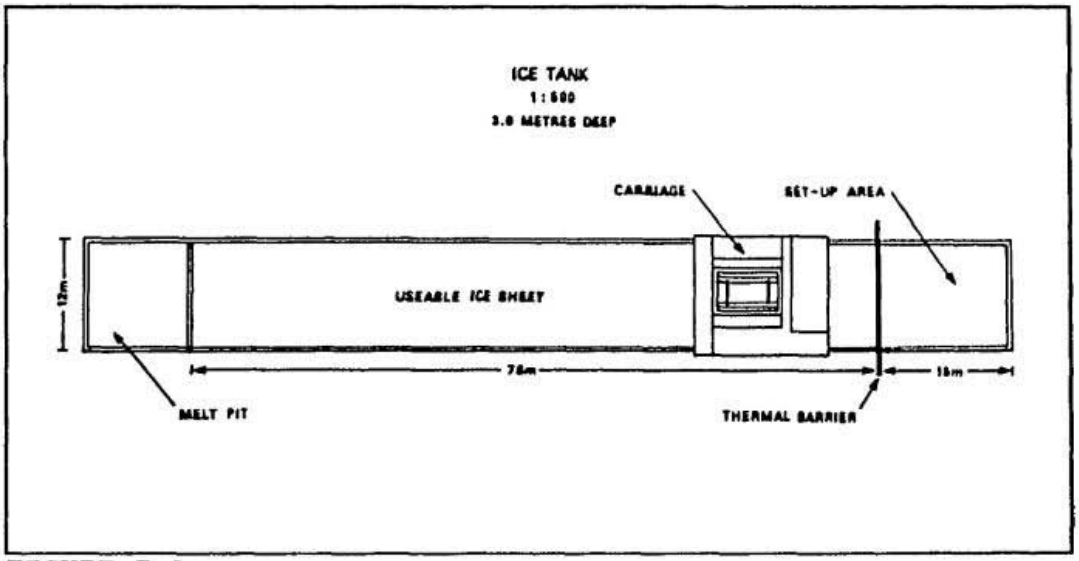

FIGURE 7.1

and an ice boom for moving the ice sheet.

The refrigeration system employs two mechanical compressors developing 1600 HP total, and uses ammonia (R-717) as the refrigerant. Cooling is provided by 26 ceiling hung evaporator units. Refrigeration plant output is computer controlled to maintain uniform temperature at the water surface. The system supplies cold air throughout the tank room with relatively still air at the tank surface to allow heat transfer by natural convection. Air temperature at the ice surface is measured by 12 thermocouples positioned about 25 mm above the surface. These provide feedback control to the refrigeration system. Air temperature can be controlled in the range of -30 to +15 degrees C. and is maintained at -20 deg. C for ice freezing and +1 deg. C for ice tempering and testing. Heating is provided by manually controlled, forced air heaters which are used to warm the room after freezing is complete.

The Ice Tank towing carriage is an 80 tonne steel structure 15 m. long by 14.2 m. wide by 3.9 m. high. The carriage rides on wheels but is propelled by a toothed gear and rack system. Motive power is provided by electric motors. Speed range is .0002 to 4 m/s. Control is provided by an on board computer which can be programmed for up to eight test speeds in a single run, with specified interval distance and acceleration rate.

Models are attached to a 150 mm dia. steel towing post.

The frame supporting the post can be traversed to either of three lateral positions in the tank, allowing tests to be run at the centreline or the quarter width points. The frame can be vertically positioned to accommodate differing model sizes. Maximum model length is 12 m. with maximum design loads of 60 kN on centreline and 30 kN on the quarter points.

The ice tank data acquisition system is a digital computer based system with analog tape back-up (Figure 7.2). It is housed in the carriage control room with signals fed by permanent cabling to and from the test frame. Transducer excitation is provided by a NEFF System 620 Series 300 signal conditioner. Transducer outputs are amplified and digitized by a NEFF System 620 Series 100 amplifier/multiplexer. Digitized data is passed to a DEC MicroVAX II computer which also controls functioning of the NEFF system. Amplified

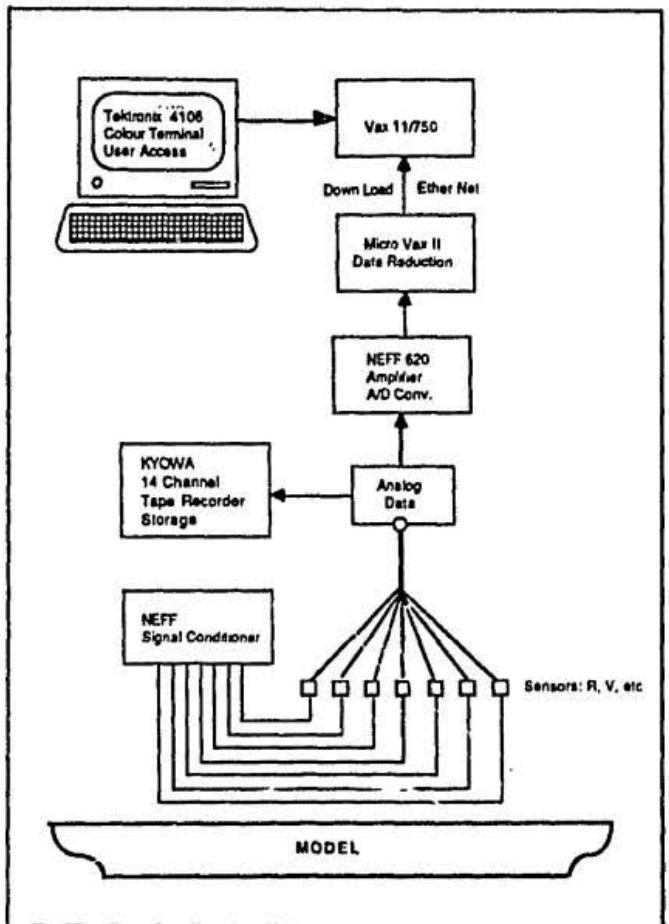

FIGURE 7.2 Data Acquisition System

analog outputs are recorded on tape by a KYOWA RTP-600B 14 channel tape recorder. This provides computer system backup but also allows subsequent analysis of analog data if required.

Digitizing is performed at 50 Hz and current memory capacity allows about seven minutes of sampling over 20 channels in a single burst. Data can be displayed and averaged over relevant intervals locally on a graphic display terminal attached to the MicroVAX. More involved analysis is performed on the main Institute computer, a DEC VAX 11/750 after transfer via communications network.

7.2 EG/AD Ice

The original EG/AD/S Ice developed by Timco is formed from a dilute aqueous solution of Ethylene Glycol, Aliphatic Detergent and Sugar in the ratios .40/.03/.04% by weight. Mechanical properties are described in detail in the reference [3.24].

The formulation used at IMD during this test series differs from the original in that the sugar component is not included and the solution is only of Ethylene Glycol and Aliphatic Detergent in the ratios .39/.027%. To distinguish from the original, this formulation will be referred to as EG/AD. This mixture was adopted because bacterial consumption of sugar in the original formulation led to excessive fouling in the tank and subsequent erosion of ice mechanical properties. Mechanical properties of the EG/AD ice are somewhat degraded from those reported for the EG/AD/S formulation apparently because of a more pronounced top layer, usually 2-3 mm thick. Generally the properties have been found to be similar to the previously used UREA (Carbamide) doped solution.

Mechanical properties of the tank ice as measured for this experimental program are presented in the second section following.

7.2.1 Ice Preparation

Prior to starting an ice sheet, tank water is cooled by circulating it through water chillers. Cooling efficiency is reduced below 1 deg. C so subsequent cooling is achieved by reducing tank room air temperature below zero and circulating tank water by means of an air bubbler system. Water temperature is monitored by thermocouples mounted in the tank walls and thermistor strings deployed in the tank.

Ice seeding is carried out with water temperatures between +.3 and -.1 deg. C and an air temperature of -20 deg. C. Remains of previous ice sheets are pushed into the melt pit. At the time of seeding, refrigeration fans are switched off to reduce air circulation. The tank is wet seeded by blowing a fine mist of warm water into the air above the water surface. This is achieved with compressed air and spray nozzles mounted on the service carriage. A dense fog of ice crystals is created over the length of the tank by moving the spray from one end of the tank to the other at about .04 m/s. At this rate it takes 30 minutes to seed a sheet and approximately 35 litres of seed water are used. The seeding process provides an even layer of fine ice crystals on the surface of the tank from which the sheet is nucleated. At the end of seeding, the refrigeration system is restarted and the freeze cycle commenced.

Ice is grown at a temperature of -20 deg. C. During

freezing, ice growth averages 2.5 mm/hr. Following completion of the freeze cycle, a warm up and tempering cycle is entered. Over a four hour warm up period, the room temperature is raised to +1 deg. C. The room is held at the 1 deg. C tempering temperature for some time. Tempering serves to weaken the ice to the desired test strength. Because ice growth continues during warm up and tempering, final ice thickness is greater than at the end of freezing (see Figure 7.3). Thus ice thickness must be calculated considering growth rates during the three stages of preparation (freeze, warm up

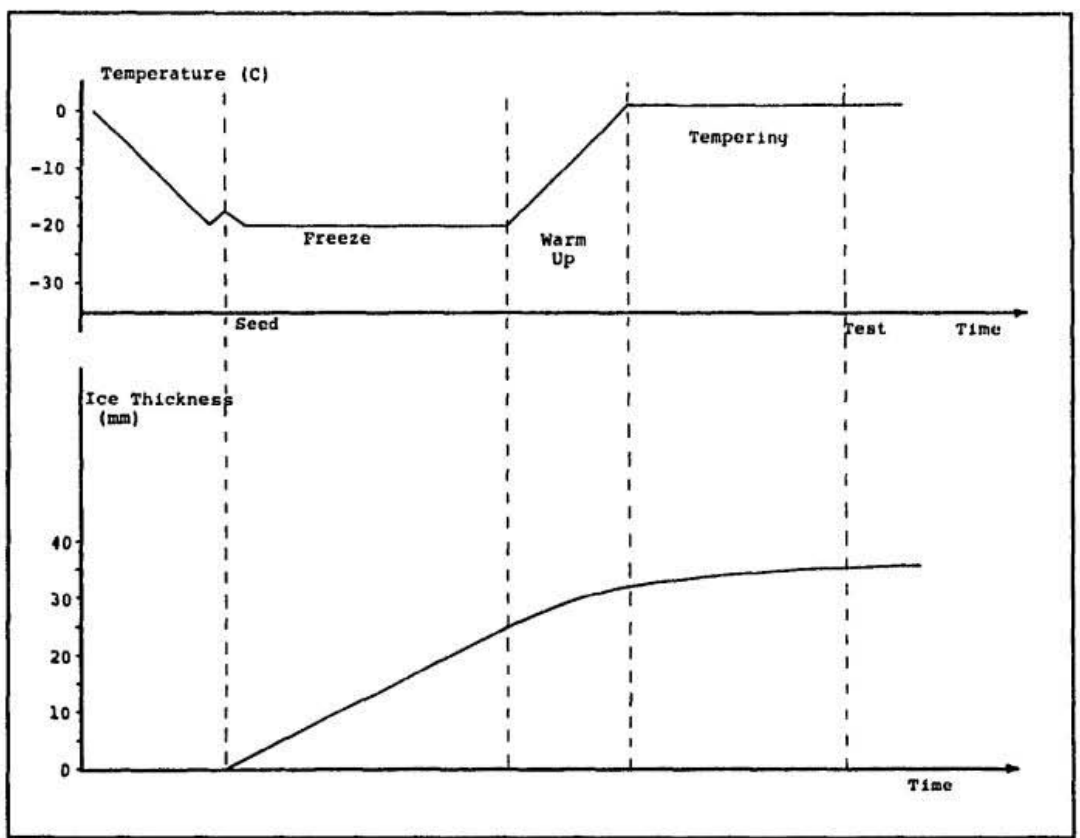

FIGURE 7.3 Ice Growth and Tempering Cycle

and tempering) and the cycle adjusted for different tempering times.

Different ice strengths are achieved by varying tempering time. As tempering time increases, ice strength decreases. The rate of decrease depends on ice thickness, but the trend for all is a negative exponential curve in time. The strength of an ice sheet cannot be maintained at any given value, so testing must be performed quickly when the strength is at the desired point.

7.3 Ice Properties

Model ice properties obviously play an important role in testing ships and structures. Model ice formulations differ substantially from the full scale material and exhibit different mechanical and physical properties. In most cases, considerable effort has gone into modifying the mechanical properties of the model ice to satisfy certain scaling requirements which are judged to be of primary importance. However, other properties may not be suitably scaled so a given ice formulation may not be ideal in all respects.

7.3.1 Thickness

Based on ice thickness surveys over the tank area, average deviation in a 40 mm ice sheet is approximately 1 mm or 2.5 %. This is typical of deviation recorded along the model track. Figure 7.4 shows a typical ice sheet thickness profile. In all test cases, ice thickness is measured along the model track and variations can be accounted for in analyzing results.

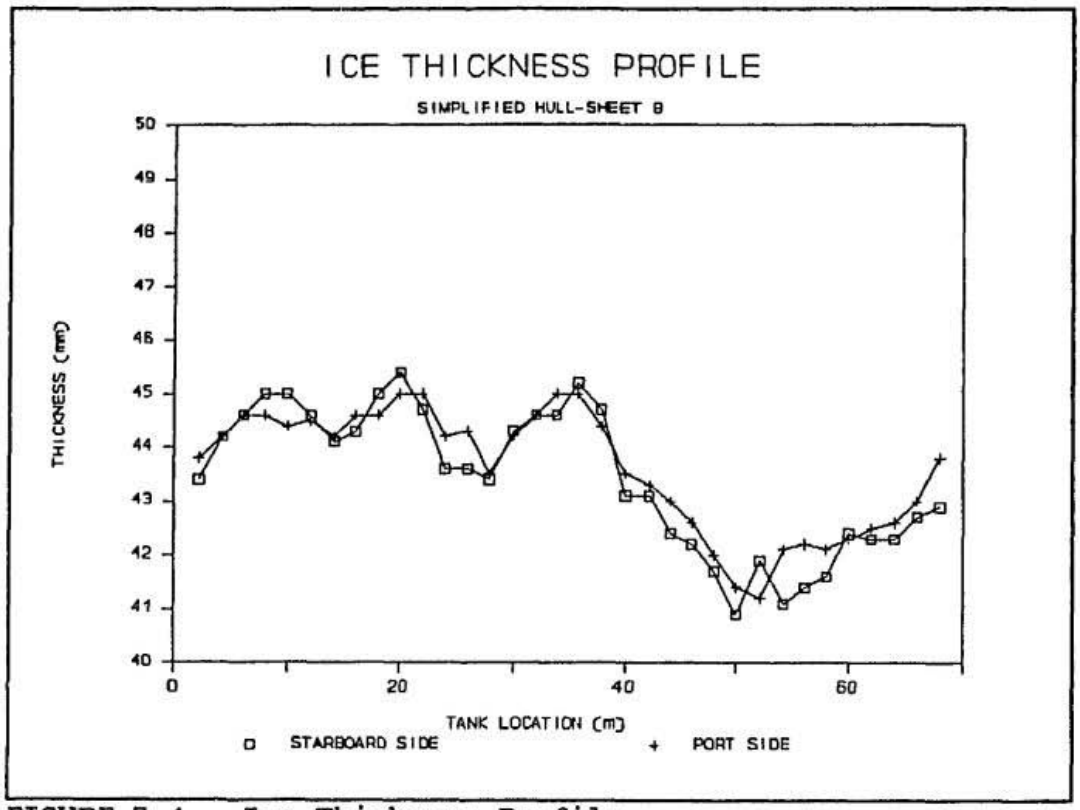

FIGURE 7.4 Ice Thickness Profile

7.3.2 Flexural Strength and Fracture Toughness

Flexural strength of EG/AD ice can be adjusted in the range of 100 kPa to 15 kPa by varying tempering time (Figure 7.5). At lower strengths the ice starts to lose structural integrity and higher strengths are difficult to achieve unless tank temperature is held below 0 deg. C during testing.

Strength is measured by in situ cantilever beam test, using a beam with a thickness:width:length ratio of 1:2:5. Failure load is applied manually using spring balances at moderate loading rates. Reported strength values are the mean

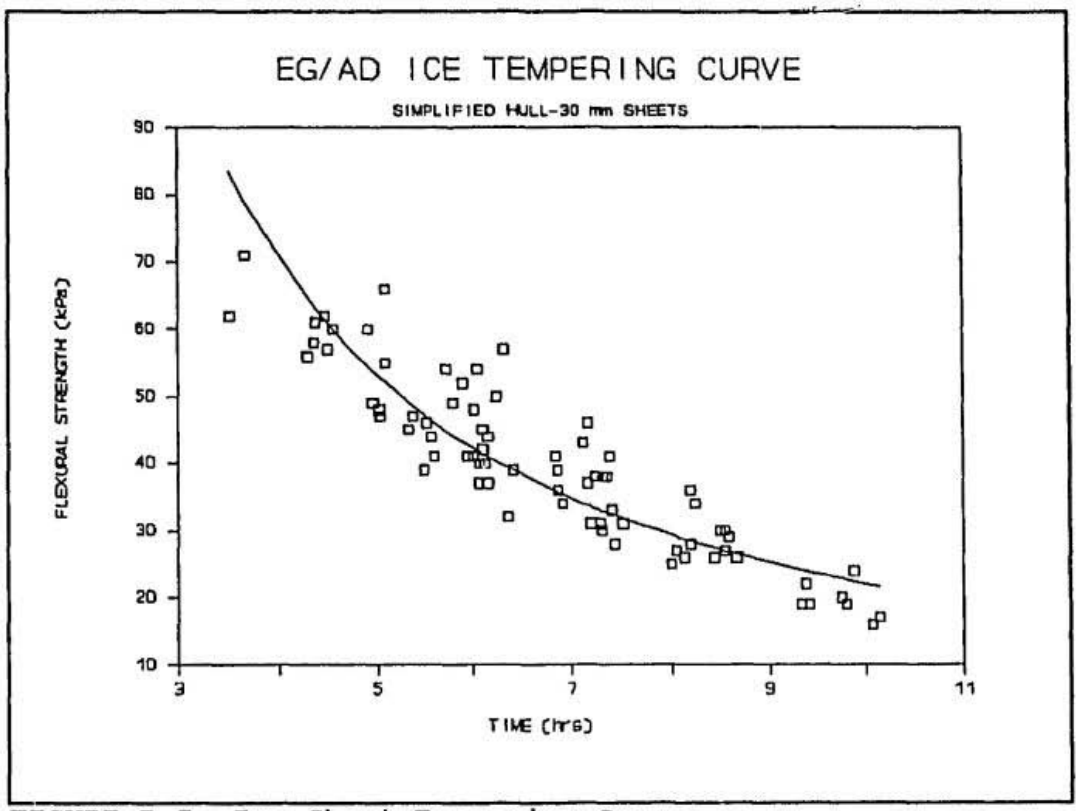

FIGURE 7.5 Ice Sheet Tempering Curve

of four samples tested at a single location.

There is some variation in flexural strength over the tank area. It is not possible to measure this variation completely, due to the time required to perform strength tests and the fact that they are destructive to the ice. Values reported for each test are taken in the middle area of the tank on either side of the model track. This has been found to represent a reasonable average for the entire sheet.

Fracture toughness in model and full scale ice is an issue that has gained increased prominence in the ice model testing field. A claim of the original EG/AD/S formulation was

much lower fracture toughness than previous formulations. Over a year of testing, fracture toughness of EG/AD ice has proven to be higher than that reported for the original EG/AD/S formulation. In addition the fracture toughness has not shown good consistency from sheet to sheet. See Reference 7.2 for a description of fracture toughness measurements.

Given the lack of consistency in fracture data for previous tests, it was not extensively recorded during these tests nor used in the analysis. Those points which were recorded are shown in Figure 7.6. As part of these experiments or any analysis of icebreaking, major interest is in failure

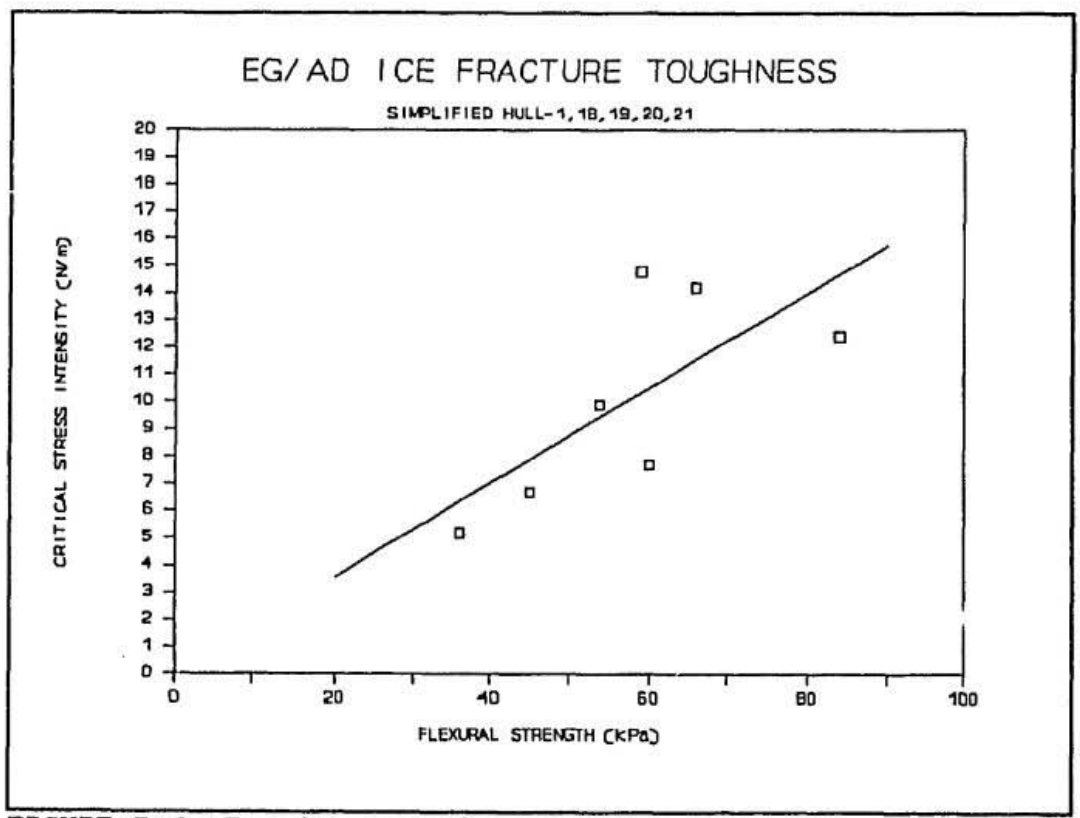

FIGURE 7.6 Fracture Toughness

of the ice cover. That this occurs by generation and/or propagation of cracks in the ice is beyond debate. However, fracture toughness as a material property is a measure of the energy required to propagate a crack. In order to predict a failure load, the distribution of pre-existing flaws must be known. If, on the other hand, these flaws are non-existent or ineffectual as crack initiation points, then the load required to nucleate cracks must be known. Thus, more information than just the fracture toughness must be in hand before the property can be used as a measure of material strength.

Flexural strength testing determines a load to induce fracture without requirement to know flaw distributions. It is not a test of any fundamental material property but an indication of the gross mechanical strength of a given sample. If it is reasonable to assume that fracture properties will interact in the same way throughout an entire ice sheet, then flexural strength is a better indication of the effective strength of the ice sheet than the fracture toughness by itself. However, because flexural strength is not a measure of any single material property, it is reasonable to assume that there will be variations due to scale or changes in geometry. Both these things have been observed in the literature on ice strength testing [3.8]. Therefore the principal use of flexural strength is as a relative indication of ice strength, much as resistance in level ice is a relative indication of icebreaking performance.

7.3.3 Compressive Strength

Compressive strength of the EG/AD ice is recorded by a uniaxial unconfined compression test performed in the in-plane direction on samples cut from the ice sheet. Compressive strength is not judged to be of primary importance in the flexural type failure, and thus it is not usually considered in analysis of ship icebreaking data. This same approach has been taken with the present study, although typical compressive strength values for this test series are given in Figure 7.7.

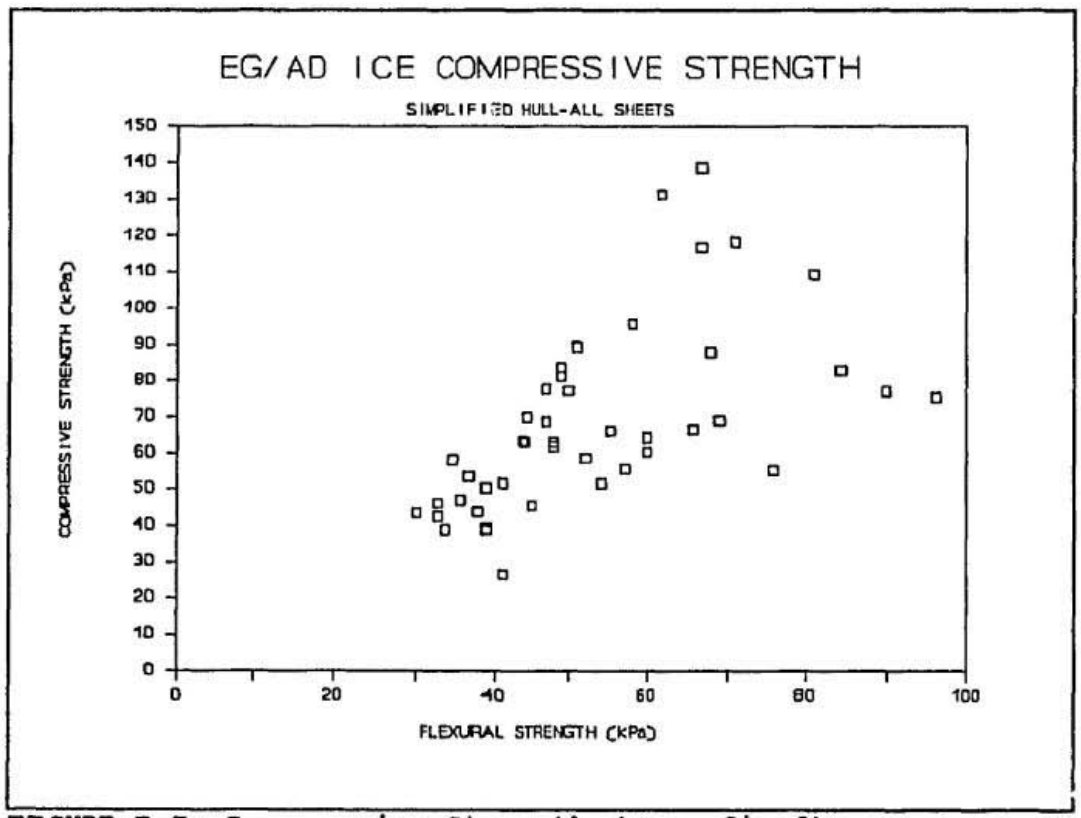

FIGURE 7.7 Compressive Strength (unconfined)

7.3.4 Elastic Modulus

Elastic modulus is measured by the static deflection method described in Reference [7.3]. This method involves recording sheet deflection at the point of application of a concentrated load. The ice sheet is assumed to be an infinite elastic plate on an elastic foundation. Modulus measurement is usually performed once per ice sheet and used to indicate the E/σ ratio for the sheet. Because the measurement is rate dependent, it is unlikely that it is a good measure of the effective elastic modulus at model speeds. At higher speeds, it is expected that the apparent elastic modulus would increase although the extent of this increase is unknown. Uncertainty associated with this parameter reduces its value in analysis of icebreaking data. Changes in elastic modulus as measured in the tank were not found to influence results recorded during this study.

7.3.5 Density

Ice density measurements are also taken once per ice sheet and have been found to correlate well with ice thickness and flexural strength. Density figures for each sheet are determined after model testing by cutting a sample from the sheet, measuring the volume and calculating density by reading

the load required to maintain submersion. The volume is calculated by manually measuring the sample dimensions.

Ice density is measured at the end of each days testing. Because density tends to increase with tempering time, this reading is higher than at test time. Ice strength and thickness are also measured in the area of the density measurement, and the density has been found to correlate well with thickness and strength (or tempering time) in the model ice. Density at test time is calculated based on thickness and strength in the test interval using a regression equation derived from all sheets in a series. Values of ice density for the EG/AD ice usually fall within the range of 925 to 950 kg/m^3.

7.4 TEST MODEL

The hullform used in the model test portion of this study is shown in Figure 7.8 and Photograph 1. The shape was tested at three different beams while maintaining overall length and bow angles. This required that the length of the bow section be increased with beam which was judged preferable to changing angles. The hull is a flat sided, barge shape designed to satisfy a number of criteria. The bow is representative of an icebreaker without the curvature and varying angles of a

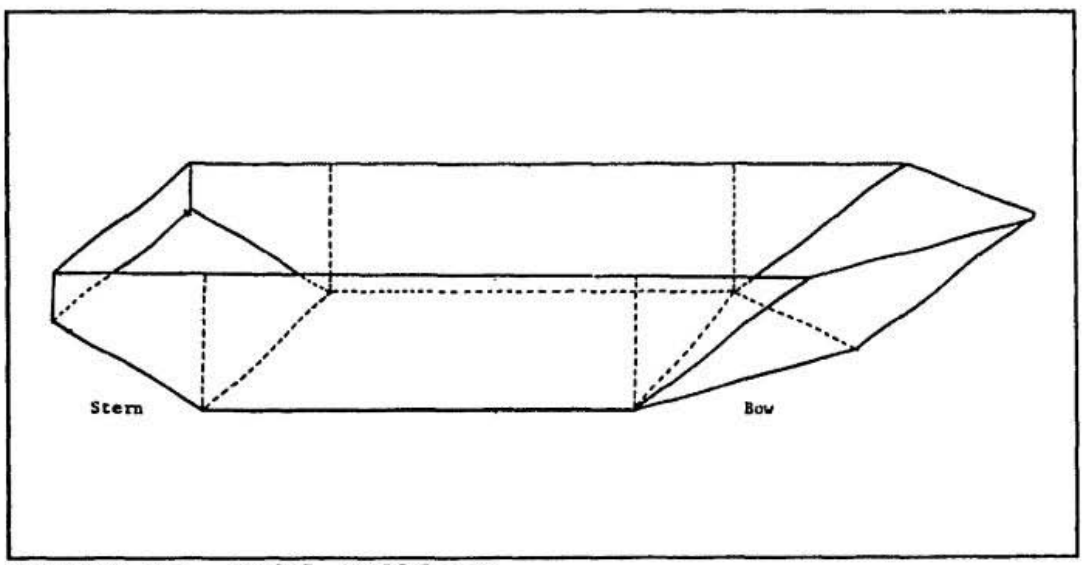

FIGURE 7.8 Model Hullform

realistic ship form. The waterline form is maintained throughout the hull depth, eliminating gross changes in icebreaking geometry with slight changes in trim. For pre-sawing tests, the form provides constant flare and waterline

angles in the bow region. This gives a chevron breaking pattern which can be easily duplicated by sawing a similar pattern in the ice.

7.4.1 Model Construction

The three models were constructed in the model shop of the IMD. All were built of polystyrene foam overcoated with epoxy resin and glass fibre matting. Internal framing is plywood. The outer surface is a smooth sanded resin body filler primed and painted with flattened automotive lacquer. This surface gives a relatively low friction coefficient with ice (approx. 0.06).

7.4.2 Test Conditions

The models were ballasted with 27 kg lead ingots to the following hydrostatic conditions (Table 7.1).

Table 7.1 Model Test Conditions

	Model A	Model B	Model C
Displaced Volume (m**3)	0.798	1.116	1.421
Wetted Surface (m**2)	5.300	6.550	7.800
Waterline Length (m)	4.430	4.430	4.430
Beam (m)	0.700	1.000	1.300
Draft (m)	0.300	0.300	0.300
VCG(centre of gravity) (m)	0.270	0.350	0.350
VCB(centre of buoyancy) (m)	0.160	0.156	0.153
KM (metacentric height) (m)	0.323	0.452	0.752
Roll Period (sec)	2.86	2.44	1.39

Model VCG was determined by performing an inclining experiment on the model in the tank and calculating VCG from the measured GM (distance from metacentre to c.g.)

7.4.3 Towing Arrangement

Two towing systems were used as part of the model test series. The first was a normal 3 degree of freedom rigid tow using the IMD Towing Gimbal (Figure 7.9, Photograph 2). This device is a combination load cell and universal joint, which when placed at the model centre of gravity allows motions in roll, pitch and heave. It also allows freedom in yaw but this motion is restrained by a yaw restraint located at the stern of the model (Photograph 3). The device has a maximum measuring capacity of approximately 6000 N and a sensitivity of about 5 N. The load cell is located on the model side of

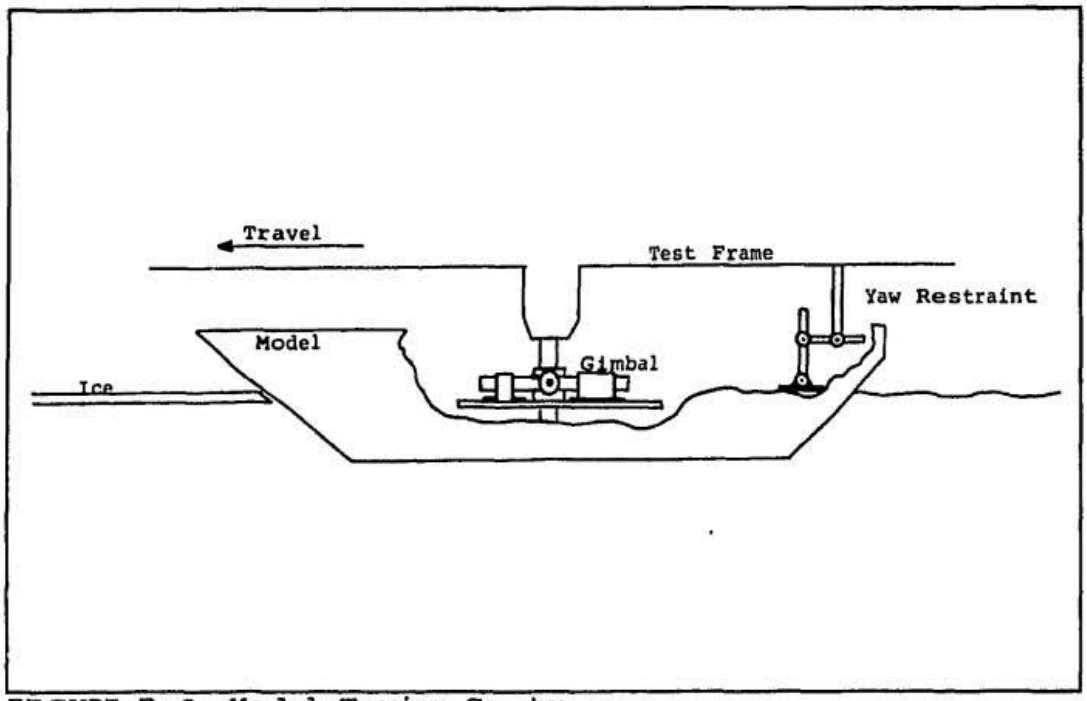

FIGURE 7.9 Model Towing System

the universal joint, and thus resistance is measured in the model coordinate system, rather than the tank coordinate system. This means that as the model pitches, the measured load is slightly reduced from that actually required to propel the model down the tank. Because pitch angles are usually less than 1 degree this error is insignificant. The natural frequency of the towing system with a 1 tonne model attached is about 8 Hz

A second towing system was used for trials where the bow section (wedge) was tested alone and at very shallow draft. For this test, it was necessary to restrain the model in all modes of motion and measure towing force. The frame used to accomplish this was attached to the carriage suspended on four

linear bearings so that it was free to move in the longitudinal direction only (Figure 7.10, Photograph 4). A small load cell was installed to restrain motion and measure tow force in this direction. The frame has a maximum measuring capacity of 500 N and a sensitivity of about 2 N. The model bow section was bolted to the underside of the frame. With this arrangement, the model was suspended in a level attitude. Draft was adjusted by moving the carriage test frame up or down.

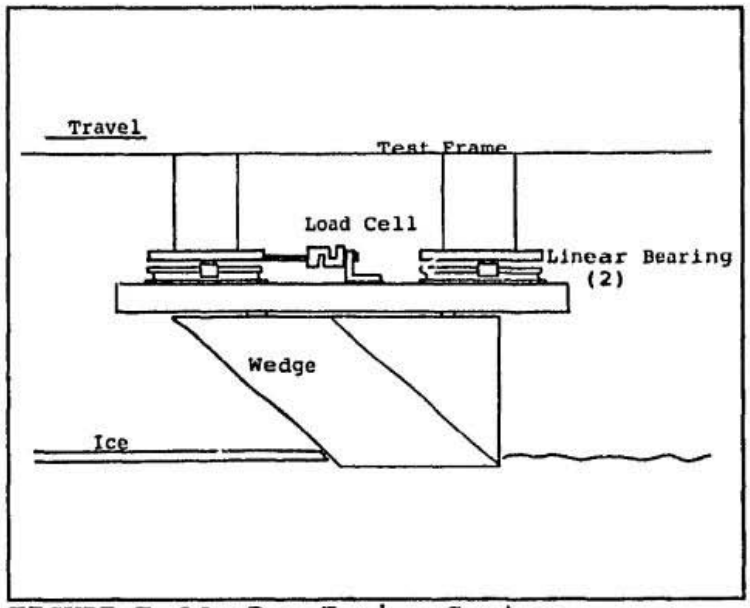

FIGURE 7.10 Bow Towing System

7.5 TEST PROCEDURE

The test series was divided into five different sub tests (numbered 1,2,3,4,5). Two of these involved verification of pre-sawing procedures, and three were standard tests on the hullform at differing beams. The tests were classified as follows:

Set 1	Variations in Pre-Sawing Pattern
Set 2	Shallow Draft Wedge
Set 3	1.0 m Beam
Set 4	1.3 m Beam
Set 5	0.7 m Beam

Numbers 1,2 and 3 were conducted in September of 1987 while 4 and 5 were conducted in October 1988 . A range of target ice thickness from 30 mm to 45 mm and ice strengths from 30 to 60 kPa was covered with some sets taking in more points than others. In general the aim was to provide a good basis for comparison within the limited ice tank time available. Table 7.1 illustrates the target test conditions.

Table 7.2 Test Ice Condition Matrix

Thickness mm	30	37.5	45
Strength kPa			
30	[1,2,3,4,5]	[3]	[2,3,4,5]
45	[2,3,4,5]	-	[2,3,4,5]
60	[3]	[3]	[3]

The general test procedure is described below.

Ice flexural strength was measured in the centre area of the tank at one hour intervals until the target strength was approached. Then, Elastic modulus of the sheet was measured.

The first model test was then carried out on the tank centreline, after which the ice flexural strength was tested and the ice thickness measured at 2 m intervals along the model track.

The model was moved over to the south quarter point in the tank and the ice prepared for a second test. This preparation consisted of placing channel spreaders in the previously cut channel to prevent the remaining ice from moving over into the area of clear water (see Fig. 7.11, and Photograph 10). Because the second test was normally the pre-sawn run, the ice was sawn in the desired pattern along the model track.

The model was then run on the quarter point, after which ice thickness was measured along the second channel and the ice strength tested a final time.

Ice density was measured once per sheet between the first and second tests.

Model tests in ice involve running at more than one speed in a given sheet of ice. The choice of test intervals and speed sequence are important aspects of a test plan. The model should be fully surrounded by ice that has been broken at the

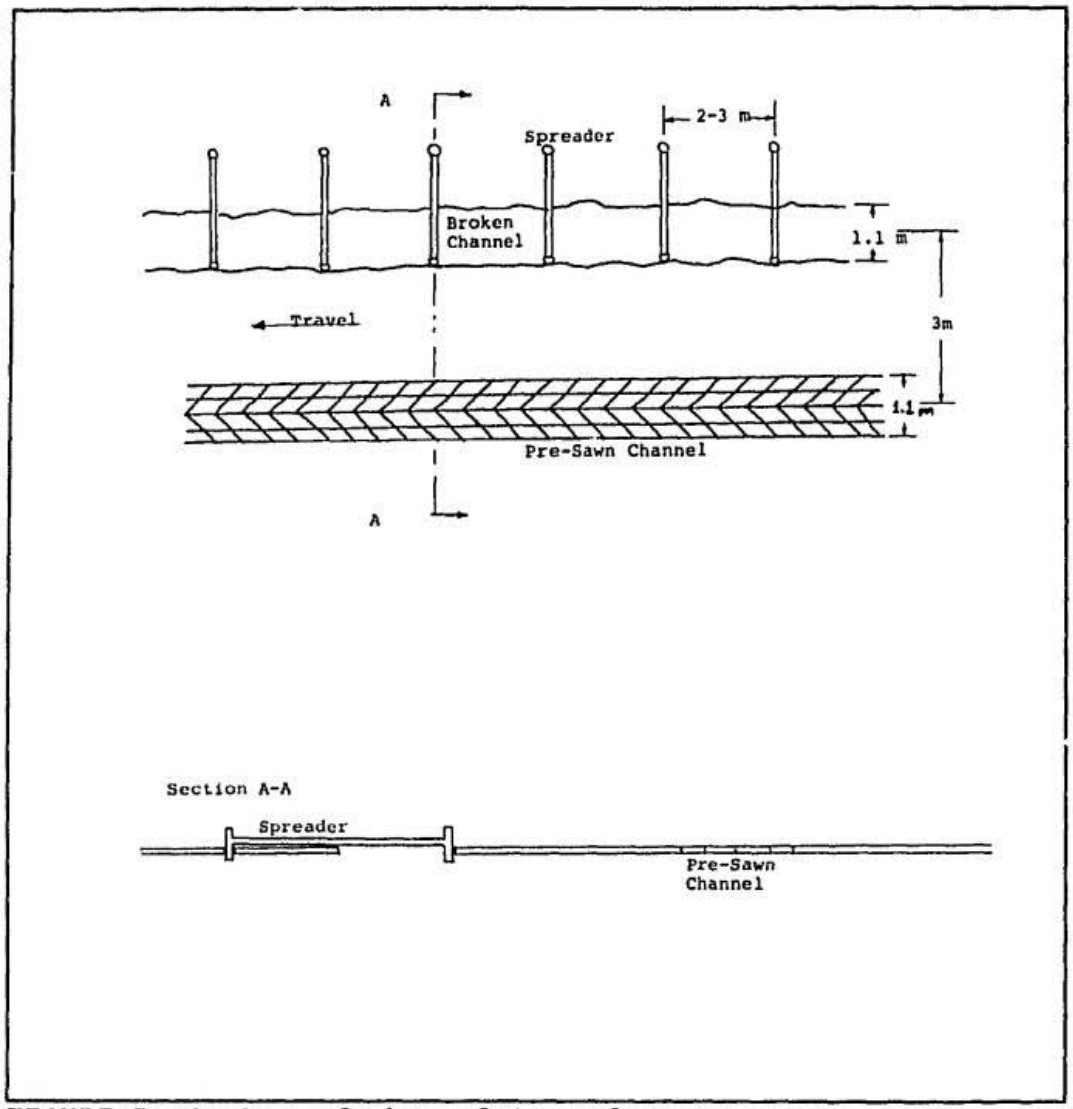

FIGURE 7.11 Use of Channel Spreaders

set speed before a legitimate measurement can be taken. Thus, at least one model length of travel is required before a measurement can be considered reliable. Also, accelerations induced by speed changes in mid run give rise to transient vibrations in the tow system which must be allowed to settle out. It has been traditional to allow a model length for

measurement after the settling period, but this leads to very short measurement time periods at high speed and to very long measurement time periods at low speeds.

To minimize these problems and make best use of available tank length, the following scheme was developed to calculate run length. In general, the settling period was taken to be the longer of one model length or 5 seconds of run at the given speed. The measurement interval was then taken to be 20 to 25 seconds after the settling period. For this model, the formula yielded the following run lengths and measurement intervals (Table 7.2).

Table 7.3 Measurement Intervals

Speed (m/s)	Run Length (m)	Settle Length (m)	Settle Time (sec)	Measurement Length (m)	Measurement Time (sec)
.10	7.5	5.0	50	2.5	25
.25	10.0	5.0	20	5.0	20
.50	16.0	5.0	10	11.0	22
1.00	25.0	5.0	5	20.0	20

The intervals are exclusive of any distance and time lost to accelerations between speeds.

Speed sequence is a related issue. Ideally the sequence of speeds would be randomized for each test in an attempt to remove any systematic variation in ice strength along the

length of the tank. However, ice strength is also varying in time, and it is desirable to avoid speed sequences that are either steadily increasing or decreasing. Thus, four speed sequences were used on a four test rotation as follows.

Table 7.4 Speed Sequence

Speed Order	1	2	3	4
Sequence ID	Speed (m/s)			
A	0.25 m/s	1.00	0.10	0.50
B	0.10	0.50	0.25	1.00
C	0.50	0.10	1.00	0.25
D	1.00	0.25	0.50	0.10

This sequencing of speeds, combined with the unequal run lengths meant that there was considerable variation in the area of the tank in which the speeds were run within the four test cycle. It was judged that this would avoid systematic errors due to repeated combinations of ice strength and model speed.

Each set of tests had certain procedural details that were peculiar to that set of tests. These are covered in the following sections.

7.5.1 Pre-Sawn Pattern Variations

For the tests of pre-sawn patterns, the 1.0 m beam hull was used with four sets of trials run in two ice sheets. Model speed was maintained at .50 m/s. Target ice thickness was 30 mm and target strength for the first test in each sheet was 30 kPa.

Prior to each run, the ice sheet was sawn to the required patterns and then photographed from above to allow subsequent determination of the exact parameters (Photograph 14). In the first sheet, four included angles were tested on the centreline run and four piece lengths on the quarter point

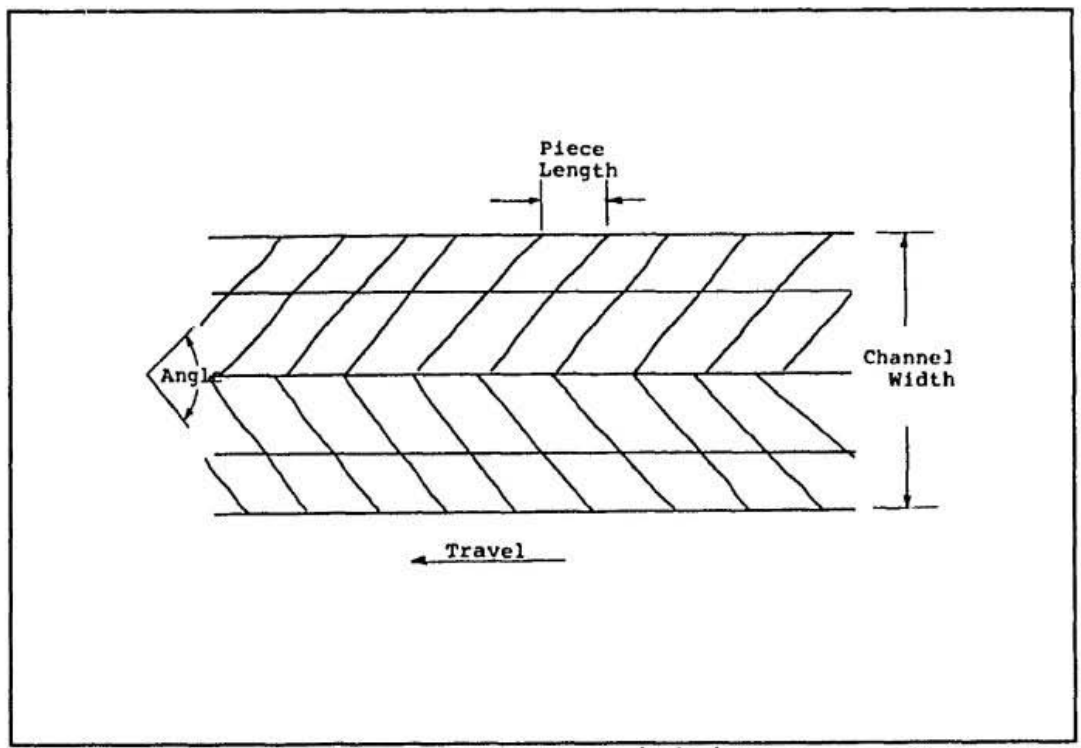

FIGURE 7.12 Pre-sawn Pattern Definitions

(See Figure 7.12). In the second sheet, four piece lengths were tested on the centreline and four channel widths on the quarter point. Ice cutting was accomplished manually using small pruning saws. Longitudinal cuts were made by holding the saws in the correct position on the service carriage, with tips in the ice, and running the service carriage down the length of the tank. Cross cuts in the chevron pattern were made by hand sawing as the service carriage moved slowly down the tank in the direction of model travel. Angle of cut was maintained by towing a large adjustable protractor behind the carriage so that individuals making the cuts would have a reference (See Photographs 8 & 9). This system worked well and generated consistent, well controlled patterns, particularly for channel width and included angle. Piece length was subject to the judgement of the individual doing the sawing and thus a little more variable.

7.5.2 Shallow Draft Wedge

The shallow draft wedge trials were conducted with only the bow section of the 1.0 m beam model. This could be done because the geometry of the bow is constant at all waterlines, and thus at shallow draft the icebreaking geometry is the same as at deeper drafts. However, in this case the resistance

associated with clearing ice, open water drag and friction is minimized because only a small section of the hull is immersed (Photograph 5). That is, the shallow draft partial hull experiences the same breaking resistance component as the full vessel, with minimal influence from the other components. The draft was set at 60 mm, just deep enough to cause the ice to crack.

Tests were conducted by running the model on the tank centreline and then repeating the run on the quarter point with a different speed sequence. This yielded two level ice tests per sheet at different ice strengths. Because the wedge did not significantly displace the ice after breaking, the ice left behind the model was very similar in pattern to the chevron pre-sawn pattern. To take advantage of this, the model was lifted out of the water at the end of the second run and carried back to the start point without disturbing the ice in the channel. A third run was then carried out over the pre-broken ice to measure resistance due to displacing the ice pieces. This was essentially a pre-sawn test although the ice was not sawn but broken by the first pass of the model.
This run was included to measure non-breaking resistance components acting on the partial hull as a check on the validity of this means of isolating the breaking resistance. It also provided data to allow the non-breaking resistance to be subtracted from the total measured in level continuous ice.

7.5.3 Full Model Tests

Tests on the simplified hullform at three different beams were conducted as a regular set of ice model tests in the IMD tank. Model resistance and carriage speed were measured in addition to roll pitch and heave motions. Video records were made of the model under tow and the flow of ice underneath the model.

Tests were carried out with the model on the tank centreline for level ice tests (Photographs 6 & 7) and on the south quarter point for pre-sawn runs (Photograph 11). Ice sawing was accomplished in the same way as described earlier. Included angle and piece size were measured at the "print" left by the model at the end of the level ice run (Photograph 12). This is the area at the end of a run where the model has advanced far enough to crack the ice but not enough to displace it. When the model is backed off, the primary cracking pattern can be observed in the ice. From this, the angle of primary cracking and approximate piece length are evident. This pattern was used as a guide for the sawing pattern for each test. As with the pre-sawn pattern tests, control of channel width and included angle was found to be very good with piece length somewhat more variable. Overall the consistency of sawn channels was judged to be very good. It was also clear that patterns of this quality could be achieved on a regular basis as part of commercial testing.

8. RESULTS OF EXPERIMENTS

The full data set recorded during six weeks of ice tank testing is presented in Appendix 1. This represents results from 47 tests conducted in 22 ice sheets and a number of open water data points. The sum is approximately 195 data points relating ice breaking and ice clearing to ship speed, ship beam, ice strength and ice thickness. Although the range of ice properties is somewhat narrow, particularly in the case of ice thickness, the range of model speeds is sufficiently wide to cover most practical applications.

In analyzing data from even a simple ice model test, the immediate problem is comparison of results between experiments. The nature of the testing is such that only model speed can be controlled sufficiently to insure consistency from run to run. All other independent variables show some variation from target values. Thus, one is faced with a non-dimensional presentation as a matter of necessity. Even a good non-dimensional presentation will be subject to some random variation. As noted in the literature review, presented earlier, there have been many formulations by different authors with limited success. Analysis of data generated for this study has been carried out using the formulation developed in Chapter 5. Results indicate that the icebreaking process can and should be divided into at least three components for presentation and scaling.

8.1.1 Primary Data Reduction

Raw data collected at the towing carriage consists of model resistance and speed. As part of standard model test procedure, model motions in roll, pitch and heave were collected but not used in analysis of the test program. Model resistance is measured at 50 Hz and presented as a digital format time series. Quoted resistance is the arithmetic mean of all samples within the time interval of the steady state run. For this test series this average was taken over the last 20 to 25 seconds of each constant speed interval as explained in 7.5. Readings of model speed are digitized at the same rate and averaged over the same interval.

Recording information on ice properties presents a problem because no aspect of the ice remains static in time. Although there are many properties of an ice sheet which can be measured, the two which are consistently used in ship-ice model and full scale trials are ice flexural strength and ice thickness.

Flexural strength is monitored by cantilever beam tests as the ice sheet tempers and once before and after each model test. Recorded data are curve fitted to a negative exponential curve in time and this curve used to interpolate ice strength at test time. Strength is usually measured in the middle section of the tank and represents an average for the entire sheet. Local variations in strength are not accounted for.

Ice thickness data are collected immediately after each test. Average thicknesses are computed for each test interval in a sheet. For reasons covered in 7.3.4 elastic modulus was not used in analysis of data from this test program, although the information was collected for each sheet to assess the E/σ ratio.

Ice density was recorded for each sheet and extrapolated to test time for each speed interval. This was achieved by deriving a regression equation in strength and thickness based on the readings for all ice sheets in a series. This equation was used to calculate density based on the average thickness and strength for each test interval.

8.1.2 Assessment of Data Quality

Some methods used in gathering data for ship ice model tests are necessarily simple and allow considerable room for error. Because final analysis of model resistance requires combinations of measurements, all subject to some degree of error, it is worthwhile to consider the quality and degree of error in each of the variables recorded and used in analysis.

Measured resistance is judged to be of good quality at higher load levels. Background electronic noise in the load cell and data acquisition system has a peak amplitude equivalent to about 5 newtons of load. This noise is high frequency and does not affect average resistances. Mechanical stickiness, hysteresis and drift have been consistently below 3-5 newtons in repeated calibrations. Thus, measured resistance is judged to have an absolute error of no more than ±5 newtons.

Model speed, provided by the towing carriage, is accurate to one part in one thousand. Consequently, model speed is judged to be the parameter least subject to variation.

Ice properties are more variable than parameters associated with the model. Ice thickness variation is usually within 5% of the mean value for a whole sheet. Locally measured thickness in an test interval is usually less variable (on the order of ±3% of the mean thickness in the interval) because values are taken over a smaller area. These

are the values used in data reduction.

Flexural strength measurements frequently exhibit 10 to 15% variation even within a narrow test region. Variation across the tank width is of similar magnitude but lengthwise variation is higher. Figure 8.1 shows a lengthwise profile of ice strength indicating a standard deviation of ±10% of the mean. Although quoted average strength is derived from a

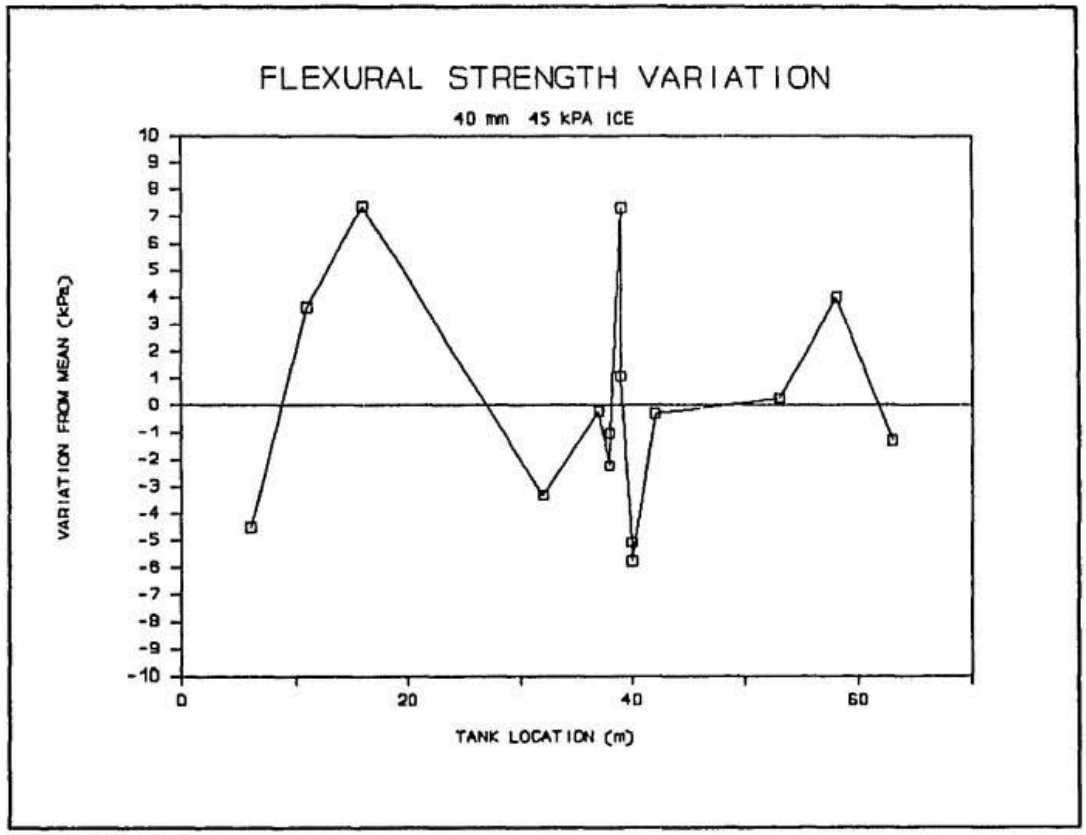

FIGURE 8.1

number of samples, usually eight, and fitted to a smooth curve in time, there can be considerable variation from the mean within an ice sheet.

Elastic modulus measurements are judged to be of good quality with up to ten measurements taken for each reported value. This is however a time consuming test and, as stated earlier, highly rate dependent. Elastic modulus and E/σ ratio are known to change with tempering time and this change is not routinely monitored making it difficult to predict the modulus at test time. Because E/σ is only used to characterize the ice sheet, this is not a major drawback.

Ice density is also only measured only once per test, but as previously mentioned, is well correlated with thickness and strength. The range of variation at maximum is only 3.5% and within the regression for density at test time the error is estimated to be less than 2% even though the measurement error is greater. The results of the foregoing discussion are summarized below (Table 8.1).

Table 8.1 Experimental Errors

PARAMETER	Maximum Expected Error
Resistance	5N or 2-5%
Speed	0.1%
Thickness	3%
Strength	15%
Density	2%

Strength is obviously the largest single source of variability in the collected data. Because the strength of the ice influences the total resistance measurement, this variable can be expected to show a random variation of about 15%. Presawn resistance is not subject to ice strength and thus should be less variable. This has been confirmed in the data. Therefore the derived clearing resistance shows less variability than the total resistance or the derived breaking resistance. Clearly, ice strength quantification is the largest source of error in ice resistance data and the area most requiring improvement.

Thus it is important that sufficiently large volumes of data be collected to allow calculation of coefficients with confidence intervals as narrow as possible.

8.2 Open Water Resistance

Periodically during the test series, runs were conducted in clear water or in the broken channel after clearing out all ice pieces. These tests provide data on the open water resistance of the hullform and give an indication of the effect of ice cover on the hydrodynamic resistance when operating in a channel.

These results must be treated with caution. Although trends are thought to be correct, lack of absolute accuracy arises because the measurement is of a relatively small load with a device designed to measure much higher loads.

Nevertheless, the resistance curves in Figure 8.2 show that resistance in a channel is slightly higher than resistance in clear water. Insufficient time and facilities were available to perform an in-depth set of experiments on the effect of running in a channel, but the recorded results give sufficient information to indicate the trend and to provide open water data for analysis of icebreaking.

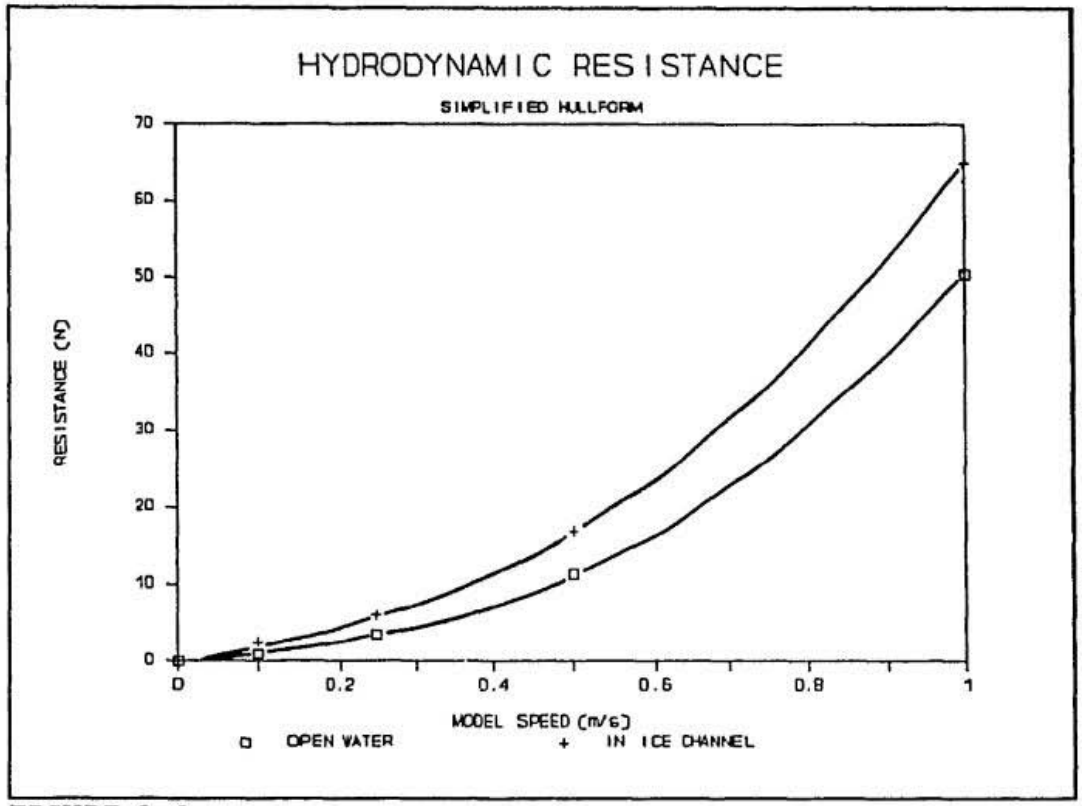

FIGURE 8.2

8.2.1 Separation of Hydrodynamic Resistance

It has been common practice in analysis of icebreaking data to separate hydrodynamic resistance by subtracting open water resistance as measured in a clear tank from the total resistance measured in ice. This neglects effects which may arise from the ice sheet on the water surface or coupling between water flow around the bow and ice pieces which are cleared aside. Data gathered for this study allows a preliminary investigation of these items. However, because of the relatively small differences in resistance and the lack

of sensitivity in the load measuring apparatus, these results are more qualitative than quantitative.

The higher resistance measured in a channel is thought to be due to the greater capacity of the covered free surface to absorb wave energy, particularly at short wavelengths. Thus, it is more difficult for the model to move water aside because of presence of the ice cover. It is expected that this effect would become more pronounced at higher speeds where larger waves are generated. However, it is not common for icebreakers to operate at these speeds, and thus the increase in resistance due to ice cover is not large in absolute terms.

Evidence of coupling between hydrodynamic flow and ice flow arises when the clear water resistance is subtracted from the pre-sawn resistance. In theory, the difference between these two should be resistance associated with clearing broken ice pieces. Increasing velocity should result in an increase in inertial forces required to push ice aside. However, as speed increases the difference between pre-sawn resistance and clear water resistance levels off or decreases (Figure 8.3). This is attributed to coupling between the flow of water over the hull and the movement of ice pieces as they pass around the model. Subtraction of the calculated viscous component alone yields an ice clearing resistance which shows more rational characteristics with increasing speed. In this case the viscous term is calculated using the ITTC 1957 Model Ship Correlation Line and the method presented in Reference

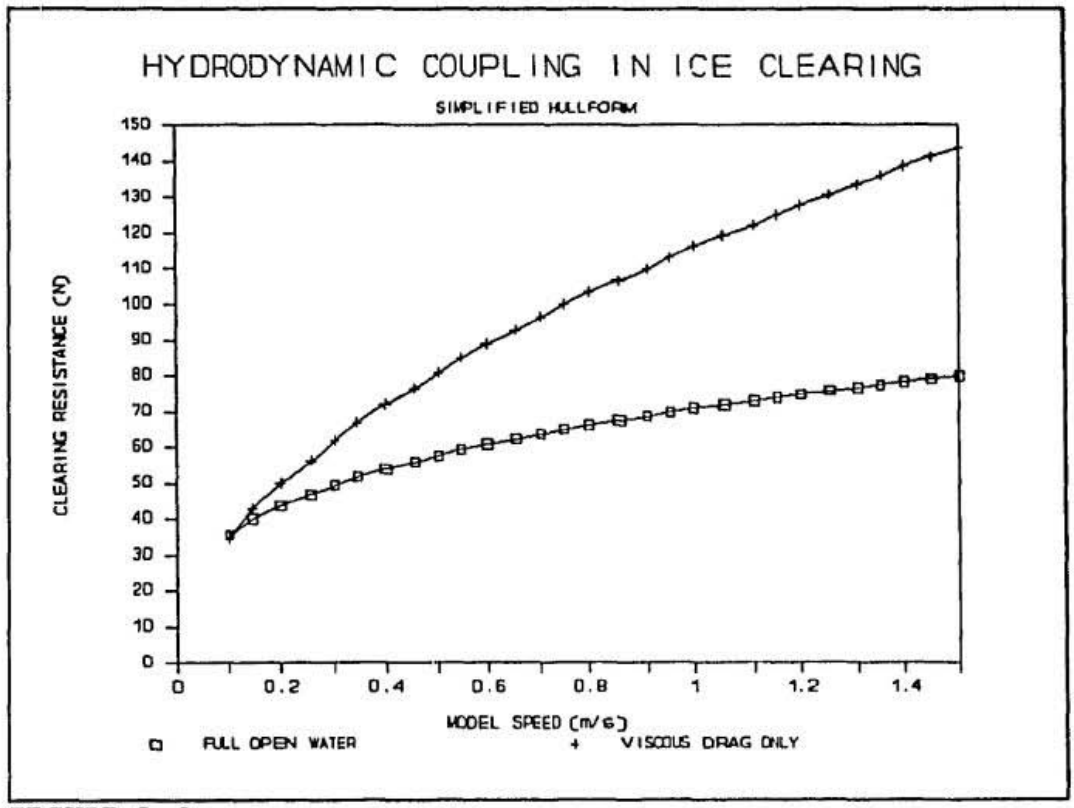

FIGURE 8.3

8.1. There is further support for this approach in that both wavemaking resistance and ice clearing resistance are dominated by Froude velocity scaling. Viscous drag on the other hand is dominated by Reynolds scaling and thus cannot rightfully be combined with the other two.

Based on these data and experience with previous pre-sawing tests, it is concluded that there is coupling between the flow of water and the flow of broken ice pieces around the vessel which masks the resistance associated with clearing ice. Thus, it is not appropriate to subtract the wavemaking component of clear water resistance from the pre-sawn

resistance. Subtracting viscous resistance on the other hand is viewed as a legitimate step in light of the different scaling requirements. This represents a departure from present practice.

Ice clearing resistance is derived by calculating viscous skin friction resistance and subtracting it from the pre-sawn resistance. The resultant ice clearing resistance is the sum of wavemaking and form drag components of hydrodynamic resistance combined with resistance of moving broken ice around the model hull. At the present time it does not appear that these mechanisms can be separated experimentally.

8.3 Isolation of The Breaking Component

Two approaches were taken toward isolating the breaking component of icebreaking resistance. The first was to use the results of the pre-sawing tests; the breaking component equals the measured total resistance less the measured pre-sawn resistance (clearing and viscous components). The second approach was more direct, in that an attempt was made to minimize the other components. A partial model was towed in such a way that the bow waterline shape was maintained but there was not any hull underneath or behind the small section breaking the ice. In this way, it was intended to measure directly the resistance associated with primary breaking of the ice cover. The two methods were compared and it was found that the breaking component derived by either method is the same. This is strong evidence that a breaking component does exist and that it can be identified by experiment. In addition, it was found that there is a slight velocity dependence in the breaking component and a qualitative explanation for this effect presented itself. The results of this investigation are presented in the following sections.

8.3.1 Pre-sawing Tests

Non-dimensional resistance coefficient data from the four tests of the 1.0 m. beam model in which pre-sawn pattern parameters were systematically varied are presented in Figures

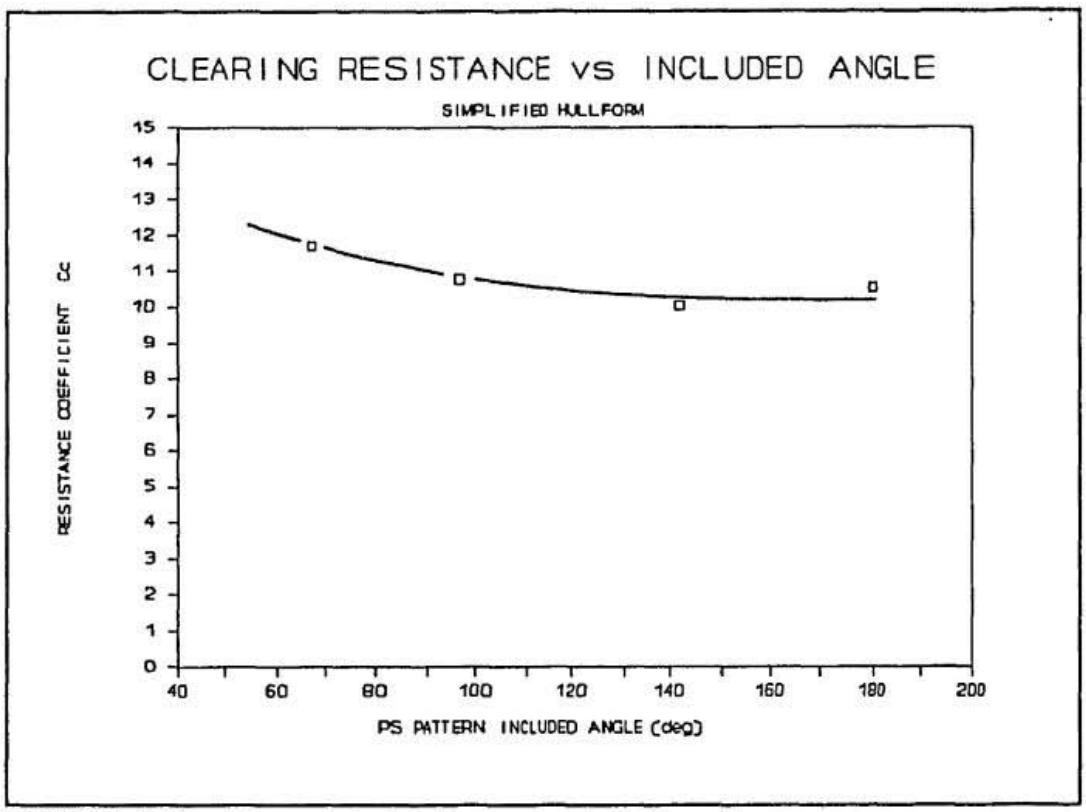

FIGURE 8.4

8.4 to 8.6. The figures include effects of variation in included angle, piece length and channel width. See Figure 7.12 for definitions of pattern parameters. Although channel width was held to a close tolerance, included angle and piece length in the pre-sawn patterns showed some random variation. However, the pattern for each test was recorded and variations

in secondary parameters are considerably less than that in the independent variable for each test.

Although scatter in the data appears to be greater than variation due to the independent parameter, each graph does show a slight trend. However, these slight trends indicate

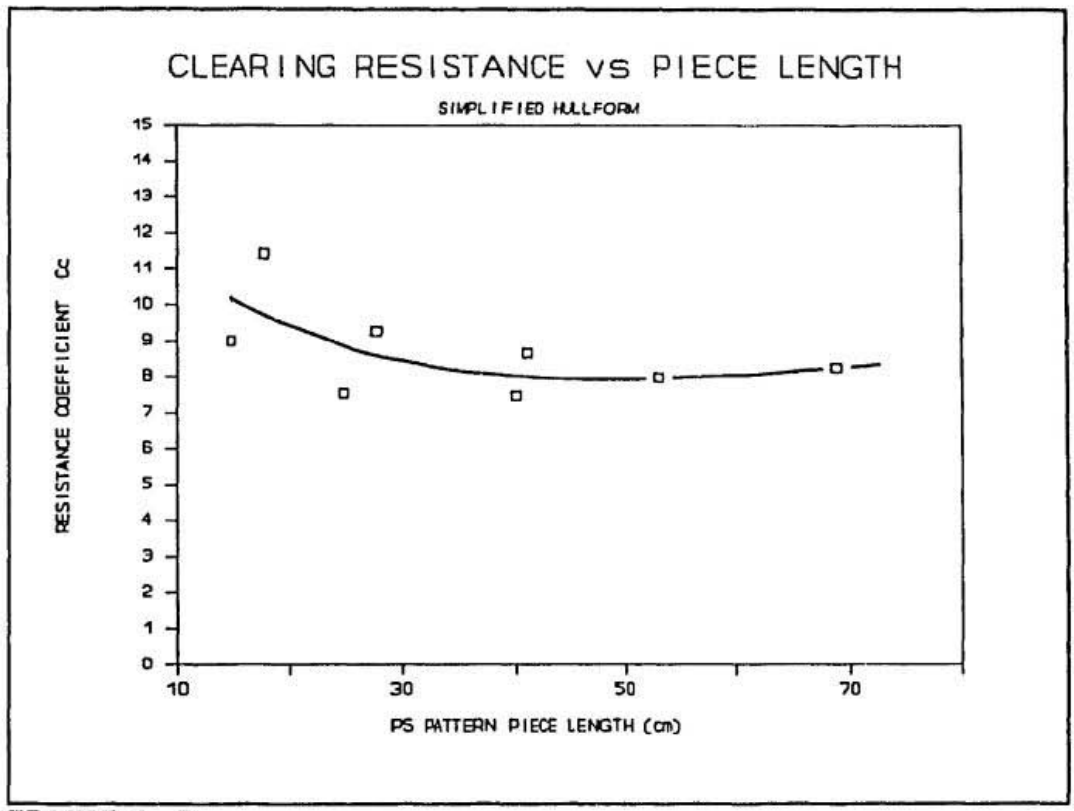

FIGURE 8.5

that the inferred clearing resistance is not sensitive to small variations in the pre-sawn pattern. This is a key prerequisite for pre-sawing to be a reliable test procedure, because small variations in pattern geometry are inevitable in routine testing.

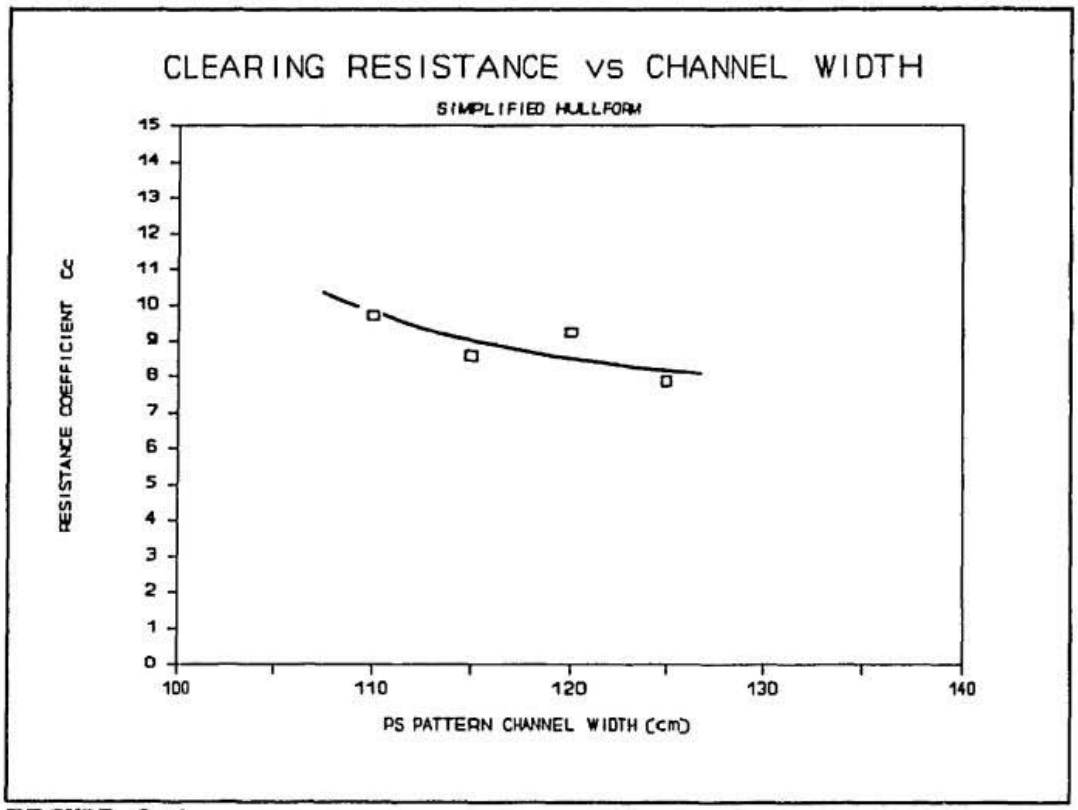

FIGURE 8.6

For these experiments and the remaining test series, pattern angle, width and piece length were measured from photographs (Figure 8.7, Photograph 14) taken over each pre-sawn channel prior to testing. This method was found to be more satisfactory than measuring the pattern directly on the ice. In determining angle or piece length for a given test all angles and piece lengths wholly within the photograph (typically 2 metres long) were measured and mean values used for data analysis.

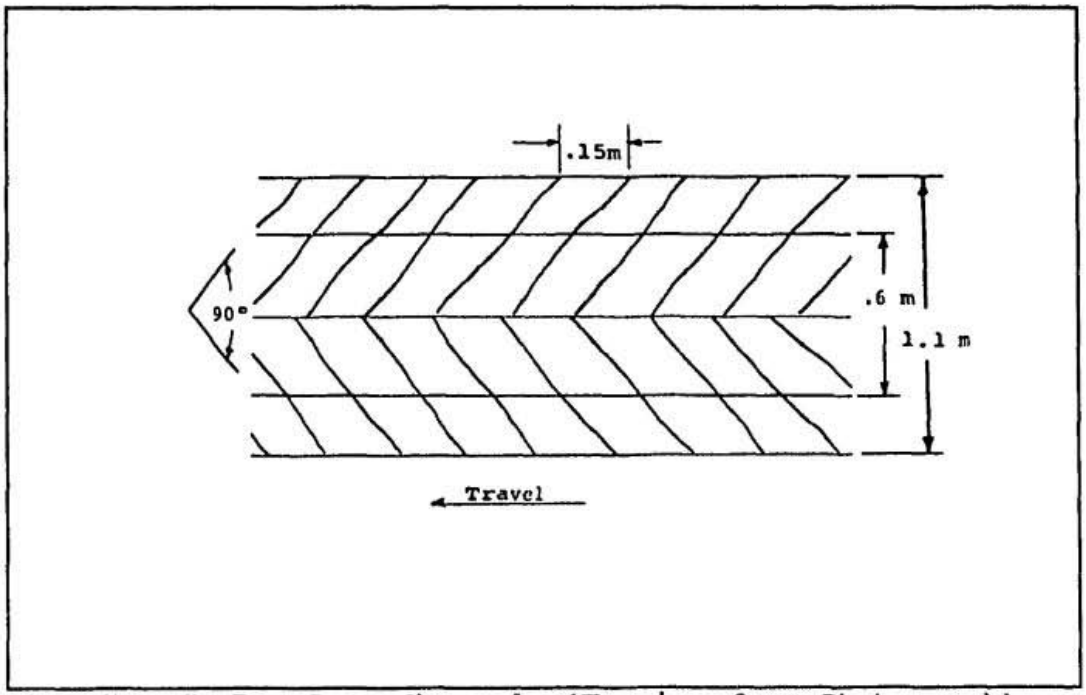

FIGURE 8.7 Pre-Sawn Channel (Tracing from Photograph)

8.3.2 Full Hull Tests

Tests on the full simplified hullform models (sets 3-5) were done to cover a range of ice strength, thickness and beam values. Both the clearing and breaking resistance components obtained from these tests are discussed below. The results show some scatter which is attributed to two main factors. The first and most important is normal variability associated with testing in ice. The second is the inability to determine accurately ice flexural strength in a given test area.

Figure 8.8 shows the non-dimensional clearing resistance coefficient for all tests on the 1.0 m beam simplified hullform. Each group of points in the figure represents a single model speed. This figure illustrates that the clearing resistance as measured by the pre-sawn method is independent of ice strength. Thus, by inference, the breaking component and the clearing component must be separate and independent.

At low speed (.10 m/s) broken pieces of ice stuck to the model bottom and moved with it rather than passing under. Apparently the combination of buoyancy and frictional forces

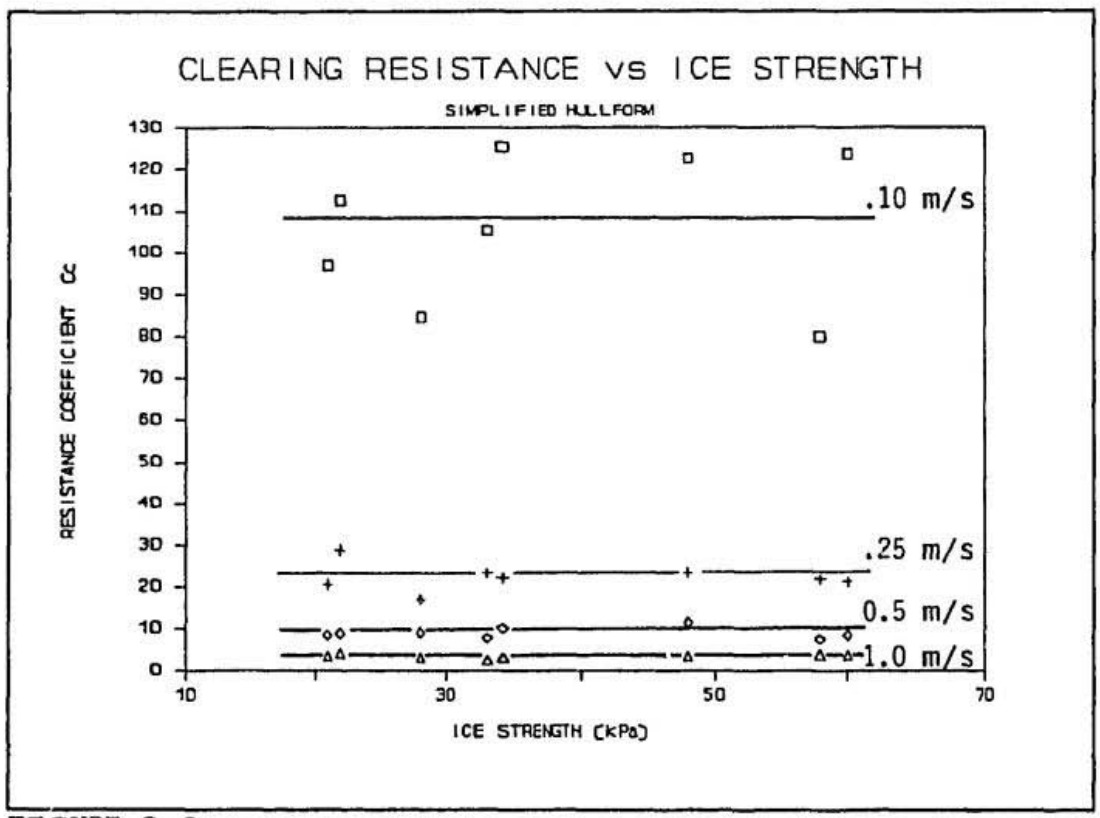

FIGURE 8.8

was greater than hydrodynamic drag on the pieces at the low speed.

To obtain the breaking resistance component from this type of ice test, the resistance measured in pre-sawn ice is subtracted from that measured in a level ice. Having established that minor variations in pre-sawn pattern do not cause major variations in resistance, nor is there an effect due to ice strength, this subtraction may now be carried out with some confidence. However, as previously noted, it is preferable to conduct the analysis using non-dimensional parameters rather than subtracting resistances directly. This was done by first obtaining the ice clearing resistances and deriving a smooth curve of clearing resistance for the hullform. Non-dimensional clearing resistance can be expressed as a function of the Thickness Froude Number (see Fig 8.9):

$$C_c = f(Fn) \tag{8.1a}$$

where

$$C_c = R_c / (\Gamma B h V^2) \tag{8.1b}$$

$$Fn = V / (gh)^{1/2} \tag{8.1c}$$

The relationship is found to be a negative power, which becomes singular as V approaches 0 and asymptotically approaches 0 as velocity goes to infinity. The singularity at zero velocity is a consequence of division by the zero velocity while the clearing resistance remains finite (the

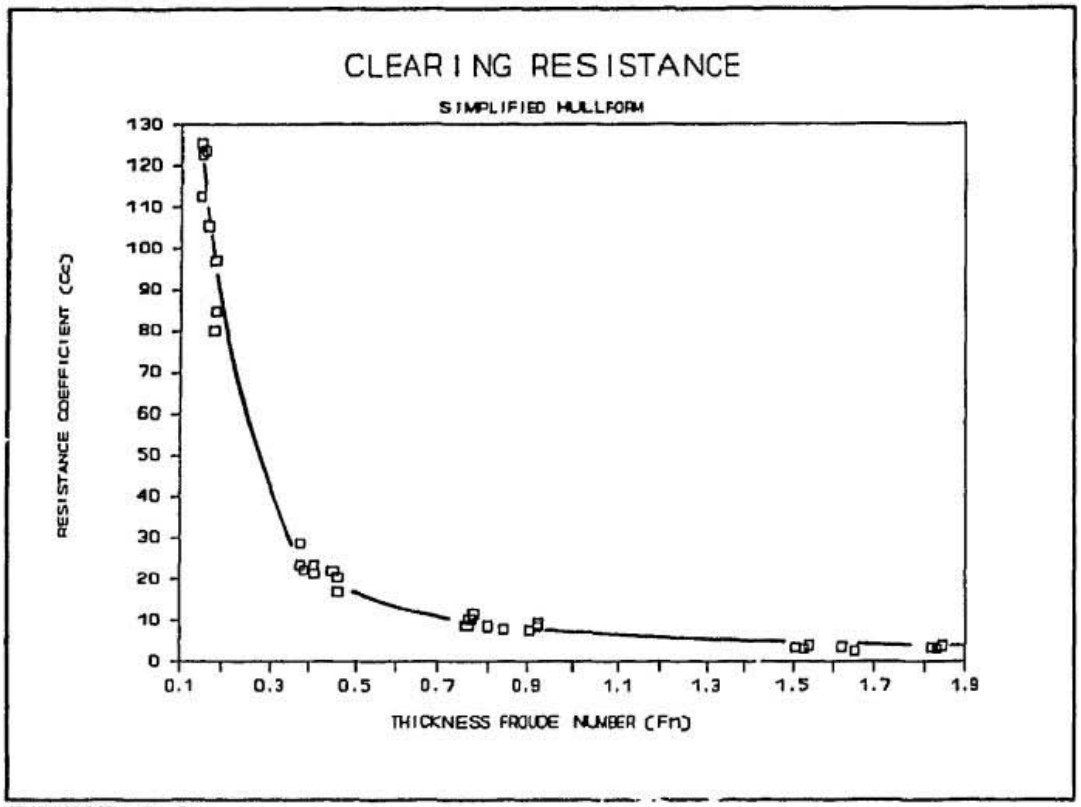

FIGURE 8.9

submergence component). The asymptotic features make it difficult to interpolate values at the extreme ends of the curve. This can be overcome by plotting values on a log-log (base 10) scale and performing a linear regression on the data. The result of this can be seen in Fig. 8.10 and is described by a best fit equation of the form:

$$C_c = k_1(Fn)^{-a} \qquad (8.2)$$

$$k_1 = 6.918$$
$$a = 1.48$$
$$r^2 = .99$$

The data can be seen to be closely grouped around the regression line and the correlation coefficient (r^2) is very good. This line is valid for all combinations of ice thickness and model velocity and thus can be used to calculate R_c for any valid (within the bounds of the regression) combination of the independent variables, via:

$$R_c = k_1 \Gamma B h V^2 (V/(gh)^{1/2})^{-a} \qquad (8.3)$$

Equation 8.3 is used to calculate values of R_c corresponding to each level ice resistance based on the measured thickness,

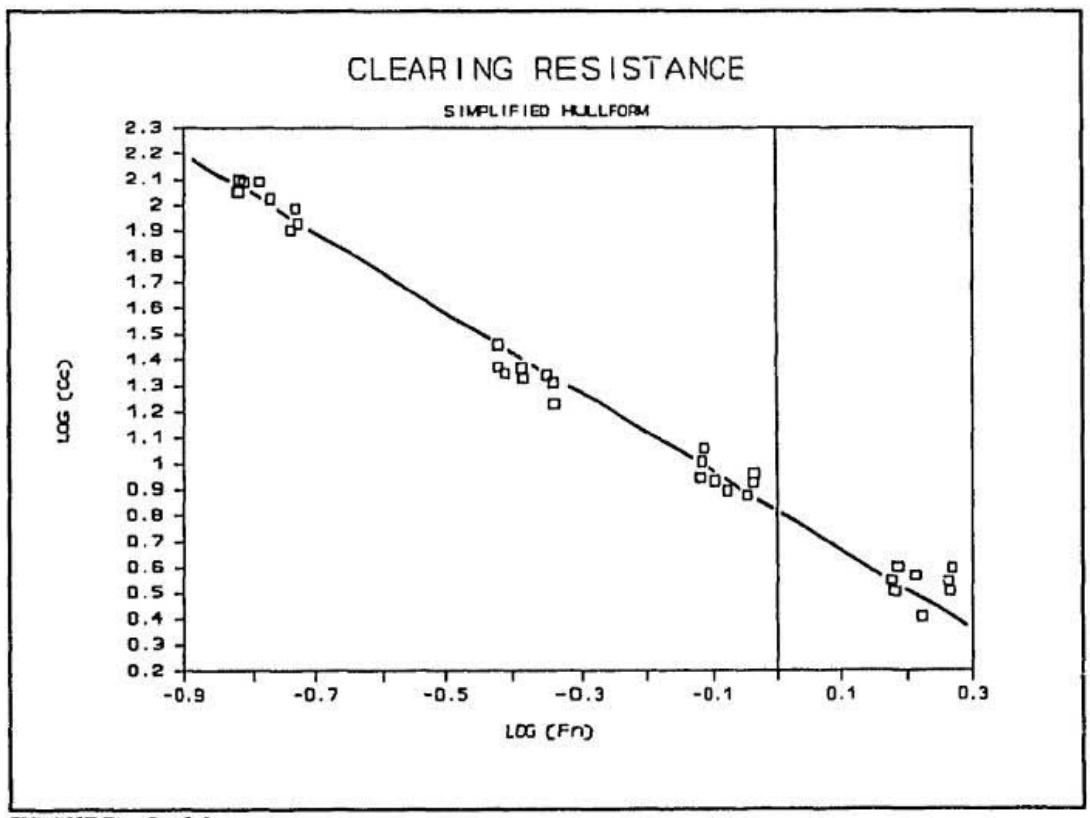

FIGURE 8.10

density and velocity. Viscous skin friction and the regression based clearing resistance are then subtracted from the total resistance to yield a breaking component R_B. Obtained in this fashion, breaking resistance may be plotted in non-dimensional form against Strength Number (Figure 8.11), and as with the clearing resistance, this reveals a negative power function:

$$C_B = g(Sn) \tag{8.4a}$$

where

$$C_B = R_B/(\Gamma bhV^2) \tag{8.4b}$$

$$Sn = V/(\sigma/\Gamma)^{1/2} \tag{8.4c}$$

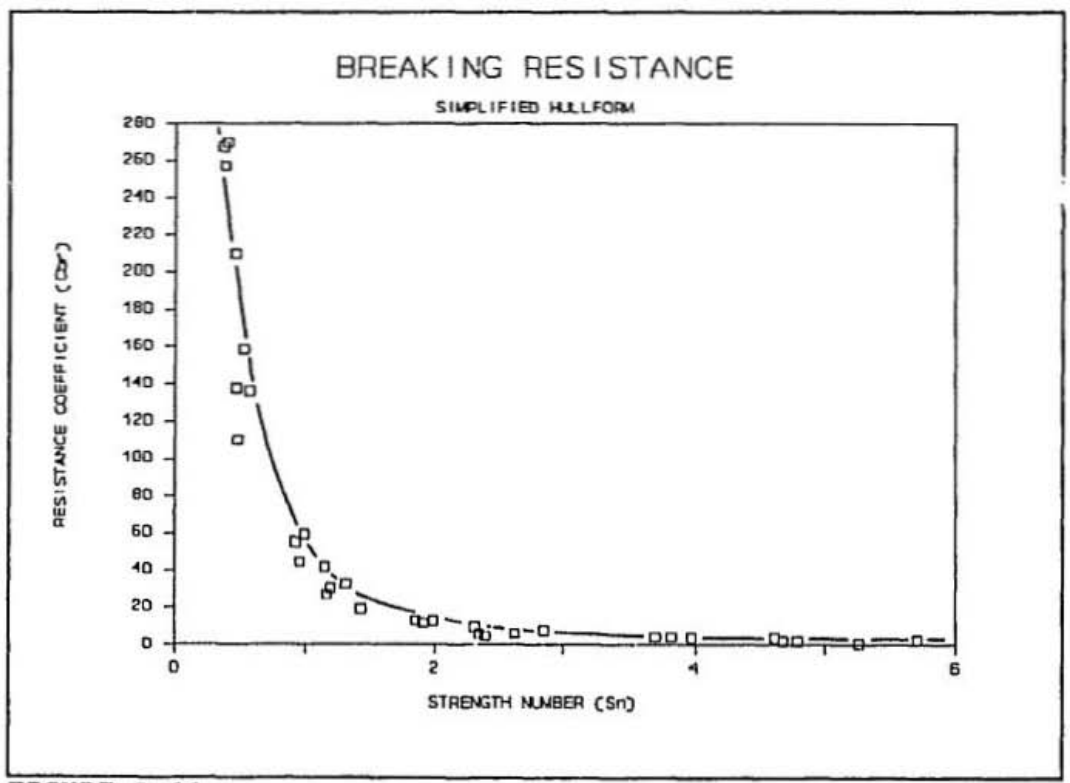

FIGURE 8.11

This function is also singular at zero velocity because of division by zero velocity and a non-zero breaking resistance at zero speed. Performing similar regression analysis on logarithmic values of the data points results in an equation of the form (see Figure 8.12):

$$C_B = k_2(Sn)^{-b} \qquad (8.5)$$

$k_2 = 42.658$
$b = 1.85$
$r^2 = .97$

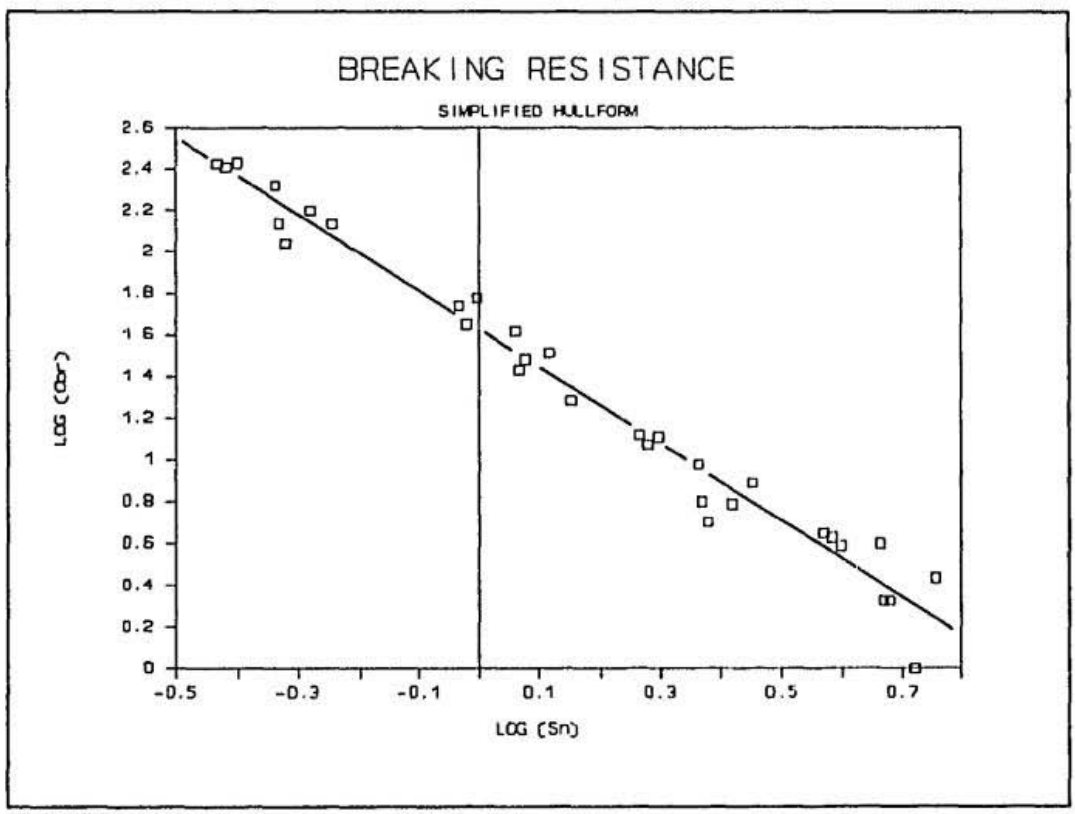

FIGURE 8.12

for which the correlation is also very good. This yields a non-dimensional expression for the breaking resistance which is valid for the tested form at all combinations of ice strength, ice thickness and model velocity.

Functional singularities at Fn = 0 and Sn = 0 indicate that the expressions are unable to predict zero speed values of the breaking or clearing components. If the equations are rearranged to solve for R_B or R_C directly, then a zero value for velocity predicts a zero value for either resistance component, unless the exponents a or b are greater than 2, in which case the resistance is infinite. Neither approach provides a satisfactory solution for predicting zero speed resistances which are, in all likelihood, both non-zero and finite.

This singularity at zero speed is not viewed as a major drawback for two reasons. Zero speed resistance is of little practical value because vessels generally have to achieve minimum speeds, well removed from zero, to maintain progress in ice. Secondly, there is undoubtedly a discontinuity in the resistance curve at zero speed because of differences in static and dynamic friction coefficients and possibly due to differences in ice failure mechanisms at speeds low enough to introduce creep deformation. Thus, any dynamic resistance formulation is unlikely to give a proper prediction of the zero speed resistance values.

8.3.3 Shallow Draft Wedge Tests

The shallow draft wedge tests showed very encouraging results in both the qualitative and quantitative sense. Measured resistances were similar both in magnitude and trend with the breaking component resistances calculated using the pre-sawing method.

Qualitatively, the tests showed that the primary icebreaking pattern for the wedge is the same as that observed for the full model. Unlike the full model, pieces behind the wedge were not significantly displaced nor did they undergo secondary breaking. The arrangement of ice pieces behind the wedge was almost identical to the pre-sawing pattern used in the full hull tests (see Figure 8.13 and Photograph 13) This is a strong endorsement of the chevron pattern as a good approximation of the primary breaking pattern for this hull form.

Analysis of data from the wedge tests was not as straightforward as originally hoped. It was intended that the clearing component should be essentially zero and thus the breaking component could be measured directly. As it turned out, it was necessary to subtract a significant clearing resistance from the total. This clearing resistance ranged from 15% to 30% of the total resistance even at this shallow draft. This compares with 35% to 65% for the full hull form. Apparently considerable energy loss is associated with initial

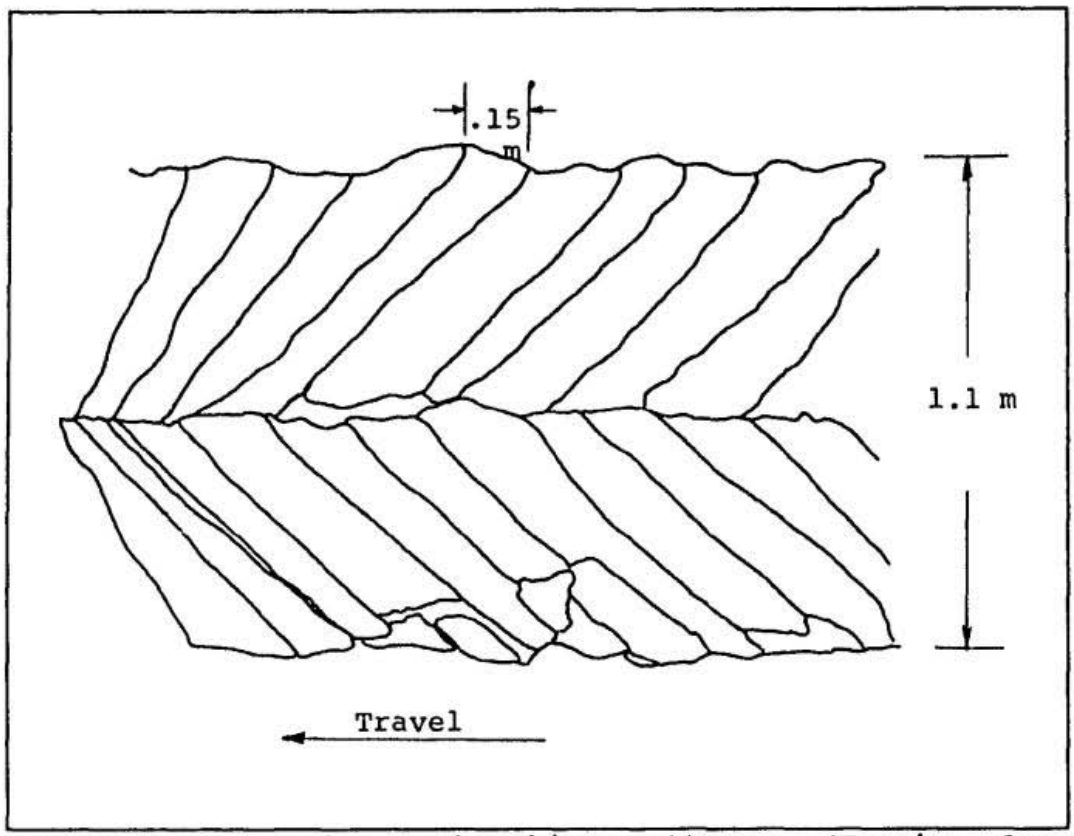

FIGURE 8.13 Wedge Icebreaking Pattern (Tracing from Photograph)

acceleration of the broken ice. Despite this, the bulk of the energy expended in towing the wedge is still attributed to primary breaking.

"Pre-sawn" measurements from the wedge tests (i.e. resistance in the broken channel) were analyzed in the same way as those from the full model trials. Clearing resistance is presented in Fig. 8.14. The regression equation from this data is used to calculate a clearing resistance for each level ice measurement. The difference between the measured level ice resistance and the smooth curve clearing resistance is

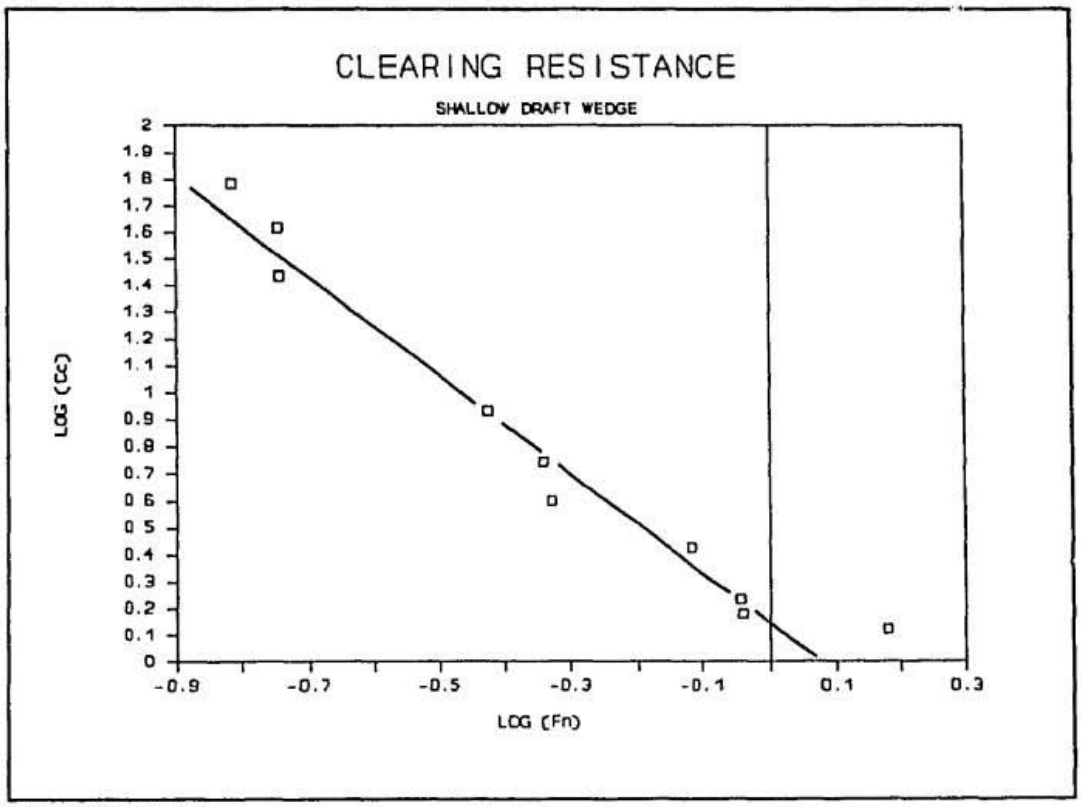

FIGURE 8.14

calculated, and the resulting breaking resistance non-dimensionalized as per the previous results. These are plotted in Fig 8.15 along with the breaking component derived by the pre-sawing method. It can be seen that the two data sets overlap. Within the data scatter, the breaking component by either method is essentially the same.

Essentially, the shallow wedge is an icebreaker with substantially reduced clearing and viscous resistances. However, because it breaks ice in the same fashion as the full hull form, it should experience the same breaking resistance component. The fact that this is so is strong confirmation

that the pre-sawing method does indeed isolate the breaking component.

Velocity effects in ice breaking were more easily observed with the wedge than they would have been with a regular model. The best example of this is again primary piece size. At low speeds the distance between transverse cracks in the chevron pattern was observed to be greater than at higher speeds. This resulted in larger primary piece sizes at lower speeds and smaller ones at higher speeds. This effect would be obscured by secondary breaking in a regular model test. It is hypothesized that this change in piece size is due to dynamic interaction between inertial forces and strength (cohesive) forces in the ice sheet. At high speeds the sheet is forced down in the area close to the bow at a rate higher than the wider area of ice can react to (inertia dominates). Thus a sharp bend is induced in the ice, close to the bow, and the ice breaks off in relatively small pieces (Photograph 6). At lower speeds the ice is able to deflect in a wider area around the bow (strength dominates) and the point of maximum stress moves away from the bow due to the larger radius of curvature (Photograph 7). Thus the ice breaks off in relatively larger pieces. This also explains why the Strength Number which is the non-dimensional ratio of inertial forces to strength forces is the parameter most relevant to the breaking component.

Increased energy absorption is attributed to an increase

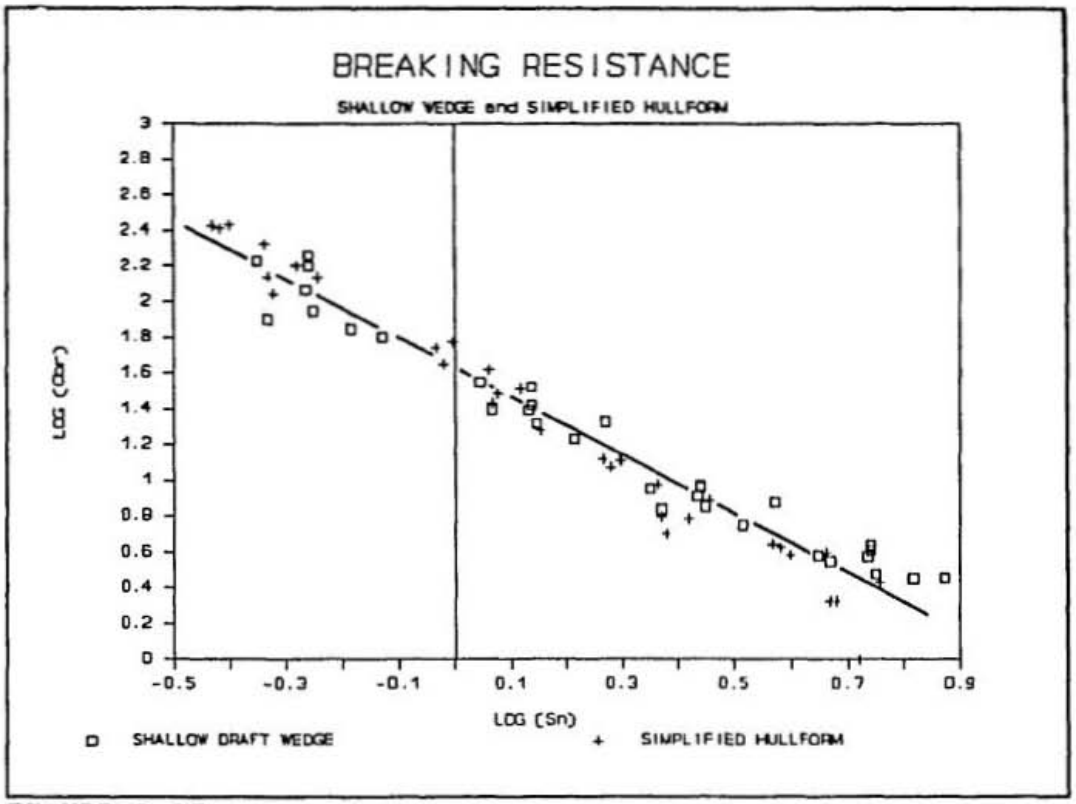

FIGURE 8.15

in created crack surface, but because fracture toughness in ice is quite low this increase is not high. This velocity dependence is borne out by the regression equation for the breaking component which can be rearranged to;

$$R_B = 42.658(BhV^{.15}\sigma^{.925}\Gamma^{.075}) \qquad (8.6)$$

showing a slight dependence on velocity in the ice breaking mechanism.

There is some question, in light of the differing deflections in the ice with vessel speed, of the role played

by elastic forces in the ice sheet. It is possible that elastic forces do not have a significant effect and that the major consumer of energy in the breaking component is the fracturing mechanism. It is also possible that the increased deflection at lower speeds results in higher energy loss to elastic mechanisms which is slightly more than compensated for by the reduction in energy lost to fracture. At the present time it is not possible to determine exactly what the interaction between deformation and fracture is, but the gross effect can be seen in the shallow velocity dependence in the ice breaking component.

8.3.4 A Case for Pre-Sawing

One of the main objectives of this study is to indicate whether or not pre-sawing ice is a legitimate model test technique and if the information gathered from such a test is of value in dividing the overall resistance into components. This is difficult to demonstrate directly, so the problem has been approached from a number of angles to see if evidence mounts for or against the test.

The first approach was to vary key parameters in the pre-sawing pattern to see what effect each of these had on the measured resistance. Results shown in Fig 8.4-8.6 indicate that the degree of scatter is higher in most cases than variation due to change in parameter. This means that the measured resistance would not vary significantly because of minor irregularities in pre-sawn pattern.

Further evidence is drawn from the data in which pre-sawn tests were performed at similar ice thickness but differing ice strength (Figure 8.8). There is no perceptible change in pre-sawn resistance with ice strength. Thus sawing the ice into an acceptable pattern effectively removes any effects of ice strength in the measured resistance.

In addition, the shallow draft wedge tests (where the ice breaking component predominated over the other two components) yielded essentially the same breaking coefficient as the pre-sawing method. That is, a large reduction in the clearing and

viscous resistance does not affect the computed breaking component.

The strongest confirmation of pre-sawing, and the chevron pattern in particular, is largely qualitative. Underwater video recordings of both level ice tests and pre-sawn tests show ice pieces flowing down around the model hull in the same manner. In addition, the primary crack pattern left by the model bow at the end of each run was observed to be almost exactly a chevron pattern. Figure 8.16 and Photograph 12 show the crack pattern left by the model at the end of a run.

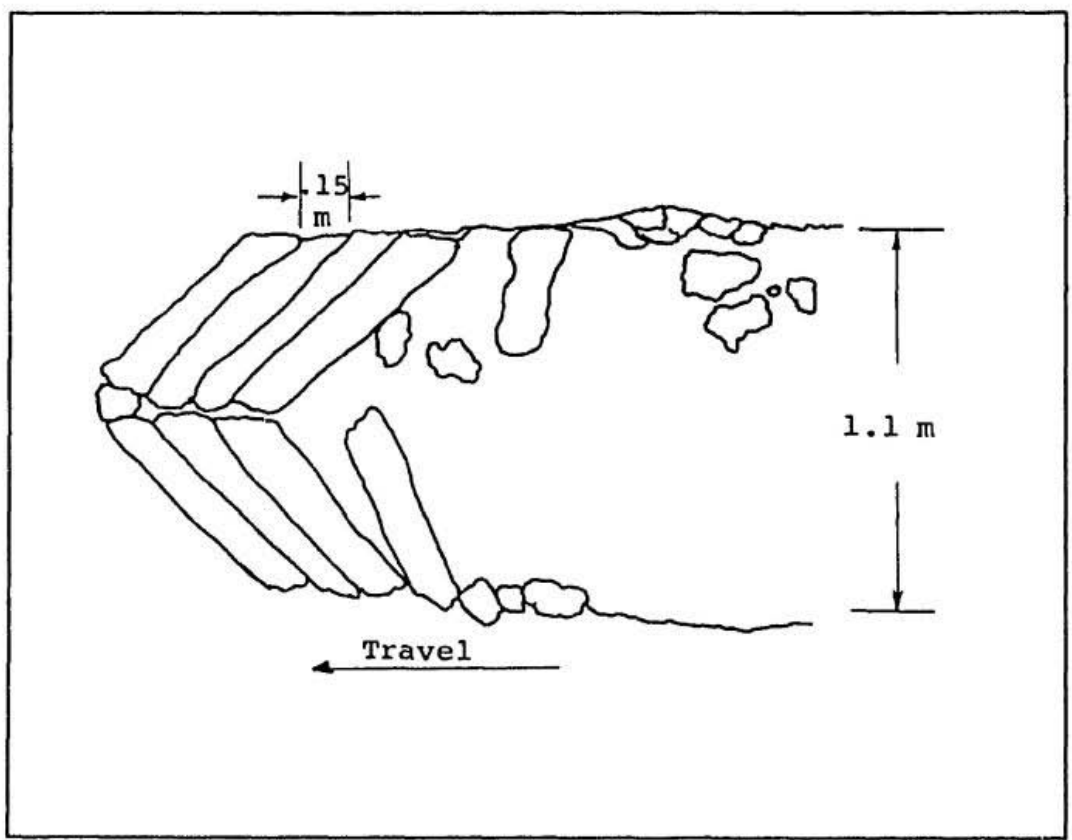

FIGURE 8.16 Broken Ice Pattern (Tracing from Photograph)

Best observations were made during the shallow draft wedge tests. During these, the ice only suffered primary cracking, breaking in the same chevron pattern with ice left behind the model arranged similarly to the pre-sawn pattern. Comparing Figures 8.16 8.13 and 8.7 or Photographs 12,13 and 14 reveals the obvious similarities.

From this evidence it is concluded that pre-sawing ice is a legitimate technique for model testing purposes. It allows the two fundamental processes, breaking ice and clearing ice, to be separated for analysis. Figure 8.17 shows the division of components for the simplified hullform.

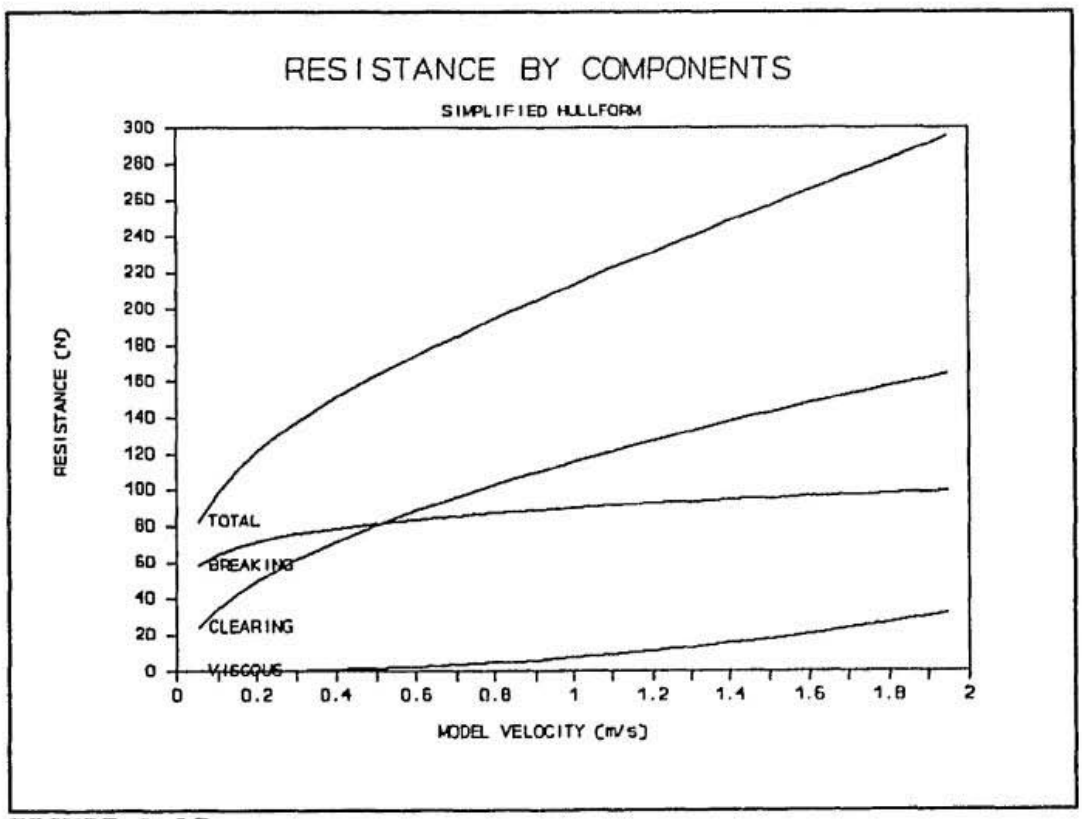

FIGURE 8.17

8.4 A Method of Analysis and Prediction

As a result of data analysis involved in the model tests, a method of presenting and analyzing data from icebreaking model tests has been developed. This method requires that presawn tests be conducted in addition to regular level ice tests. It is desirable that as many data points as possible be collected to improve confidence in the curve derived from the data. This method offers some advantages over previous methods. The primary advantage is that all data, regardless of ice strength, ice thickness or model velocity, applies to the same non-dimensional curve. This makes the most efficient use possible of results from all tests. The required parameters are non-dimensional and based on ice material properties and vessel dimensions that are easily and routinely measured at all ice model tanks, and in many full scale trials.

The basic steps in the method are:

a) Measure model resistance in level ice (R_L) and pre-sawn ice (R_p) at a range of velocity, thickness and strength suitable to cover the required range of Thickness Froude and Ice Strength Numbers:

$$\text{Measure} \qquad R_L(\sigma,h,\Gamma,V) \text{ and } R_p(h,\Gamma,V)$$

b) Calculate viscous drag on the model by an appropriate method (in this case the ITTC method) and subtract it from the pre-sawn resistance to yield an ice clearing resistance:

$$R_c(h,\Gamma,V) = R_p(h,\Gamma,V) - R_f(V) \tag{8.7}$$

c) Plot $R_c/(\Gamma BhV^2)$ vs. $V/(gh)^{1/2}$ (Thickness Froude Number) and perform a LOG-LOG linear regression to determine two constants in the equation:

$$R_c/(\Gamma BhV^2) = K_c[V/(gh)^{1/2}]^{-a} \tag{8.8}$$

d) Using the clearing regression equation (8.8) calculate R_C for each R_L and subtract it and the viscous resistance from each R_L to yield the ice breaking resistance:

$$R_B(\sigma,h,\Gamma,V) = R_L(\sigma,h,\Gamma,V) - R_C(h,\Gamma,V) - R_f(V) \quad (8.9)$$

e) Plot $R_B/(\Gamma BhV^2)$ vs. $V/(\sigma/\Gamma)^{1/2}$ (Ice Strength Number) and perform a LOG-LOG linear regression to yield two constants in the equation:

$$R_B/(\Gamma BhV^2) = K_B[V/(\sigma/\Gamma)^{1/2}]^{-b} \quad (8.10)$$

f) Using appropriate vessel and ice data, calculate model or full scale resistances based on the two regression equations and a suitable method for calculating viscous drag (skin friction):

$$R_T = R_B + R_C + R_f \quad (8.11)$$

This method provides a means of making full scale predictions or comparing model tests. It eliminates the need to accurately hit target ice conditions in order to compare or scale. The results of this analysis are non-dimensional coefficients (ice breaking and ice clearing) which are form and friction factor dependent. The drawback of the method is that the friction factor cannot be explicitly separated and

its effect can only be determined by conducting repeat tests at a number of friction factors.

In Chapter 9 this procedure is applied to a number of ship forms.

8.5 The Effect of Beam on Breaking and Clearing

One of the original intentions of this study was to demonstrate the effect of ship beam on the measured resistance independent of other form parameters. In addition it was intended to verify that beam was the most critical linear ship dimension for the purposes of non-dimensionalization. Thus, three models of the same basic shape with differing widths were tested for ice resistance. There is a problem with changing the width of a ship shape without changing any other parameters. In fact it cannot be done without changing either the length of the forebody or the bow waterline angles. In this case, it was decided to change the length of the forebody and hold constant the waterline angles. Indeed, the choice of the simplified hullform was largely dictated by the desire to vary the beam with as little impact on other form parameters as possible.

Results from these tests, broken out by component and analyzed by the method presented in the previous section, are shown in Figures 8.18 and 8.19. It can be seen that the breaking resistance coefficient is independent of beam within the bounds of the scatter exhibited in previous ice data. The clearing resistance on the other hand shows a trend of increasing coefficient with increasing beam. It is hypothesized that this is due to the hydrodynamic resistance which is buried in the clearing component. A non-linear

increase in hydrodynamic resistance with ship beam (for constant length) would be expected. Thus, it would be necessary to separate the hydrodynamic and ice clearing components before the beam effect on ice clearing could be properly demonstrated. However, as stated earlier, these two effects appear to be coupled, and their separation would require considerable additional study.

Nevertheless, the breaking component is sufficiently independent to draw conclusions about it alone. Within the bounds of the data scatter, this coefficient is essentially independent of vessel beam. Thus, the actual breaking

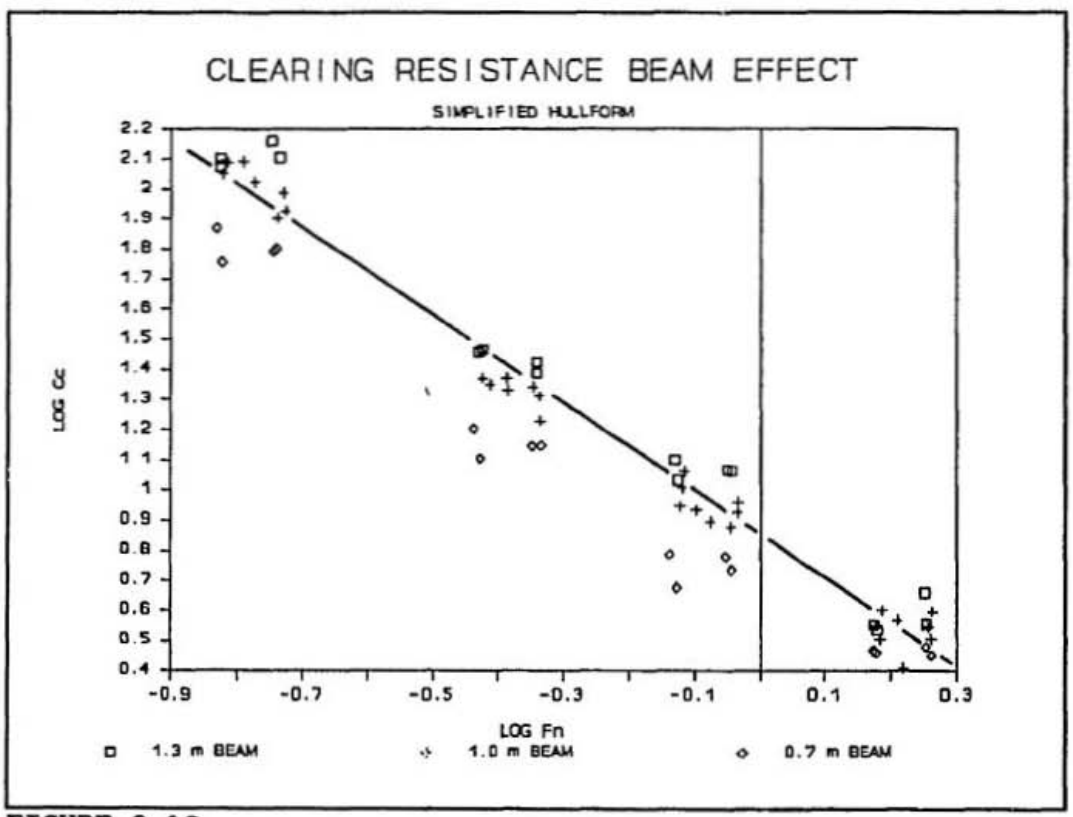

FIGURE 8.18

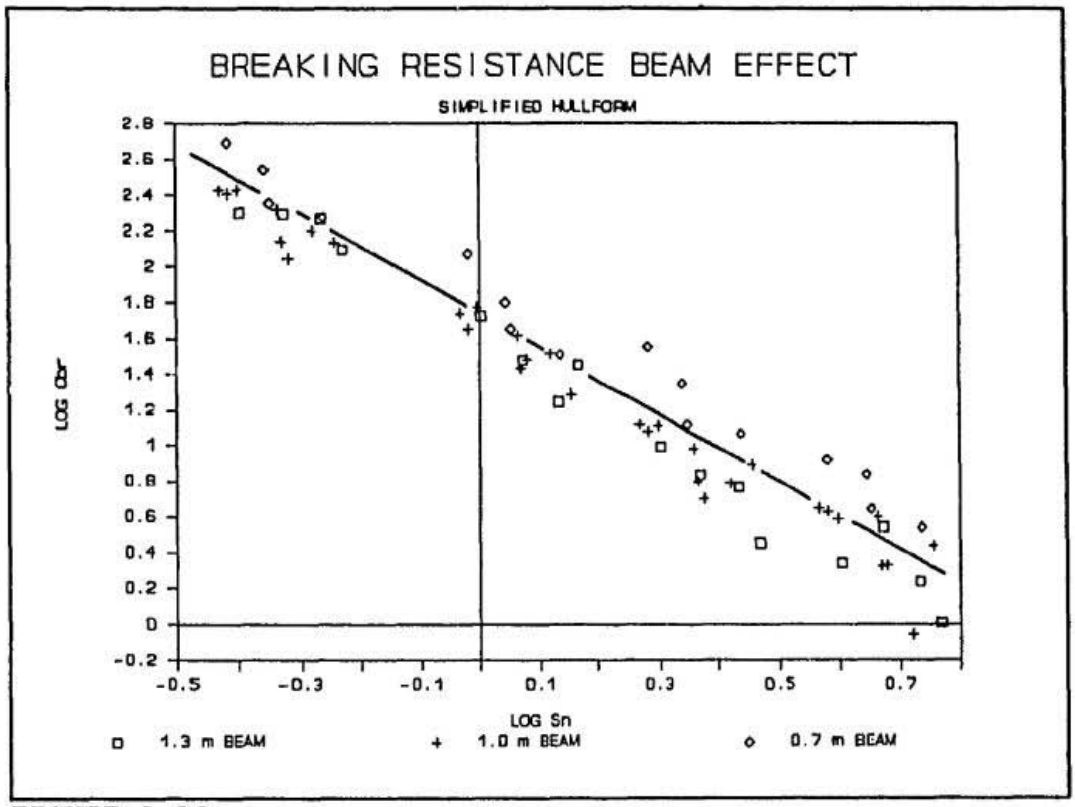

FIGURE 8.19

resistance would be linear with vessel beam. This will be further demonstrated in the following chapter with data from a realistic icebreaker form at a number of different model scales.

9. APPLICATION TO ICEBREAKER FORMS

Having developed a method of analyzing icebreaking model tests, an appropriate step is to apply the methodology to a number of icebreaker forms to provide verification of its applicability. Over a year of tank work at IMD, a number of vessels were tested, of which three hullforms are well suited to this purpose. Pre-sawing tests were carried out in all cases, and in two of the three, full scale data are readily available. Additional full scale data from a towed resistance test are also available for one vessel. Although model test data are not available for this vessel, the two component method of analysis is applied with good results.

Where pre-sawn model test data were available, the non-dimensional reduction and analysis is by the method presented in the previous chapter. All show similar relationships between parameters, with slight variations in constants and exponents. Full scale prediction presents a problem in that the components cannot be independently verified without performing a full scale pre-sawing test. This is clearly not very practical. However a full scale prediction can be made for the total resistance at any combination of parameters based on the regression lines derived at model scale. This prediction is compared to measured full scale data.

The following sections contain data from the CCGS LOUIS ST. LAURENT, the CCG R-Class Hull, the M.V. ARCTIC and the

USCGC MOBILE BAY. With the exception of the MOBILE BAY, each of these was tested in the IMD ice tank over the year 1987. The MOBILE BAY was towed in ice at full scale in 1986 and the results reported in [9.6]. In the other cases, pre-sawn and level ice tests were conducted and the data re-analyzed using the method developed in this study. Despite the fact that all the vessels presented in this chapter have curved bow forms, characteristic of icebreakers, the basic chevron pattern was used for the pre-sawing trials. Raw data for all tests and full scale trials are contained in Appendix 2.

9.1 Louis St. Laurent

Model test data for the CCGS LOUIS St. LAURENT in its original configuration(A) and with two new bow forms(B,C) are presented in Figures 9.1 and 9.2. These data were gathered as part of a study to evaluate two new bow designs with reference to the original. It can be seen that all data follow the same trend in both clearing and breaking resistances. The new bow designs both exhibit lower resistance than the original but are not significantly different from each other. For each configuration, the data are closely grouped about the mean

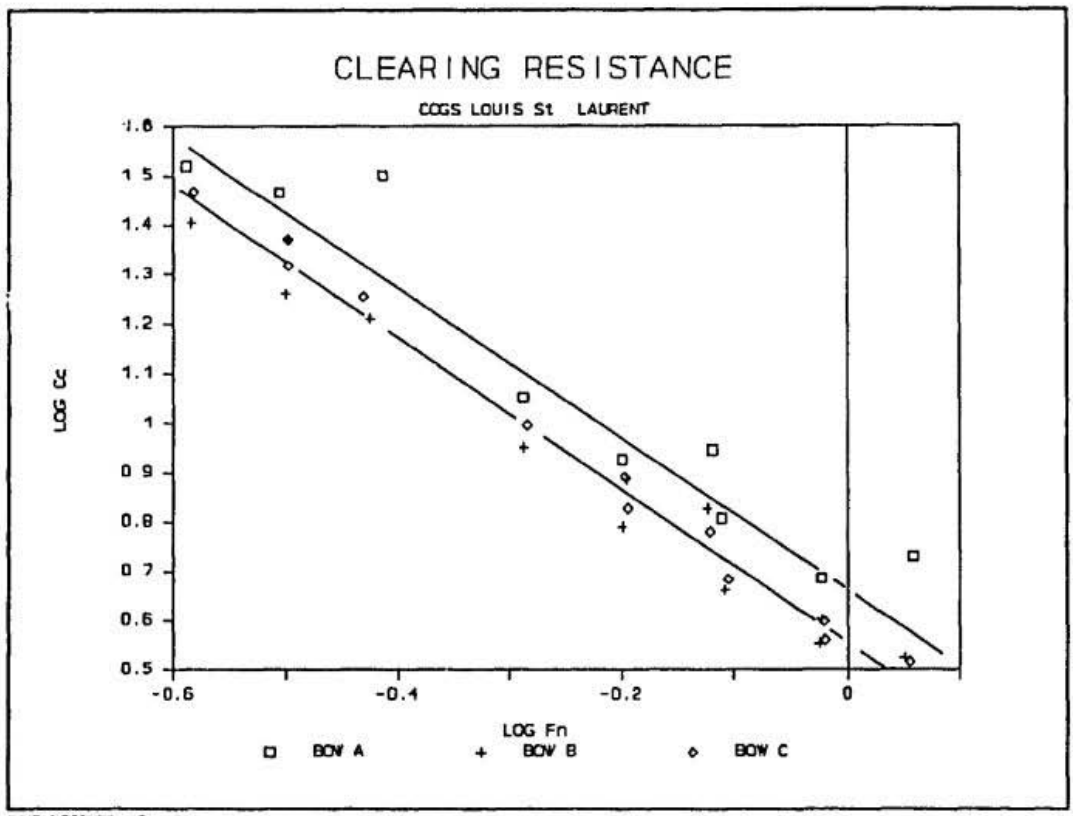

FIGURE 9.1

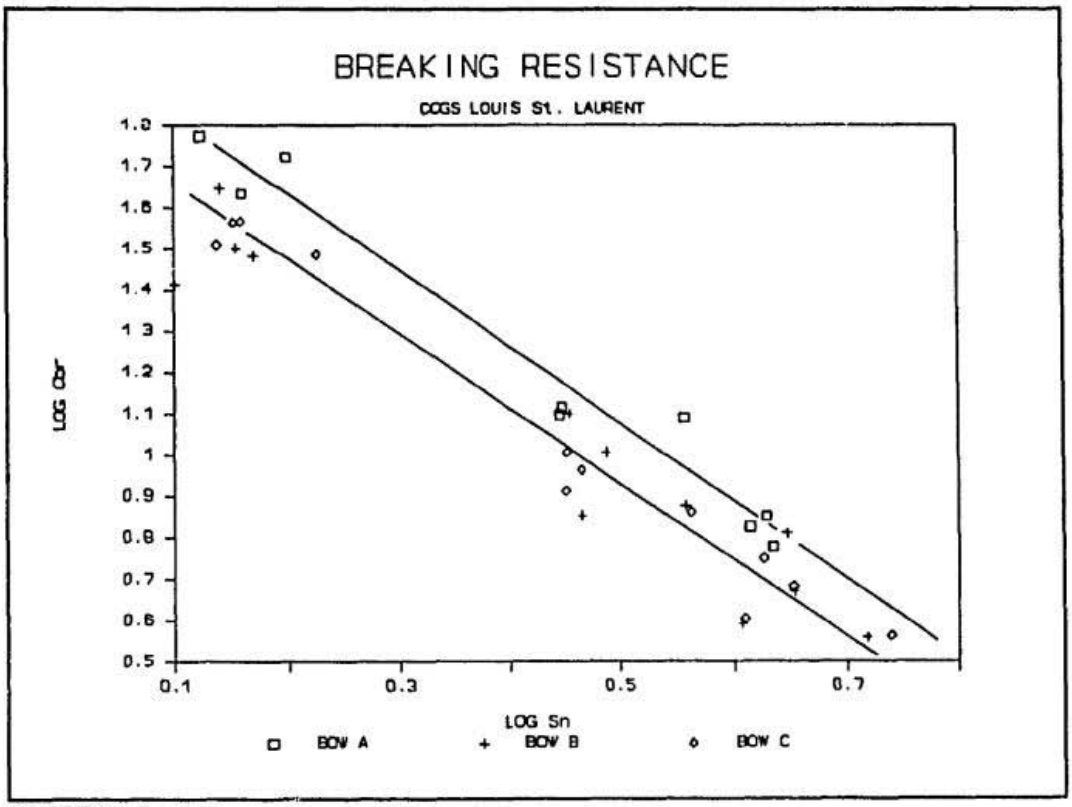

FIGURE 9.2

lines. This test series is better than many because ice strength was measured locally in each test interval rather than averaged for the entire sheet. This reduced the error associated with variations in ice strength.

Some full scale data for the original LOUIS St. LAURENT are available [9.1] and predictions for these data are made using the three component scaling method. A deviation plot for these predictions is shown in Figure 9.3. The reported data is for ice estimated to be of very low strength (155-159 kPa). The predicted resistances agree reasonably well with measured full scale values. Large scatter in the full scale data

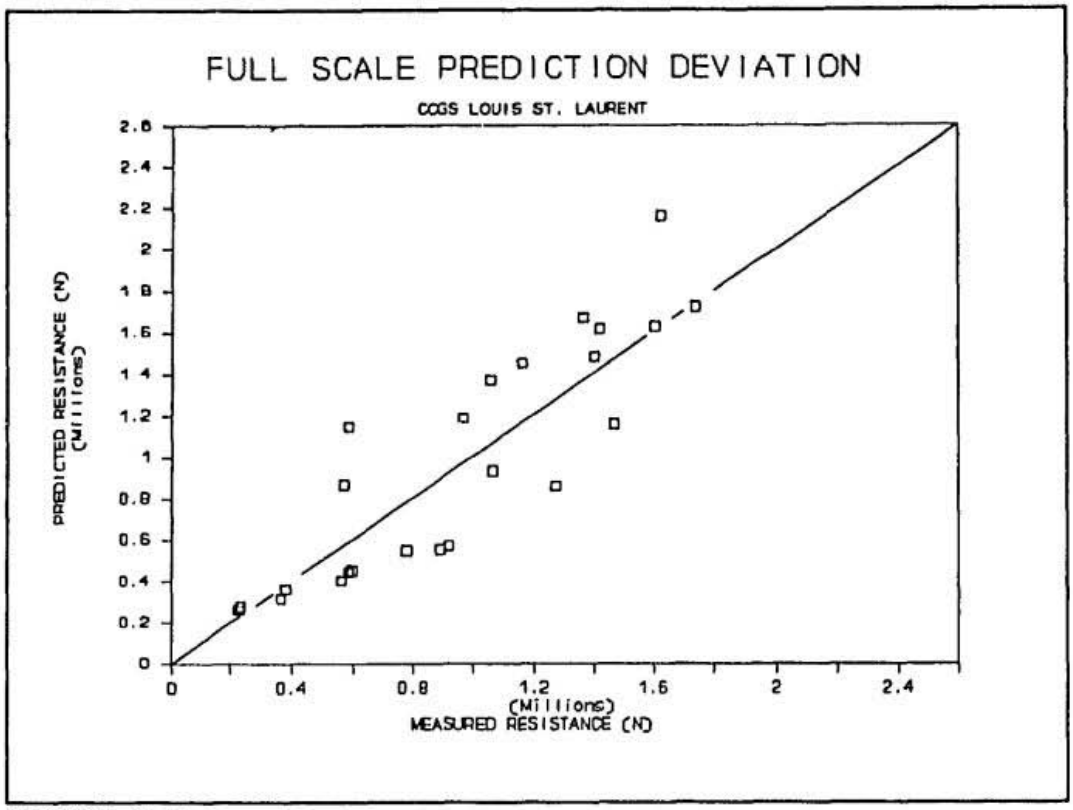

FIGURE 9.3

reflects the relatively poor quality. This is thought to be due primarily to poor strength measurements.

9.2 M.V. Arctic

The M.V. Arctic with its new bow shape was model tested using a number of differing surface coatings on the bow and mid section. Analysis of these data indicates that the midbody friction coefficient has a minor effect on overall resistance when compared to the bow friction coefficient [9.2]. Level ice and pre-sawn test data were analyzed by grouping results by bow friction coefficient. These data are plotted in Figures 9.4 and 9.5. No clear relationship is evident between the slopes of the regression lines (exponents a and b) and the friction coefficient. However, constants k_c and k_B did show

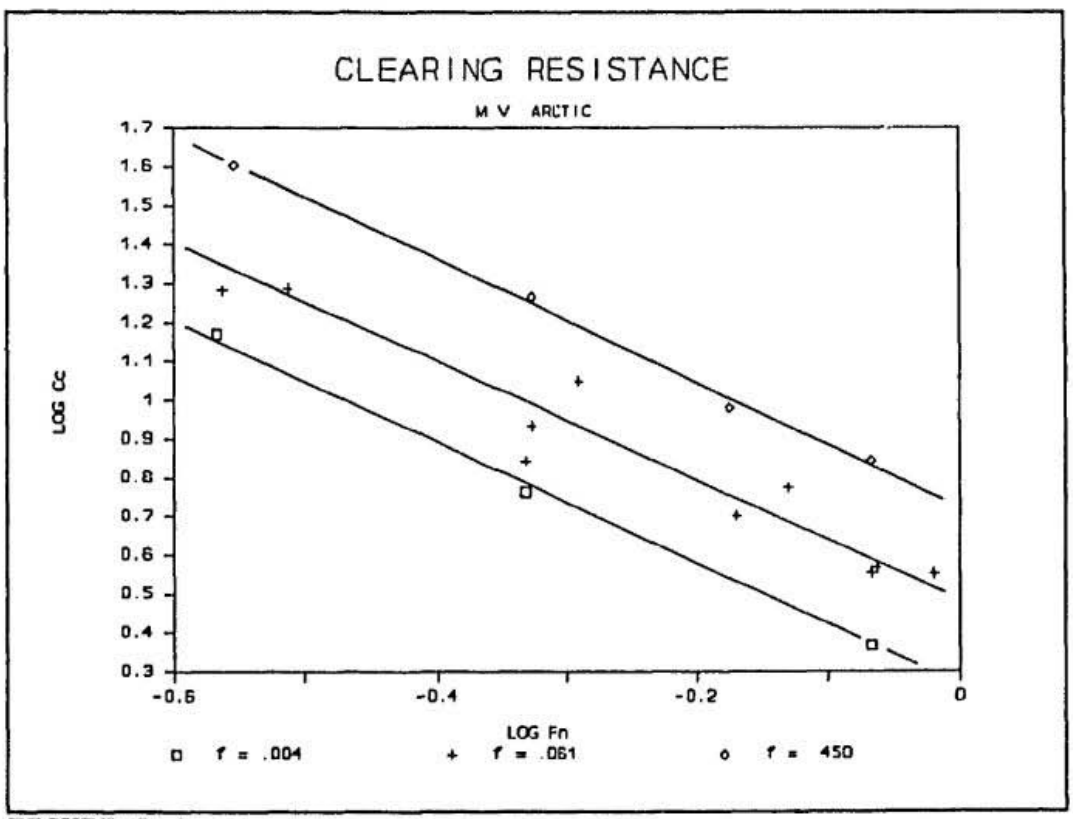

FIGURE 9.4

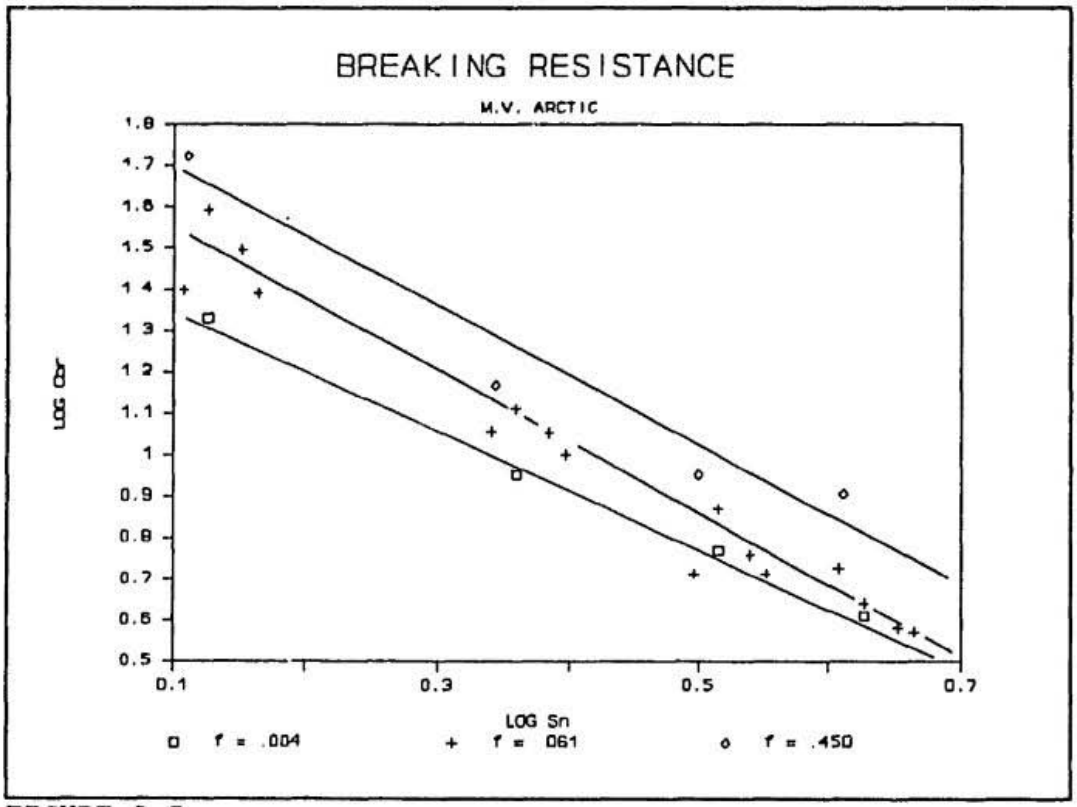

FIGURE 9.5

clear trends with bow friction coefficient. These relationships are plotted in Figure 9.6 and are remarkably well defined.

Unlike previous work,[2.8,2.10] indicating that effects of friction are linear with friction coefficient and equally applicable to all components of resistance, these data show the effect is non linear and of different magnitude for each component. This suggests expressions including effects of friction:

$$C_C = k_{CF}(\mu)^c(Fn)^{-a} \qquad (9.1)$$

$$C_B = k_{BF}(\mu)^d(Sn)^{-b} \qquad (9.2)$$

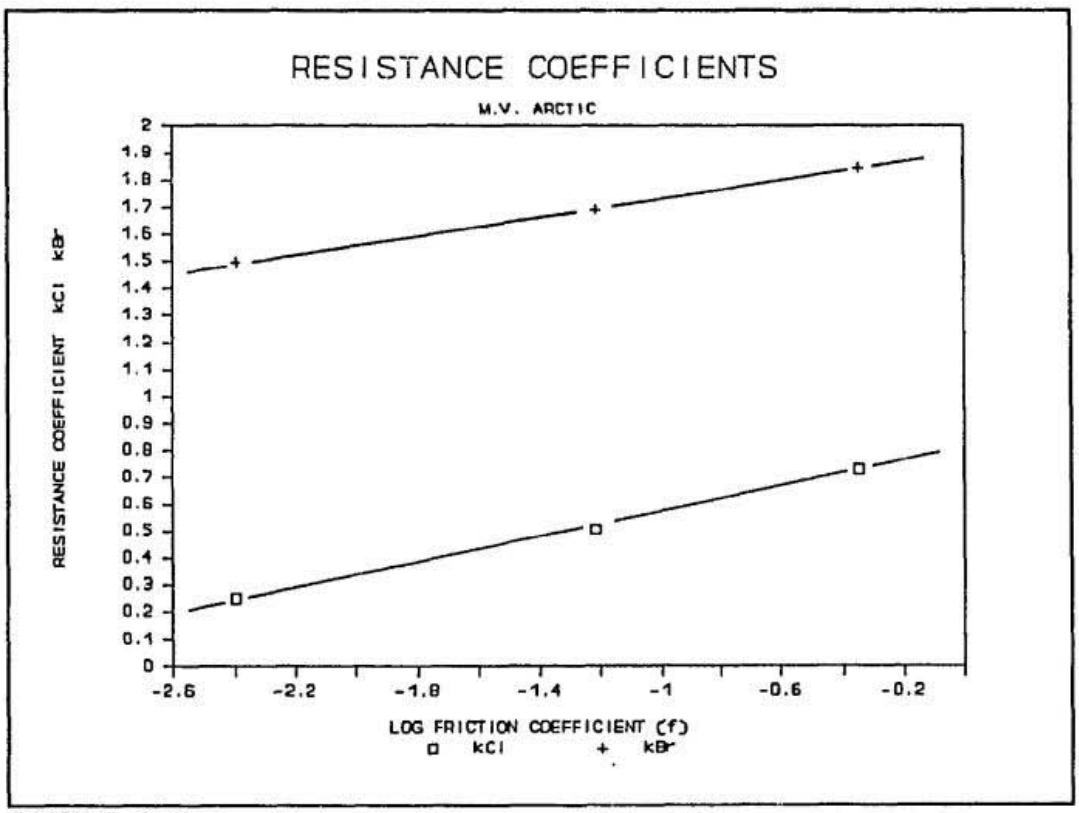

FIGURE 9.6

The equations can be combined to give an expression for total ice resistance coefficient C_I, for which coefficients and exponents are derived from model tests conducted at differing friction coefficients.

$$C_I = k_{CF}(\mu)^c(Fn)^{-a} + k_{BF}(\mu)^d(Sn)^{-b} \qquad (9.3)$$

For the M.V. Arctic model data, values of these coefficients are:

k_{CF} = 6.310
k_{BF} = 79.80
a = 1.52
b = 1.64
c = .232
d = .170

Unfortunately, full scale data for the M.V. Arctic with this new bow are not readily available and thus comparison cannot be made.

9.3 R-Class Hullform

In recent years, a large volume of data has been collected on the R-Class hullform at various facilities around the world [9.4]. More recent work at IMD has involved testing the hull at three scale factors (40,20 and 8) [9.3,9.5]. These data are shown in Figures 9.7 and 9.8. The three data sets fall into the same range for clearing and breaking components.

Clearing resistance at all three scales is essentially the same across the range of Thickness Froude Numbers. Within the bounds of data scatter there is no apparent scale effect in this component.

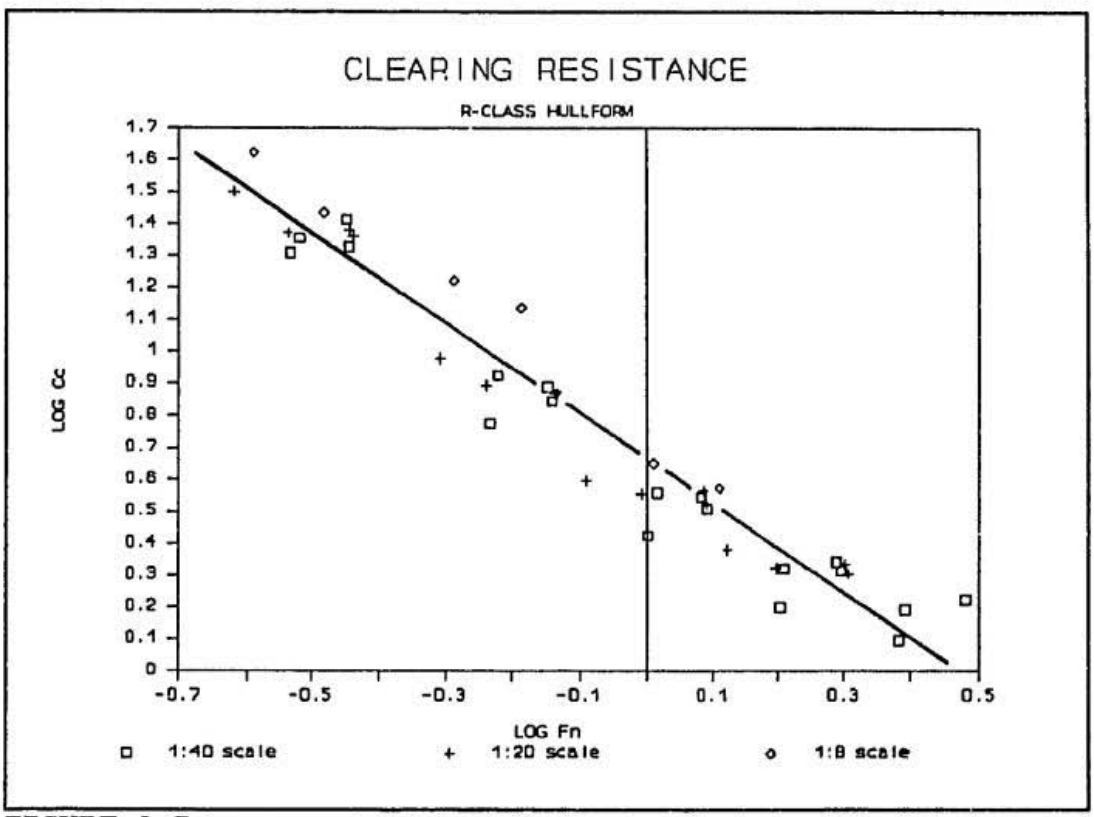

FIGURE 9.7

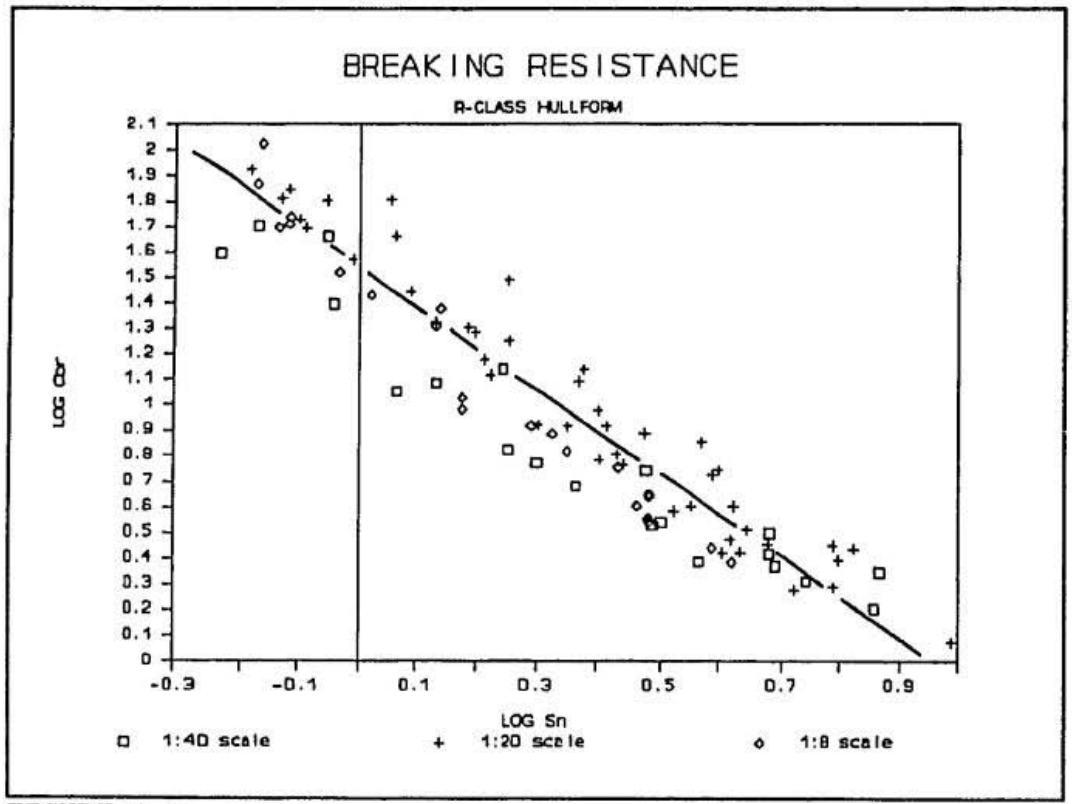

FIGURE 9.8

Breaking resistance shows more variance and some separation of the data groups. However the trend is not consistent. Results from 1:20 scale tests are higher than the other two in the middle range of Strength Number while at the ends of the curve, the three data groups converge. The 1:40 and 1:8 groups are equal across the range. Regression lines exhibit the same slope and no discernable trend in magnitude with scale. Friction coefficients for all tests were nominally the same (f=0.1) so slightly higher resistances at 1:20 are unlikely to be due to frictional effects.

If outliers are removed from consideration, the data groups are close and of similar trend. It appears that the variation exhibited in these data is more due to difference in experimental procedure than to any genuine scale effect.

Full scale data are available for two of the R-Class vessels (CCGS PIERRE RADISSON and CCGS SIR JOHN FRANKLIN). Of these, the RADISSON data from the Saugenay River showed a number of points in level ice with little or no snow cover. These data are compared with the two component model equation using coefficients derived from the 1:8 scale model tests (Figure 9.9). On average the equation is about 30% higher than

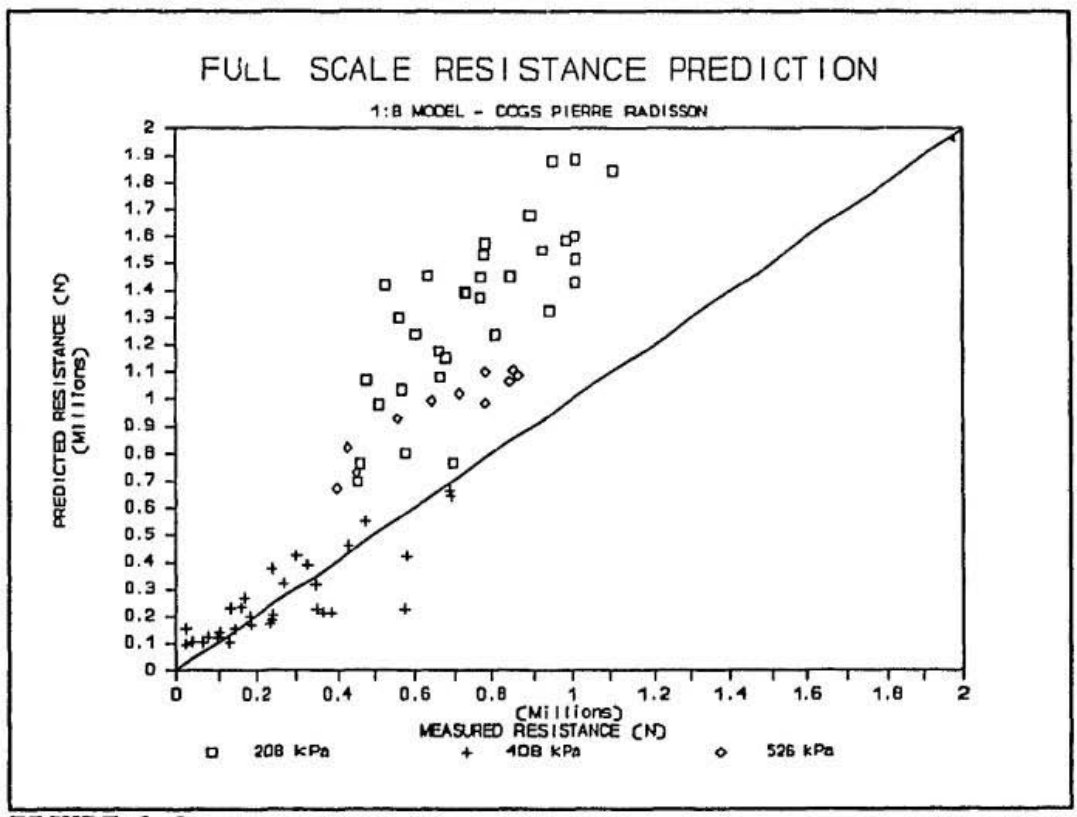

FIGURE 9.9

the data. However, only two ice strengths are quoted, and it is unlikely that over 10 trials were conducted in ice that was consistently of only one strength. The points are highly scattered but this is not unexpected with full scale data.

As with the previous two hullforms, tank data show encouraging trends in that they are closely grouped about lines of similar form. In comparison with full scale data there is a great deal of scatter. This may be due to different friction coefficients or unknown factors in the measurements.

9.4 USCGC Mobile Bay

In 1986, full scale towing tests were carried out with the USCGC MOBILE BAY (Reference [9.6]). Although the two component method cannot be applied to these data directly, because model test results are not available, the method is applied in an indirect manner. This was thought to be worthwhile because the data appears to be of good quality and full scale towed data do not have the problems of converting thrust to resistance that self propelled data have. To develop a two component regression equation, certain limiting assumptions were applied. Based on these assumptions, the method was found to be very successful.

Total reported resistance is assumed to be made up of a breaking component, a clearing component and the viscous resistance component. The viscous component is calculated by the ITTC formulation and subtracted from the total resistance to yield ice resistance:

$$R_I = R_T - R_V \tag{9.5}$$

where

$$R_I = R_C + R_B \tag{9.6}$$

The previously developed general expressions are then substituted:

$$C_I = k_C(Fn)^{-a} + k_B(Sn)^{-b} \tag{9.7}$$

It is assumed that the exponents a and b and the constants k_c and k_s are confined to the ranges previously established. Regression analysis of the data applied to the above expression results in the following:

$$k_c = 12.82$$
$$a = 1.45$$
$$k_s = 55.38$$
$$b = 1.65$$

For these constants, the data exhibited a .97 correlation coefficient (r^2) and a mean standard error of 14% See Figure 9.10). This is better than the formulation given in the reference [9.4] which shows an r^2 of .83 and a mean standard

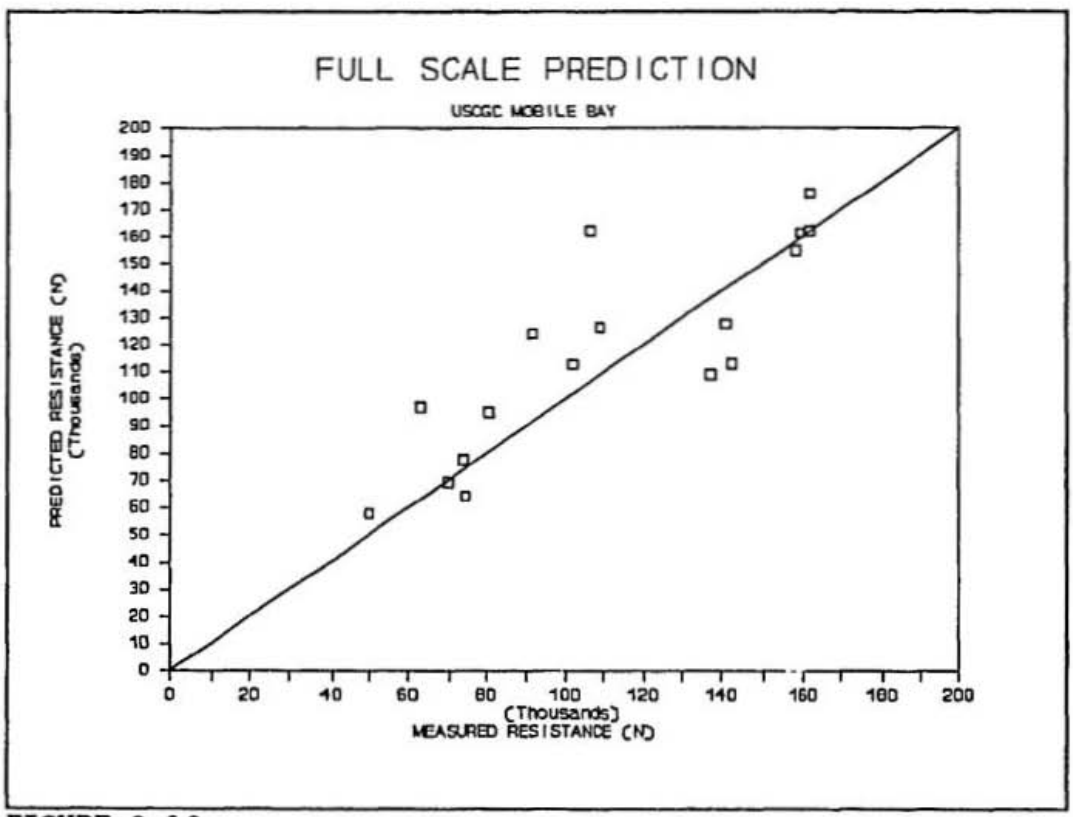

FIGURE 9.10

error of 19%. Although hardly a rigorous test of the above expression, it does provide further evidence of good fit and general applicability.

10. DISCUSSION

Although the concept of icebreaking components has been recognized for many years, little has been done to identify and explore the nature of these components. The purpose of this research has been to demonstrate that two major components of icebreaking, breaking and clearing, can be measured experimentally. Further objectives have been to develop methods of testing, analysis and scaling, and to explore characteristics of the components under varying parameters.

The analytical work has been to apply principles of dimensional analysis and force similitude to individual components of the problem rather than to the entire resistance as a whole. This has demonstrated that each mechanism is functionally dependent on different non-dimensional parameters and thus requires a separate scaling law. It is believed that this is the primary reason that, up to now, it has been so difficult to non-dimensionalize and scale the results of icebreaking tests. Without measuring both components, it is impossible to say what fraction of the total resistance is made up of either.

Choice of an inertial term (ΓBhV^2) as the common parameter on which to base the analysis is borrowed from clearwater resistance prediction and an intuitive sense that inertia in the ice sheet plays a role in both breaking the

ice sheet and clearing the broken pieces. Although the resulting Thickness Froude Number is evident in many previous developments, the Strength Number relevant to the breaking component has not been previously presented, although it is similar to the Cauchy Number. This appears to be largely because the breaking component has traditionally been assumed to be velocity independent. Although the dependence on velocity is not strong, it has consistently appeared in data collected for this study.

As part of the experimental program, two methods were used to isolate the breaking component. The direct measurement method was carried out as a verification for the pre-sawing method. The fact that the results of both techniques were nearly identical is strong evidence that the breaking component can be isolated experimentally. It is recognized that the hullform used in these experiments had a bow shape which is particularly applicable to the chevron pattern used in sawing the ice. Nevertheless, tests in which the piece size and pattern angle were varied did not result in appreciable changes in measured resistance. This indicates that the technique is robust and that minor variance in the sawn pattern does not significantly alter results of the pre-sawn test. Data for more regular icebreaker forms, for which the same chevron pattern was used, has shown the same and equally consistent trends.

The direct measurement technique is also promising as a model test procedure to measure the ice breaking component. The advantage of the test is that the ice does not have to be sawn or prepared in any way. It does, however, require construction of a separate model of the bow with the below waterline section removed. It also requires a special towing system to adequately support the model during the tow. Despite this additional expense the test does reveal interesting details about icebreaking mechanisms which are not evident in regular icebreaking tests. Alternately, because the broken pieces are not significantly displaced in the channel, the partial model could be used to prepare a pre-broken channel. The pattern in this case would presumably be the one broken by the full hull. This would eliminate the need for pre-sawing the simpler chevron pattern. For the purposes of this research, the method provided a good second approach to verify the pre-sawing technique.

In analyzing data generated for this study, a new method and presentation was developed as part of the analytical investigation. This method uses two non-dimensional groups which, while not entirely new in themselves, have been combined to give a unique method of analysis and presentation for icebreaking data. Originally it was believed that plots of the breaking or clearing coefficients against their respective non dimensional numbers would result in smooth but not necessarily mathematically definable curves. However, for

all data generated thus far, curves have been consistent in trend and definable by a single function within the range of data available. Consistency between hullforms and from scale to scale has been encouraging (See Table 10.1). The only negative aspect has been a high degree of scatter evident in all data sets. Better design of icebreaking tests may serve to reduce this scatter in the future.

Table 10.1 Resistance Coefficients

VESSEL	CLEARING				BREAKING			
	k_c	a	r^2	DF	k_B	b	r^2	DF
Simp. 0.7 m	8.13	1.492	.98	14	42.36	1.995	.98	14
Form 1.0 m	6.90	1.475	.99	30	42.76	1.854	.97	30
1.3 m	4.94	1.332	.97	14	73.96	1.749	.98	14
Louis St. A	5.19	1.462	.92	7	99.54	1.865	.97	7
Laurent B	3.64	1.479	.96	10	54.95	1.662	.93	10
C	3.64	1.565	.99	10	64.86	1.775	.97	10
R-Class 1:40	4.52	1.261	.93	18	20.65	1.354	.92	18
1:20	4.38	1.386	.96	14	41.30	1.653	.94	42
1:8	5.58	1.516	.96	4	32.43	1.898	.97	20
M.V. Arctic μ=.004	1.78	1.605	1.0	1	31.33	1.427	1.0	2
μ=.061	3.20	1.419	.93	8	49.20	1.705	.96	14
μ=.450	5.35	1.591	1.0	2	69.98	1.680	1.0	2
Mobile Bay	12.88	1.450	.97	15	54.95	1.650	.97	15

DF = Degrees of Freedom

In looking at curves for breaking or clearing coefficients an important aspect is the negative power relationship which appears for both and the implications of the value of the exponent. For both components the relationship is of the form:

$$C_R = k(Nn)^{-P} \qquad (10.1)$$

where Nn = Thickness Froude Number or Strength Number.

The exponent P ranges from 1.26 to 1.61 for the clearing component and 1.43 to 2.00 for the breaking component.

This range of exponents for the clearing component indicates a lower power in velocity for the clearing resistance than expected from theoretical considerations. With P ranging from 1.26 to 1.61, the exponent on the velocity term for R_c ranges from .26 to .61, respectively. This is considerably less than V^2 arising from simple inertial considerations. It is likely that the low power in velocity arises from interaction between a number of effects, each with widely different dependencies on velocity. These include inertia in the ice, buoyancy, friction, added mass and viscous drag.

The ice breaking resistance component shows a weaker dependence on velocity, with powers in the range 0.0 to .57, and it is easy to see how this could be interpreted as velocity independence in data sets with a high degree of scatter. Although weak, this velocity dependence has appeared consistently in all data analyzed to date. Velocity effect in the breaking component can be explained by interplay between inertial and strength forces in the ice sheet. At low speeds, strength forces dominate and the sheet deflects significantly, leading to larger curvature and a break at some distance from the point of displacement. At higher speeds inertial forces come into play and the sheet is less prone to deflection. The radius of curvature in the sheet is decreased, and the break

occurs at a point closer to the point of displacement. Thus, the distance between primary cracks decreases leading to a decrease in primary broken piece size. Because crack extent in the lateral direction is not changed significantly, more energy is expended in propagating a larger number of cracks per unit length of travel. In the terminology of fracture mechanics, more crack surface area is created, requiring more energy. Given that fracture toughness of ice is very low it is not expected that the velocity effect would be very strong and this has been the case with data to date.

Although this velocity effect has not been demonstrated at full scale, it has been with a very large model (1:8 scale R-Class). In addition, use of the three component method on data from the Mobile Bay trials showed better correlation than the method presented with that data. Figure 10.1 shows the relationship between piece sizes and model velocity measured during trials with the shallow draft wedge. It can be seen that the primary piece size is clearly related to the vessel speed.

Dependence on ice strength is nearly linear and quite consistent. It is difficult to see how so many investigators have declared resistance to be uncorrelated to ice strength. It appears likely that the inability to discern the effects of ice strength is due to poor or inadequate measurement. This is particularly true of full scale trials.

Relative magnitudes of breaking and clearing components

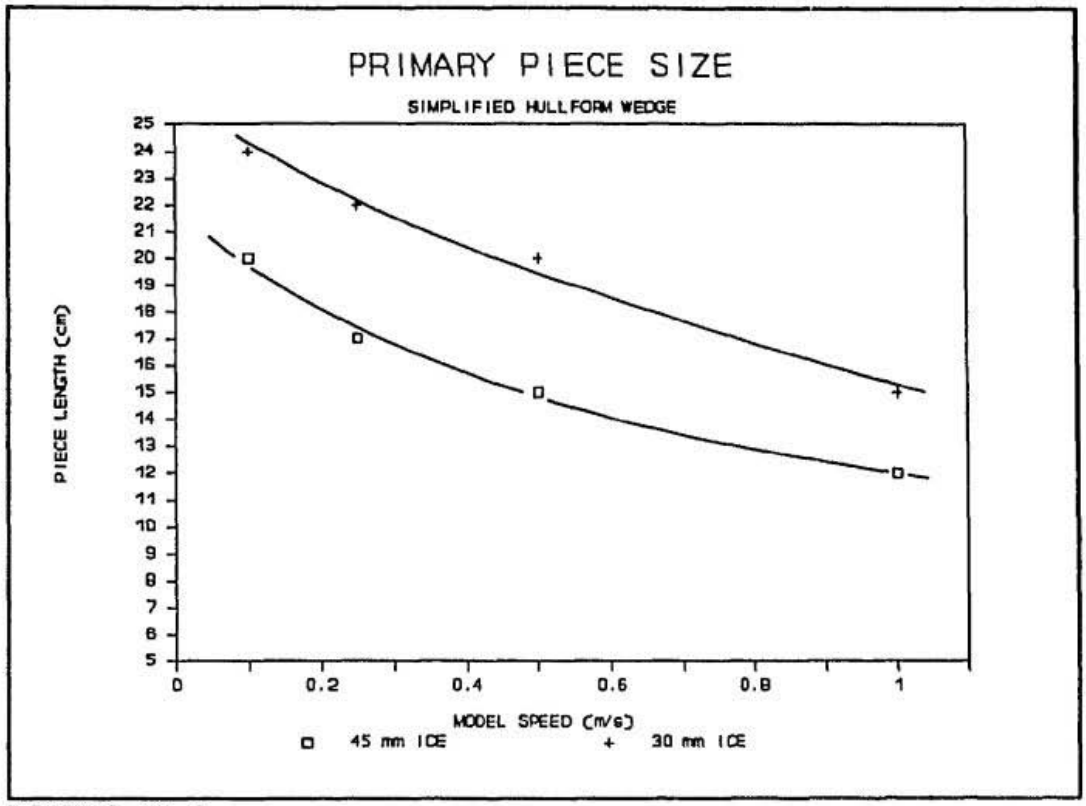

FIGURE 10.1

across a range of velocities for the simplified hullform are shown in Figure 10.2. The breaking component occupies a larger fraction of the total resistance (60-80%) at lower speeds but the proportion drops off as speed increases. Within the practical limits of vessel speeds (0 to 1.2 m/s on the graph) the relative magnitude of the breaking component drops by 20 - 30%. This is in the same range reported by Enkvist [10.1].

In separating the water induced resistance it is not yet entirely clear whether the wavemaking component can be separated from the ice clearing. For purposes of this analysis they have been left together because of apparent coupling

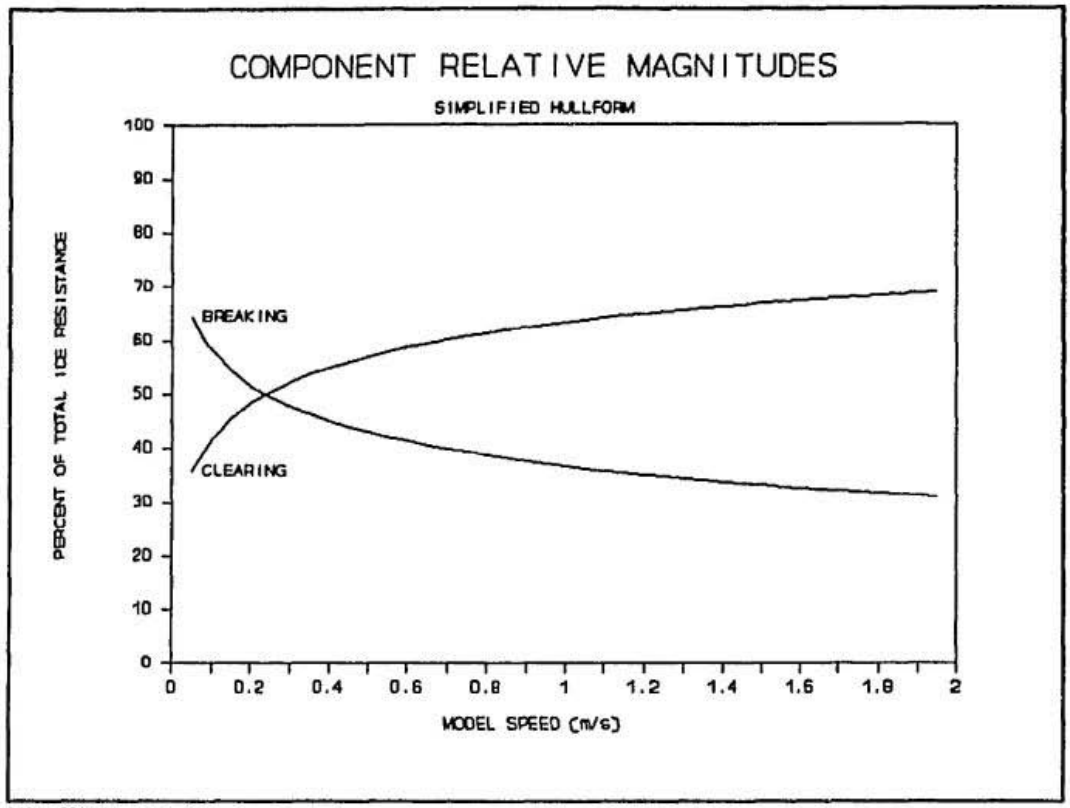

FIGURE 10.2

between the flow of water and the flow of ice around the hull. This however is based on a specific interpretation of the data and a theoretically based notion of how the clearing component should behave with velocity. Regardless of what approach is taken with open water resistance, it does not affect values of the breaking component. If, however, the full open water resistance value is subtracted from the pre-sawn resistance, this tends to make the power (P) in the clearing resistance expression,

$$C_c = k(Fn)^{-P} \qquad (10.2)$$

even more negative. The effect of this is to move the expression closer to velocity independence. Given that this dependence is already less than linear, this does not appear to be a desirable thing to do. There is, however, no conclusive data either in this study or anywhere else that indicates which is the correct approach. Subtracting only the viscous component appears to be more sensible, and this is the approach which has been taken.

Effects of friction between ice and hull have not been extensively dealt with, but the available data has enabled a few conclusions. The first is that effects of friction are not the same for both breaking and clearing components. This can be expressed as differing friction coefficients or as different constants and exponents applied to the same friction coefficient. The approach of using different coefficients has been presented previously [2.15] but no evidence has been given as to what they may be. Development of a power relationship for each resistance component based on a common friction coefficient is preferred because it is simpler to derive given the measurement and reporting of friction coefficients, and because it gives a clearer indication of velocity effects or other changes in frictional effect between the two components.

A second indication has been that the dependence of measured resistance on friction is not linear but logarithmic and at powers considerably less than one. This is not an

unexpected result, because even though the friction coefficient has been shown to be important, it is unreasonable to expect that a ten fold reduction in friction coefficient would result in a similar reduction in total ice resistance. Unfortunately, even the treatment presented in this analysis remains quite simple and does not adequately reveal effects due to sliding velocity or changing pressure.

Features identified in this study, strictly speaking, apply only at model scale and in EG/AD ice. Comparison with other data gives reasonable results but only on total predicted resistance because of the lack of pre-sawn data. Although the degree of agreement experienced thus far provides confidence in the method, it would be desirable to carry out further verification. To perform this verification completely, it is necessary to carry out level ice and pre-sawn tests across a range of velocities and friction coefficients, in addition to ice strengths and thicknesses. Although this could be easily done in other tanks and other model ice formulations, it is not very practical at full scale. Better quality full scale data could be used to verify total predictions based on model test data. The method of testing and analysis presented here provides a consistent method of ship ice model testing which makes best use of available data and provides better comparison between hullforms. The method also allows true non-dimensional scaling.

To this point, results of the analysis have been

consistent and encouraging over a number of data sets. However, comparison with earlier sets is of very limited benefit due to lack of pre-sawn data. It is hoped that this method will be applied to future icebreaking resistance trials. This should provide a degree of consistency in reported test results.

11. CONCLUSIONS AND RECOMMENDATIONS

The primary conclusion of this study is that the concept of icebreaking components is valid and offers an improved method of analyzing the results of icebreaking models. Over the course of this work the technique of pre-sawing the ice to allow separation of resistance into components has become a standard procedure at IMD. The data gathered over a two year period has proven the method to be consistent and robust enough to withstand the variability associated with normal ice tank testing.

Unfortunately, conclusions can only be drawn about model tests at the present time. Full scale data is still of poor quality and difficult to analyze with confidence. Although it is unlikely that testing to isolate icebreaking components will be routinely conducted at full scale, tests at different model scales have been consistent with each other. In addition, towed trials at full scale (USCGC Mobile Bay) have shown good agreement with two component based predictions. These facts lead to the conclusion that the major problem with self propelled full scale trials is the measurement and translation of thrust to resistance. This is compounded by the problem of making extensive and accurate ice strength measurements. These are clearly areas requiring further effort. Despite the lack of good full scale data, the model test results show reasonable correlation with most data sets.

In analyzing data on the components of icebreaking, two points which had not been previously dealt with were evident. The first is a weak but consistent velocity dependence in the breaking component of resistance. Previous developments have proceeded on the basis that this component is independent of ship velocity. This assertion was made without experimental evidence and is inconsistent with fracture theory and considerations of time dependent deformation in ice. Evidence in this study shows a clear velocity effect and the use of a non-dimensional coefficient including an inertial (velocity dependent) term has allowed a more compact and consistent presentation of data.

The second point is that there is considerable coupling between the flow of ice and the flow of water around a ships hull, particularly at higher speeds. This effect complicates analysis of ice clearing resistance and makes it difficult to identify ice mass or submergence effects. For the purpose of this research, it has been found adequate to leave the wavemaking and ice clearing components together and only separate the viscous component of hydrodynamic resistance. This, however, begs the question of interaction between ice pieces and the flow of water around the hull. There is also energy lost in the propagation of flexural and gravity waves from the ship bow. The gravity waves are considerably modified by the surface ice sheet. In further pursuit of resistance components, the area of ice-water interaction is the next

logical avenue of research. It is believed that an improved understanding of ice-water flow could improve hull design and possibly reduce problems with propeller ice ingestion. This may be particularly true as the trend in icebreaker design has been towards increasingly angular and less hydrodynamicly efficient hullforms.

The method of conducting, and more importantly, analyzing ship ice model test results developed for this study is felt to offer a greatly improved method over previous presentations. It allows all test data to be used to generate two basic curves which fully describe the icebreaking efficiency of a given hullform. It also allows more rational comparison between forms, test media or analysis of frictional effects. Friction is particularly important because the parameter has been abused as an overall correction factor in many previous developments. A consistent method of gathering and analyzing results may also offer some hope in reconciling widely varying results from different ice towing tanks.

The dimensionless parameters presented in this study are new in some respects but consistent with previous developments in the field. They parallel similar presentations for fluid flow and open water ship model testing. Use of these coefficients has shown extremely good results in terms of consistency and physical relevance to the icebreaking problem. Data presentation based on these numbers is more compact and understandable than previous methods of presenting ice

resistance.

The objectives of this study are deemed to be successfully complete in that a sound, physically-based method of analyzing icebreaking resistance has been developed and experimentally verified. In developing the method, a number of questions deserving of further research have come to light:

(a) Methods of conducting full scale trials in ice to measure the true level ice resistance.

(b) The effect of water flow on the flow of broken ice around a ships hull.

(c) Frictional effects in the interaction between ship hulls and ice.

It is hoped that these and other issues in the development of icebreaking theory can be tackled in a rational manner, with experimental support to adequately illustrate understanding of the problem

REFERENCES

2.1 Kashteljan, V.I., Poznjak, I.I., Ryvlin, A.Ja. Ice Resistance to Motion of a Ship Sudostroenie Leningrad 1968 Translation by Marine Computer Application Corp. 1969

2.2 White, R.M. Dynamically Developed Forces at the Bow of an Icebreaker D.Sc. Thesis, Massachusetts Institute of Technology, 1965.

2.3 White, R.M. Prediction of Icebreaker Capability Transactions of The Royal Institute of Naval Architects Vol. 112, 1970.

2.4 Lewis, J.W.;Edwards, R.Y. Methods for Predicting Icebreaking and Ice Resistance Characteristics of Icebreakers Transactions of The Society of Naval Architects and Marine Engineers Vol. 78, 1970.

2.5 Edwards, R.Y;Lewis,J.W.;Wheaton,J.W.;Coburn,J. Full Scale and Model Tests of a Great Lakes Icebreaker Transactions of The Society of Naval Architects and Marine Engineers. Vol. 80, 1972.

2.6 Milano, V.R. Ship Resistance to Continuous Motion in Ice Transactions of The Society of Naval Architects and Marine Engineers. Vol. 81, 1973.

2.7 Milano, V.R. Variation of Ship/Ice Parameters on Ships Resistance to Continuous Motion in Ice SNAME, Ice Tech. 1975, Montreal.

2.8 Enkvist, E. On The Ice Resistance Encountered by Ships Operating in the Continuous Mode of Icebreaking The Swedish Academy of Engineering Science in Finland Report No. 24, Helsinki, 1972.

2.9 Enkvist, E. A Survey of Experimental Indications of the Relation Between the Submersion and Breaking Components of Level Ice Resistance to Ships POAC, Helsinki, 1983.

2.10 Vance, G.P. A Modelling System for Vessels in Ice Ph.D Thesis, University of Rhode Island 1974.

2.11 Vance, G.P. A Scaling System for Vessels Modeled in Ice Ice Tech. 75, SNAME, Montreal, 1975.

2.12 Naegle, J.N. Ice Resistance Prediction and Motion Simulation For Ships Operating in the Continuous Mode of Icebreaking Ph.D Thesis, University of Michigan 1980.

2.13 Kotras, T.V., Baird, A.V., Naegle, J.N. Predicting Ship Performance in Level Ice Transactions, SNAME, Vol. 91 1983.

2.14 Carter, D. Ship Resistance to Continuous Motion in Level Ice Transportation Development Centre Report TP3679E, Transport Canada, Montreal, 1983.

2.15 Poznjak, I.I., Ionov, B.P. The Division of Icebreaker Resistance into Components Ice Tech, 81, SNAME, Ottawa, 1981.

2.16 Report of The Performance in Ice Covered Waters Committee The 17th International Towing Tank Conference Goteborg, Sweden. 1984

2.17 Atkins, A.G. Icebreaker Modelling Journal of Ship Research, Vol. 14, No. 1, 1975.

2.18 Atkins, A.G. and Caddell, R.M. The Laws of Similitude and Crack Propagation International Journal of Mechanical Sciences, Vol. 16, No. 8, 1974.

2.19 Timco, G.W. Ice Forces on Structures: Physical Modelling Techniques IAHR Symposium on Ice, Hamburg, 1984.

2.20 Lewis, J.W., DeBord, F.W., Bulat, V.A. Resistance and Propulsion of Ice Worthy Ships Transactions, SNAME, Vol. 90, 1982.

2.21 Vance, G.P., Goodwin, M.J., Gracewski, A.S., Full Scale Icebreaking Test of the USCGC Katmai Bay Ice Tech. 81, SNAME, Ottawa. 1981.

2.22 Albery, Pullerits, Dickson and Associates. M.V. Arctic Ice Transiting Performance-Continuous Mode Transportation Development Centre Report No. TP5170, Montreal, 1984.

2.23 Kim, J.K. et al Final Report, Full Scale/Model Scale Correlation Study Using Louis S. St. Laurent Hull Form Arctec Canada for German & Milne Inc., Unpublished, 1975.

2.24 Edwards, R.Y.;Dunne,M.A.;Johnson,B. Results of Full Scale Trials of CCGS Pierre Radisson Ice Tech. 81, SNAME, Ottawa, 1981.

2.25 Michailides, M., Murdey, D.C., Performance of CCGS Franklin in Lake Melville, 1980 Ice Tech. 81, SNAME, Ottawa, 1981.

3.1 Michel,B.; Ice Mechanics , Laval University Press Quebec 1978

3.2 Lovell,M.C.;Avery,A.J.;Vernon,M.W.; Physical Properties of Materials , Van Nostrand Reinhold Toronto 1976

3.3 Mellor,M.; Mechanical Properties of Polycrystalline Ice IUTAM Symposium Copenhagen Denmark

3.4 Croasdale,K.R.; Ice Engineering II Ice Forces on Offshore Structures , Symposium on Offshore Mechanics and Cold Ocean Engineering 1983

3.5 Hallam,S.D.; The Role of Fracture in Limiting Ice Forces IAHR Ice Symposium Iowa City 1986

3.6 Sinha,N.K.; Rate Sensitivity of Compressive Strength of Columnar Grained Ice Experimental Mechanics Vol 21 1981

3.7 Sanderson,T.J.O.; A Pressure Area Curve For Ice ,IAHR Ice Symposium Iowa City 1986

3.8 Frederking,R.;Hausler,F.U.; The Flexural Behavior of Ice From In Situ Cantilever Beam Tests IAHR Symposium on Ice Problems Sweden 1978

3.9 Sodhi,D.S.; Flexural and buckling failure of Floating Ice Sheets Against Structures IAHR Ice Symposium Iowa City 1986

3.10 Sinha,N.K.;Timco,G.W.;Frederking,R.; Recent Advances in Ice Mechanics in Canada , Proceedings OMAE Houston 1987

3.11 Frederking,R.;Timco,G.W.; Field Measurements of the Shear Strength of Columnar Grained Sea Ice , IAHR Ice Symposium Iowa City 1986

3.12 Hobbs,P.V.; Ice Physics , Clarendon Press, Oxford, 1974

3.13 Oksanen,P.; Friction and Adhesion of Ice Technical Research Centre of Finland, Laboratory of Structural Engineering Publication 10 1983

3.14 Tusima,K.; Friction of a Steel Ball on a Single Crystal of Ice , Journal of Glaciology, Vol. 19 No. 81, 1977

3.15 Forland,K.A.; Tatinclaux,J.C.; Experimental Investigation of the Kinetic Friction Coefficient of Ice , CRREL Report No. 85-6, Hanover NH., 1985

3.16 Tusima,K; Tabata,T; Friction Measurements of Sea Ice on Flat Plates of Metals, Plastics and Coatings , POAC 1979

3.17 Miller,K.J.; The Application of Fracture Mechanics to Ice Problems , IUTAM Physics and Mechanics of Ice Symposium Copenhagen 1979

3.18 Goodman,D.J.; Tabor,D; Fracture Toughness of Ice: A Preliminary Account of Some New Experiments Journal of Glaciology No. 21 1978

3.19 Goodman,D.J.; Critical Stress Intensity Factor (K_{IC}) Measurements at High Loading Rates for Polycrystalline Ice , IUTAM Physics and Mechanics of Ice Symposium Copenhagen 1979

3.20 Urabe,N.; Iwasaki,T.; Yoshitake,A; Fracture Toughness of Sea Ice , Cold Regions Science and Technology No. 3 1980

3.21 Urabe,N.; Yoshitake,A.; Fracture Toughness of Sea Ice In-Situ Measurement and its Application , POAC 81 Quebec 1981

3.22 Urabe,N.; Yoshitake,A.; Strain Rate Dependent Fracture Toughness (K_{IC}) of Pure Ice and Sea Ice IAHR Symposium on Ice Quebec 1981

3.23 Weeks,W.;Assur,A.; The Mechanical Properties of Sea Ice Cold Regions Science and Engineering Monograph 11-C3 U.S. Army 1967

3.24 Timco,G.W.; EG/AD/S: A New Type of Model Ice for Refrigerated Towing Tanks , Cold Regions Science and Technology Vol 12 1986

5.1 Sharp,J.J.; Hydraulic Modelling Butterworths Toronto 1981

7.1 Jones,S.J.; Canada's New Ice Tank 21st American Towing Tank Conference 1987

7.2 Parsons,B.L.;Snellen,J.B.;Hill,B; Physical Modelling and the Fracture Toughness of Sea Ice Fifth International OMAE Symposium Tokyo, 1986

7.3 Hirayama,K.; Properties of Urea-Doped Ice in the CRREL Test Basin CRREL Report 83-8P 1983

8.1 Principles of Naval Architecture Ed. J.P. Comstock Society of Naval Architects and Marine Engineers New York 1967

9.1 Lewis,J.W. et al; A Semi Empirical Ice Resistance Model Arctec Canada Report to Transport Canada TP4375E Transport Canada Montreal

9.2 Williams,F.M.;Snellen,J.B.;Bell,J.; The Effect of Surface Friction on Ship Model Resistance in Level Ice NRCC Report TR-AVR-02 1987

9.3 Newbury, S. "R" Class Icebreaking Experiments with Model 327 and Comparison with 1:40 Scale and Full Scale Results NRCC Report, LTR-SH-383, 1984.

9.5 Colbourne,D.B.; Model Tests in Ice of a 1:8 Scale Model of the CCG R-Class Hull NRCC Report TR-AVR-07 1987

9.6 Zahn,P.B.;Humphreys,D.;Phillips,L.; Full Scale Towed Resistance Trials of the USCGC Mobile Bay in Uniform Level Ice SNAME Transactions 1987

PHOTOGRAPHS

List of Photographs

PHOTOGRAPH 1 SIMPLIFIED HULLFORM 1.0 m BEAM

PHOTOGRAPH 2 TOWING GIMBAL

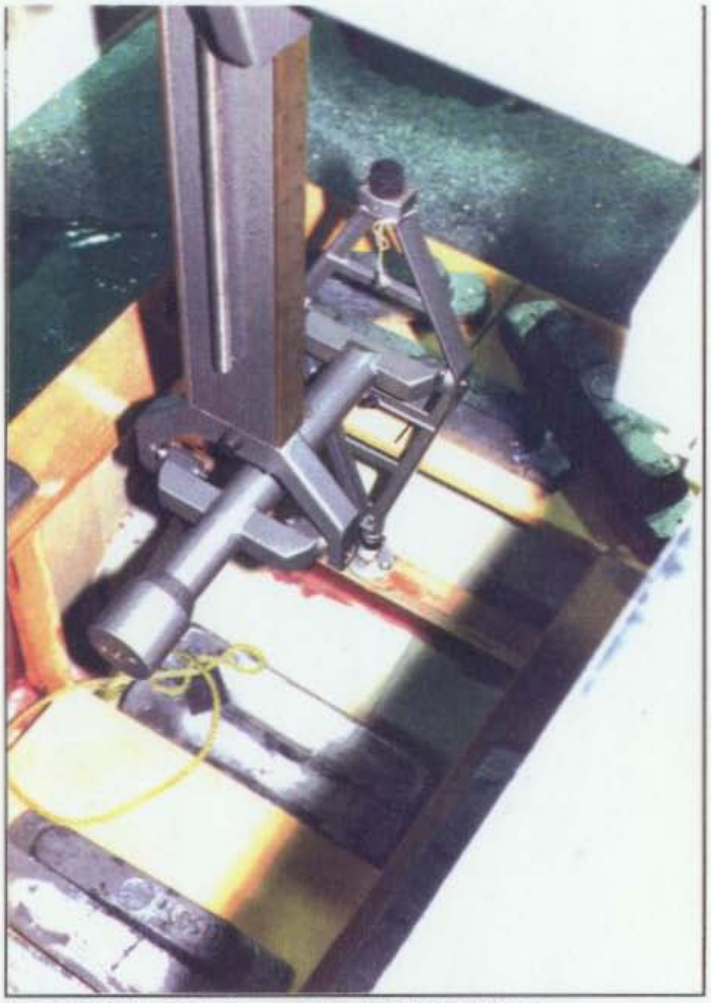

PHOTOGRAPH 3 YAW RESTRAINT

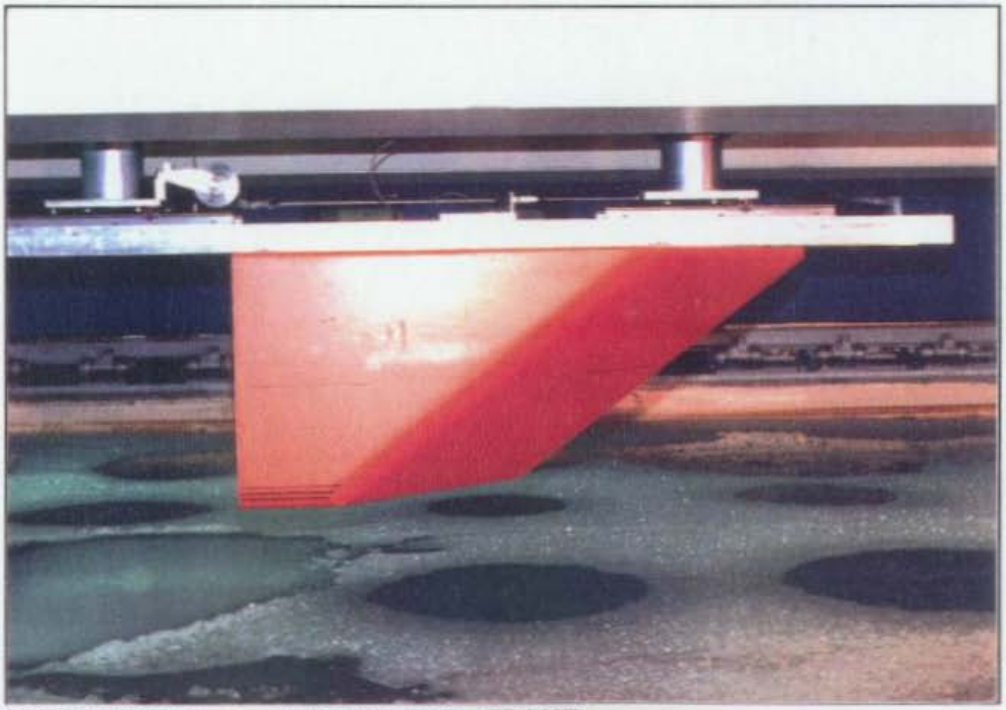

PHOTOGRAPH 4 WEDGE TOW FRAME

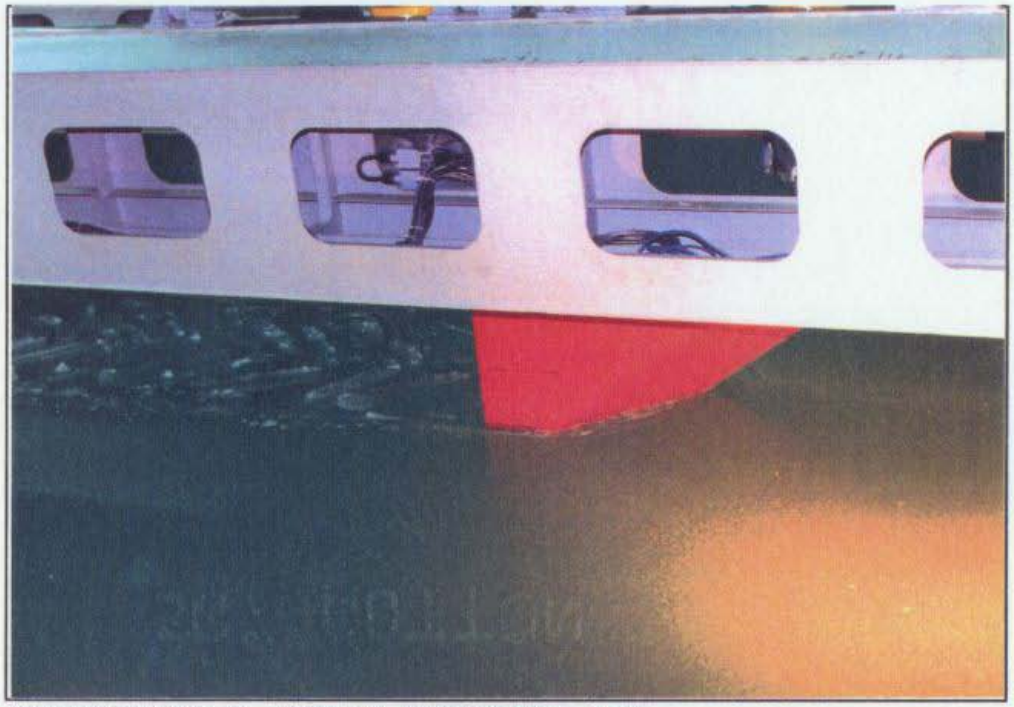

PHOTOGRAPH 5 WEDGE BREAKING ICE

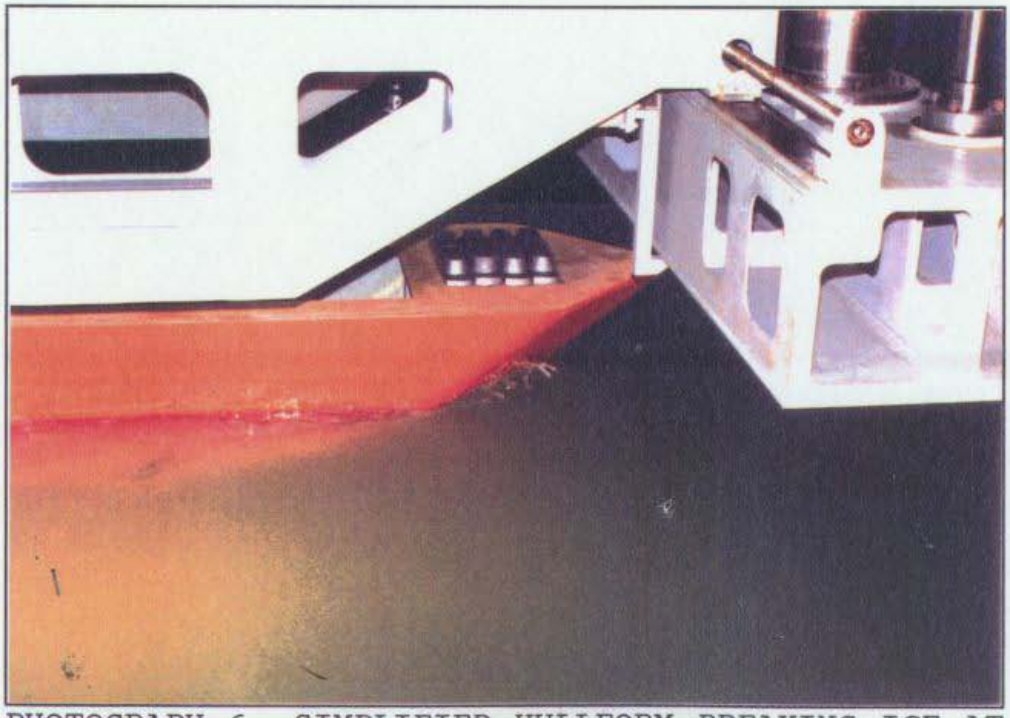

PHOTOGRAPH 6 SIMPLIFIED HULLFORM BREAKING ICE AT HIGH SPEED (1.0 m/s)

PHOTOGRAPH 7 SIMPLIFIED HULLFORM BREAKING ICE AT LOW SPEED (0.1 m/s)

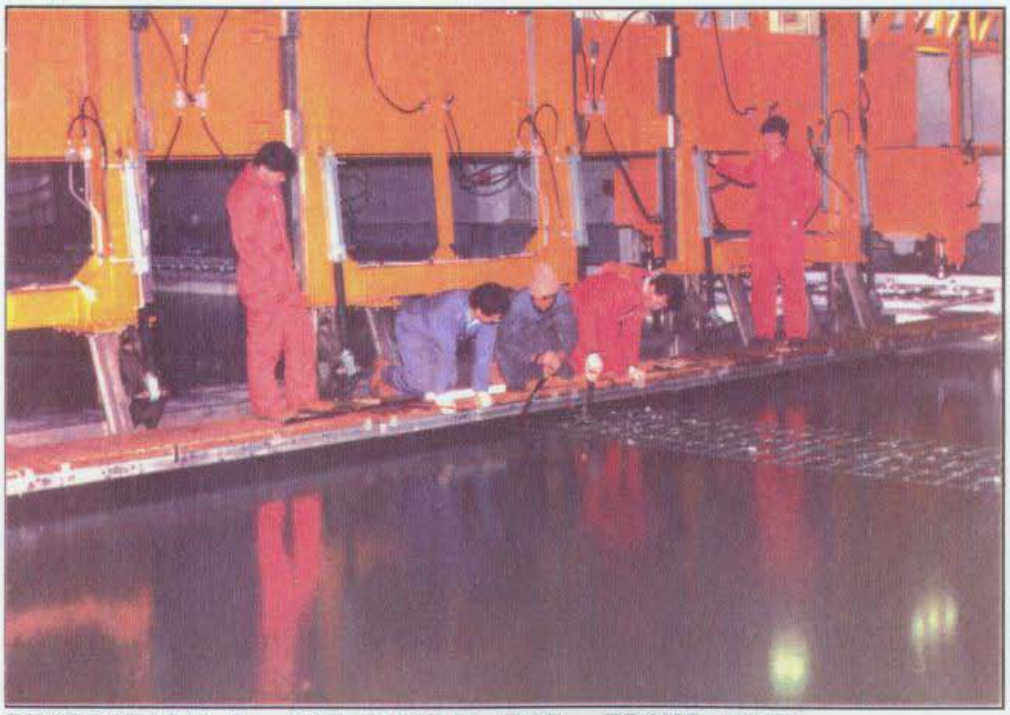

PHOTOGRAPH 8 PRE-SAWING ICE, FRONT VIEW

PHOTOGRAPH 9 PRE-SAWING ICE, SIDE VIEW

PHOTOGRAPH 10 PRE-SAWN CHANNEL BEFORE TEST

PHOTOGRAPH 11 SIMPLIFIED HULLFORM IN PRE-SAWN CHANNEL

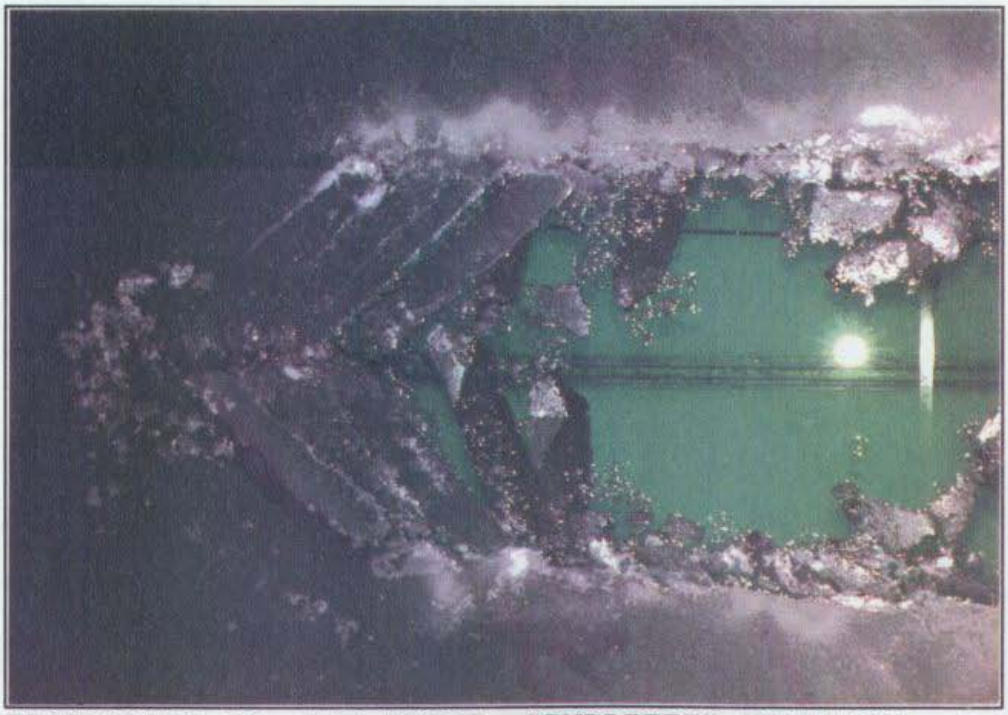

PHOTOGRAPH 12 BOW PRINT, SIMPLIFIED HULLFORM

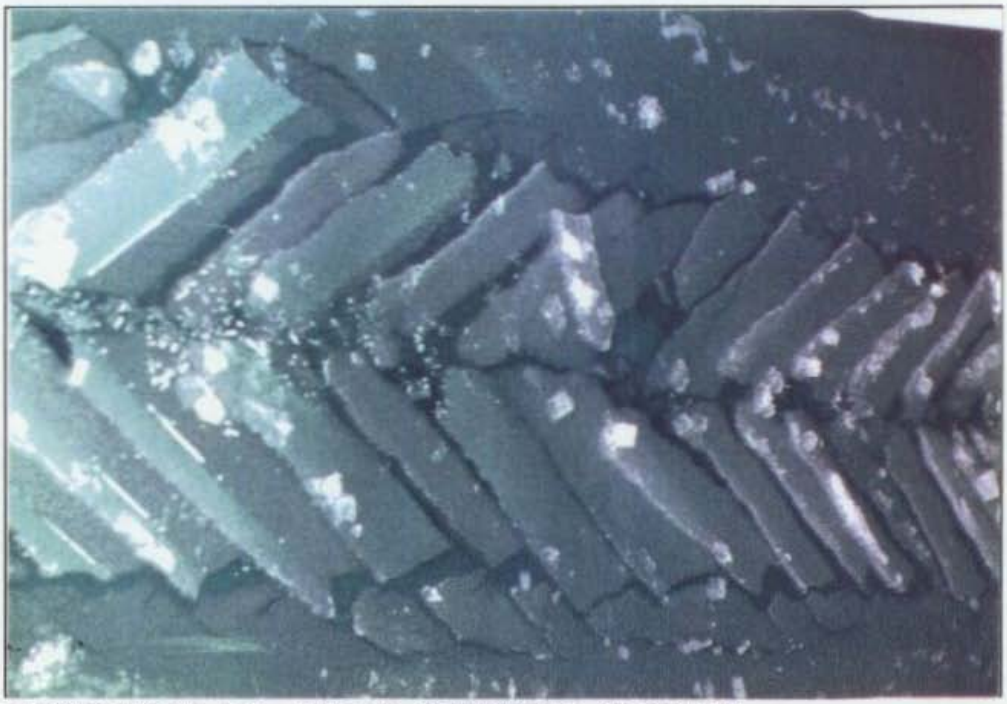

PHOTOGRAPH 13 WEDGE BREAKING PATTERN

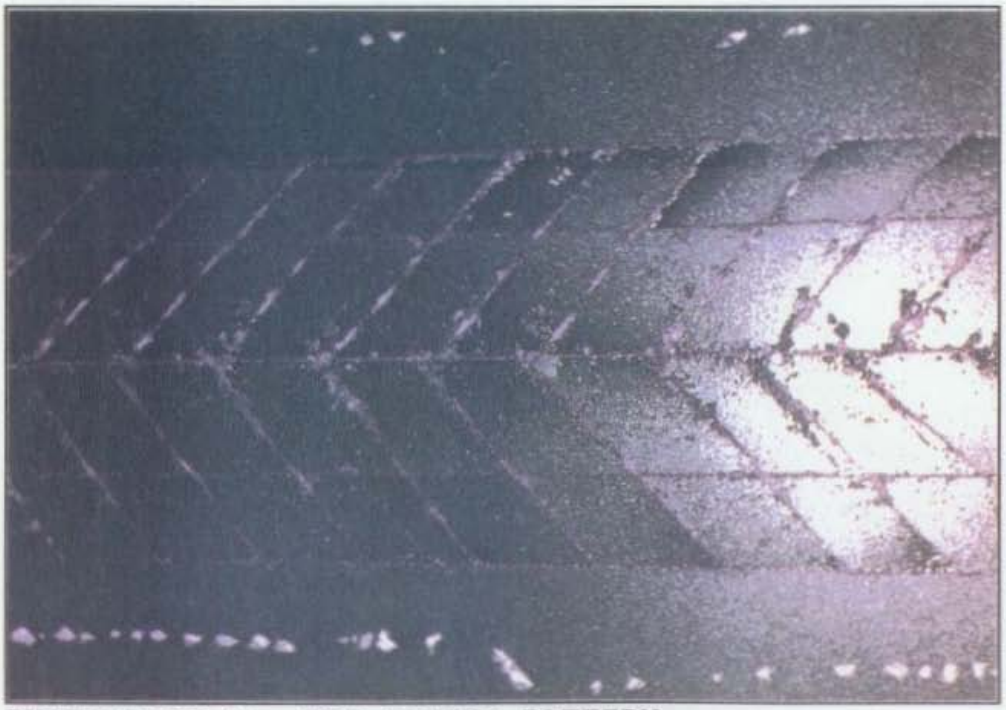

PHOTOGRAPH 14 PRE-SAWING PATTERN

APPENDIX 1

SIMPLIFIED HULLFORMS

MODEL TEST DATA

Contents

Nomenclature

TEST NO.	Ice Sheet, Run, Test ie. 1A2	Ice Sheet 1 Run A Test 2
WIDTH	Sawn Channel Width in cm.	
ANGLE	Chevron Pattern Included Angle in deg.	
LENGTH	Distance Between Lateral Cuts in the Direction of Travel	
MODEL SPEED	Average Model Speed in the Test Interval (m/sec) 0.5 m/s when not specified	
ICE THICK.	Average Ice Thickness in the Test Interval (mm)	
ICE STR.	Average Ice Strength for a Run (kPa)	
DENSITY	Regression Based Density for the Test Interval (kg/cubic metre)	
RES.	Average Tow Force Measured in the Test Interval (Newtons)	
VISC.	Calculated Viscous Skin Friction Resistance (Newtons)	
NET.	Net Resistance ie. RES. - VISC. (Newtons)	
CLEAR.	Regression Based Ice Clearing Resistance (Newtons)	
BREAK.	Calculated Breaking Resistance ie. NET. - CLEAR. (Newtons)	
Fn	Ice Thickness Froude Number	
Sn	Ice Strength Number	
Cc	Clearing Resistance Coefficient	
Cbr	Breaking Resistance Coefficient	

SIMPLIFIED HULLFORM OPEN WATER DATA

SPEED m/s	OPEN WATER N	THIN ICE CHANNEL N	30 MM CHANNEL N	45 MM CHANNEL N	THIN ICE N
0.10	-	-	-	-	18.80
0.25	3.10	-	6.00	-	30.40
0.50	11.30	21.80	-	16.90	39.30
0.75	31.30	-	-	-	-
1.00	50.20	58.80	69.00	62.40	70.00

BOW ONLY OPEN WATER

SPEED	RESISTANCE
1.00	10.40

INTERPOLATED VALUES

SPEED m/s	OPEN WATER N	CHANNEL N	BOW ONLY N	CALCULATED FRICTIONAL N	RESIDUARY N	CHANNEL N
0.10	1.00	2.50	0.00	0.20	0.80	1.50
0.25	3.50	6.00	0.00	1.00	2.50	2.50
0.50	11.50	17.00	0.50	3.50	8.00	5.50
1.00	50.50	65.00	10.50	12.20	38.30	14.50

SIMPLIFIED HULLFORM PRESAWN CHANNEL RESISTANCE DATA

TEST NO.	PRESAWN CHANNEL WIDTH cm	ANGLE deg.	LENGTH cm.	ICE THICK. mm	ICE STR. kPa	DENSITY kg/m^3	RES. N	NET N	Cc
1A1	110.00	67.00	28.00	30.30	33.00	942.39	87.10	83.60	11.71
1A2	110.60	97.00	21.00	30.20	33.00	942.42	80.20	76.70	10.78
1A3	110.00	142.00	16.00	28.50	33.00	942.95	71.00	67.50	10.05
1A4	110.00	180.00	17.00	28.40	33.00	942.98	74.00	70.50	10.53
1B1	110.00	106.00	15.00	30.80	26.00	944.40	69.00	65.50	9.01
1B2	110.00	99.00	25.00	30.60	26.00	944.46	58.00	54.50	7.54
1B3	110.00	94.00	41.00	28.80	26.00	945.02	62.50	59.00	8.67
1B4	110.00	92.00	69.00	28.70	26.00	945.05	59.50	56.00	8.26
2A1	110.00	93.00	18.00	30.40	28.00	943.91	85.40	81.90	11.42
2A2	110.00	99.00	28.00	30.20	28.00	943.97	69.60	66.10	9.27
2A3	110.00	104.00	40.00	29.60	28.00	944.15	55.70	52.20	7.47
2A4	110.00	95.00	53.00	28.70	28.00	944.43	57.60	54.10	7.98
2B1	110.00	107.00	23.00	30.30	22.00	945.80	73.10	69.60	9.71
2B2	115.00	107.00	24.00	30.30	22.00	945.80	65.00	61.50	8.58
2B3	120.00	94.00	24.00	29.60	22.00	946.01	68.20	64.70	9.24
2B4	125.00	95.00	23.00	29.00	22.00	946.20	57.50	54.00	7.87

SIMPLIFIED HULLFORM RESISTANCE DATA

PRESAWN RESULTS

TEST NO.	MODEL SPEED m/s	ICE THICK. mm	ICE STR. kPa	DENSITY kg/m^3	RES. N	VISC N	NET N	Fn	Cc
0.7 m BEAM									
1581	0.25	44.90	21.30	937.81	101.00	1.27	99.73	0.38	29.15
1582	1.00	44.80	21.30	937.84	203.00	15.16	187.84	1.51	3.44
1583	0.10	45.90	21.30	937.48	67.00	0.25	66.75	0.15	119.32
1584	0.50	45.20	21.30	937.71	153.00	4.37	148.63	0.75	10.79
1681	0.10	45.90	58.50	929.25	70.00	0.25	69.75	0.15	125.79
1682	0.50	46.10	58.50	929.18	180.00	4.37	175.63	0.74	12.62
1683	0.25	46.10	58.50	929.18	101.00	1.27	99.73	0.37	28.65
1684	1.00	45.60	58.50	929.35	212.00	15.16	196.84	1.50	3.57
1781	0.50	31.80	29.80	940.23	118.00	4.37	113.63	0.90	11.69
1782	0.10	32.00	29.80	940.16	57.00	0.25	56.75	0.18	145.09
1783	1.00	31.40	29.80	940.36	153.00	15.16	137.84	1.80	3.59
1784	0.25	30.40	29.80	940.69	58.00	1.27	56.73	0.46	24.41
1881	1.00	31.90	40.00	937.94	193.00	15.16	177.84	1.79	4.57
1882	0.25	30.40	40.00	938.43	63.00	1.27	61.73	0.46	26.63
1883	0.50	30.70	40.00	938.33	113.00	4.37	108.63	0.91	11.6u
1884	0.10	30.10	40.00	938.53	47.00	0.25	46.75	0.18	127.29
1.0 m BEAM									
383	0.10	29.50	21.00	946.31	27.30	0.20	27.10	0.19	97.08
381	0.25	29.90	21.00	946.18	37.30	1.00	36.30	0.46	20.53
384	0.50	29.70	21.00	946.25	62.80	3.50	59.30	0.93	8.44
382	1.00	31.00	21.00	945.84	115.30	12.20	103.10	1.81	3.52
481	0.10	44.90	22.00	941.23	47.80	0.20	47.60	0.15	112.63
483	0.25	44.90	22.00	941.23	77.10	1.00	76.10	0.38	28.81
482	0.50	44.60	22.00	941.32	96.40	3.50	92.90	0.76	8.85
484	1.00	43.20	22.00	941.76	175.00	12.20	162.80	1.54	4.00

582	0.10	44.40	34.00	937.63	52.40	0.20	52.20	0.15	125.39
584	0.25	42.40	34.00	938.25	56.60	1.00	55.60	0.39	22.36
581	0.50	44.00	34.00	937.75	109.10	3.50	105.60	0.76	10.24
583	1.00	43.90	34.00	937.78	144.30	12.20	132.10	1.52	3.21
684	0.10	29.00	28.00	944.27	23.40	0.20	23.20	0.19	84.72
682	0.25	29.80	28.00	944.02	30.90	1.00	29.90	0.46	17.01
683	0.50	29.60	28.00	944.09	67.60	3.50	64.10	0.93	9.18
681	1.00	30.50	28.00	943.81	104.50	12.20	92.30	1.83	3.21
783	0.10	43.40	48.00	933.55	49.90	0.20	49.70	0.15	122.67
781	0.25	44.70	48.00	933.15	62.40	1.00	61.40	0.38	23.55
784	0.50	43.30	48.00	933.58	120.00	3.50	116.50	0.77	11.53
782	1.00	45.00	48.00	933.06	161.80	12.20	148.60	1.51	3.54
1281	0.10	30.60	58.00	934.38	23.10	0.20	22.90	0.18	80.09
1283	0.25	31.20	58.00	934.20	41.00	1.00	40.00	0.45	21.96
1282	0.50	31.10	58.00	934.23	58.70	3.50	55.20	0.91	7.60
1284	1.00	30.10	58.00	934.54	123.40	12.20	111.20	1.84	3.95
1382	0.10	39.00	60.00	931.16	45.10	0.20	44.90	0.16	123.64
1384	0.25	37.20	60.00	931.71	47.40	1.00	46.40	0.41	21.42
1381	0.50	39.90	60.00	930.88	83.50	3.50	80.00	0.80	8.62
1383	1.00	38.80	60.00	931.22	146.20	12.20	134.00	1.62	3.71
1484	0.10	36.00	33.00	940.54	35.90	0.20	35.70	0.17	105.44
1482	0.25	37.50	33.00	940.08	52.60	1.00	51.60	0.41	23.42
1483	0.50	36.20	33.00	940.48	70.50	3.50	67.00	0.84	7.87
1481	1.00	37.30	33.00	940.14	102.20	12.20	90.00	1.65	2.57

1.3 m BEAM

1981	0.25	45.50	57.70	929.56	24.50	0.86	23.64	0.37	12.77
1982	1.00	45.10	57.70	929.69	95.00	10.29	84.71	1.50	2.89
1983	0.10	45.50	57.70	929.56	17.00	0.17	16.83	0.15	56.84
1984	0.50	45.60	57.70	929.52	38.20	2.96	35.24	0.75	4.75
2081	0.10	47.20	40.50	932.80	23.00	0.17	22.83	0.15	74.07
2082	0.50	47.90	40.50	932.57	51.00	2.96	48.04	0.73	6.14
2083	0.25	47.80	40.50	932.61	32.00	0.86	31.14	0.37	15.97
2084	1.00	46.00	40.50	933.20	98.00	10.29	87.71	1.49	2.92
2181	0.50	31.10	27.60	940.95	31.00	2.96	28.04	0.91	5.47
2182	0.10	30.90	27.60	941.01	13.00	0.17	12.83	0.18	63.02
2183	1.00	30.40	27.60	941.18	67.00	10.29	56.71	1.83	2.83
2184	0.25	29.50	27.60	941.47	18.00	0.86	17.14	0.46	14.10

22B1	1.00	31.70	37.60	938.54	73.00	10.29	62.71	1.79	3.01	
22B2	0.25	31.50	37.60	938.60	19.00	0.86	18.14	0.45	14.02	
22B3	0.50	32.30	37.60	938.34	35.00	2.96	32.04	0.89	6.04	
22B4	0.10	31.50	37.60	938.60	13.00	0.17	12.83	0.18	61.98	

BREAKING RESISTANCE

TEST NO.	MODEL SPEED m/s	ICE THICK. mm	ICE STR. kPa	DENSITY kg/m^3	RES. N	VISC N	NET N	CLEAR. N	BREAK. N	Sn	Cbr
0.7 m BEAM											
15A1	0.25	46.50	27.10	936.00	228.00	1.27	226.73	126.57	100.16	1.47	28.32
15A2	1.00	45.00	27.10	936.49	313.00	15.16	297.84	241.92	55.92	5.88	1.02
15A3	0.10	45.80	27.10	936.23	147.00	0.25	146.75	77.39	69.36	0.59	124.43
15A4	0.50	45.90	27.10	936.20	220.00	4.37	215.63	176.02	39.61	2.94	2.84
16A1	0.10	47.50	57.70	928.90	197.00	0.25	196.75	81.83	114.92	0.40	200.35
16A2	0.50	46.60	57.70	929.19	322.00	4.37	317.63	179.38	138.25	2.01	9.82
16A3	0.25	45.90	57.70	929.42	308.00	1.27	306.73	122.86	183.87	1.00	53.05
16A4	1.00	46.50	57.70	929.23	393.00	15.16	377.84	254.19	123.65	4.01	2.20
17A1	0.50	31.90	32.00	939.71	155.00	4.37	150.63	93.60	57.03	2.71	5.85
17A2	0.10	31.30	32.00	939.91	111.00	0.25	110.75	39.97	70.78	0.54	185.06
17A3	1.00	31.70	32.00	939.77	214.00	15.16	198.84	131.69	67.15	5.42	1.73
17A4	0.25	30.70	32.00	940.10	104.00	1.27	102.73	61.58	41.15	1.36	17.55
18A1	1.00	32.40	42.30	937.26	289.00	15.16	273.84	136.44	137.40	4.71	3.48
18A2	0.25	31.20	42.30	937.66	136.00	1.27	134.73	63.17	71.56	1.18	30.10
18A3	0.50	31.30	42.30	937.63	160.00	4.37	155.63	90.35	65.28	2.35	6.84
18A4	0.10	30.80	42.30	937.79	113.00	0.25	112.75	38.78	73.97	0.47	197.00
1.0 m BEAM											
3A3	0.10	29.40	29.00	943.83	60.90	0.20	60.70	22.85	37.85	0.57	136.40
3A1	0.25	29.20	29.00	943.90	70.70	1.00	69.70	36.52	33.18	1.43	19.26
3A4	0.50	29.40	29.00	943.83	110.90	3.50	107.40	53.17	54.23	2.85	7.82
3A2	1.00	30.80	29.00	943.40	174.60	12.20	162.40	82.89	79.51	5.70	2.74
4A1	0.10	44.30	34.00	937.66	112.40	0.20	112.20	46.29	65.91	0.53	158.68

4A3	0.25	44.90	34.00	937.47	163.40	1.00	162.40	76.62	85.78	1.31	32.61
4A2	0.50	44.70	34.00	937.54	177.30	3.50	173.80	109.38	64.42	2.63	6.15
4A4	1.00	42.70	34.00	938.15	193.10	12.20	180.90	145.42	35.48	5.25	0.89
5A2	0.10	44.20	44.00	934.56	132.90	0.20	132.70	45.95	86.75	0.46	210.00
5A4	0.25	41.90	44.00	935.27	170.70	1.00	169.70	67.78	101.92	1.15	41.61
5A1	0.50	44.40	44.00	934.50	210.30	3.50	206.80	107.76	99.04	2.30	9.55
5A3	1.00	43.30	44.00	934.84	322.20	12.20	310.00	148.47	161.53	4.61	3.99
6A4	0.10	28.80	43.00	939.64	59.40	0.20	59.20	21.95	37.25	0.47	137.65
6A2	0.25	30.20	43.00	939.20	87.60	1.00	86.60	38.53	48.07	1.17	27.11
6A3	0.50	29.00	43.00	939.57	98.30	3.50	94.80	51.68	43.12	2.34	6.33
6A1	1.00	30.50	43.00	939.11	154.10	12.20	141.90	81.13	60.77	4.67	2.12
7A3	0.10	43.00	59.00	930.23	151.70	0.20	151.50	43.60	107.90	0.40	269.74
7A1	0.25	44.40	59.00	929.80	229.40	1.00	228.40	74.53	153.87	0.99	59.64
7A4	0.50	42.60	59.00	930.36	231.50	3.50	228.00	99.84	128.16	1.99	12.94
7A2	1.00	44.90	59.00	929.64	331.10	12.20	318.90	157.25	161.65	3.97	3.87
12A1	0.10	29.70	64.00	932.78	94.50	0.20	94.30	22.99	71.31	0.38	257.42
12A3	0.25	30.70	64.00	932.47	120.40	1.00	119.40	39.36	80.04	0.95	44.73
12A2	0.50	30.40	64.00	932.56	143.50	3.50	140.00	55.68	84.32	1.91	11.90
12A4	1.00	29.40	64.00	932.87	205.00	12.20	192.80	75.60	117.20	3.82	4.27
13A2	0.10	38.50	68.00	928.81	131.80	0.20	131.60	35.93	95.67	0.37	267.55
13A4	0.25	36.90	68.00	929.30	173.10	1.00	172.10	54.01	118.09	0.92	55.10
13A1	0.50	39.90	68.00	928.37	214.40	3.50	210.90	88.91	121.99	1.85	13.17
13A3	1.00	37.90	68.00	928.99	286.30	12.20	274.10	117.05	157.05	3.70	4.46
14A4	0.10	35.20	41.00	938.28	67.70	0.20	67.50	31.06	36.44	0.48	110.33
14A2	0.25	37.00	41.00	937.73	121.70	1.00	120.70	54.75	65.95	1.20	30.41
14A3	0.50	35.60	41.00	938.16	119.50	3.50	116.00	73.70	42.30	2.39	5.07
14A1	1.00	37.40	41.00	937.60	202.40	12.20	190.20	115.44	74.76	4.78	2.13

1.3 m BEAM

19A1	0.25	47.50	63.70	927.57	264.00	0.86	263.14	36.27	226.87	0.95	117.70
19A2	1.00	45.50	63.70	928.23	340.00	10.29	329.71	85.31	244.40	3.82	8.27
19A3	0.10	46.10	63.70	928.03	167.00	0.17	166.83	18.71	148.11	0.38	494.58
19A4	0.50	46.10	63.70	928.03	326.00	2.96	323.04	54.86	268.18	1.91	35.82
20A1	0.10	47.60	48.00	931.01	128.00	0.17	127.83	19.80	108.02	0.44	348.23
20A2	0.50	47.60	48.00	931.01	234.00	2.96	231.04	58.05	172.99	2.20	22.31
20A3	0.25	47.50	48.00	931.05	159.00	0.86	158.14	36.40	121.73	1.10	62.92
20A4	1.00	46.80	48.00	931.28	309.00	10.29	298.71	89.70	209.01	4.40	6.85
21A1	0.50	31.30	31.50	940.02	92.00	2.96	89.04	29.15	59.88	2.73	11.63

21A2	0.10	30.70	31.50	940.21	48.00	0.17	47.83	9.63	38.20	0.55	189.04
21A3	1.00	30.80	31.50	940.18	126.00	10.29	115.71	45.11	70.61	5.46	3.48
21A4	0.25	30.50	31.50	940.28	59.00	0.86	58.14	17.58	40.56	1.37	32.33
22A1	1.00	32.20	46.50	936.40	152.00	10.29	141.71	48.38	93.33	4.49	4.42
22A2	0.25	31.40	46.50	936.66	77.00	0.86	76.14	18.38	57.76	1.12	44.89
22A3	0.50	32.60	46.50	936.27	104.00	2.96	101.04	31.07	69.96	2.24	13.10
22A4	0.10	31.50	46.50	936.63	57.00	0.17	56.83	10.01	46.81	0.45	226.67

SIMPLIFIED HULLFORM SHALLOW DRAFT WEDGE RESISTANCE DATA

PRESAWN RESISTANCE

TEST NO.	MODEL SPEED m/s	ICE THICK. mm	ICE STR. kPa	DENSITY kg/m^3	RES. N	VISC. N	NET N	Fn	Cc
9C3	0.10	43.50	27.00	940.10	25.00	0.02	24.98	0.15	61.08
9C1	0.25	44.90	27.00	939.67	22.80	0.12	22.68	0.38	8.60
9C4	0.50	43.40	27.00	940.13	27.80	0.39	27.41	0.77	2.69
9C1	1.00	44.90	27.00	939.67	57.30	1.31	55.99	1.51	1.33
10C2	0.10	31.10	19.00	946.44	8.10	0.02	8.08	0.18	27.45
10C4	0.25	29.20	19.00	947.03	7.00	0.12	6.88	0.47	3.98
10C1	0.50	31.00	19.00	946.47	11.50	0.39	11.11	0.91	1.51
10C3	1.00	30.90	19.00	946.50	27.10	1.31	25.79	1.82	0.88
11C1	0.10	31.40	32.00	942.28	12.30	0.02	12.28	0.18	41.50
11C3	0.25	30.90	32.00	942.43	10.20	0.12	10.08	0.45	5.54
11C2	0.50	31.50	32.00	942.25	13.10	0.39	12.71	0.90	1.71
11C4	1.00	29.50	32.00	942.86	28.70	1.31	27.39	1.86	0.98

BREAKING RESISTANCE

TEST NO.	MODEL SPEED m/s	ICE THICK. mm	ICE STR. kPa	DENSITY kg/m^3	RES. N	VISC. N	NET N	CLEAR. N	BREAK. N	Sn	Cbr
8A2	0.10	43.80	31.00	938.75	81.70	0.02	81.68	16.45	65.23	0.5503	158.65
8A4	0.25	42.50	31.00	939.16	87.90	0.12	87.78	22.02	65.76	1.3760	26.36
8A1	0.50	44.60	31.00	938.51	129.90	0.39	129.51	31.19	98.32	2.7511	9.40
8A3	1.00	42.90	31.00	939.03	204.10	1.31	202.79	37.78	165.01	5.5038	4.10
8B4	0.10	43.10	17.00	943.35	41.80	0.02	41.78	16.05	25.73	0.7449	63.28
8B2	0.25	44.30	17.00	942.98	79.80	0.12	79.68	23.83	55.85	1.8619	21.39
8B3	0.50	42.80	17.00	943.45	106.10	0.39	105.71	29.10	76.61	3.7248	7.59
8B1	1.00	44.40	17.00	942.95	162.00	1.31	160.69	40.38	120.31	7.4477	2.87
9A4	0.10	44.70	47.00	933.46	87.30	0.02	87.28	16.97	70.31	0.4457	168.51
9A2	0.25	43.90	47.00	933.71	114.00	0.12	113.88	23.21	90.67	1.1143	35.39
9A3	0.50	42.70	47.00	934.08	119.20	0.39	118.81	28.69	90.12	2.2290	9.04
9A1	1.00	44.80	47.00	933.43	202.80	1.31	201.49	40.62	160.87	4.4565	3.85
9B3	0.10	43.50	31.00	938.85	90.90	0.02	90.88	16.25	74.63	0.5503	182.75
9B1	0.25	44.90	31.00	938.41	112.00	0.12	111.88	24.30	87.58	1.3755	33.26
9B4	0.50	43.40	31.00	938.88	124.00	0.39	123.61	29.70	93.91	2.7517	9.22
9B2	1.00	44.90	31.00	938.41	227.00	1.31	225.69	41.00	184.69	5.5019	4.38
10A1	0.10	31.30	30.00	942.93	35.10	0.02	35.08	8.99	26.09	0.5606	88.40
10A3	0.25	31.20	30.00	942.96	51.30	0.12	51.18	12.63	38.55	1.4016	20.97
10A2	0.50	30.70	30.00	943.12	68.40	0.39	68.01	15.93	52.08	2.8034	7.19
10A4	1.00	29.70	30.00	943.43	105.90	1.31	104.59	19.50	85.09	5.6078	3.04
10B2	0.10	31.10	22.00	945.50	29.50	0.02	29.48	8.91	20.57	0.6556	69.96
10B4	0.25	29.20	22.00	946.09	40.90	0.12	40.78	11.24	29.54	1.6394	17.11
10B1	0.50	31.00	22.00	945.53	58.40	0.39	58.01	16.26	41.75	3.2779	5.70
10B3	1.00	30.90	22.00	945.56	106.00	1.31	104.69	21.00	83.69	6.5559	2.86
11A3	0.10	29.40	43.00	939.45	29.90	0.02	29.88	8.00	21.88	0.4674	79.24
11A1	0.25	30.70	43.00	939.05	57.40	0.12	57.28	12.21	45.07	1.1683	25.01
11A4	0.50	29.20	43.00	939.51	62.60	0.39	62.21	14.50	47.71	2.3372	6.96

11A2	1.00	30.70	43.00	939.05	124.80	1.31	123.49	20.61	102.88	4.6731	3.57
11B1	0.10	31.40	32.00	942.28	43.50	0.02	43.48	9.03	34.45	0.5426	116.42
11B3	0.25	30.90	32.00	942.43	57.80	0.12	57.68	12.40	45.28	1.3567	24.88
11B2	0.50	31.50	32.00	942.25	77.90	0.39	77.51	16.68	60.83	2.7132	8.20
11B4	1.00	29.50	32.00	942.86	125.80	1.31	124.49	19.25	105.24	5.4281	3.78

APPENDIX 2

ICEBREAKER

MODEL AND FULL SCALE DATA

Contents

Nomenclature

TEST NO.	Test Identifier
SPEED	Average Speed in the Test Interval
ICE THICK.	Reported Average Ice Thickness in the Test Interval (mm)
ICE STR.	Reported Average Ice Strength for a Run (kPa)
DENSITY	Reported Density for the Test Interval (kg/cubic metre)
RES.	Average Tow Force Measured in the Test Interval (Newtons) Calculated from thrust measurements for full scale trials.
VISC.	Calculated Viscous Skin Friction Resistance (Newtons)
NET.	Net Resistance ie. RES. - VISC. (Newtons)
CLEAR.	Regression Based Ice Clearing Resistance (Newtons)
BREAK.	Calculated Breaking Resistance ie. NET. - CLEAR. (Newtons)
Fn	Ice Thickness Froude Number
Sn	Ice Strength Number
Cc	Clearing Resistance Coefficient
Cbr	Breaking Resistance Coefficient
Cr	Net Ice Resistancce Coefficient

CCGS LOUIS ST. LAURENT MODEL SCALE RESISTANCE DATA

PRESAWN RESISTANCE

TEST NO.	SPEED m/s	THK. mm	STR. kPa	DENSITY kg/m^3	RES N	VISC. N	NET N	Fn	Cc
BOW A									
1	0.26	69.65	20.00	938.90	209.00	2.02	206.98	0.31	29.28
	0.52	68.01	32.20	935.87	240.00	7.00	233.00	0.63	8.47
	0.77	67.96	11.30	941.29	316.00	14.53	301.47	0.95	4.84
2	0.26	45.68	21.80	940.37	149.00	2.02	146.98	0.39	31.65
	0.52	46.97	24.40	939.59	176.00	7.00	169.00	0.76	8.86
	0.77	46.67	22.40	940.13	244.00	14.53	229.47	1.14	5.38
3	0.26	102.09	17.60	936.90	344.00	2.02	341.98	0.26	33.08
	0.52	102.08	20.30	936.20	473.00	7.00	466.00	0.52	11.28
	0.77	101.89	14.40	937.75	612.00	14.53	597.47	0.77	6.43
BOW B									
4	0.26	99.89	14.90	937.78	259.00	1.98	257.02	0.26	25.43
	0.52	101.95	19.70	936.37	376.00	6.86	369.14	0.52	8.96
	0.77	100.39	13.40	938.13	435.00	14.24	420.76	0.78	4.60
5	0.26	67.22	21.40	938.73	162.00	1.98	160.02	0.32	23.50
	0.52	66.97	19.20	939.32	216.00	6.86	209.14	0.64	7.70
	0.77	67.92	16.20	940.03	262.00	14.24	247.76	0.95	4.00
6	0.26	67.78	24.50	937.89	127.00	1.98	125.02	0.32	18.23
	0.52	67.97	24.90	937.77	177.00	6.86	170.14	0.63	6.18
	0.77	68.58	20.40	938.88	238.00	14.24	223.76	0.94	3.58
7	0.26	48.00	24.20	939.56	81.00	1.98	79.02	0.38	16.24
	0.52	48.01	24.40	939.51	138.00	6.86	131.14	0.75	6.74
	0.77	48.30	14.40	942.08	162.00	14.24	147.76	1.12	3.34
BOW C									
8	0.26	99.05	15.10	937.80	296.00	1.98	294.02	0.26	29.34
	0.52	100.63	23.40	935.52	410.00	6.86	403.14	0.52	9.92
	0.77	99.15	14.70	937.89	450.00	14.24	435.76	0.78	4.83
9	0.26	67.06	20.20	939.06	161.00	1.98	159.02	0.32	23.40
	0.52	67.17	17.80	939.67	219.00	6.86	212.14	0.64	7.79
	0.77	67.06	16.80	939.94	257.00	14.24	242.76	0.95	3.97
10	0.26	67.06	23.80	938.12	143.00	1.98	141.02	0.32	20.77
	0.52	66.47	25.00	937.86	188.00	6.86	181.14	0.64	6.73
	0.77	66.96	24.40	937.98	236.00	14.24	221.76	0.95	3.64
11	0.26	49.28	21.10	940.26	92.00	1.98	90.02	0.37	18.00
	0.52	47.47	26.10	939.11	123.00	6.86	116.14	0.76	6.04
	0.77	47.29	19.60	940.81	156.00	14.24	141.76	1.14	3.28

BREAKING RESISTANCE

TEST NO.	SPEED m/s	THK. mm	STR. kPa	DENSITY kg/m^3	RES N	VISC. N	NET N	CLEAR N	BREAK. N	Sn	Cbr
BOW A											
1	0.26	69.20	25.00	937.64	571.00	2.02	568.98	198.65	370.33	1.58	52.80
	0.52	67.80	19.30	939.23	624.00	7.00	617.00	278.92	338.08	3.60	12.28
	0.77	67.50	33.20	935.65	770.00	14.53	755.47	342.97	412.50	4.11	6.71
2	0.26	45.20	29.80	938.33	295.00	2.02	292.98	95.12	197.86	1.45	43.16
	0.52	46.50	32.40	937.56	388.00	7.00	381.00	144.95	236.05	2.78	12.52

		0.77	46.20	30.40	938.10	446.00	14.53	431.47	178.39	253.08	4.30	6.00
	3	0.26	101.60	35.20	932.38	995.00	2.02	992.98	384.01	608.97	1.33	59.47
		0.52	101.70	32.00	933.20	1100.00	7.00	1093.00	559.08	533.92	2.79	13.01
		0.77	101.40	31.00	933.49	1362.00	14.53	1347.47	692.08	655.39	4.25	7.12
BOW B												
	4	0.26	99.40	32.50	933.26	714.00	1.98	712.02	265.30	446.72	1.38	44.55
		0.52	101.60	31.00	933.47	920.00	6.86	913.14	395.42	517.72	2.83	12.62
		0.77	99.90	28.60	934.23	1077.00	14.24	1062.76	474.60	588.16	4.42	6.48
	5	0.26	66.70	28.40	936.96	341.00	1.98	339.02	133.05	205.97	1.48	30.49
		0.52	66.60	19.20	939.35	402.00	6.86	395.14	190.85	204.29	3.61	7.55
		0.77	67.40	20.70	938.90	478.00	14.24	463.76	240.52	223.24	5.21	3.63
	6	0.26	67.30	30.50	936.37	354.00	1.98	352.02	135.06	216.96	1.43	31.85
		0.52	67.60	26.40	937.41	480.00	6.86	473.14	195.46	277.68	3.07	10.13
		0.77	68.10	27.90	936.98	549.00	14.24	534.76	244.39	290.37	4.49	4.68
	7	0.26	47.50	39.20	935.71	200.00	1.98	198.02	73.61	124.41	1.26	25.89
		0.52	47.60	29.40	938.24	251.00	6.86	244.14	106.27	137.87	2.91	7.14
		0.77	47.80	34.40	936.93	317.00	14.24	302.76	132.01	170.75	4.04	3.92
BOW C												
	8	0.26	98.60	29.80	934.02	663.00	1.98	661.02	293.80	367.22	1.44	36.89
		0.52	100.30	29.40	933.99	789.00	6.86	782.14	409.40	372.74	2.91	9.20
		0.77	98.70	31.40	933.60	994.00	14.24	979.76	474.31	505.45	4.22	5.64
	9	0.26	66.60	22.20	938.58	356.00	1.98	354.02	146.69	207.33	1.68	30.68
		0.52	66.80	18.80	939.44	404.00	6.86	397.14	199.52	197.62	3.65	7.28
		0.77	66.60	18.80	939.46	474.00	14.24	459.76	236.72	223.04	5.47	3.66
	10	0.26	66.60	30.80	936.35	396.00	1.98	394.02	146.34	247.68	1.42	36.74
		0.52	66.10	31.40	936.23	474.00	6.86	467.14	195.14	272.00	2.82	10.16
		0.77	66.50	28.00	937.08	542.00	14.24	527.76	235.49	292.27	4.48	4.82
	11	0.26	48.80	33.10	937.19	246.00	1.98	244.02	84.14	159.88	1.37	32.34
		0.52	47.10	31.60	937.71	270.00	6.86	263.14	106.82	156.32	2.81	8.19
		0.77	46.80	34.10	937.09	312.00	14.24	297.76	125.89	171.87	4.06	4.03

CCGS LOUIS ST. LAURENT FULL SCALE DATA

TEST NO.	SPEED m/s	THICK. mm	STR. kPa	RES. N	Fn	Sn	Cr	VISCOUS N
1	1.94	0.74	154.90	570947	0.72	4.71	61858	11632
2	2.10	0.88	154.90	588059	0.71	5.09	85778	13412
3	2.68	0.84	154.90	969530	0.93	6.50	133473	21120
4	2.32	0.70	154.90	1272061	0.88	5.61	82974	16089
5	2.97	0.80	154.90	1467127	1.06	7.19	155897	25535
6	1.85	1.07	154.90	1161167	0.57	4.49	81212	10631
7	2.21	1.14	154.90	1737367	0.66	5.35	122883	14722
8	2.12	1.13	154.90	1365201	0.64	5.15	112815	13711
9	1.40	1.11	154.90	1054815	0.42	3.39	48076	6320
10	0.77	1.00	154.90	1062994	0.24	1.86	12983	2075
11	1.29	1.27	154.90	1419586	0.36	3.12	46484	5407
12	1.36	1.18	154.90	1402280	0.40	3.30	48514	6022
13	1.71	1.18	154.90	1605872	0.50	4.15	76629	9199
14	2.03	1.36	154.90	1624345	0.56	4.91	123677	12571
15	1.34	0.39	154.90	361691	0.68	3.24	15441	5811
16	2.47	0.39	158.60	563551	1.26	5.91	52659	18134
17	4.78	0.39	158.60	778864	2.45	11.46	197701	62130
18	5.20	0.39	158.60	921450	2.66	12.45	233219	72481
19	4.89	0.39	158.60	891292	2.50	11.71	206306	64648
20	3.29	0.39	158.60	597671	1.68	7.89	93615	30965
21	3.14	0.39	158.60	588409	1.60	7.52	85061	28323
22	1.90	0.39	158.60	380345	0.97	4.56	31283	11181
23	0.87	0.39	158.60	233850	0.45	2.09	6599	2647
24	0.72	0.39	158.60	227194	0.37	1.72	4478	1851

1:8 R-CLASS ICE RESISTANCE TEST RESULTS

PRESAWN RESISTANCES

TEST NO.	SPEED m/s	THICK. mm	STR. kPa	DENSITY kg/m^3	RES. N	VISC. N	NET N	Fn	Cc
1.00	0.48	55.10	95.00	926.93	404.00	13.70	390.30	0.65	13.71
3.00	0.48	88.00	90.00	923.59	766.00	13.70	752.30	0.52	16.60
4.00	0.24	89.20	68.00	925.27	487.00	3.20	483.80	0.26	42.05
5.00	0.95	87.90	37.00	927.97	851.00	50.70	800.30	1.02	4.49
6.00	0.95	55.20	45.00	931.04	472.00	50.70	421.30	1.29	3.75
8.00	0.24	54.00	75.00	928.70	193.00	3.20	189.80	0.33	27.15

BREAKING RESISTANCES

TEST NO.	SPEED m/s	THICK. mm	STR. kPa	DENSITY kg/m^3	RES. N	VISC. N	NET N	CLEAR. N	BREAK. N	Sn	Cbr
1.00	0.48	54.40	95.00	927.01	610.00	13.70	596.30	296.92	299.38	1.50	10.65
1.00	0.48	53.40	95.00	927.12	567.00	13.70	553.30	287.43	265.87	1.50	9.63
2.00	0.95	55.50	98.00	926.64	931.00	50.70	880.30	427.76	452.54	2.92	4.03
2.00	0.24	54.40	98.00	926.76	566.00	3.20	562.80	212.27	350.53	0.74	49.88
2.00	0.24	56.30	63.00	929.43	471.00	3.20	467.80	226.12	241.68	0.92	33.13
3.00	0.24	90.50	116.00	921.17	1380.00	3.20	1376.80	516.27	860.53	0.68	74.05
3.00	0.48	90.60	116.00	921.16	1690.00	13.70	1676.30	723.37	952.93	1.35	20.48
4.00	0.95	88.60	90.00	923.53	1643.00	50.70	1592.30	970.25	622.05	3.04	3.48
4.00	0.24	88.70	48.00	926.98	813.00	3.20	809.80	501.49	308.31	1.05	26.90
5.00	0.48	90.40	48.00	926.78	1098.00	13.70	1084.30	724.97	359.33	2.11	7.69
5.00	0.95	88.30	48.00	927.02	1453.00	50.70	1402.30	968.13	434.17	4.17	2.43
6.00	0.48	57.40	56.00	929.88	587.00	13.70	573.30	327.32	245.98	1.96	8.27
6.00	0.95	58.00	56.00	929.81	842.00	50.70	791.30	463.80	327.50	3.87	2.78
7.00	0.24	134.10	111.00	916.61	2850.00	3.20	2846.80	1025.58	1821.22	0.69	106.29
7.00	0.48	134.60	111.00	916.56	3100.00	13.70	3086.30	1443.55	1642.75	1.38	23.88
7.00	0.95	129.40	111.00	917.15	3400.00	50.70	3349.30	1875.33	1473.97	2.73	5.69
8.00	0.95	55.90	90.00	927.25	990.00	50.70	939.30	433.49	505.81	3.05	4.47
9.00	0.24	90.10	90.00	923.36	1149.00	3.20	1145.80	513.48	632.32	0.77	54.53
9.00	0.95	88.80	90.00	923.50	1810.00	50.70	1759.30	974.08	785.22	3.04	4.38
10.00	0.70	47.00	91.00	928.18	643.00	28.40	614.60	275.95	338.65	2.24	6.55
10.00	0.95	47.30	91.00	928.15	721.00	50.70	670.30	323.48	346.82	3.03	3.62
10.00	0.24	44.40	91.00	928.48	446.00	3.20	442.80	148.80	294.00	0.77	51.16

1:20 R-CLASS ICE RESISTANCE TEST RESULTS

PRESAWN RESISTANCES

TEST NO.	SPEED m/s	THICK. mm	STR. kPa	DENS. kg/m^3	RESIST. N	VISC. N	NET N	Fn	Cc
27	0.17	22.20	10.80	951	14.00	0.44	13.56	0.36	22.95
27	0.35	23.00	10.80	951	21.00	1.58	19.42	0.74	7.49
27	0.58	22.50	10.80	951	27.00	3.90	23.10	1.23	3.31
27	0.92	21.00	10.80	952	42.00	8.93	33.07	2.03	2.02
28	0.17	34.80	36.00	942	22.00	0.44	21.56	0.29	23.52
28	0.35	37.10	36.00	941	34.00	1.58	32.42	0.58	7.83
28	0.58	35.40	36.00	941	43.00	3.90	39.10	0.98	3.60
28	0.92	34.50	36.00	942	65.00	8.93	56.07	1.58	2.11
30	0.17	51.30	31.20	936	43.00	0.44	42.56	0.24	31.67
30	0.35	51.70	31.20	936	56.00	1.58	54.42	0.49	9.48
30	0.58	52.10	31.20	936	67.00	3.90	63.10	0.81	3.97
30	0.92	48.90	31.20	937	99.00	8.93	90.07	1.33	2.40
32	0.17	22.90	31.70	947	15.00	0.44	14.56	0.36	24.01
32	0.35	23.40	31.70	947	21.00	1.58	19.42	0.73	7.39
32	0.58	23.00	31.70	947	30.00	3.90	26.10	1.22	3.68
32	0.92	21.50	31.70	947	45.00	8.93	36.07	2.00	2.16

BREAKING RESISTANCE

TEST NO.	SPEED m/s	THICK. mm	STR. kPa	DENS. kg/m^3	RES. N	VISC. N	NET N	CLEAR N	BREAK N	Sn	Cbr
23	0.17	37.00	48.80	938	88.00	0.44	87.56	24.54	63.02	0.75	64.90
23	0.35	38.10	48.80	938	127.00	1.58	125.42	40.17	85.25	1.53	20.12
23	0.58	36.50	48.80	938	123.00	3.90	119.10	50.97	68.13	2.54	6.11
23	0.92	34.30	48.80	939	140.00	8.93	131.07	60.96	70.11	4.04	2.66
24	0.17	34.80	20.20	945	65.00	0.44	64.56	22.28	42.28	1.16	45.97
24	0.35	36.10	20.20	944	94.00	1.58	92.42	36.92	55.50	2.39	13.73
24	0.58	34.90	20.20	945	111.00	3.90	107.10	47.57	59.53	3.97	5.55
24	0.92	32.40	20.20	946	127.00	8.93	118.07	55.74	62.33	6.29	2.48
25	0.17	33.90	28.80	943	55.00	0.44	54.56	21.28	33.28	0.97	37.20
25	0.35	36.10	28.80	942	72.00	1.58	70.42	36.85	33.57	2.00	8.32
25	0.58	35.30	28.80	943	94.00	3.90	90.10	48.40	41.70	3.32	3.85
25	0.92	35.30	28.80	943	125.00	8.93	116.07	64.25	51.82	5.26	1.90
26	0.17	49.20	20.90	939	123.00	0.44	122.56	39.81	82.75	1.14	64.01
26	0.35	51.40	20.90	938	139.00	1.58	137.42	66.74	70.68	2.35	12.36
26	0.58	50.40	20.90	939	174.00	3.90	170.10	88.07	82.03	3.89	5.32
26	0.92	47.70	20.90	940	187.00	8.93	178.07	106.62	71.45	6.17	1.95
27	0.17	22.00	18.10	950	27.00	0.44	26.56	10.31	16.25	1.23	27.80
27	0.35	22.80	18.10	950	43.00	1.58	41.42	17.05	24.37	2.54	9.49
27	0.58	22.30	18.10	950	54.00	3.90	50.10	22.40	27.70	4.20	4.02
27	0.92	20.80	18.10	950	80.00	8.93	71.07	26.45	44.62	6.67	2.76
28	0.17	34.50	42.90	940	71.00	0.44	70.56	21.85	48.71	0.80	53.68
28	0.35	36.70	42.90	939	101.00	1.58	99.42	37.77	61.65	1.64	15.08
28	0.58	35.00	42.90	940	120.00	3.90	116.10	47.56	68.54	2.72	6.40
28	0.92	34.20	42.90	940	140.00	8.93	131.07	60.74	70.33	4.31	2.67
29	0.17	34.70	8.40	947	51.00	0.44	50.56	22.23	28.33	1.81	30.81
29	0.35	36.30	8.40	947	68.00	1.58	66.42	37.36	29.06	3.72	7.13
29	0.58	36.10	8.40	947	86.00	3.90	82.10	50.47	31.63	6.16	2.84
29	0.92	34.50	8.40	947	103.00	8.93	94.07	62.09	31.98	9.77	1.19

30	0.17	50.80	35.10	936	127.00	0.44	126.56	41.87	84.69	0.88	63.68
30	0.35	51.20	35.10	936	169.00	1.58	167.42	66.10	101.32	1.81	17.83
30	0.58	51.60	35.10	936	217.00	3.90	213.10	91.33	121.77	2.99	7.75
30	0.92	48.40	35.10	937	224.00	8.93	215.07	108.92	106.15	4.75	2.86
31	0.17	35.40	62.50	936	101.00	0.44	100.56	22.72	77.84	0.66	83.98
31	0.35	36.40	62.50	936	124.00	1.58	122.42	37.10	85.32	1.35	21.13
31	0.58	35.00	62.50	936	139.00	3.90	135.10	47.36	87.74	2.24	8.22
31	0.92	33.80	62.50	937	173.00	8.93	164.07	59.30	104.77	3.56	4.04
32	0.17	22.70	41.10	945	41.00	0.44	40.56	10.81	29.75	0.82	49.58
32	0.35	23.20	41.10	945	53.00	1.58	51.42	17.47	33.95	1.68	13.06
32	0.58	22.80	41.10	945	68.00	3.90	64.10	23.14	40.96	2.78	5.84
32	0.92	21.30	41.10	945	90.00	8.93	81.07	27.39	53.68	4.41	3.25
33	0.17	34.80	46.10	939	87.00	0.44	86.56	22.16	64.40	0.77	70.42
33	0.35	35.30	46.10	939	113.00	1.58	111.42	35.36	76.06	1.58	19.35
33	0.58	35.70	46.10	939	143.00	3.90	139.10	49.14	89.96	2.62	8.24
33	0.92	33.40	46.10	940	144.00	8.93	135.07	58.33	76.74	4.15	2.98

1:40 R-CLASS ICE RESISTANCE TEST RESULTS

PRESAWN RESISTANCES

TEST NO.	SPEED m/s	THK. mm	STR. kPa	DENS. kg/m^3	RES. N	VISC. N	NET N	Fn	Cc
2	0.12	11.40	37.4	949	1.60	0.00	1.60	0.36	21.22
2	0.24	11.30	37.4	949	2.10	0.00	2.10	0.72	7.02
2	0.41	11.20	37.4	949	2.80	0.00	2.80	1.24	3.24
2	0.65	11.00	37.4	949	4.40	0.00	4.40	1.98	2.06
2	0.98	10.70	37.4	949	7.90	0.01	7.89	3.02	1.67
3	0.12	11.60	12.1	956	2.00	0.00	2.00	0.36	25.89
3	0.24	11.60	12.1	956	2.40	0.00	2.40	0.71	7.77
3	0.41	11.70	12.1	955	3.20	0.00	3.20	1.21	3.52
3	0.65	11.40	12.1	956	4.90	0.00	4.90	1.94	2.20
3	0.98	10.70	12.1	956	8.00	0.01	7.99	3.02	1.68
4	0.12	16.00	17.1	952	2.40	0.00	2.40	0.30	22.60
4	0.24	16.10	17.1	952	3.60	0.00	3.60	0.60	8.42
4	0.41	16.00	17.1	952	4.50	0.00	4.50	1.03	3.63
4	0.65	16.40	17.1	952	6.70	0.00	6.70	1.62	2.10
4	0.98	16.10	17.1	952	11.10	0.01	11.09	2.47	1.56
5	0.12	17.10	14.7	952	2.30	0.00	2.30	0.29	20.26
5	0.24	17.00	14.7	952	2.70	0.00	2.70	0.59	5.98
5	0.41	17.00	14.7	952	3.50	0.00	3.50	1.00	2.66
5	0.65	16.90	14.7	952	5.20	0.00	5.20	1.60	1.59
5	0.98	16.30	14.7	952	9.30	0.01	9.29	2.41	1.25

BREAKING RESISTANCE

TEST NO.	SPEED m/s	THK. mm	STR. kPa	DENS. kg/m^3	RES. N	VISC. N	NET N	CLEAR. N	BREAK N	Sn	Cbr
2	0.12	11.40	40.0	948	4.20	0.00	4.20	1.24	2.96	0.58	39.31
2	0.24	11.30	40.0	948	5.40	0.00	5.40	2.04	3.36	1.17	11.25
2	0.41	11.20	40.0	948	8.10	0.00	8.10	2.99	5.11	2.00	5.92
2	0.65	11.00	40.0	948	11.50	0.00	11.50	4.08	7.42	3.16	3.48
2	0.98	10.70	40.0	948	17.70	0.01	17.69	5.28	12.41	4.77	2.63
3	0.12	11.60	16.9	954	3.20	0.00	3.20	1.28	1.92	0.90	24.85
3	0.24	11.60	16.9	954	4.20	0.00	4.20	2.14	2.06	1.80	6.67
3	0.41	11.70	16.9	954	6.30	0.00	6.30	3.23	3.07	3.08	3.38
3	0.65	11.40	16.9	954	9.60	0.00	9.60	4.35	5.25	4.88	2.36
3	0.98	10.70	16.9	955	15.90	0.01	15.89	5.32	10.57	7.37	2.23
4	0.12	16.00	29.7	949	7.50	0.00	7.50	2.15	5.35	0.68	50.53
4	0.24	16.10	29.7	949	8.80	0.00	8.80	3.63	5.17	1.36	12.13
4	0.41	16.00	29.7	949	11.30	0.00	11.30	5.34	5.95	2.32	4.82
4	0.65	16.40	29.7	949	15.60	0.00	15.60	7.82	7.78	3.67	2.44
4	0.98	16.10	29.7	949	24.90	0.01	24.89	10.28	14.61	5.54	2.06
5	0.12	17.10	17.6	951	7.60	0.00	7.60	2.41	5.19	0.88	45.78
5	0.24	17.00	17.6	952	10.20	0.00	10.20	3.98	6.22	1.76	13.79
5	0.41	17.00	17.6	952	13.20	0.00	13.20	5.92	7.28	3.01	5.53
5	0.65	16.80	17.6	952	18.50	0.00	18.50	8.16	10.34	4.78	3.16
5	0.98	16.80	17.6	952	23.00	0.01	22.99	11.06	11.93	7.21	1.61

CCGS PIERRE RADISSON FULL SCALE DATA

TEST NO.	SPEED m/s	THICK. m.	STR. kPa	RES. N	Fn	Sn	Cr	VISC. N
1	0.82	0.23	408.47	80728	0.55	1.23	3436	1780
2	1.85	0.23	408.47	151830	1.24	2.76	17397	7979
3	2.73	0.23	408.47	203017	1.82	4.07	37692	16352
4	3.81	0.23	408.47	282182	2.54	5.68	73513	30432
5	4.99	0.23	408.47	320205	3.33	7.45	126299	50375
6	5.81	0.23	408.47	454576	3.88	8.68	171395	66964
7	7.00	0.23	408.47	517752	4.67	10.44	248325	94642
9	5.81	0.23	408.47	430776	3.88	8.68	171395	66964
10	2.93	0.23	408.47	257949	1.96	4.38	43604	18723
12	0.72	0.21	408.47	130863	0.50	1.07	2400	1391
13	1.75	0.20	408.47	110136	1.25	2.61	13483	7176
16	0.62	0.21	408.47	67035	0.43	0.92	1788	1047
17	2.32	0.21	408.47	118466	1.62	3.46	24572	12071
18	3.14	0.25	408.47	205442	2.00	4.68	54745	21242
19	0.62	0.43	408.47	169145	0.30	0.92	3660	1047
20	1.44	0.46	408.47	249198	0.68	2.15	21219	5006
21	2.16	0.43	408.47	338961	1.05	3.22	44850	10614
22	3.13	0.45	408.47	453529	1.50	4.68	96748	21179
23	3.83	0.33	408.47	383597	2.13	5.71	106727	30730
24	1.75	0.48	408.47	309610	0.81	2.61	32590	7176
25	3.76	0.48	408.47	513779	1.73	5.60	150220	29663
26	5.76	0.48	408.47	756477	2.65	8.60	353715	65872
27	6.28	0.48	408.47	767044	2.89	9.37	419636	77256
28	1.11	0.35	408.47	162397	0.60	1.66	9541	3098
29	3.13	0.35	408.47	294307	1.69	4.68	75877	21179
30	6.82	0.35	408.47	718384	3.68	10.18	360789	90271
31	1.29	0.34	408.47	134579	0.71	1.93	12404	4090
60	4.09	0.69	525.89	890499	1.57	5.37	255772	34699
61	3.83	0.72	525.89	825017	1.44	5.04	233649	30820
62	3.06	0.71	525.89	662132	1.16	4.02	146454	20221
63	2.42	0.72	525.89	569030	0.91	3.19	92977	13138
64	1.61	0.72	525.89	435606	0.60	2.12	41510	6156
65	1.33	0.70	525.89	459501	0.51	1.75	27185	4304
66	1.05	0.69	525.89	403828	0.40	1.39	17027	2811
67	3.13	0.72	525.89	735254	1.18	4.11	155387	21116
68	3.79	0.72	525.89	902658	1.43	4.98	227002	30120
69	3.87	0.72	525.89	894758	1.46	5.09	238390	31361
70	3.62	0.68	525.89	818900	1.41	4.76	196720	27738
71	2.72	1.22	207.75	1107945	0.79	5.68	199171	16241
72	2.19	1.22	207.75	891907	0.63	4.58	129023	10853
73	1.92	1.22	207.75	985383	0.55	4.02	99430	8523
75	1.88	1.22	207.75	784850	0.54	3.94	95734	8229
76	2.30	1.17	207.75	1007797	0.68	4.81	136853	11917
77	3.34	1.17	207.75	947455	0.99	6.99	288675	23842
78	1.48	1.17	207.75	938790	0.44	3.10	56792	5273
79	1.25	1.17	207.75	810477	0.37	2.62	40457	3853
80	1.11	1.17	207.75	659420	0.33	2.31	31673	3073
82	3.91	0.96	207.75	772486	1.27	8.18	324739	31983
83	3.29	0.98	207.75	728020	1.06	6.89	234998	23221
84	2.71	1.03	207.75	732857	0.85	5.67	167508	16185
86	3.70	1.00	207.75	1011833	1.18	7.75	303577	28918
87	3.96	1.12	207.75	1011922	1.20	8.29	388868	32764

88	2.78	1.05	207.75	847570	0.87	5.81	179309	16936
89	2.57	0.93	207.75	675604	0.85	5.38	136119	14678
91	1.34	1.03	207.75	566021	0.42	2.80	40742	4364
92	0.87	0.95	207.75	461341	0.29	1.83	16057	1989
93	3.61	1.02	207.75	922350	1.14	7.56	294301	27581
94	2.73	1.02	207.75	769823	0.86	5.71	167721	16352
95	2.21	0.93	207.75	662632	0.73	4.63	100681	11094
96	1.13	1.04	207.75	510008	0.35	2.37	29438	3202
97	0.62	0.98	207.75	455059	0.20	1.29	8255	1047
98	1.34	0.88	207.75	575668	0.46	2.80	34803	4364
99	1.49	1.12	207.75	601928	0.45	3.12	55173	5346
100	1.75	0.80	207.75	695657	0.62	3.66	54136	7176
101	2.21	1.15	207.75	781557	0.66	4.63	124524	11094
102	3.50	0.98	207.75	1007666	1.13	7.32	265329	25997

M.V. ARCTIC RESISTANCE DATA
BOW FRICTION COEFFICIENTS f= .061, .004, .450

PRESAWN RESISTANCE

TEST NO.	SPEED m/s	THICK. mm	STR. kPa	DENSITY kg/m^3	RES. N	VISC. N	NET N	Fn	Cc
3	0.19	39.0	12.0	950.1	20.5	0.74	19.76	0.31	19.39
	0.33	41.0	12.0	949.2	37.0	1.92	35.08	0.51	11.20
	0.47	40.0	12.0	949.6	41.0	3.65	37.35	0.74	5.97
	0.60	40.0	12.0	949.6	43.0	5.77	37.23	0.96	3.57
5	0.33	49.0	11.0	945.9	34.0	1.92	32.08	0.47	8.60
	0.60	49.0	11.0	945.9	53.0	5.77	47.23	0.87	3.71
12	0.19	49.0	15.0	944.2	25.2	0.74	24.46	0.27	19.22
	0.33	50.0	15.0	943.8	28.5	1.92	26.58	0.46	7.00
	0.47	48.0	15.0	944.7	41.3	3.65	37.65	0.68	5.04
	0.60	50.0	15.0	943.8	52.5	5.77	46.73	0.86	3.61
4	0.19	50.0	14.0	944.2	20.0	0.74	19.26	0.27	14.83
	0.33	50.0	14.0	944.2	24.0	1.92	22.08	0.46	5.81
	0.60	50.0	14.0	944.2	36.0	5.77	30.23	0.86	2.33
13	0.19	47.0	15.0	945.2	49.9	0.74	49.16	0.28	40.23
	0.33	49.0	15.0	944.2	70.7	1.92	68.78	0.47	18.47
	0.47	49.0	15.0	944.2	76.6	3.65	72.95	0.67	9.57
	0.60	50.0	15.0	943.8	96.4	5.77	90.63	0.86	7.00

BREAKING RESISTANCE

TEST NO.	SPEED m/s	THICK. mm	STR. kPa	DENSITY kg/m^3	RES. N	VISC. N	NET N	CLEAR. N	BREAK. N	Sn	Cbr
2	0.19	49.0	19.0	942.6	76.0	0.74	75.26	25.50	49.76	1.34	39.17
	0.33	51.0	19.0	941.6	89.0	1.92	87.08	37.25	49.83	2.29	12.89
	0.47	49.0	19.0	942.6	103.0	3.65	99.35	42.87	56.48	3.28	7.42
	0.60	49.0	19.0	942.6	111.0	5.77	105.23	49.71	55.52	4.23	4.38
3	0.19	39.0	17.0	948.0	50.0	0.74	49.26	17.36	31.90	1.42	31.37
	0.33	41.0	17.0	947.1	63.0	1.92	61.08	25.80	35.28	2.43	11.29
	0.47	40.0	17.0	947.5	70.0	3.65	66.35	30.46	35.89	3.47	5.75
	0.60	40.0	17.0	947.5	81.0	5.77	75.23	35.32	39.91	4.48	3.84
5	0.19	48.0	16.0	944.3	56.0	0.74	55.26	24.66	30.60	1.46	24.54
	0.33	49.0	16.0	943.8	74.0	1.92	72.08	34.87	37.21	2.50	10.00
	0.47	49.0	16.0	943.8	86.0	3.65	82.35	42.93	39.42	3.57	5.17
	0.60	49.0	16.0	943.8	103.0	5.77	97.23	49.78	47.45	4.61	3.74
12	0.19	49.0	20.7	941.9	58.0	0.74	57.26	25.48	31.78	1.28	25.04
	0.33	50.0	20.7	941.4	81.1	1.92	79.18	36.00	43.18	2.19	11.40
	0.47	48.0	20.7	942.3	83.6	3.65	79.95	41.38	38.57	3.14	5.18
	0.60	50.0	20.7	941.4	126.0	5.77	120.23	51.40	68.83	4.05	5.33
4	0.19	49.0	19.0	942.6	46.0	0.74	45.26	18.06	27.20	1.34	21.41
	0.33	50.0	19.0	942.1	59.0	1.92	57.08	23.14	33.94	2.29	8.95
	0.47	50.0	19.0	942.1	76.0	3.65	72.35	26.66	45.69	3.27	5.89

	0.60	50.0	19.0	942.1	88.0	5.77	82.23	29.48	52.75	4.22	4.08
13	0.19	47.0	20.4	942.9	114.6	0.74	113.86	49.41	64.45	1.29	52.87
	0.33	49.0	20.4	942.0	122.9	1.92	120.98	66.24	54.74	2.21	14.73
	0.47	49.0	20.4	942.0	148.7	3.65	145.05	76.69	68.36	3.16	8.99
	0.60	50.0	20.4	941.5	198.3	5.77	192.53	88.21	104.32	4.08	8.08

USCGC MOBILE BAY FULL SCALE TOWED RESISTANCE DATA

ICE STRENGTHS

DATE	TEST	THK	PSI	KPA
18	1	21.00	41.11	283.54
19	3	19.50	47.69	328.93
20	4	20.00	56.59	390.31
	5	21.00	51.56	355.62
23	6	17.00	70.75	487.98
	7	17.00	69.06	476.32
24	9	15.00	70.42	485.70
	10	15.00	94.69	653.09
	11	16.00	64.21	442.87
	12	15.00	91.99	634.47
25	13	16.00	72.31	498.74
	14	12.50	59.23	408.52
	15	17.00	64.83	447.14

RESISTANCE RESULTS

DATE	TEST	SPEED (kts)	THK (in)	Rt (lbs)	SPEED (m/s)	THK (m)	STR (kpa)	RES (N)	VISC	NET	Cr	Fn	Sn
19	1	4.00	20.60	24417	2.06	0.52	329.00	108650	2116	106534	14.45	0.91	3.42
20	2	5.00	18.70	37104	2.57	0.47	373.00	165105	3197	161908	15.48	1.19	4.02
	3	2.50	19.90	31903	1.29	0.51	373.00	141962	890	141072	50.70	0.58	2.01
21	4	1.80	19.90	23021	0.93	0.51	409.00	102439	486	101952	70.68	0.42	1.38
	5	4.80	18.00	36186	2.47	0.46	409.00	161020	2964	158056	17.03	1.17	3.68
	6	3.70	14.10	14535	1.90	0.36	409.00	64678	1833	62845	14.55	1.02	2.84
22	7	2.80	14.90	18369	1.44	0.38	446.00	81738	1096	80642	30.86	0.75	2.06
	8	6.30	12.60	32000	3.24	0.32	446.00	142393	4902	137491	12.29	1.83	4.63
		6.80	12.60	33324	3.50	0.32	446.00	148285	5647	142637	10.94	1.97	5.00
23	9	1.10	14.90	16706	0.57	0.38	482.00	74338	197	74141	183.81	0.29	0.78
		1.30	14.90	15743	0.67	0.38	482.00	70053	268	69785	123.87	0.35	0.92
	10	4.90	14.90	25209	2.52	0.38	482.00	112175	3079	109095	13.63	1.31	3.46
24	12	1.20	13.00	11229	0.62	0.33	527.00	49967	231	49735	118.75	0.34	0.81
	13	7.60	15.00	37367	3.91	0.38	527.00	166275	6940	159335	8.22	2.02	5.14
25	14	2.10	14.10	16718	1.08	0.36	451.00	74392	646	73746	53.01	0.58	1.53
	15	7.40	16.70	37854	3.81	0.42	451.00	168442	6605	161837	7.91	1.87	5.41
	16	4.40	15.50	21215	2.26	0.39	451.00	94402	2524	91878	13.69	1.15	3.22

BIBLIOGRAPHY

List of References and other works consulted but not cited. Alphabetically by author.

Albery, Pullerits, Dickson and Associates. M.V. Arctic Ice Transiting Performance-Continuous Mode Transportation Development Centre Report No. TP5170, Montreal, 1984.

Arvetis,C.;Palmer,C;Buckley,J Why Does it Float? Rand Mc Nally New York 1983

Atkins, A.G. Icebreaker Modelling Journal of Ship Research, Vol. 14, No. 1, 1975.

Atkins, A.G. and Caddell, R.M. The Laws of Similitude and Crack Propagation International Journal of Mechanical Sciences, Vol. 16, No. 8, 1974.

Bowden,F.P.; Friction on Snow and Ice , Proceedings of the Royal Society, Vol 187 , London 1953

Cammaert,A.B.;Muggeridge,D.B. Ice Interaction with Offshore Structures Van Nostrand New York 1988

Carter, D. Ship Resistance to Continuous Motion in Level Ice Transportation Development Centre Report TP3679E, Transport Canada, Montreal, 1983.

Carter, J.E. Colbourne, B., Small Waterplane Area Twin (SWATH) Vessel Ice Tests Transportation Development Centre, Report No. TP6681E, 1985, Montreal.

Colbourne,D.B.; Model Tests in Ice of a 1:8 Scale Model of the CCG R-Class Hull NRCC Report TR-AVR-07 1987

Croasdale,K.R.; Ice Engineering II Ice Forces on Offshore Structures , Symposium on Offshore Mechanics and Cold Ocean Engineering

Edwards, R.Y;Lewis,J.W.;Wheaton,J.W.;Coburn,J. Full Scale and Model Tests of a Great Lakes Icebreaker Transactions of The Society of Naval Architects and Marine Engineers. Vol. 80, 1972.

Edwards, R.Y.;Dunne,M.A.;Johnson,B. Results of Full Scale Trials of CCGS Pierre Radisson Ice Tech. 81, SNAME, Ottawa, 1981.

Enkvist, E. On The Ice Resistance Encountered by Ships Operating in the Continuous Mode of Icebreaking The Swedish Academy of Engineering Science in Finland Report No. 24, Helsinki, 1972.

Enkvist, E. A Survey of Experimental Indications of the Relation Between the Submersion and Breaking Components of Level Ice Resistance to Ships POAC, Helsinki, 1983.

Ettema, R., Matsuishi, M. Influence of Ice Rubble Size on Resistance to Ship Hull Motion Through a Thick Layer of Ice Rubble POAC 85 Narssarssuaq, Greenland September 1985

Forland, K.A. and Tatinclaux, J.C. Experimental Investigation of the Kinetic Friction Coefficient of Ice CRREL, Report No. 85-6, Hanover, N.H., 1985.

Frederking,R.;Hausler,F.U.; The Flexural Behavior of Ice From In Situ Cantilever Beam Tests IAHR Symposium on Ice Problems Sweden 1978

Frederking,R.;Timco,G.W.; Field Measurements of the Shear Strength of Columnar Grained Sea Ice , IAHR Ice Symposium Iowa City 1986

Friction on Snow and Ice , Department of the Army Project 8-66-02-001 (DA-11-190-ENG-1), Prepared by R.C. Jordan et al University of Minnesota, June 1955

Goodman,D.J.; Tabor,D; Fracture Toughness of Ice: A Preliminary Account of Some New Experiments Journal of Glaciology No. 21 1978

Goodman,D.J.; Critical Stress Intensity Factor (K_{IC}) Measurements at High Loading Rates for Polycrystalline Ice , Physics and Mechanics of Ice Symposium Copenhagen 1979

Hallam,S.D.; The Role of Fracture in Limiting Ice Forces IAHR Ice Symposium Iowa City 1986

Hirayama,K.; Properties of Urea-Doped Ice in the CRREL Test Basin CRREL Report 83-8P 1983

Hobbs,P.V.; Ice Physics , Clarendon Press, Oxford, 1974

Jones,S.J.; Canada's New Ice Tank 21st American Towing Tank Conference 1987

Kashteljan, V.I., Poznjak, I.I., Ryvlin, A.Ja. Ice Resistance to Motion of a Ship Sudostroenie Leningrad 1968 Translation by Marine Computer Application Corp. 1969

Kim, J.K. et al Final Report, Full Scale/Model Scale Correlation Study Using Louis S. St. Laurent Hull Form Arctec Canada for German & Milne Inc., Unpublished, 1975.

Kotras, T.V., Baird, A.V., Naegle, J.N. Predicting Ship Performance in Level Ice Transactions, SNAME, Vol. 91 1983.

Lewis, J.W. and Edwards, R.Y. Methods for Predicting Icebreaking and Ice Resistance Characteristics of Icebreakers Transactions of The Society of Naval Architects and Marine Engineers Vol. 78, 1970.

Lewis, J.W., DeBord, F.W., Bulat, V.A. Resistance and Propulsion of Ice Worthy Ships Transactions, SNAME, Vol. 90, 1982.

Liljestrom, G., Lindberg, K. Performance of the Icebreaker Ymer on the Swedish Arctic Expedition "Ymer 80" POAC 81 Quebec, 1981.

Lovell,M.C.;Avery,A.J.;Vernon,M.W.; Physical Properties of Materials , Van Nostrand Reinhold Toronto 1976

Mellor,M.; Mechanical Properties of Polycrystalline Ice IUTAM Symposium Copenhagen Denmark

Michailides, M., Murdey, D.C., Performance of CCGS Franklin in Lake Melville, 1980 Ice Tech. 81, SNAME, Ottawa, 1981.

Michel, B. Ice Mechanics Laval University Press, Quebec, 1978.

Milano, V.R. Ship Resistance to Continuous Motion in Ice Transactions of The Society of Naval Architects and Marine Engineers. Vol. 81, 1973.

Milano, V.R. Variation of Ship/Ice Parameters on Ships Resistance to Continuous Motion in Ice SNAME, Ice Tech. 1975, Montreal.

Miller,K.J.; The Application of Fracture Mechanics to Ice Problems , Physics and Mechanics of Ice Symposium Copenhagen 1979

Naegle, J.N. Ice Resistance Prediction and Motion Simulation For Ships Operating in the Continuous Mode of Icebreaking Ph.D Thesis, University of Michigan 1980.

Newbury, S. "R" Class Icebreaking Experiments with Model 327 and Comparison with 1:40 Scale and Full Scale Results NRCC Report, LTR-SH-383, 1984.

Oksanen,P.; Friction and Adhesion of Ice Technical Research Centre of Finland, Laboratory of Structural Engineering Publication 10 1983

Poznjak, I.I., Ionov, B.P. The Division of Icebreaker Resistance into Components Ice Tech, 81, SNAME, Ottawa, 1981.

Principles of Naval Architecture Ed. J.P. Comstock Society of Naval Architects and Marine Engineers New York 1967

Report of The Performance in Ice Covered Waters Committee The 17th International Towing Tank Conference Goteborg, Sweden.

Riska, K., Varsta, P. State of the Art Review of Basic Ice Problems for a Naval Architect Technical Research Centre of Finland. Ship Laboratory Report No. 2, 1977.

Saeki,H.;Ozaki,A.;Kubo,Y.; Experimental Study on Flexural Strength and Elastic Modulus of Sea Ice POAC 81 Quebec 1981

Sanderson,T.J.O.; A Pressure Area Curve For Ice ,IAHR Ice Symposium Iowa City 1986

Scarton, H.A. On the Role of Bow Friction in Icebreaking Journal of Ship Research, Vol. 19, No. 1, 1975.

Sharp, J.J. Hydraulic Modelling Butterworths, Toronto, 1981.

Sinha,N.K.; Rate Sensitivity of Compressive Strength of Columnar Grained Ice Experimental Mechanics Vol 21 1981

Sinha,N.K.;Timco,G.W.;Frederking,R.; Recent Advances in Ice Mechanics in Canada , Proceedings OMAE Houston 1987

Sodhi,D.S.; Flexural and buckling failure of Floating Ice Sheets Against Structures IAHR Ice Symposium Iowa City 1986

Tatinclaux,J.C. Ship Model Testing in Level Ice CRREL Report 88-15 Hanover N.H. 1988

Timco,G.W.; Ice Forces on Structures: Physical Modelling Techniques IAHR Symposium on Ice Hamburg 1984

Timco,G.W.; EG/AD/S: A New Type of Model Ice for Refrigerated Towing Tanks , Cold Regions Science and Technology Vol 12 1986

Tusima,K.; Friction of a Steel Ball on a Single Crystal of Ice , Journal of Glaciology, Vol. 19 No. 81, 1977

Tusima,K; Tabata,T; Friction Measurements of Sea Ice on Flat Plates of Metals, Plastics and Coatings , POAC 1979

Urabe,N.; Iwasaki,T.; Yoshitake,A; Fracture Toughness of Sea Ice , Cold Regions Science and Technology No. 3 1980

Urabe,N.; Yoshitake,A.; Fracture Toughness of Sea Ice - In Situ Measurement and its Application , POAC 81 Quebec 1981

Urabe,N.; Yoshitake,A.; Strain Rate Dependent Fracture Toughness (K_{IC}) of Pure Ice and Sea Ice IAHR Symposium on Ice Quebec 1981

Vance, G.P. A Modelling System for Vessels in Ice Ph.D Thesis, University of Rhode Island 1974.

Vance, G.P. A Scaling System for Vessels Modeled in Ice Ice Tech. 75, SNAME, Montreal, 1975.

Vance, G.P., Goodwin, M.J., Gracewski, A.S., Full Scale Icebreaking Test of the USCGC Katmai Bay Ice Tech. 81, SNAME, Ottawa. 19[illegible].

Voelker, R.P., Kim, J.K. Summary Results of Ice Resistance Tests for Great Lakes Bulk Carriers from the Wartsila Model Test Series Arctec, Inc. for Maritime Administration U.S. Dept of Commerce, Washington NTIS Report No. MA-RD-940-77069

Weeks,W.;Assur,A.; The Mechanical Properties of Sea Ice Cold Regions Science and Engineering Monograph 11-C3 U.S. Army 1967

White, R.M. Dynamically Developed Forces at the Bow of an Icebreaker D.Sc. Thesis, Massachusetts Institute of Technology, 1965.

White, R.M. Prediction of Icebreaker Capability Transactions of The Royal Institute of Naval Architects Vol. 112, 1970.

Williams,F.M.;Snellen,J.B.;Bell,J.; The Effect of Surface Friction on Ship Model Resistance in Level Ice NRCC Report TR-AVR-02 1987

Younger, M.S. A First Course in Linear Regression, 2nd. Ed. Duxbury Press, Boston, 1985.

Zahn,P.B.;Humphreys,D.;Phillips,L.; Full Scale Towed Resistance Trials of the USCGC Mobile Bay in Uniform Level Ice SNAME Transactions 1987